Development of Optimal Energy Infrastructures for the Oil Sands Industry in a CO_2-constrained World

by

J. Guillermo Ordorica-Garcia

A thesis
presented to the University of Waterloo
in fulfillment of the
thesis requirement for the degree of
Doctor of Philosophy
in
Chemical Engineering

Waterloo, Ontario, Canada, 2007

I hereby declare that I am the sole author of this thesis. This is a true copy of the thesis, including any required final revisions, as accepted by my examiners.

I understand that my thesis may be made electronically available to the public.

Abstract

Western Canadian bitumen is becoming a predominant source of energy for North American markets. The bitumen extraction and upgrading processes in the oil sands industry require vast quantities of energy, in the form of power, H_2, steam, hot water, diesel fuel, and natural gas. These energy commodities are almost entirely produced using fossil feedstocks/fuels, which results in significant CO_2 atmospheric emissions.

CO_2 capture and storage (CCS) technologies are recognized as viable means to mitigate CO_2 emissions. Coupling CCS technologies to H_2 and power plants can drastically reduce the CO_2 emissions intensity of the oil sands industry. The CO_2 streams from such plants can be used in Enhanced Oil Recovery, Enhanced Coal Bed Methane, and underground CO_2 storage. The above CO_2 sinks currently exist in Alberta and roughly half of its territory is deemed suitable for geological storage of CO_2.

This study investigates the relationship between energy demands, energy costs and CO_2 emissions associated with current and proposed oil sands operations using various energy production technologies. Accordingly, two computer models have been developed to serve as energy planning and economic optimization tools for the public and private sectors. The first model is an industry-wide mathematical model, called the Oil Sands Operations Model (OSOM). It serves to quantify the demands for power, H_2, steam, hot water, process fuel, and diesel fuel of the oil sands industry for given production levels of bitumen and synthetic crude oil (SCO), by mining and/or thermal extraction techniques. The second model is an optimal economic planning model for large-scale energy production featuring CCS technologies to reduce CO_2 emissions in the oil sands industry. Its goal is to feasibly answer the question: *What is the optimal combination of energy production technologies, feedstocks, and CO_2 capture processes to use in the oil sands industry that will satisfy energy demands at minimal cost while attaining CO_2 reduction targets for given SCO and bitumen production levels?*

In 2003, steam, H_2, and power production are the leading sources of CO_2 emissions, accounting for approximately 80% of the total emissions of the oil sands industry. The CO_2 intensities calculated by the OSOM range from 0.080 to 0.087 tonne CO_2 eq/bbl for

SCO and 0.037 tonne CO_2 eq/bbl for bitumen. The energy costs in 2003 are $13.63/bbl and $5.37/bbl for SCO and bitumen, respectively.

The results from the OSOM indicate that demands for steam, H_2, and power will catapult between 2003 and 2030. Steam demands for thermal bitumen extraction will triple between 2003-2012 and triple again between 2012-2030. The H_2 demands of the oil sands industry will triple by 2012 and grow by a factor of 2.7 thereafter. Power demands will roughly double between 2003 and 2012 and increase by a factor of 2.4 by 2030.

The optimal energy infrastructures featured in this work reveal that natural gas oxyfuel and combined-cycle power plants plus coal gasification H_2 plants with CO_2 capture hold the greatest promise for optimal CO_2-constrained oil sands operations.

In 2012, the maximum CO_2 reduction level attainable with the optimal infrastructure is 25% while in 2030 this figure is 39% with respect to "business as usual" emissions. The optimal energy costs at maximum CO_2 reduction in 2012 are $21.43/bbl (mined SCO), $22.48/bbl (thermal SCO) and $7.86/bbl (bitumen). In 2030, these costs are $29.49/bbl (mined SCO), $31.03/bbl (thermal SCO), and $10.32/bbl (bitumen). CO_2 transport and storage costs account for between 2-5% of the total energy costs of SCO and are negligible in the case of bitumen.

The optimal energy infrastructures are mostly insensitive to variations in H_2 and power plant capital costs. The energy costs are sensitive to changes in natural gas prices and insensitive to changes in coal prices. Variations in CO_2 transport and storage costs have little impact on SCO energy costs and a null impact on bitumen energy costs. Likewise, all energy costs are insensitive to changes in the length of the CO_2 pipeline for transport.

Acknowledgements

I thank Prof. Peter Douglas for his unwavering support and invaluable advice throughout my years at Waterloo. You always helped me improve and calmed me down when I fretted about work. Thanks for your friendship.

I thank Prof. Ali Elkamel for always having words of encouragement for me and helping me think more mathematically. I look forward to collaborating with you on many future projects. Thanks for believing in me.

I thank Prof. Eric Croiset for being quick to point out opportunities for improvement in my work. You taught me to think more critically about my work and to look for weak points in my approaches. Thanks for the fun times at trips and conferences.

I thank CANMET for providing financial assistance for my research project.

I thank God for the first 31 years of my journey and for life, the universe, and everything.

To Shelley, my wife.

You are *my* optimal infrastructure

Table of Contents

CHAPTER 1: INTRODUCTION

CHAPTER 2: THE OIL SANDS OPERATIONS MODEL

CHAPTER 3: GAMS OPTIMIZATION MODEL

CHAPTER 4: RESULTS AND DISCUSSION

CHAPTER 5: SENSITIVITY ANALYSES

CHAPTER 6: CONCLUSIONS AND RECOMMENDATIONS

Nomenclature

A1 = Mined bitumen upgraded by LCF+FC+HT

A2 = Mined bitumen upgraded by DC+HT

A3 = Mined bitumen upgraded by LCF+HT

ATB = atmospheric-topped bitumen

B1 = SAGD bitumen upgraded by LCF+FC+HT

B2 = SAGD bitumen upgraded by DC+HT

B3 = SAGD bitumen upgraded by LCF+HT

BAU = business as usual

BBL = barrels of oil

BC = base case

BIT = SAGD bitumen

C = SAGD diluted bitumen

CCO2 = CO_2 captured

CCS = carbon dioxide capture and storage

DB = diluted bitumen

DC = delayed coking

DRU = diluent recovery unit

E = CO_2 emissions

ECBM = enhanced coal bed methane

EOR = enhanced oil recovery

FC = fluid coking

FPS = future production scenario

GHG = greenhouse gas

HEX = additional H_2 demands in the optimization model (optional)

HGO = heavy gas-oil

HT = hydrotreatment

HWP = hot water process

IGCC = integrated gasification combined-cycle power plant

LCF = LC-fining

LGO = light gas-oil

MEA = monoethanolamine

MEA = mono-ethanolamine

MILP = mixed integer linear program

MSCO = mined SCO

NG = natural gas

NGCC = natural gas combined-cycle power plants

OSOM = oil sands operations model

PC = supercritical pulverized coal power plant

PEX = additional power demands in the optimization model (optional)

PSA = pressure swing adsorption

PSV = primary separation vessel

SAGD = steam assisted gravity drainage

SB = boiler - 6,300 kPa and 500 °C steam

SCFD = standard cubic feet per day

SCO = synthetic crude oil

SMR/SR = steam methane reforming hydrogen plant

SOR = steam-to-oil ratio

SSB = boiler - 80% steam at 8,000 kPa

SSU = secondary separation unit

TOR = tailings oil recovery unit

TSCO = SAGD SCO

VDU = vacuum distillation unit

VTB = vacuum-topped bitumen

WCSB = western Canadian sedimentary basin

X = natural gas

Y = coal

Z = alternative (opportunity) fuel

OSOM Variables

ATB = atmospheric-topped bitumen [tonne/h]

B = bitumen production rate via SAGD [tonne/h]

BF = bitumen content of primary froth [mass %]

D = diesel demands [l/h]

DB = diluted bitumen [tonne/h]

E = CO_2 emissions [tonne/h]

F = process fuel demands [MJ/h]

FR = bitumen froth produced in primary extraction [tonne/h]

h = head requirements for pumping [m]

H = hydrogen demands [tonne/h]

HGO = heavy gas-oil [tonne/h]

LGO = light gas-oil [tonne/h]

N = number of units in mining [integer]

NAP = naphtha [tonne/h]

OS = oil sands mining rate [tonne/h]

P = power demands [kW]

PC = power demands for bitumen centrifugation [kW]

PF = pumping factor for bitumen slurry [kWh/tonne m]

PS = power demands for SAGD extraction [kW]

PTA = power demands for pumping tailings [kW]

RES = LC-Finer bottoms [tonne/h]

S = process steam demands [tonne/h]

SG = SAGD solution gas [tonne/h]

SS = steam demands for SAGD extraction [tonne/h]

TP = pumping factor for tailings [kWh/tonne m]

uf = utilization factor [%]

VTB = vacuum-topped bitumen [tonne/h]

W = hot water demands [tonne/h]

WF = water content of primary froth [mass %]

x = bitumen content of oil sand [mass %]

X = natural gas demands [Nm^3/h]

OSOM Parameters

ERS = power requirements for SAGD bitumen extraction [kW/tonne bitumen]

f = engine diesel fuel consumption [l/h]

FCH = fuel consumption rate in hydrogen plant [MJ/tonne H_2]

FEF = fuel emissions factor [tonne CO_2 /Nm^3]

FRD = fuel requirements of delayed coker [MJ/tonne feed]

FRL = fuel requirements of LC-finer [MJ/tonne feed]

HDR = heat requirements of diluent recovery unit [MJ/tonne feed]

HEF = unitary CO_2 emissions of hydrogen plant [tonne CO_2/tonne H_2]

HFC = heat requirements of fluid coker [MJ/tonne feed]

HHG = hydrogen requirements for hydrotreatment – HGO [tonne/bbl feed]

HHV = high heating value [MJ/Nm^3]

HLG = hydrogen requirements for hydrotreatment – LGO [tonne/bbl feed]

HLH = hydrogen requirements for high-conversion LC-finer [tonne/tonne feed]

HLL = hydrogen requirements for low-conversion LC-finer [tonne/tonne feed]

HNP = hydrogen requirements for hydrotreatment – naphtha [tonne/bbl feed]

HRP = heat rate of power plant [MJ/kWh]

HVD = heat requirements of vacuum distillation unit [MJ/tonne feed]

PDC = power requirements of delayed coker [kW/tonne feed]

PFC = power requirements of fluid coker [kW/tonne feed]

PLH = power requirements of high-conversion LC-finer [kW/tonne feed]

PLL = power requirements of low-conversion LC-finer [kW/tonne feed]

PSP = percentage of boiler capacity used for steam production [%]

SCS = solids content of bitumen slurry [mass %]

SF = sand content of primary froth [mass %]

SOL = SAGD solution gas production [tonne gas/tonne bitumen]

SOR = steam-to-oil ratio [tonne steam/tonne bitumen]

SSE = steam requirements for secondary bitumen extraction [tonne steam/tonne froth]

WWE = wash water requirements for bitumen extraction [tonne water/tonne oil sand]

ΔHS = enthalpy of steam [MJ/tonne]

ΔHW = enthalpy of hot water [MJ/tonne]

η_B = steam boiler thermal efficiency [%]

ρ= density of oil fraction [tonne/bbl]

GAMS Model Variables

AF = annual amortization factor [%]

BIT_{CO2} = optimized CO_2 intensity of SAGD bitumen [tonne CO_2/bbl bitumen]

C = CO_2 captured [tonne/h]

CAP = annual capital cost of plant [$/year]

C_h = CO_2 captured in hydrogen plants [tonne/h]

C_p = CO_2 captured in power plants [tonne/h]

CS_{cost} = CO_2 injection/storage costs [$/y]

CT_{cost} = CO_2 transport costs [$/y]

D_D = Diesel fuel demand [l/h]

DIE_{msco} = optimized unitary cost of diesel fuel [$/bbl SCO]

E = CO_2 emitted [tonne/h]

E_b = CO_2 emissions of boilers [tonne/h]

E_{DF} = CO_2 emissions of diesel fuel [tonne/h]

E_h = CO_2 emissions of hydrogen plants [tonne/h]

E_p = CO_2 emissions of power plants [tonne/h]

E_{PF} = CO_2 emissions of process fuel [tonne/h]

H_D = hydrogen demand [tonne/h]

H_h = hydrogen from H_2 plants [tonne/h]

HOT_{CO2} = average unitary CO_2 emissions of hot water [tonne CO_2/tonne]

HOT_{cost} = average unitary cost of hot water [$/tonne]

HOT_{msco}= optimized unitary cost of hot water [$/bbl SCO]

H_{OUT} = hydrogen supply [tonne/h]

HYD_{CO2} = average unitary CO_2 emissions of optimized hydrogen [tonne CO_2/tonne H_2]

HYD_{cost} = average unitary cost of optimized hydrogen [$/tonne H_2]

HYD_{msco} = optimized unitary cost of hydrogen [$/bbl SCO]

$MSCO_{CO2}$ = optimized CO_2 intensity of mined SCO [tonne CO_2/bbl SCO]

OM = annual non-fuel O&M cost of plant [$/year]

P = power supply [kW]

P_{CO2} = power required for CO_2 transport [kW]

P_D = power demand [kW]

PF_D = process fuel demand [Nm^3/h]

P_h = power co-produced or consumed in hydrogen plants [kW]

P_{H2} = power for hydrogen plants [kW]

POW_{CO2} = average unitary CO_2 emissions of optimized power [tonne CO_2/kWh]

POW_{cost} = average unitary cost of optimized power [$/kWh]

POW_{msco} = optimized unitary cost of power [$/bbl SCO]

P_p = power from power plants [kW]

PRO_{CO2} = average unitary CO_2 emissions of process fuel [tonne CO_2/GJh]

PRO_{cost} = average unitary cost of process fuel [$/GJh]

PRO_{msco} = optimized unitary cost of process fuel [$/bbl SCO]

RED = net CO_2 reduction of the fleet [tonne/h]

S = process steam supply [tonne/h]

S_b = process steam from boilers [tonne/h]

S_D = process steam demand [tonne/h]

S_h = process steam from H_2 plants [tonne/h]

SS = SAGD steam supply [tonne/h]

SS_b = SAGD steam from boilers [tonne/h]

SS_D = SAGD steam demand [tonne/h]

SST_{CO2} = average unitary CO_2 emissions of SAGD steam [tonne CO_2/tonne]

SST_{cost} = average unitary cost of SAGD steam [$/tonne]

STM_{CO2} = average unitary CO_2 emissions of process steam [tonne CO_2/tonne]

STM_{cost} = average unitary cost of process steam [$/tonne]

STM_{msco} = optimized unitary cost of process steam [$/bbl SCO]

TOT_{msco} = total optimized energy cost [$/bbl SCO]

$TSCO_{CO2}$ = optimized CO_2 intensity of thermal SCO [tonne CO_2/bbl SCO]

W = hot water supply [tonne/h]

W_b = hot water from boilers [tonne/h]

W_D = hot water demand [tonne/h]

X = natural gas demand [Nm^3/h]

X_b = natural gas demand in boilers [Nm^3/h]

X_h = natural gas demand in hydrogen plants [Nm^3/h]

X_i = natural gas consumption in unit i [Nm^3/h]

X_p = natural gas demand in power plants [Nm^3/h]

X_{PF} = natural gas demand for process fuel [Nm^3/h]

Y= coal demand [kg/h]

Y_h = coal demand in hydrogen plants [kg/h]

Y_i = coal consumption in unit i [kg/h]

Y_p = coal demand in power plants [kg/h]

Y_{PF} = coal demand for process fuel [kg/h]

Binary Variables

IB_b	= 1	if boiler b exists in the fleet	
	= 0	otherwise	$b \in S_B \cup S_{SB}$
IH_h	= 1	if hydrogen plant h exists in the fleet	
	= 0	otherwise	$h \in \bigcup_{i=1}^{5} S_{H_i}$
IP_p	= 1	if power plant p exists in the fleet	
	= 0	otherwise	$p \in \bigcup_{i=1}^{9} S_{P_i}$

GAMS Model Parameters

AOM = non-fuel operating cost factor [% of total overnight capital costs]

book life = plant book life [years]

CC = unitary overnight capital costs [$/unit of installed design capacity]

CCH = CO_2 captured in hydrogen plants [tonne CO_2 captured/tonne H_2]

CCP = CO_2 captured in power plants [tonne CO_2 captured/kWh]

CCT = unitary CO_2 transport costs [$/tonne CO_2/100 km]

CF = plant availability (capacity) factor [%]

CST = unitary CO_2 injection/storage costs [$/tonne CO_2]

D = diesel demands [l/h]

EBL = baseline CO_2 emissions for given year [tonne/h]

EFP = unitary CO_2 emissions of power plant [tonne CO_2/kWh]

ERG = target CO_2 reduction percentage [% of baseline emissions for given year]

ERS = power requirements for SAGD bitumen extraction [kW/tonne bitumen]

ESC = capital cost escalation factor [adimensional]

f = engine diesel fuel consumption [l/h]

F = process fuel demands [MJ/h]

FCH = fuel consumption rate in hydrogen plant [MJ/tonne H_2]

FEF_C = fuel emissions factor of coal [tonne CO_2/tonne C in coal]

FEF_{DIE} = fuel emissions factor of diesel fuel [tonne CO_2/l]

FEF_{NG} = fuel emissions factor of natural gas [tonne CO_2/Nm^3]

FRD = fuel requirements of delayed coker [MJ/tonne feed]

FRL = fuel requirements of LC-finer [MJ/tonne feed]

fuel cost = natural gas or coal cost [$/GJ]

H = hydrogen demands [tonne/h]

HCAP = hydrogen plant design capacity [tonne/h]

HDR = heat requirements of diluent recovery unit [MJ/tonne feed]

HEF = unitary CO_2 emissions of hydrogen plant [tonne CO_2/tonne H_2]

HFC = heat requirements of fluid coker [MJ/tonne feed]

HHE = additional Hydrogen production [tonne/h]

HHG = hydrogen requirements for hydrotreatment – HGO [tonne/bbl feed]

HHV_C = high heating value of coal [MJ/tonne]

HHV_{NG} = high heating value of natural gas [MJ/Nm^3]

HLG = hydrogen requirements for hydrotreatment – LGO [tonne/bbl feed]

HLH = hydrogen requirements for high-conversion LC-finer [tonne/tonne feed]

HLL = hydrogen requirements for low-conversion LC-finer [tonne/tonne feed]

HNP = hydrogen requirements for hydrotreatment – naphtha [tonne/bbl feed]

HPW = power co-production/demands in hydrogen plants [kWh/tonne H_2]

HRP = heat rate of power plant [MJ/kWh]

HVD = heat requirements of vacuum distillation unit [MJ/tonne feed]

N_H = fuel consumption in H_2 plant [MJ/tonne H_2]

P = power demands [kW]

PCT = unitary power demands for CO_2 transport [kWh/tonne CO_2/100 km]

PDC = power requirements of delayed coker [kW/tonne feed]

PEX = excess power [kW]

PFC = power requirements of fluid coker [kW/tonne feed]

PKM = CO_2 pipeline length [km]

PLH = power requirements of high-conversion LC-finer [kW/tonne feed]

PLL = power requirements of low-conversion LC-finer [kW/tonne feed]

POUT = power plant nominal output [kW]

PSP = percentage of boiler capacity used for steam production [%]

RET = annual capital charge rate [%]

S = process steam demands [tonne/h]

SBC = standard boiler capacity [tonne steam/h]

SCS = solids content of bitumen slurry [mass %]

SF = sand content of primary froth [mass %]

SOL = SAGD solution gas production [tonne gas/tonne bitumen]

SOR = steam-to-oil ratio [tonne steam/tonne bitumen]

SS = SAGD steam demands [tonne/h]

SSE = steam requirements for secondary bitumen extraction [tonne steam/tonne froth]

SSR = steam produced in H_2 plant [tonne/tonne H_2 produced]

t = annual hours of operation [h/year]

W = hot water demands [tonne/h]

water cost = fresh water cost [$/tonne]

WWE = wash water requirements for bitumen extraction [tonne water/tonne oil sand]

ΔHS = enthalpy of steam [MJ/tonne]

ΔHW = enthalpy of hot water [MJ/tonne]

η_B = boiler thermal efficiency [%]

ρ= density of oil fraction [tonne/bbl]

Indices

b = boiler

D = diesel fuel

E = extraction stage

F = LC-finer feed

H = hydrotransport stage

h = hydrogen plant

i = oil sands operator

j = process unit in upgrading scheme

k = upgrading scheme

L = LC-finer unit

NG = natural gas fuel

p = power plant

ref = reference mining fleet

s = shovels

T = hydrotreater unit

t = trucks

U = upgrading stage

V = VDU feed

Chapter 1

Introduction

1.1 The Oil Sands Industry

Canada possesses sizeable energy resources in the form of hydrocarbon. Most of these are located in Western Canada, specifically in Alberta. The Western Canadian Sedimentary Basin (WCSB) is the largest producer of oil and natural gas in the country. In addition to these resources, Alberta is home to the world's largest oil sands deposit, with estimated ultimate bitumen reserves in the order of 400 billion cubic metres (2,516 billion bbl) [1].

Current global market and political environments have caused oil prices to soar in the past 3 years. Concurrently, oil supply concerns in North America have contributed to an explosion of new oil sands developments in Canada, as seen in Figure 1-1. As a result, the nation's oil sands are now considered strategic for sustained economic growth and stability. Beyond Canada, markets in the United States and Asia have unequivocally expressed their interest in Canada's oil resources. Within this framework, the importance of Canada's oil sands industry is evident in both the present and foreseeable future.

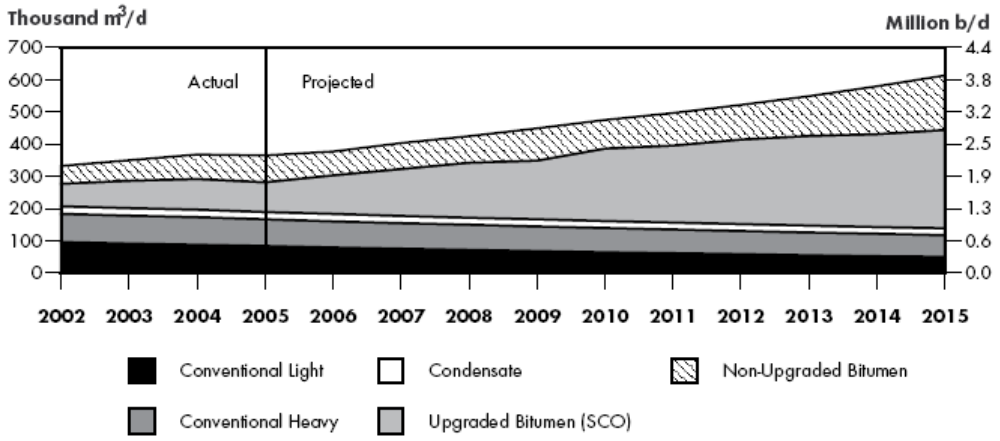

Figure 1-1. Projected crude oil production in WCSB [2]

The challenges to develop and exploit the oil sands resource, however, are substantial. In simple terms, these challenges are: 1) recoverability and 2) economics. As with most underground oil deposits, only a fraction of the reservoir is either technically or economically recoverable. Current technology allows bitumen recovery levels between one third and one half of the total reserves in the Athabasca region [3]. Also, the recovered bitumen must be upgraded to synthetic crude oil (SCO) before it can be marketed. The combined capital investments required to extract and upgrade bitumen are elevated, which makes SCO production more expensive than conventional oil production.

Oil companies in Alberta extract bitumen from the oil sands and upgrade a good portion of it to SCO. In the extraction and upgrading processes, vast quantities of energy in the form of electricity, hydrogen, steam, hot water, diesel fuel, and natural gas are consumed. This energy is almost entirely produced using fossil feedstocks/fuels (whether directly or indirectly), which inevitably results in significant greenhouse gas (GHG) atmospheric emissions. The combined CO_2 emissions from energy production for bitumen extraction and upgrading make the oil sands industry the single largest contributor to GHG emissions growth in Canada [4].

As social and environmental concerns over GHG emissions and their implications on climate change grow, the pressure on industrial users has begun to mount. In an increasingly CO_2-constrained world, reducing the CO_2 emissions of the oil industry is likely to become a top priority in the short and medium terms.

Canada has expressed its strong desire to mitigate its GHG emissions with economically sound and sustainable approaches. Carbon dioxide capture and storage (CCS) technologies are being increasingly accepted by the scientific community as well as governments around the world, as viable mid-term strategies to mitigate GHG emissions. Furthermore, the coupling of CCS technologies with large stationary fossil energy producers such as hydrogen and power generation plants has great potential to reduce CO_2 emissions and their mitigation cost. The concentrated CO_2 streams from such plants can be utilized in value-added applications such as Enhanced Oil Recovery (EOR) using current commercial practices, as demonstrated in the Weyburn project in Saskatchewan, Canada [5]. Also, in the immediate future, the CO_2 captured could also be used for Enhanced Coal Bed Methane (ECBM) natural gas recovery [5]. Both the above

carbon dioxide sinks as well as underground CO_2 storage are quite attractive provided that suitable locations exist in proximity to the CO_2 sources.

The province of Alberta's geography and geology, including the WCSB are largely favourable for CO_2 -based EOR, ECBM, and underground storage. According to Figure 1-2, roughly half of the province's territory has "good" or "very good" suitability for geological storage of CO_2. Many major CO_2 emitters in the province are either located on areas suitable for underground storage or within a reasonable distance of them, as is the case with some SCO producers. In short, it appears that Alberta has the unique ability to absorb the CO_2 it produces from large fossil energy operations.

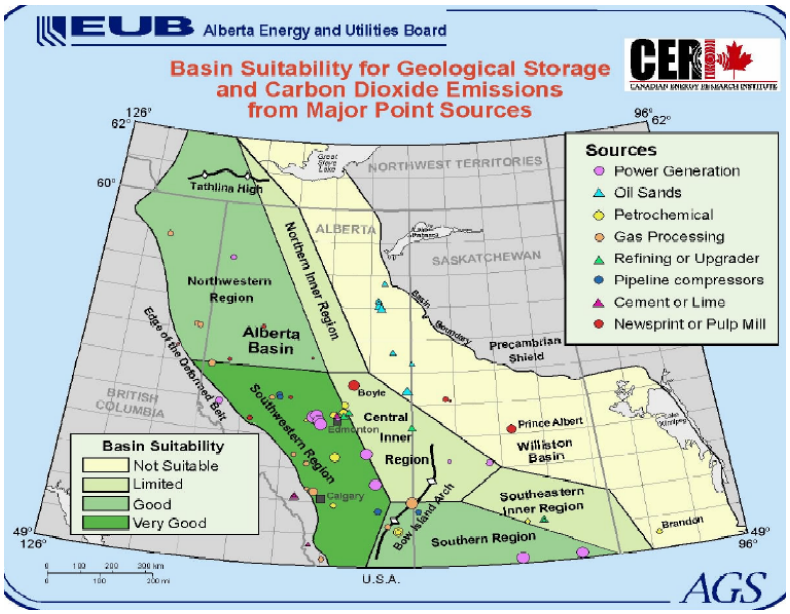

Figure 1-2. Basin suitability for underground CO_2 storage in Western Canada [6]

A key component in the development of effective CCS-based GHG mitigation strategies for Canada's oil sands industry is an inventory of their energy demands and associated GHG emissions. It is vital for the decision-making processes of policy-makers as well as industries and investors to forecast how much energy is required to realize any given future SCO and/or bitumen production level.

The energy demands for oil sands operations, being as substantial as they are, are intrinsically tied to the anticipated growth in bitumen extraction and upgrading. Energy commodities such as power, hydrogen, and steam are produced in power plants, hydrogen plants, boilers, and other units. Thus, if production levels rise, so will the

energy demands of the oil sands industry, which will in turn require that more energy-producing units be built and commissioned to uninterruptedly sustain operations.

In addition to energy demands, growth strategies for the oil sands industry in an increasingly CO_2-constrained world must be based on a sound knowledge of the magnitude of its GHG emissions and their sources. To implement CCS as a GHG abatement strategy in an economic fashion, it is imperative to first develop a CO_2 inventory that quantifies emissions associated with fossil fuel use in energy-producing units within the oil sands industry. The resulting benefits for the industry would be significant reductions in CO_2 emissions while ensuring affordable energy availability for sustained SCO and bitumen production growth.

The potential economic advantages derived from implementing CCS in oil sands operations include the potential revenue from CO_2 credits or commercially supplying CO_2 for EOR or ECBM to nearby users, once a suitable CO_2 distribution infrastructure is in place. Furthermore, future environmental legislation limiting GHG intensity and emissions in oil sands operations in Canada could well drive oil sands operators in Alberta to incorporate CCS schemes in their operations.

As the oil sands industry continues its accelerated expansion, serious economic and environmental impacts are expected. These impacts will be largely shaped by the magnitude of the bitumen and SCO production levels and by the technologies used. The above two variables combined will also dictate the composition and scale of the energy demands for oil sands operations. Ultimately, energy production for bitumen extraction and upgrading is responsible for all non-fugitive GHG emissions of the oil sands industry. Likewise, the cost associated with meeting these demands has a large influence on the production costs in oil sands operations.

The energy balance in oil sands operations consists of the energy demand side and the energy supply side. The former is related to the processes used to extract and upgrade bitumen and is a function of oil production. The latter is a combination of energy producing plants, typically employing different technologies, in numbers sufficient to match the energy demands. This is what in this work is referred to as the “energy infrastructure.” This term shall be used extensively in this work and is also the focus of both modeling and optimization efforts.

The reminder of section 1.1 will review the bitumen extraction and upgrading processes found in the oil sands industry as well as relevant energy production technologies used in this work.

1.1.1 Bitumen extraction

The only commercial technologies presently used for extracting bitumen from oil sands are in-situ or surface mining. According to some estimates [7], less than one-tenth of the total in-place bitumen reserves can be extracted by mining. The remainder must be recovered by using in-situ technologies.

Surface mining is a well-established technology that has seen its share of improvements sine its inception in the 1960's in Canada. As such, the bitumen recovery rates are high, in excess of 95%. The main operators employing this technology in Alberta are Syncrude Canada [8] and Suncor Energy [9].

In-situ technology will account for the majority of the growth in oil sands operations in the next 20 years [10]. The technology used in in-situ projects was developed in the 1970's and to date, the research in this area is squarely aimed at improving recoveries and reducing steam consumption. Interest in this technology is high among oil companies. A recent example is the Long Lake project – operated by Opti Canada Inc. and Nexen Inc – which is expected to begin operations in late 2007 [11].

Surface mining involves three stages: overburden removal, oil sands mining, and bitumen extraction. The layer covering the oil sands must be removed prior to mining. This layer, commonly known as overburden consists of sub-layers of decaying vegetation, stagnant water, wet sands and clay. In Alberta, trucks and shovels strip off the rocky, clay-like overburden and place it in mined-out pits. Once the overburden is removed, the thick deposit of oil sand is exposed.

Current oil sands mining technologies can be divided as conventional and hydrotransport. Conventional mining techniques were developed in the early 1950's while the hydrotransport method was developed in the late 1980's by Syncrude. In conventional mining processes, walking dragline/reclaimers or shovel/trucks transport the sand to the bitumen extraction plant. Conventional mining has been almost completely phased out in oil sands operations and has been replaced by oil sands hydrotransport. In

the hydrotransport process, hydraulic shovels dig the oil sand and feed trucks which deliver the material into a crusher. A mixer combines the oil sand from the crusher with hot water (35-50 ºC) to create a slurry that is pumped via pipeline to the extraction plant. By the time the slurry reaches the plant, it is already conditioned and thus the first step in the Hot Water Process (see Figure 1-3 below) can be omitted. Hydrotransport technology improves the energy efficiency and environmental performance of mining operations, as less hot water is required to process the mined sand.

The only commercially proven process to extract bitumen from mined oil sands is known as the Hot Water Process (HWP). It was developed between 1940 and 1960. A schematic of the HWP is shown in Figure 1-3. The process consists of three main steps: 1) conditioning, 2) separation, and 3) froth treatment.

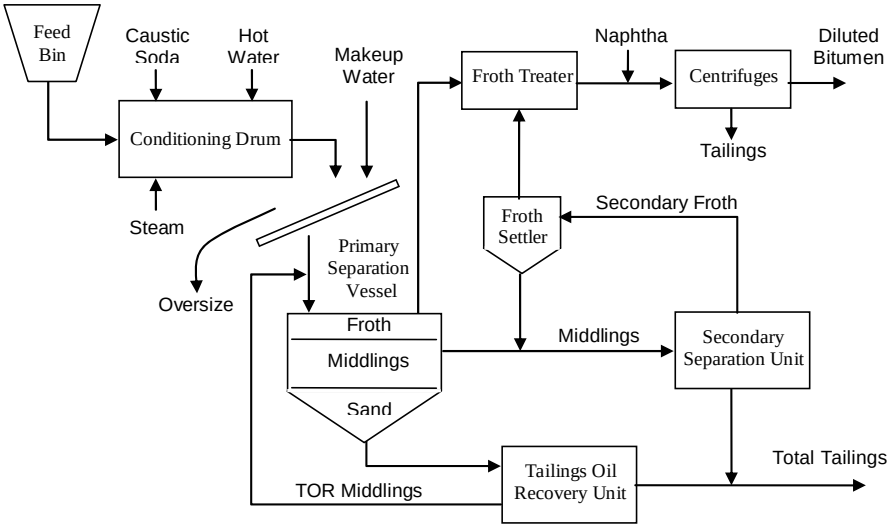

Figure 1-3. Hot water process flowchart

In the conditioning stage, hot water (35-50 ºC) and caustic soda are added to the mined oil sand. The resulting slurry is agitated in rotary drums known as *tumblers*. The temperature in the tumblers is maintained by steam injection. Bitumen is stripped from the individual sand grains in this step. The resulting slurry is a mixture containing water, sand grains, and bitumen globules of nearly identical size.

The conditioned slurry passes through a vibrating screen before entering the Primary Separation Vessel (PSV). Oversized rocks, clay lumps, and metal pieces from excavation equipment are screened out and sent back to the mine as oversized overburden.

Once screened, the slurry is diluted with water and a sand-rich mixture called *middlings*, which is recycled from a downstream unit. In the PSV, mineral particles readily settle. At the same time, bitumen globules float to the top, forming a bitumen-rich froth. The bitumen froth layer is skimmed off and sent to treatment, which is the last stage in the bitumen extraction process.

The bottom stream leaving the PSV contains mostly water-saturated sand, clay, and fines. However, some bitumen is entrained in this sludge, called *tailings*. The tailings are processed in the Tailings Oil Recovery (TOR) unit, where additional bitumen is recovered and sent back to the PSV.

The intermediate layer in the PSV is known as the *middlings*. These middlings are mainly constituted of water and solids, but they also contain suspended silt and clay fines. A middlings stream is continuously withdrawn from the PSV and sent to the Secondary Separation Unit (SSU) for further bitumen extraction. A bituminous froth is formed in the SSU, which is later sent to a settler, to improve its quality. The treated SSU froth is mixed with the PSV froth, heated and deareated in the froth treater. The treated froth is later diluted with naphtha to reduce the bitumen's specific gravity/viscosity. In the final step, the entrained solids and water are removed in a two-stage centrifugation process. The resulting bitumen product contains less than 0.5 % solids and 4-7 % water (mass).

In addition to water-based bitumen extraction technology, some development work has been conducted on solvent-based bitumen extraction methods. A key problem with this approach is the solvent recovery from the sand after bitumen extraction. Most of the time, large quantities of solvent are lost, through intersitial transport in the sand.

No solvent-based method is commercially used for bitumen extraction from oil sands. Most of the methods have only been developed at a conceptual stage, or at laboratory scale. More details about solvent-based processes can be found in [7].

In-situ technology was originally developed to recover heavy oil from deep underground reservoirs. However, the shared characteristics of bitumen and heavy oil favoured the application of the above technology in oil sand operations. Two main in-situ recovery technologies for oil sands exist: thermal and emulsification processes. The former involve the injection of one or combinations of the following: steam, air, or water. The latter technology involves the use of steam plus chemicals. These chemicals promote

emulsification so that the bitumen may be transported to the surface. There is almost no literature available on in-situ emulsification techniques. The bulk of the in-situ research is focused on thermal recovery techniques, as it is generally acknowledged as the best in-situ recovery technology.

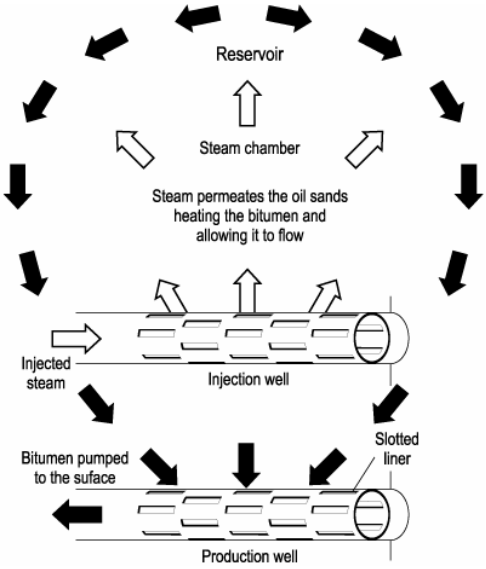

Figure 1-4. Steam Assisted Gravity Drainage (SAGD) [12]

The focus of this work is exclusively on thermal in-situ technologies, as they are the only ones that have been successful commercial application. Specifically, bitumen recovery by steam injection using Steam-Assisted Gravity Drainage (SAGD) is the technology of choice in this study. SAGD extraction involves drilling of horizontal well pairs in the reservoir. Steam injected via the upper well rises through the deposit and heats the bitumen. The hot bitumen separates from the sand and is collected along with condensed steam (water) into the lower well and is then pumped to the surface. A schematic of this process is shown in Figure 1-4.

1.1.2 Bitumen upgrading

The raw bitumen recovered from oil sand resembles a thick black tar with an extremely high specific gravity of about 9 API. This makes impossible in practice to pipeline the bitumen to refineries. One alternative is to dilute the bitumen with naphtha so that it can be transported. Alternatively, the bitumen can be processed at the oil sand site to produce a higher quality product suitable to be transported by pipeline. Such a process

is usually referred to as “upgrading” and its product is known as synthetic crude oil (SCO) or synthetic crude.

Another reason to upgrade bitumen is to remove undesirable species –sulphur, nitrogen, carbon, aromatics, vanadium and nickel – to a degree required for refinery processing. Many refineries, especially in the United States, are designed to handle conventional light and sweet crudes and are ill equipped to process heavy oils or bitumen. Thus, bitumen upgrading to SCO is required to reach these markets.

Meyers [13] provides the following summary of the key properties of bitumen that have prompted the development of upgrading technologies:

1. Extremely high viscosity at ambient temperatures which renders pipeline transportation virtually impossible without the addition of substantial quantities of diluent (natural gas condensate or naphtha).
2. Hydrogen deficiency relative to conventional light and medium-gravity crude oils.
3. Large percentage of high-boiling-point material which limits the volume of virgin transportation fuels that may be recovered by simple separation processes.
4. Substantial quantities of resins and asphaltenes which act as undesirable coke precursors in high-temperature refining operations.
5. High sulphur and/or nitrogen content, which necessitates severe hydroprocessing of the distillate fractions to produce fuels or intermediate products for refineries
6. High metals content, particularly vanadium and nickel which causes deactivation of downstream cracking catalysts

Generally speaking, bitumen upgrading technologies can be classified as: 1) coking processes and 2) hydrotreating processes. The above processes convert raw bitumen into synthetic crude oil by using heat and hydrogen as cracking agents, respectively. Traditional oil sands upgrading plants relied heavily on thermal-based coking in the past. Currently, coking technologies are supplemented by hydrocracking processes in various process configurations. These combinations result in increased liquid fraction yields, lower-sulphur products, and higher bitumen conversions to SCO.

All of the upgrading plants in existing oil sands projects follow a similar process steps sequence for SCO production. A generalised sequence is shown in Figure 1-5. In each case, bitumen is fed to a primary upgrading process in which conversion of the high-boiling range components in the bitumen occurs. Overall, the products of upgrading are:

- Hydrocarbon off-gases – single, double, and triple-bonded with 3-6 C atoms
- Cracked liquid distillates – naphtha and light and heavy gas oils
- Residue fraction – petcoke or pitch

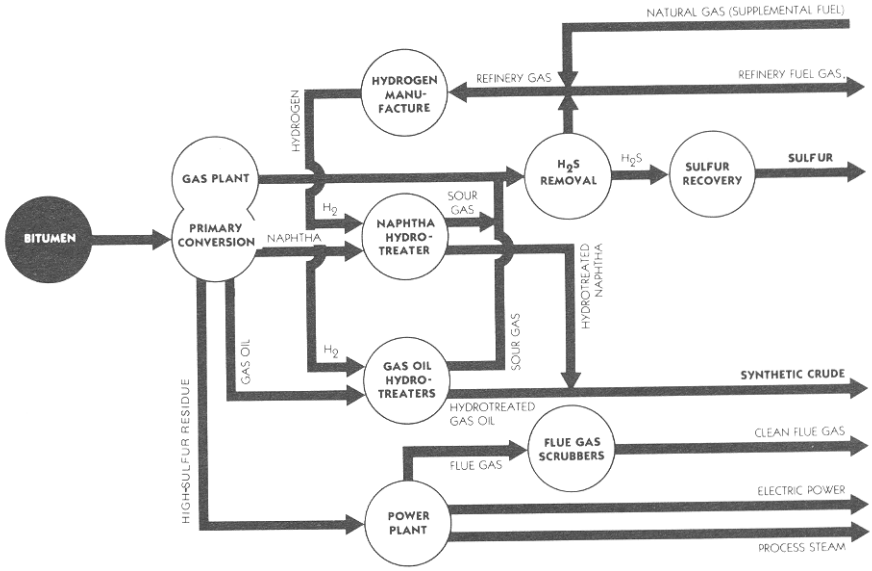

Figure 1-5. Generalized conventional bitumen upgrading sequence [13]

The liquid distillate fractions contain large concentrations of nitrogen and sulphur. These cracked liquid distillates also contain aromatic species and in the case of the naphtha fraction, substantial olefins. These distillates are therefore hydrotreated before being blended into marketable SCO. The effects of hydrotreatment are as follow:

1. Olefin and diolefin saturation to provide a stable synthetic crude
2. Sulphur and nitrogen concentration reductions to levels suitable for downstream refining to finished products
3. Limited saturation of aromatic compounds to improve the cetane number and smoke point of diesel and jet fuels
4. A shift to more naphtha and distillates through hydrocracking of the gas-oil fractions

The sour offgas from hydroprocessing is combined with the offgas from primary upgrading followed by H_2S removal and conversion to elemental sulphur. The resulting sweet gas is then available for use as fuel or as feed to hydrogen production plants.

The coke residue contains a large part of the sulphur and nitrogen and essentially all of the metals and ash. Unfortunately, the high sulphur content of this coke makes it generally unacceptable as a fuel without some form of sulphur removal – which would greatly increase operating costs.

In Alberta, some of the by-product coke is stockpiled and natural gas is typically used as the preferred refinery and boiler fuel. However, this practice is not sustainable in the long-term. Decreased natural gas production combined with steep price hikes are forecasted within the next decade, as conventional gas sources are depleted. Innovative ways to minimize coke production and maximize its utilization must be developed and implemented in oil sands refining operations.

There are six major bitumen upgrading processes that are currently used:

- Delayed coking
- Fluid coking
- Flexicoking
- LC-Fining
- The H-Oil process
- The CANMET hydrocracking process

The first three are thermal coking technologies while the rest are hydrogen-based. In this study, only delayed and fluid coking and LC-Fining are considered, as these are the technologies currently used in large-scale commercial operations in the oil sands industry in Alberta.

The delayed coking process (shown in Figure 1-6) is used at Suncor [9]. In their process, the diluted bitumen coming from extraction is first distilled to recover the naphtha and recycled back to the extraction plant. The bitumen is then preheated before entering high-temperature coking drums, where it resides for an extended period of time. Light hydrocarbons are vaporized in the coking drums and sent to a fractionating tower where they are separated into four main streams:

1. Light gases which are desulphurised and used as fuels

2. Naphtha which can be upgraded to gasoline
3. Distillate for the production of jet fuels
4. Gas-oil used as a heating fuel or for diesel production

The severe conditions inside the delayed-coker produce a significant amount of coke. The above, coupled with low conversion efficiencies are the major issues of this process.

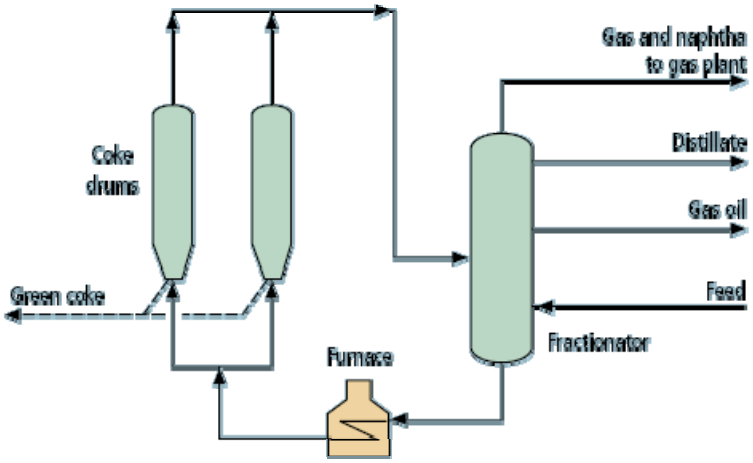

Figure 1-6. Delayed coking process flowsheet [14]

The largest bitumen fluid coking units in the world belong to Syncrude Canada Ltd. Each one of these units process more than 50,000 tons per day [7]. The process schematic of fluid coking technology is shown in Figure 1-7. Diluent-free bitumen is fed to the fluid coker. Gas streams containing butanes, naphtha, and gas-oils are generated in the coking drum along with petcoke. The gases are sent to a fractionator and are blended into SCO downstream. The petcoke generated in the reactor is burned in a separate vessel, providing all the heat for the thermal cracking reactions. Unburned coke is withdrawn from the burner and stockpiled.

The liquid fraction conversion in fluid coking is higher than in delayed coking. However, coke co-production is still an issue, although the net petcoke production of the former is lower than the latter. Coke removal and carryover are challenges in fluid coking processes and unscheduled shutdowns can occur.

The LC-Fining process is unique among hydrocracking technologies because it can handle the entrained solids in bitumen and operates at relatively low pressures. Currently, Syncrude Canada and Shell Canada employ this technology in their upgrading processes. The former is a low-conversion process (60%) while the latter can reach up to 90%

bitumen conversion rates [15]. Due to the above, LC-Fining is Shell's only primary upgrading strategy whereas the upgrading scheme of Syncrude involves fluid coking in addition to LC-Fining.

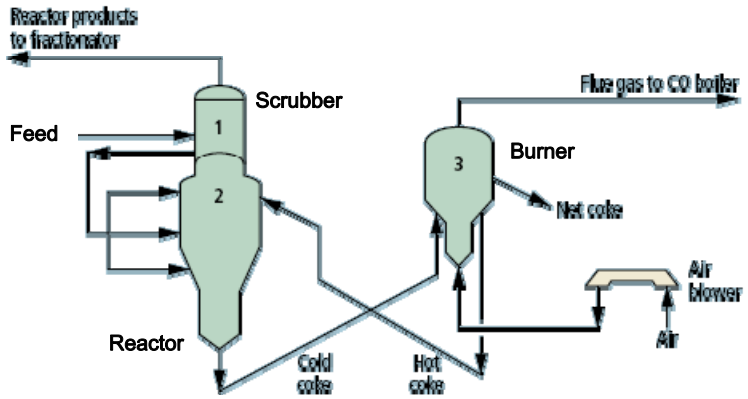

Figure 1-7. Fluid coking process flowsheet [14]

The process, which is shown in Figure 1-8, employs an expanding-bed reactor. Bitumen and hydrogen react in the presence of the catalyst, which is intermittently added and/or withdrawn to control product quality. The stream leaving the reactor is flashed in two steps to recover unreacted hydrogen before arriving at a gas fractionator. The final products include high quality distillate gases, naphtha, and gas-oil. The heavy unconverted fraction is a feed suitable for coking or solvent deasphalter.

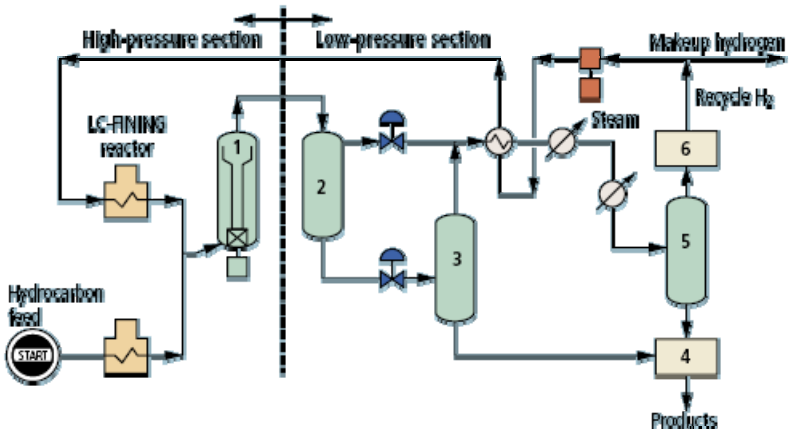

Figure 1-8. LC-Fining process flowsheet [14]

The unreacted hydrogen is recovered and purified at low pressure, before being mixed with make-up hydrogen and recycled to the reactor. This reduces capital and hydrogen production costs.

An advantage of the LC-Fining process over coking processes is that aside from the high possible bitumen-to-liquids conversion levels, deep sulphur and metal removal rates can be simultaneously achieved in the reactor. In coking processes, the recovered oil fractions require more severe hydrotreatment downstream to achieve product specifications.

1.1.3 Energy production

The extraction of bitumen and upgrading to SCO consumes vast quantities of energy. Each process stage consumes energy in different forms, as shown in Figure 1-9.

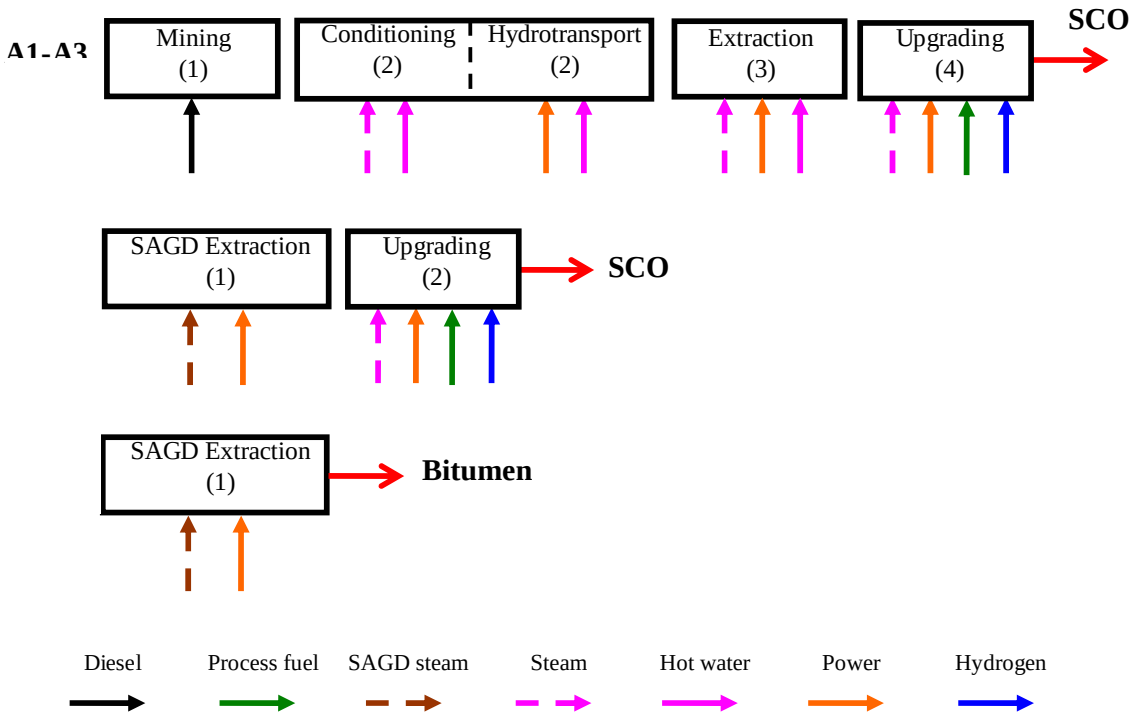

Figure 1-9. Energy consumption in oil sands operations according to process stage

Of all the energy commodities shown in Figure 1-9, steam, power, and hydrogen are produced in auxiliary units in oil sands operations. Diesel and process fuel (natural gas) are either produced internally or purchased. In this work, it is assumed that all diesel and natural gas are purchased commodities whereas steam, hot water, power, and hydrogen, are produced internally for all oil sands producers. In the following sections, power and hydrogen production processes used in this work are briefly reviewed. Boiler technology for hot water and steam generation is a comparatively undemanding process that is covered elsewhere [16] and thus, will not be reviewed in this work.

1.1.3.1 Hydrogen

Bitumen upgrading to synthetic crude consumes sizeable quantities of hydrogen. The hydrogen requirements to produce refined petroleum products from bitumen are estimated to be 5-10 times larger than those to produce the equivalent refined products from conventional crude. It is anticipated that the projected expansion in oil sands upgrading operations over the next decade will quadruple the current western Canadian hydrogen production capacity from about 500 million SCFD to approximately 2,000 million SCFD [17]. This could well place the world's largest concentration of hydrogen plants in Alberta.

Presently, the most prevalent method of hydrogen production for bitumen upgrading and refining operations in the oil sands is the steam reforming of natural gas. Figure 1-10 shows a schematic of a typical steam methane reforming (SMR) plant. The gas is first treated to remove poisons such as sulphur and chloride to maximize the life of the downstream reformer and catalysts. Steam is produced in a boiler and natural gas reacts with it over a catalyst in the reformer. The CO in the hydrogen-rich gas leaving the reformer is shifted with additional steam to produce CO_2 and more H_2 in the shift reactor. The shifted gas is treated in an amine absorption column, where bulk removal of CO_2 occurs. The clean H_2 gas is then refined in a Pressure Swing Adsorption (PSA) system, to a purity of 99.99%. The tail gas from the PSA is compressed and recycled to the reformer, where it is burned as a fuel. CO_2 and H_2 are the final products of the plant.

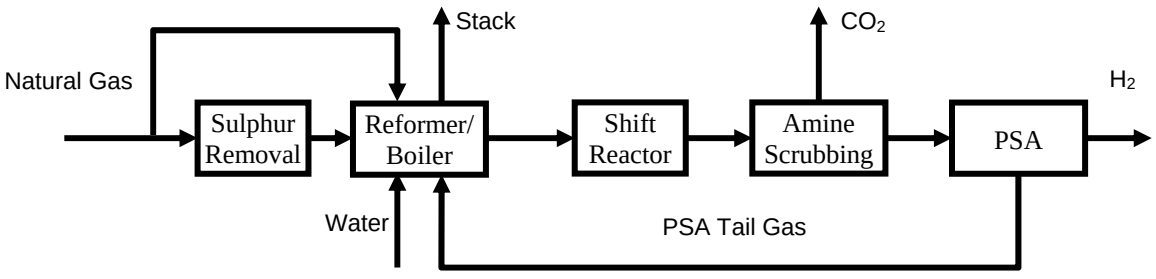

Figure 1-10. Natural gas steam reforming plant with CO_2 capture

The SMR plant in Figure 1-10 can operate in both CO_2 capture and no CO_2 capture modes. In the former, the CO_2 recovered in the amine unit is dehydrated and compressed whereas in the latter, the CO_2 is vented to the atmosphere. The SMR plants used in this study are based on techno-economic studies by Simbeck et al [18, 19].

An emerging hydrogen production technology is the gasification of hydrocarbons. Gasification in essence refers to the reaction of hydrocarbons with oxygen and steam to yield a hydrogen-rich synthetic gas. This synthetic gas (or syngas) can be used directly as fuel in a power plant or as a feed to synthesize other gaseous or liquid chemicals. Currently, about one-fifth of the hydrogen in the world is produced by this route [20].

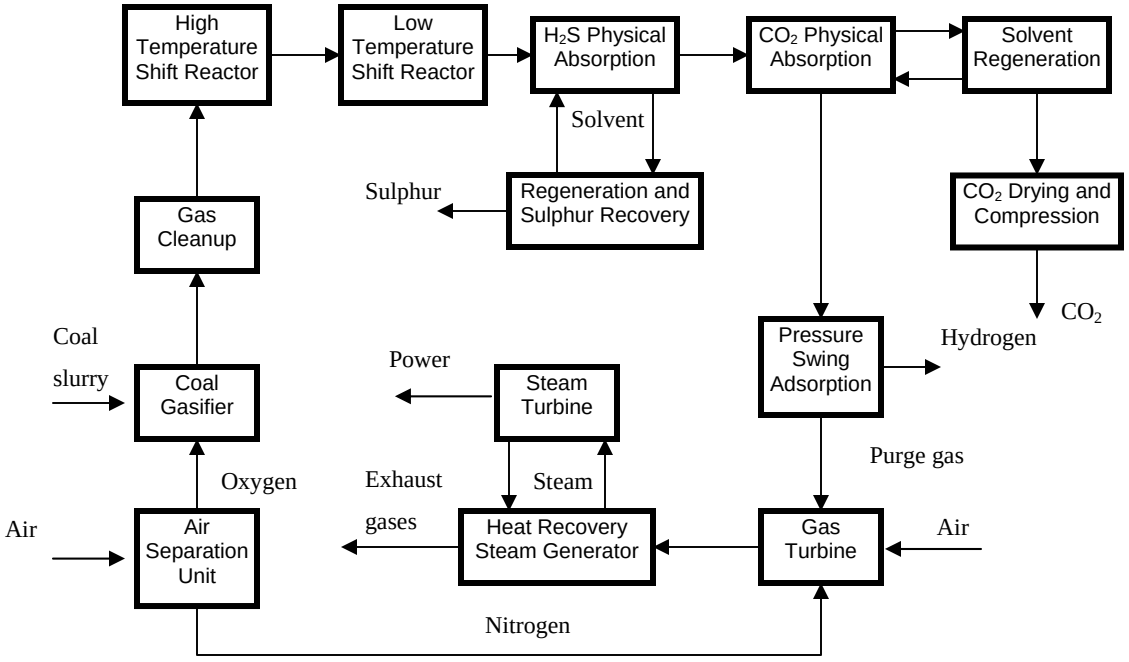

Figure 1-11. Coal gasification plant with CO_2 capture

Figure 1-11 depicts a flow diagram of a typical gasification plant using coal as a feedstock. The coal is pulverised and slurried with water before being injected to the gasifier where it reacts with steam and oxygen. The raw syngas is then cleaned of particulate matter by water quenching. The solids-free coal gas is then shifted with steam on a high/low (temperature) catalytic reaction, consisting of two reactors. The shifted gas, containing mainly hydrogen and CO_2 is cooled prior entering a physical absorption system. H_2S is removed first. Sulphur is recovered in a Claus/SCOT plant. The sulphur-free coal gas enters a CO_2 absorption system, where the bulk of the carbon dioxide is captured. When operating as a CO_2 capture hydrogen plant, the captured CO_2 is dried and compressed, and is ready for export. Otherwise, the CO_2 is removed from the syngas and vented to the atmosphere when the solvent is regenerated. The hydrogen-rich gas leaving

the CO_2 absorption system is purified in a PSA unit, thus generating hydrogen with a purity of 99.99%. The PSA purge gas is burned in a combined-cycle to generate electricity and steam for internal plant consumption.

The gasification hydrogen plants featured in this study are based on the plants described in [21, 22], an excellent report covering the performance, emissions, and costs of hydrogen production via gasification with and without CO_2 capture.

Although other techniques, such as water electrolysis, exist for hydrogen production, their limited scope of application and high cost [20] precluded their inclusion in this work. Likewise, hydrogen production via thermonuclear processes [23] although promising, is currently at the early conceptual stages of its development. The reader must note that the scope of this project is predominantly on technologies that have commercial status and thus, have the potential to be readily implemented in the oil sands industry within a two decade timeframe.

1.1.3.2 Power

The following power generation technologies are featured in this work: natural gas combined-cycle (NGCC), supercritical pulverized coal (PC), integrated gasification combined-cycle (IGCC), and oxyfuel. These power plants can have CO_2 capture and without. The former can be divided in three categories, according to CO_2 capture mode: post-combustion, pre-combustion, and oxy-combustion. The plants with post-combustion CO_2 capture in this study include NGCC and PC units. The pre-combustion plants in this study are IGCCs. The oxyfuel plants are fuelled by coal or natural gas. Schematics of the above plants and capture processes are depicted in Figure 1-12.

NGCC and PC plants are the most common types of power plants in the present. The NGCC and PC plants featured in this study are taken from [24]. PC plants burn coal in a boiler to raise steam, which drives a turbine thus generating electricity. NGCC plants burn gas in a turbine where a portion of the power is produced. The hot combustion gases exiting the turbine are then used for steam production in a heat recovery steam generator. The steam is subsequently used in a steam turbine where additional power is generated. In conventional NGCC and PC plants, the flue gases are vented to the atmosphere through stacks.

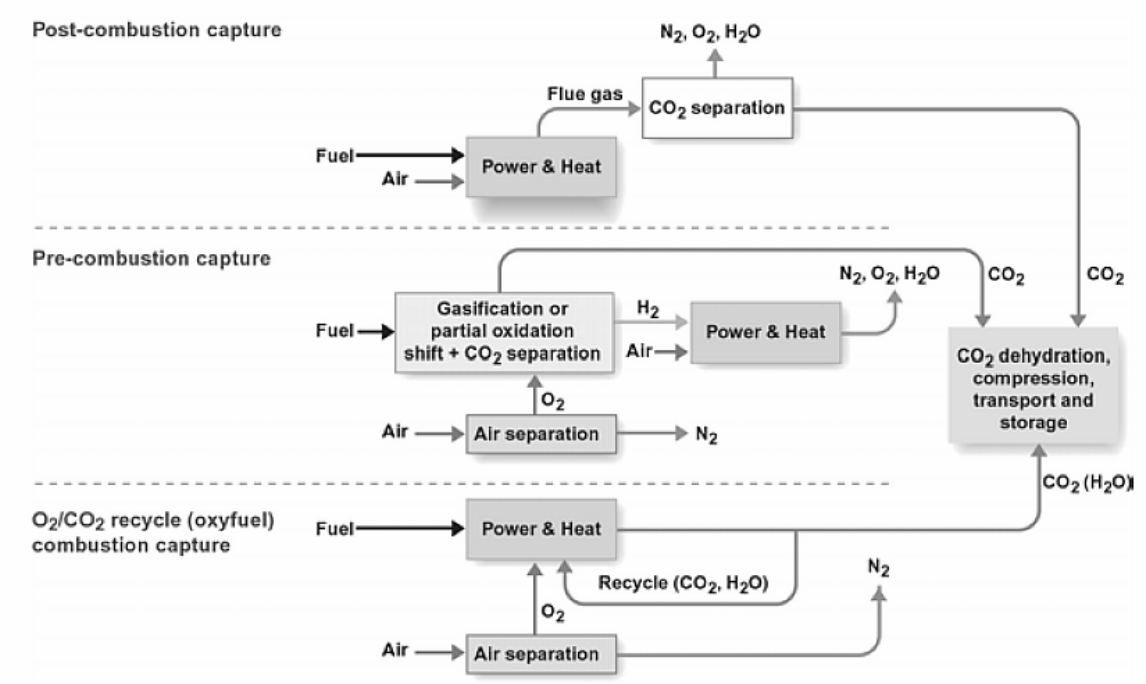

Figure 1-12. Power plants with CO_2 capture [25]

When operating in CO_2-capture mode, NGCC and PC plants employ a chemical solvent to wash the flue gas downstream of the turbine in a scrubber. The most commonly used solvent is monoethanol amine (MEA). The CO_2 dissolves in the MEA, and is then thermally recovered in a stripping column, where the solvent is regenerated. The recovered CO_2 is then dried and compressed for export. The MEA is recycled to the scrubber and the cycle is repeated.

IGCC power plants are quickly gaining popularity as they offer higher efficiencies than conventional coal-fired plants with lower overall emissions. More important, IGCC plants produce syngas streams with high CO_2 concentrations at high pressure. This reduces the overall volume of gas to be treated when CO_2 capture is contemplated, which positively impacts the costs of CO_2 removal.

A flow diagram of an IGCC power plant with and without CO_2 capture is shown in Figure 1-13. This IGCC plant operates in an almost identical way as the hydrogen production plant shown in Figure 1-11 and described earlier. When operating without CO_2 capture, the CO in the syngas is not steam-shifted after particulate removal. Hence, only H_2S is removed in the acid gas removal system and the syngas (containing H_2, CO, and $CO_{2)}$ is burned in the gas turbines. In CO_2-capture mode (represented by dotted lines)

all the CO_2 in the syngas is shifted to CO_2 yielding a syngas composed mostly of H_2 and CO_2. The CO_2 and H_2S are then removed separately in the acid gas removal unit and the hydrogen-rich syngas is burned with oxygen in a turbine for power generation.

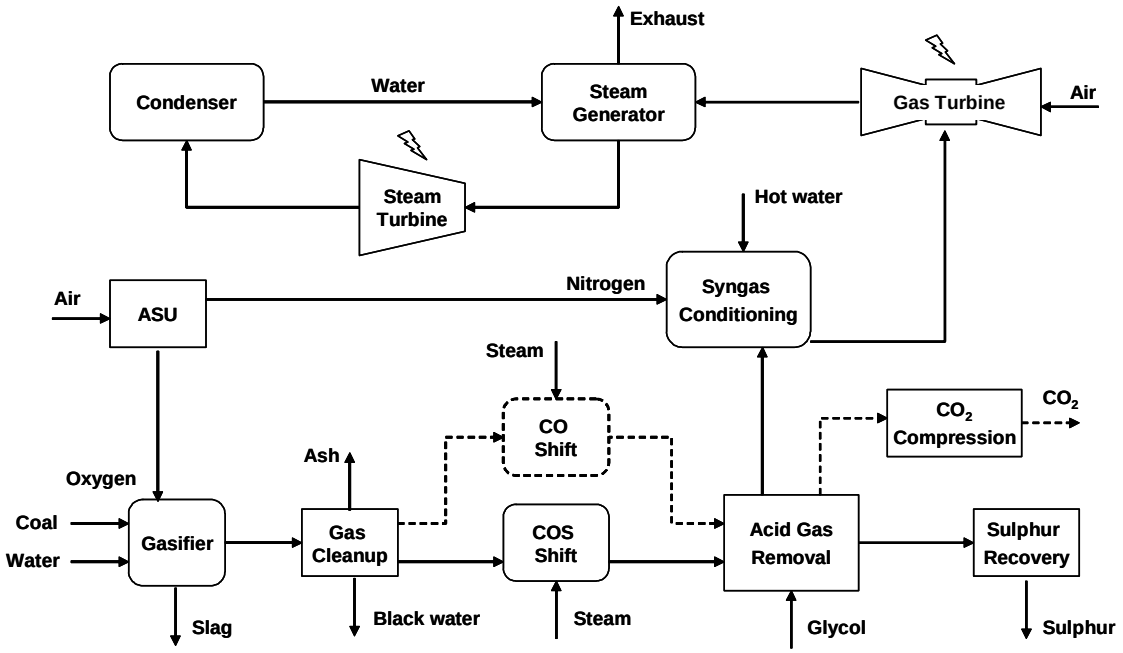

Figure 1-13. IGCC power plant with and without CO_2 capture flow diagram

The acid gas removal section of an IGCC plant typically removes CO_2 and H_2S from the syngas in a two-step process, as seen in Figure 1-13. An alternative configuration in which CO_2 and H_2S are co-captured simultaneously is possible, however. This results in the elimination of the sulphur recovery step and in a much simpler acid gas removal process, which greatly reduces the capital costs of the IGCC plant. Hence, in this work, both *separate* CO_2 and H_2S and CO_2 + H_2S *co-capture* power and H_2 plants are included.

The IGCC plants included in this project are based on a comprehensive techno-economic study of IGCC plants without CO_2 capture, with CO_2 capture, and with CO_2 and H_2S co-capture [26]. The simulation and economic evaluation of the above plants are the subject of the author's Master's thesis [27].

Oxyfuel plants, as the name suggests, burn fuel (coal or natural gas) with pure oxygen instead of air in boilers (coal-fired) or turbines (gas operation). The resulting high combustion temperatures necessitate that a portion of the flue gas be recycled back to the boiler/turbine, to moderate the temperature and prevent damage to materials. The flue gas

of this process is composed mostly of CO_2 and H_2O. Once dehydrated, the resulting stream has an elevated CO_2 purity, suitable for underground storage or other uses. If the CO_2 is utilized, the atmospheric emissions of oxyfuel plants are negligible.

In principle, any fossil feedstock can be used in oxyfuel combustion, which makes this technology attractive in refinery applications, where fuel gas and other low-value feedstocks are available [25]. In practice, however, most of the research into oxyfuel technology centres around coal and natural gas fired power plants. Consequently, in this study only the above two feedstocks are considered for the oxyfuel plants. The reference oxyfuel plants in this study are taken from [28].

1.2 Modeling and Optimization of Oil Sands Operations

The motivation for this work is based on five key facts:

1) The sustained growth of the oil sands industry in Alberta is poised to drive the energy demands in the region to unprecedented levels.
2) Most of this energy will likely have to come from fossil fuels, which exist locally and are customarily used in oil sands operations.
3) In a CO_2-constrained world, the emissions of the oil sands industry must be reduced. Otherwise, financial/environmental penalties are likely to result.
4) CO_2 capture and storage (CCS) technology, when coupled to energy production offer a viable way to mitigate emissions from oil sands operations.
5) The province of Alberta has an ideal geology for underground CO_2 storage and use in value added operations such as EOR and ECBM.

Although the above issues are reasonably-well understood individually, a clear, comprehensive approach to integrate the advantages offered by each one is currently lacking. Although the notion of using “clean” energy production technology to reduce GHG emissions is clear, a strategic way to apply them in the context of the oil sands industry is less so. Further, the uncertainty surrounding environmental legislation, fuel supply and prices, and future bitumen and SCO production levels add to the complexity of an already formidable challenge.

What is required, thus, is an optimal mechanism to apply the current knowledge of CCS and energy production technologies with an emphasis on oil sands operations in

Alberta under the assumption of a CO_2-constrained environment to achieve meaningful emissions reductions. This study proposes that the above can be accomplished by using a process systems engineering approach, making extensive use of process modelling and optimization of the oil sands operations. Ultimately, this project investigates the relationships between bitumen extraction and upgrading processes, their energy requirements, CO_2 emissions and emissions abatement, and the costs associated with energy production and CO_2 abatement. The specific objectives of this study are discussed in the next section.

1.2.1 Project objectives

The overarching object of this research is the development of mathematical models to be used as analysis and planning tools for the oil sands industry. More specifically, the models are designed to:

1) Quantify the energy demands and associated GHG emissions of bitumen extraction and upgrading.
2) Optimize the energy production on an industry-wide level in a CO_2-contrained environment by determining the "best" energy infrastructure.
3) Investigate the impacts of using CCS combined with power and hydrogen production technologies in the oil sands industry.

A chief aim of this study is to determine the magnitude and distribution of the energy demands associated with bitumen extraction and upgrading as a function of the production levels of bitumen and SCO. Likewise, establishing the magnitude and sources of CO_2 emissions due to oil sands operations is another goal of this study.

Once the energy demands for a given production level of bitumen and SCO are known, the second objective of the study is the optimization of this energy production on an industry-wide level. The optimization in this work is understood as the minimization of the costs associated with supplying all the required energy for oil sands operations, subject to specified reductions in CO_2 emissions of the fleet. The ultimate aim is to determine the number of energy-producing units and their types that fully meet the energy demands of the oil sands industry at given production levels while simultaneously

attaining target CO_2 emissions reductions. Or in other words, the development of optimal energy infrastructures to meet given CO_2 emissions constraints in the oil sands industry.

The third and final objective of this research is the quantification of financial and environmental impacts that result when the optimal energy infrastructure (or a user-specified infrastructure) is used in the oil sands industry. The above impacts are clearly manifested by changes in the costs of energy production and in the CO_2 emissions of the industry. In practical terms, however, they are measured as unitary energy costs (in $/bbl) and CO_2 emissions intensities (in tonne CO_2/bbl) of either bitumen or SCO in this study.

1.2.2 Study overview

This work is divided in the following five major sections, which also correspond to individual manuscript chapters:

The Oil Sands Operations Model – Chapter 2. This section describes the functionality and features of the OSOM. This model is used to study the energy demands of bitumen extraction and upgrading processes used in the oil sands industry. The OSOM comprises two distinct situations, namely: the base case and the future production scenarios. The former case represents the manner of operations of the oil sands industry in the base year of 2003. The future production scenarios are the energy demands of the oil sands industry in the years of 2012 and 2030 estimated by the OSOM and are used as inputs to the optimization model.

The GAMS Optimization Model – Chapter 3. The development of the optimization model used to generate optimal energy infrastructures for the years 2012 and 2030 is the subject of this chapter. This section contains details concerning the objective function, constraints, balances, and other relevant equations used in the optimizer.

Results and Discussion – Chapter 4. In this section, an extensive array of model results are presented and discussed. Sections 4.1 and 4.2 cover the OSOM base case and future production scenarios respectively. The energy demands and emissions (base case only) of bitumen and SCO production are presented, for different bitumen upgrading technologies. The remainder of the chapter features the recommended optimal energy infrastructures for the years 2012 and 2030 and their associated costs and CO_2 emissions.

Sensitivity Analyses – Chapter 5. This work includes sensitivity studies for both the OSOM and GAMS models. The sensitivities of the model outputs to a comprehensive set of process variables and model parameters are presented in this section. The variables are hydrogen and power demands. The process parameters analysed include: IGCC plant availability, steam boiler thermal efficiency, CO_2 pipeline length. Economic parameters include: fuel prices, annual capital charge rates, plant overnight capital costs, and CO_2 transport and storage costs.

Conclusions and Recommendations – Chapter 6. The most relevant conclusions from the project are presented in this section, along with suggested areas for future development of this work.

1.2.3 Research outcomes

The main contribution of this project is the development of the OSOM and GAMS optimization models. These models serve as flexible tools to generate and evaluate alternative energy production scenarios and CO_2 reduction strategies, among other possible analyses, quickly and inexpensively.

Another key contribution of this project is the development of optimal energy infrastructures for forecasted bitumen and SCO production levels in the years 2012 and 2030. The energy infrastructures featured in this work meet the energy demands of the oil sands industry at minimal cost while attaining substantial CO_2 emissions reductions. Also, the optimal infrastructures serve as an indication of which power and H_2 production technologies are most promising in the future, for varying CO_2 reduction levels.

The results of this work quantify the financial and environmental impacts of implementing the optimal energy infrastructures in the oil sands industry. The changes in the cost of energy production and CO_2 emissions per barrel of product are obtained from the optimization model for a range of possible CO_2 reduction levels. Thus, this model answers the question: *How much would it cost to reduce the CO_2 emissions associated with energy use in the oil sands industry by x percent?*

Finally, this research makes it possible to determine the maximum possible CO_2 reductions attainable by implementing CCS in hydrogen and power generation in the oil sands industry, on the basis of (but not limited to) current plant designs.

Chapter 2

The Oil Sands Operations Model

This chapter introduces a mathematical model of the energy demands and GHG emissions associated with current and future operations of the oil sands industry in Alberta. The model is based on plant- and process-specific data for bitumen extraction and upgrading to SCO. This industry-wide model, called the Oil Sands Operations Model (OSOM), quantifies the demands for power, H_2, steam, hot water, natural gas, and diesel fuel of the oil sands industry for given production levels of SCO and bitumen. Alongside the demands, the model estimates the resulting CO_2 emissions and CO_2 emissions intensity of SCO and bitumen production, using current energy-production technologies.

The OSOM comprises two scenarios: the base case and a future production scenario. The former represents the mode of operation of the oil sands industry in Alberta in 2003. In the latter case, the energy demands of SCO and bitumen production are computed for aggregate production estimates for the years 2012 and 2030. These estimates are taken from the *Oil Sands Technology Roadmap* [10] which outlines a future vision for the oil sands industry in Canada.

2.1 Features

Bitumen can be extracted by surface or in-situ techniques. Surface techniques involve mining the oil sands and separating the bitumen by using the hot-water process [13]. In-situ techniques involve injecting an external agent in the underground reservoir thus forcing the bitumen (and other substances) out of the basin. Steam-Assisted Gravity Drainage (SAGD), which uses steam to extract bitumen from oil sands, is currently the prevalent in-situ technology in the oil sands industry and is thus the technology of choice for the OSOM.

The bitumen produced by mining or in-situ methods can be upgraded to SCO or diluted with naphtha solvent before being sold to refineries. To reflect such variety of commercial oil sands operations in Alberta, the OSOM includes the following products:

A) Mined bitumen, upgraded to SCO

B) SAGD bitumen, upgraded to SCO

C) SAGD bitumen, diluted

Likewise, several technologies are employed in the upgrading process. In the OSOM, the following three are considered for all mass and energy balances:

1) LC-Fining (LCF) + Fluid coking (FC) + Hydrotreatment (HT) - Syncrude
2) Delayed coking (DC) + Hydrotreatment - Suncor
3) LC-Fining + Hydrotreatment – Shell-Albian Sands

The above bitumen upgrading schemes correspond to the three leading oil sands operators which currently extract and upgrade bitumen commercially to SCO in the Athabasca region [29]. The OSOM is based on published information for upgrading processes 1-3 as well as plant-specific data, where available.

The oil sands producers included in the OSOM, grouped by bitumen extraction technology and upgrading scheme are shown in Table 2-1. This table also shows each producer's aggregate production estimate for this study.

Table 2-1. Aggregate production estimates for all OSOM producers

Producer	Description	Daily barrels (1000 bbl/d)		
		2003*	2012	2030
A1	Mined bitumen upgraded by LCF+FC+HT	231	400	800
A2	Mined bitumen upgraded by DC+HT	213	325	650
A3	Mined bitumen upgraded by LCF+HT	94	250	550
A	Total mined SCO production	538	975	2,000
B1	SAGD bitumen upgraded by LCF+FC+HT	0	125	400
B2	SAGD bitumen upgraded by DC+HT	0	150	600
B3	SAGD bitumen upgraded by LCF+HT	0	250	1000
B	Total SAGD SCO production	0	525	2,000
A+B	Total SCO production	538	1,500	4,000
C	Total SAGD diluted bitumen production	350	500	1,000

* Base year

SCO production from mined bitumen (producers A1-A3) is accomplished in four stages: 1) Mining, 2) Conditioning/Hydrotransport, 3) Extraction, and 4) Upgrading. In stage 1, the oil sand is mined out of the ground by hydraulic shovels and transported by truck to the next process stage. In stage 2, the sand is mixed with hot water and chemicals and agitated to separate the bitumen from the sand. In stage 3, the resulting slurry is washed with hot water in separation cells, in which air and steam addition cause the bitumen to rise to the surface. The bitumen froth is then mechanically separated from the mostly-water and sand slurry, deaerated and diluted with naphtha. The diluted bitumen is then centrifuged to remove traces of sand and water and is then ready for upgrading. In stage 4, the naphtha solvent is distilled from the bitumen and sent back to stage 3. The bitumen is then processed in a vacuum distillation unit where the lighter oil fractions are recovered. The bottoms are then cracked either thermally or by hydrogen addition processes or by a combination of both. The resulting products include naphtha, light and heavy gas oils, and petroleum coke, depending on the cracking method. Finally, all the oil fractions are sent to hydrotreaters in which sulphur and nitrogen compounds are removed by hydrogen addition. The treated fractions are blended together into a SCO, with a high API number and low sulphur content.

The production of SCO from SAGD bitumen (producers B1-B3) involves two stages: 1) In-situ extraction and 2) Upgrading. In stage 1, steam is injected into the underground bitumen reservoir through an injection well. The heated bitumen alongside condensates and solution gas is collected in a second well (parallel to the injection well) and pumped out of the reservoir. Once condensate and solution gas have been removed from the bitumen, diluent naphtha is added, and the diluted bitumen is sent to upgrading. Stage 2 for producers B1-B3 is much the same as stage 4 for producers A1-A3, as the upgrading schemes considered in this study are the same.

The production of bitumen via SAGD (producers C) only involves stage 1 as described above for producers B1-B3.

The OSOM calculates the mass and energy balances of each of the above process stages for producers A1-A3, B1-B3, and C. The CO_2 emissions associated with SCO and bitumen production are calculated in the OSOM by determining each stage's net demand for a variety of fossil fuel-intensive inputs, as shown in Figure 2-1. In the base case alone,

each one of these "energy commodities" is produced in specific plants or units, which are modelled in the OSOM, based on their real world counterparts. For instance; all of the H_2 required for bitumen upgrading for producer A2 is produced in natural gas steam reforming plants. The OSOM will calculate the amount of natural gas required to produce the H_2 and also the associated CO_2 emissions, among other pertinent model outputs. Likewise, the demands for all of the other commodities are computed, along with their corresponding fossil feedstock/fuels consumption and resulting CO_2 emissions. The OSOM base case results hence include the CO_2 emissions per process stage, per SCO producer, as well as their CO_2 intensity. The CO_2 intensity is defined as the amount of CO_2/GHG emitted per unit of SCO or bitumen produced (given in tonnes of CO_2 eq./bbl).

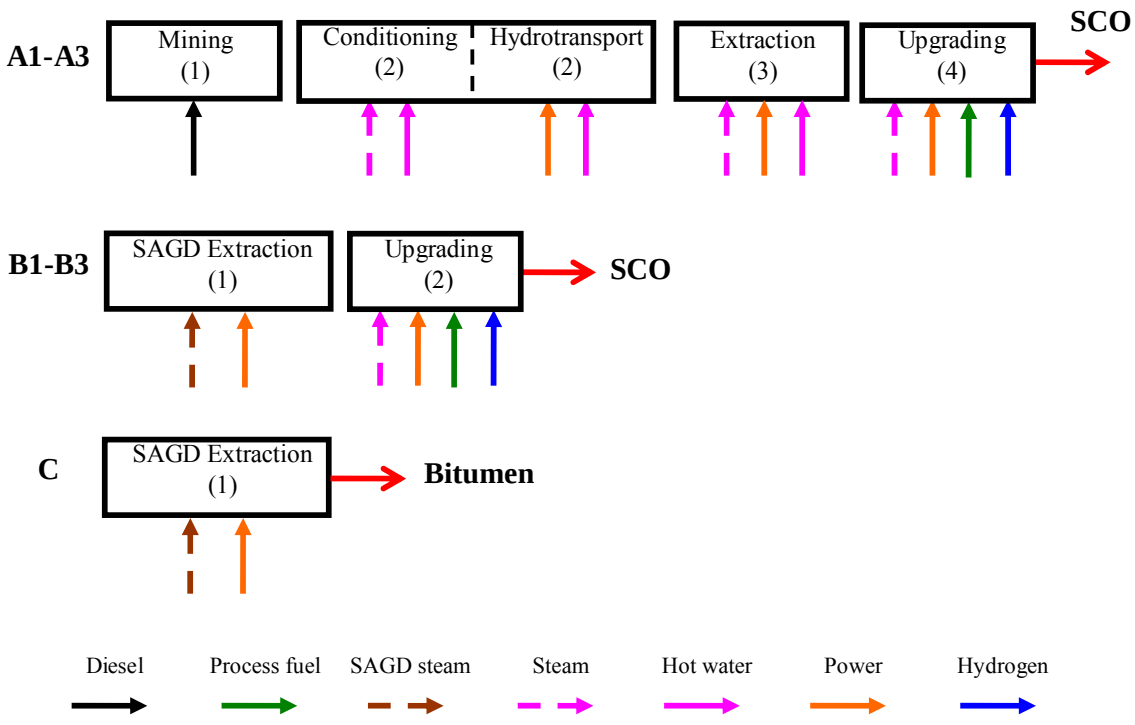

Figure 2-1. Energy commodities/inputs to OSOM process stages for producers A1-A3, B1-B3, and C

2.2 Base Case

In the OSOM, the base case (OSOM-BC) represents the SCO and bitumen production operations in Alberta in 2003. This year was selected because it conforms to the Oil Sands Technology Roadmap production estimates [10] and also because sufficient SCO and bitumen production data for that year were readily available [29]. For the former reason, all energy production operations are based on conventional technologies

and no CO_2 capture is considered in this case. Consequently, natural gas (NG) and steam methane reforming (SMR) are the fuel and technology of choice for H_2 production, respectively. All the steam and hot water are produced in natural gas-fired boilers (SB and SSB). The steam produced in SB boilers is used in mining-based SCO production and in bitumen upgrading processes, whereas the steam produced in SSB boilers is destined for SAGD bitumen extraction alone. NG is also employed for power generation in combined-cycle (NGCC) plants and as process fuel in upgrading. The resulting superstructure for the base case is shown in Figure 2-2.

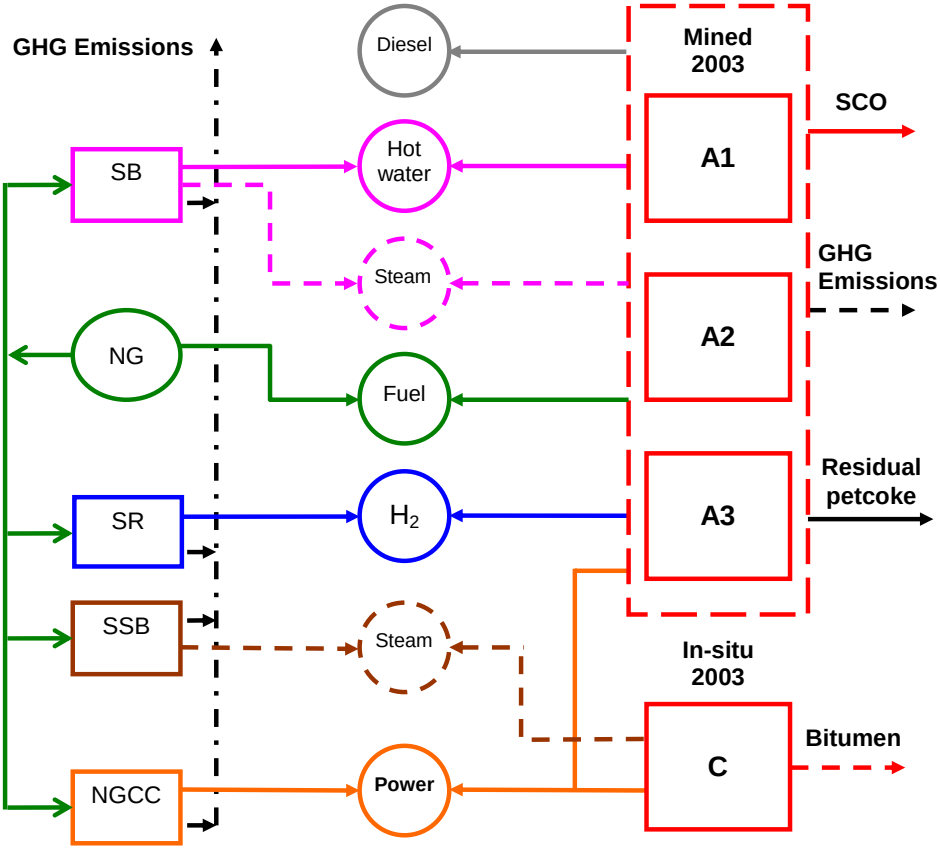

Figure 2-2 OSOM-BC superstructure

The right side of the OSOM-BC superstructure represents the energy demand side. The large boxes correspond to bitumen and SCO producers, which require certain amounts of each one of the seven energy commodities symbolized by circles in Figure 2-2. These commodities are produced in the units shown on the left side, which together represent the supply side. The OSOM-BC determines the energy demands of producers A1-A3 and C, based on historical (2003) oil sands mining and bitumen extraction rates

and mass/energy balances particular to each producer. The model then computes feedstock consumption as well as associated CO_2 emissions on the supply side, based on mass and energy balances for all energy-producing units. The model follows the constraint that the total energy supply must equal the total energy demands, to ensure that mass/energy balances on both demand and supply sides are realized.

On the demand side, each SCO and bitumen producer requires different energy inputs depending on that particular producer's *modus operandi*. For instance, producer A2 uses surface mining to extract bitumen from the sand and upgrades it by delayed coking followed by hydrodesulphurisation. On the other hand, producer C uses SAGD technology to extract bitumen from underground reservoirs and dilutes it with naphtha – without upgrading it. In the OSOM, oil producers are characterised by the technologies they use to extract and upgrade bitumen and thus, their operations are considered to take in place in distinct process stages. These stages, for modelling purposes, are defined based on the operations of actual oil sands producers, as shown in Figure 2-3.

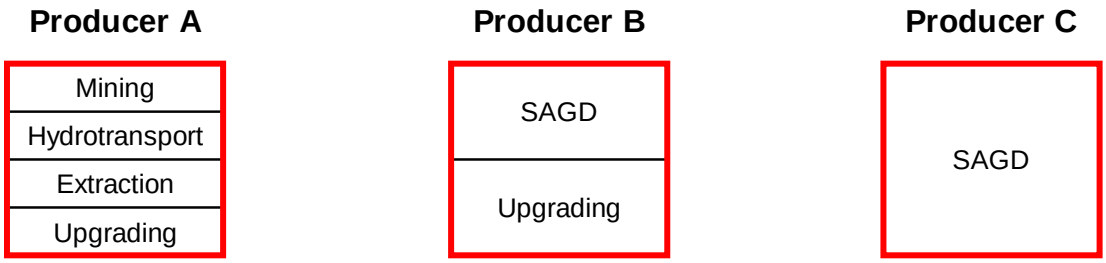

Figure 2-3 OSOM assumed process/modelling stages per bitumen/SCO producer

The modelling task is greatly facilitated by partitioning the operations of all producers into stages. An important approach for modelling these stages is that only the energy inputs specified in Figure 2-1 are considered in the OSOM. This implies that, for example, the presence of additives in the bitumen hydrotransport or extraction stages (producers A1-A3) is excluded from the mass balances for these stages. Only bitumen, hot water, steam, and power are included in such balances. The goal of the model is to quantify energy requirements and CO_2 emissions associated with SCO/bitumen production. Hence, substances/processes that neither consume energy nor cause GHG emissions are not modelled in the OSOM. Nevertheless, substance handling and

processing, if it involves energy consumption, is accounted for in the OSOM (e.g., power required to mix additives or to pump the bitumen slurry in mining operations).

2.2.1 Mining

The energy demands in this stage consist solely of diesel fuel for shovels and trucks, which are used to mine the oil sands. In the OSOM-BC, historical data of oil sands mining rates as well as the oil sand's bitumen saturation, taken from [29] are used to calculate the fuel demands of the above units.

A hypothetical fleet consisting of a variety of diesel-powered mechanical shovels and trucks is shown in Table 2-2. This fleet includes several commercial shovel and truck models, all of which have different mining capacities and varying mechanical specifications. These specifications were taken from each unit's product brochure available on their respective manufacturer's website. In the OSOM-BC, the type and number of units in service was specified to yield an oil sands mining fleet which is generic enough to adequately represent the performance of a real mining fleet, such as the ones used by Syncrude or Suncor [8, 9].

Table 2-2. OSOM-BC reference mining shovel and truck fleet

Type	Model	Units	Engine	Capacity (tonnes)*	Net power (kW)	Fuel consumption (l/h)
Shovel	LeTourneau-L2350	4	Cummins QSK 60	72	1,715	375
Shovel	CAT-994D	2	CAT 3516B EUI	63	1,011	248
Shovel	LeTourneau-1850	1	Cummins QSK 60	45	1,492	330
Shovel	Terex-RH400	4	2 Cummins QSK 60C	85	3,280	740
Truck	CAT-793C XQ	20	CAT 3516B HD EUI	218	1,611	406
Truck	Komatsu-930E	11	Komatsu SSDA16V160	290	1,902	447
Truck	Terex-MT5500B	6	Cummins QSK 78	327	2,445	580
Truck	CAT-797B	4	2 CAT 3512B	345	2,513	579
Truck	Liebherr-T282B	2	Cummins QSK 78	363	2,445	580

* Assumed oil sand density of 2.095 tonnes/banked cubic metre [30]

In the mining stage, the OSOM-BC determines the shovels' and trucks' mining rates based on their specified volumetric/mass capacities. The total reference mining fleet's

fuel consumption (D) is then calculated, based on each unit's specified engine and individual fuel consumption (f) values as shown in the following equations:

$$D_t = \sum_t f_t N_t \tag{2-1}$$

$$\mathrm{D_s} = \sum_s \mathrm{f_s N_s} \tag{2-2}$$

Where N_t and N_s, are the number of trucks and shovels in the reference fleet, respectively. Individual truck and shovel utilization for each producer in the OSOM-BC are calculated based on the producers' mining rates. The fuel demands of shovel and trucks corresponding to the calculated mining rates are then determined by calculating a shovel and truck utilization factor (uf) for each producer with respect to the reference mining fleet.

$$D_{P_i} = uf_{t,P_i} D_t + uf_{s,P_i} D_s \tag{2-3}$$

While the utilization factors are defined as:

$$uf_{t,P_i} = \frac{OS_{P_i}}{OS_{t,ref}} \tag{2-4}$$

$$uf_{s,P_i} = \frac{OS_{P_i}}{OS_{s,ref}} \tag{2-5}$$

OS is the oil sand mining rate of each producer and OS_{ref} is the mining rate of shovels/trucks of the reference fleet. Aside from diesel demands, the oil sand composition for each producer is determined on the basis of the specified oil sand mining rate and its bitumen saturation. The reason for this is that individual mass flows of sand and bitumen are required in the mass balance of downstream stages in the OSOM-BC.

2.2.2 Hydrotransport

In this stage, the mined oil sand is slurried with hot water and pumped to the extraction stage. Hence, energy demands calculated by the OSOM-BC model include hot water and power. The slurry has an assumed solids content (SCS) of 70 % (mass) [13, 30]. The water temperature is 35°C [30]. The hot water demands (W) per producer based on the above parameters are given by:

$$W_{H,P_i} = \frac{OS_{P_i}(1-SCS)}{SCS} \tag{2-6}$$

The power requirements for pumping bitumen slurry were determined by simulating the pumping of slurries of oil sands with different bitumen saturations in Aspen Plus. The resulting power demands were plotted as a function of bitumen saturation and head requirements. The following empirical pumping power factor (PF) was thus obtained, which is used in the OSOM to calculate the power demands for pumping bitumen slurries of varying qualities.

$$PF_{H,P_i} = 0.026x_{P_i} + 0.0007 \tag{2-7}$$

Where x is the bitumen content of the oil sand. The power demands (P) for each producer are calculated based on the total slurry produced and user-supplied head values (h) according to:

$$P_{H,P_i} = PF_{H,P_i}(W_{H,P_i} + OS_{P_i})h_{P_i} \tag{2-8}$$

2.2.3 Bitumen extraction

All producers in the OSOM-BC use the 2-stage hot water process (HWP) for bitumen extraction, as outlined in [13] and shown in Figure 2-4. In primary extraction, bitumen is separated from the oil sand slurry as froth, using hot water and steam. In secondary extraction, the bitumen froth is diluted with naphtha and centrifuged to remove traces of sand and water.

Energy demands of this process include hot water, steam, and power. The OSOM-BC determines hot (wash) water demands based on the mass balances presented in [13] for each producer according to:

$$W_{E,P_i} = OS_{P_i} WWE \tag{2-9}$$

Where $W_{E,Pi}$ is the hot water demand for producer i in the extraction stage and WWE is a model parameter that represents the wash water requirements for primary extraction. The composition of bitumen froth produced in primary extraction is determined using the following empirical correlations:

$$BF_{P_i} = 2.75x_{P_i} + 0.6 \tag{2-10}$$

$$WF_{P_i} = 0.6738x_{P_i} + 0.0204 \quad (2\text{-}11)$$

Where BF and WF are the bitumen and the water mass fraction of the froth, respectively and x is the mass percentage of bitumen in the oil sand. Equations (2-10) and (2-11) are empirical models, derived from mass balances for oil sands with different bitumen saturations, presented in [13]. The bitumen froth (FR) produced in primary extraction is given by the expression:

$$FR_{P_i} = WF_{P_i}(W_{E,P_i} + W_{H,P_i}) + BF_{P_i}OS_{P_i}x_{P_i} + OS_{P_i}(1 - x_{P_i})SF \quad (2\text{-}12)$$

Where SF is the sand content of primary froth, a model parameter.

Aside from determining the amount of froth produced and its composition, the OSOM-BC also calculates the percentage bitumen recovery in primary extraction as well as the quantity of primary tailings produced. The tailings are mostly composed of sand and water, with traces of bitumen. These tailings are treated for additional bitumen recovery prior being pumped (together with secondary tailings) to storage ponds.

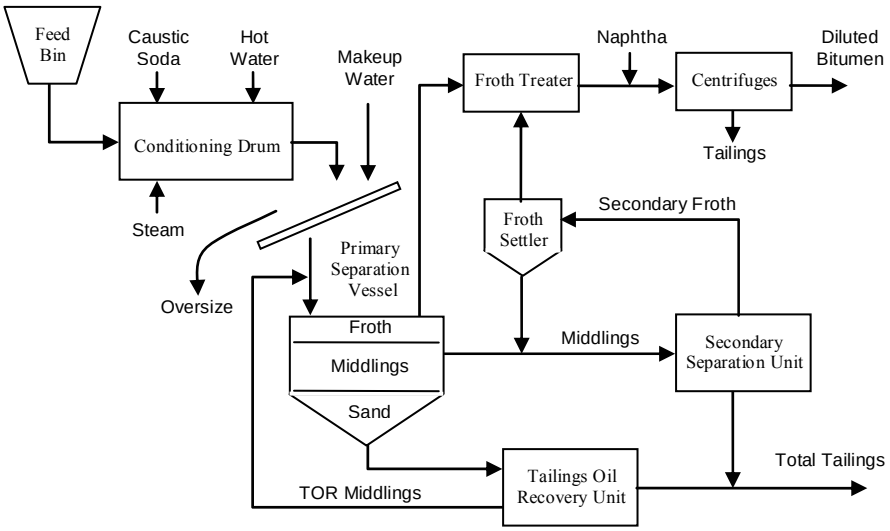

Figure 2-4 Hot water process flowchart

In secondary extraction, the OSOM-BC calculates naphtha diluent requirements and steam demands (S) according to mass balances from [13]. The steam demands are a function of the bitumen froth.

$$S_{E,P_i} = FR_{P_i}SSE \quad (2\text{-}13)$$

Where SSE is a model parameter required to compute steam requirements in bitumen extraction. The overall power demands (P) in this stage comprise of the power required to pump tailings to disposal (PTA) and the power for diluted bitumen centrifugation (PC):

$$P_{E,P_i} = PTA_{P_i} + PC_{P_i} \quad (2\text{-}14)$$

Similarly to the hydrotransport stage, the power requirements for tailings transport were determined by simulating the pumping of oil sands tailings with varying bitumen saturations in Aspen Plus. The following empirical equation was thus obtained:

$$TP_{P_i} = 0.001x_{P_i} + 0.0013 \quad (2\text{-}15)$$

Where TP is the pumping power factor and x is the bitumen content of the oil sand. The power demands for each producer are calculated based on their pumping power factor as calculated above and their overall tailing production and user-supplied head values.

The power demands for diluted bitumen centrifugation (2 stages) are calculated based on the specifications of an Alpha Laval CH-36B centrifuge [31], which is a machine suitable for mining applications. The model calculates the secondary tailings production as well as the composition of the centrifuged diluted bitumen, together with the overall bitumen recovery in the extraction stage. The diluted bitumen product can either be sold to refineries, or upgraded to SCO, as is the case with producers A in the OSOM.

2.2.4 SAGD extraction

The thermal extraction of bitumen by in-situ methods in the OSOM is modelled according to the data corresponding to Opti-Nexen's Long Lake project, [32]. The main energy demands calculated by the OSOM are steam and electricity. The steam raised for SAGD extraction has a quality of 80% and a pressure of 8000 kPa. After separation, the resulting saturated steam is injected underground at a SOR (Steam-to-Oil Ratio) of 2.4 [32], which is a typical value of an economically viable SAGD operation.

The OSOM-BC uses mass and energy data from the aforementioned source to compute the steam demands of producers B-C, as well as the amount of solution gas produced and the power demands for SAGD extraction. The solution gas is assumed to

be burned in the steam boilers, thus the amount of natural gas required for SAGD steam production is lowered accordingly in all calculations.

$$SS_{P_i} = B_{P_i} SOR \tag{2-16}$$

$$PS_{P_i} = B_{P_i} ERS \tag{2-17}$$

$$SG_{P_i} = B_{P_i} SOL \tag{2-18}$$

Where SS and PS are the steam and power demands per producer and SG is the solution gas produced during bitumen extraction. B is the bitumen production rate from SAGD operations.

2.2.5 Bitumen upgrading

The diluted bitumen from mining and/or thermal operations is upgraded to SCO in the upgrading stage. The modelling of this stage is complex, as it encompasses three possible upgrading routes for bitumen, which are shown in Figure 2-5.

Energy consumption in this stage is significant. The upgrading of bitumen to SCO requires vast amounts of hydrogen, steam, and power. Additionally, certain upgrading technologies also consume process fuel for heating. The OSOM-BC calculates energy demands for each one of the upgrading schemes shown in Figure 2-5, based on their individual amounts of bitumen processed.

The first step in the upgrading process is the recovery of naphtha solvent in a distillation column. The recovered naphtha is sent back to the bitumen extraction stage. The OSOM-BC computes the steam requirements for the diluent recovery unit (DRU), based on mass and energy balances obtained from an ASPEN Plus model of the DRU.

The products from the DRU are naphtha, light gas-oil (LGO) and atmospheric-topped bitumen (ATB). The LGO is sent to an LGO hydrotreater for sulphur and nitrogen removal. The ATB can either be sent to the Vacuum distillation unit (VDU) or split its flow between the VDU and the LC-Finer. In the latter case, the user can specify an ATB flow split fraction between 0-1, which is done only for upgrading scheme 1 in the base case. In upgrading scheme 2, all of the ATB is channelled to the Delayed coker, since this unit is specified as a “bottom of the barrel” process.

The VDU was modelled in Aspen Plus, based on the fractional yields presented in [38]. The OSOM-BC calculates heat requirements (in MJ/tonne feed) in the VDU and expresses them in terms of steam demands (tonnes steam/h) and also calculates LGO and HGO (heavy gas-oil) produced in the VDU. The bottoms of the VDU, called vacuum-topped bitumen (VTB) together with any ATB from the DRU are then sent to the LC-Finer (producers A-B 1) or to the Delayed coker (producers A-B 2) while the LGO and HGO proceed to hydrotreatment for further processing.

The LC-Finers in the OSOM use hydrogen to convert the feed (ATB and/or VTB) into LGO, HGO, and naphtha products. The LC-Finer in upgrading scheme 1 has a lower liquid yield that that of scheme 3 (60% vs. 90%). The specifications for the former LC-Finer were taken from [33], [34], and [35]. The high-conversion LC-Finer was modelled based on data from [13] and [36]. In addition to hydrogen demands, the OSOM-BC calculates total electricity and fuel demands, which are modelled based on the specifications found in [14].

The product streams from the LC-Finer (LGO, HGO, and naphtha) are sent to hydrotreatment. Some fuel gas is also generated in this unit. In the OSOM, this fuel gas is collected and after scrubbing with MEA (mono-ethanolamine), it can be used in the hydrogen plant as fuel (optional). Finally, the bottoms of the low-conversion LC-Finer are sent to the Fluid coker (A-B 1). In the case of the high conversion LC-Finer (A-B 3), the residuum is considered to be a saleable by-product and is not further processed.

The cokers in the OSOM process the bottoms of upstream units, yielding further LGO, HGO, and naphtha together with petroleum coke and sour coker gas by-products. Although the delayed coker consumes a fraction of the total petcoke for fuel, total petcoke production from the cokers is substantial. In the OSOM-BC, just as in most real-world operations, the petcoke by-product is not used for energy production, due to its high sulphur and metals content. This petcoke is stockpiled until a better use can be found for it. The sour coker gas, similarly to the LC-Finer fuel gas, is treated with MEA and can be used as fuel in the hydrogen plants in the model (optional).

The fluid coker in the OSOM is modelled based on yield data from [33] and [34]. The energy demands for steam, power, and process fuel were taken from [13]. The modelling

data for the delayed coker includes yields from [37] and energy demands (electricity/process fuel) found in [14].

The last step in the upgrading process is the hydrodesulphurisation of the oil fractions. In the OSOM, this is accomplished in individual hydrotreaters for LGO, HGO, and naphtha. The flows of the above fractions from all units upstream of the hydrotreaters are fed to their corresponding hydrotreater.

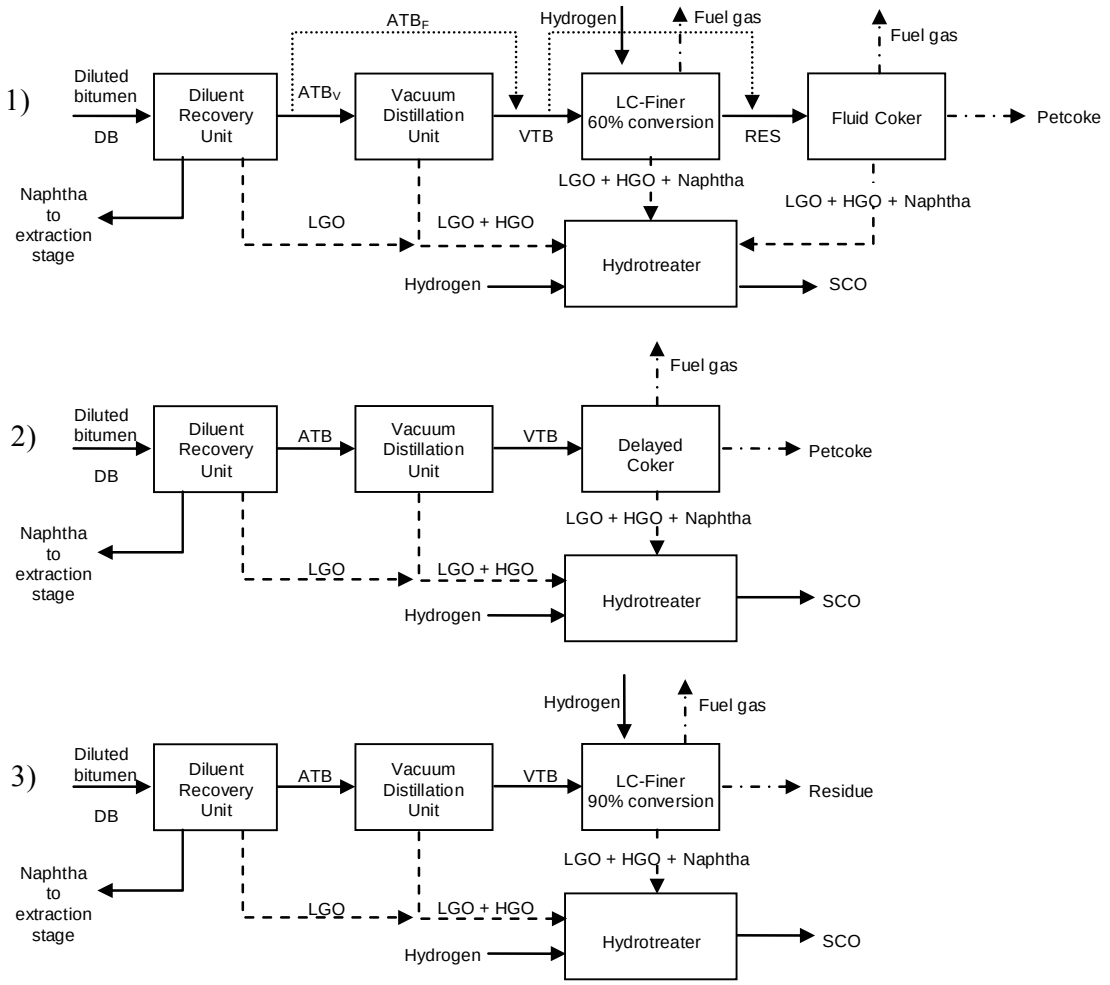

Figure 2-5. OSOM bitumen upgrading schemes for producers A1-A3 and B1-B3

The hydrogen demands for hydrotreatment in the model are calculated based on yield data presented in [33]. Additional density data for the oil fractions is taken from [38]. After hydrotreatment, the treated fractions are blended together into SCO. The properties of the SCO, such as composition and density (which are a function of the upgrading

scheme used) are calculated by the model, together with the overall bitumen conversion to SCO.

The sulphurous gas removed from the fractions in the hydrotreaters is sent to the MEA plant for treatment. The OSOM-BC computes the elemental sulphur production as well as atmospheric SO_2 emissions, based on the sulphur content of the acid gas and specified sulphur removal levels in the MEA scrubber. Aside from the sulphur balance, the model calculates the total sweet fuel gas (from LC-Finer and coker gases) that is available for use as fuel in the hydrogen plants (optional).

The breakdown of the energy demands of the upgrading stage per unit is shown in Table 2-3 for each of the upgrading processes used in this study.

Table 2-3. Energy demands distribution for upgrading schemes 1-3

Commodity	Units	1	2	3
Power	kW	LC-Finer Fluid coker	Delayed coker	LC-Finer
Hydrogen	tonne/h	LC-Finer Hydrotreater	Hydrotreater	LC-Finer Hydrotreater
Steam	tonne/h	DRU VDU Fluid coker	DRU VDU	DRU VDU
Process fuel	GJ/h	LC-Finer	Delayed coker	LC-Finer

Accordingly, the following equations are used in the OSOM model to determine power demands (P) for each upgrading scheme:

$$P_{U\text{-}1,P_i} = PLL(ATB_F + VTB)_{P_i} + PFC \cdot RES_{P_i} \quad (2\text{-}19)$$

$$P_{U\text{-}2,P_i} = PDC \cdot VTB_{P_i} \quad (2\text{-}20)$$

$$P_{U\text{-}3,P_i} = PLH \cdot VTB_{P_i} \quad (2\text{-}21)$$

Where PLL, PLH, PFC, and PDC are model parameters used to compute power demands of high conversion LC-Finer, low-conversion LC-Finer, Fluid coking, and Delayed coking, respectively. ATB, VTB, and RES are feed streams to the above processes.

The steam demands (S) of each producer are given by:

$$S_{U\text{-}k,P_i} = \frac{DB_{P_i} \cdot HDR + (ATB - ATB_F)_{P_i} \cdot HVD + RES_{P_i} \cdot HFC}{\Delta HS} \quad (2\text{-}22)$$

DB is the diluted bitumen entering the DRU. HDR, HVD, and HFC are model parameters representing the heat requirements of the DRU, VDU, and fluid coker, respectively. ΔHS is the enthalpy of the steam consumed in upgrading. When using equation (2-22) to calculate the steam demands of upgrading schemes 2 and 3, the last term is neglected in the OSOM.

Hydrogen demands for upgrading are divided into hydrogen for hydrodesulphurisation (H_T, equation 2-23) and hydrogen for hydrocracking (H_L, equations 2-24 and 2-25). The former hydrogen is consumed in the hydrotreaters while the latter is a feedstock to LC-Fining units.

$$H_{T,P_i} = \left(\sum_j \frac{LGO_{P_i,j}}{\rho_{LGO_{P_i}}} \right) \cdot HLG + \left(\sum_j \frac{HGO_{P_i,j}}{\rho_{HGO_{P_i}}} \right) \cdot HHG + \left(\sum_j \frac{NAP_{P_i,j}}{\rho_{NAP_{P_i}}} \right) \cdot HNP \quad (2\text{-}23)$$

$$H_{L\text{-}1,P_i} = (VTB + ATB_F)_{P_i} \cdot HLL \quad (2\text{-}24)$$

$$H_{L\text{-}2,P_i} = VTB_{P_i} \cdot HLH \quad (2\text{-}25)$$

LGO, HGO, and NAP represent the flow rates of each oil fraction from individual process units (j) in upgrading. HLG, HHG, and HNP are model parameters which specify the hydrogen consumption of LGO, HGO, and naphtha hydrotreaters. Two other parameters, HLL and HLH denote the hydrogen requirements of low-conversion and high-conversion LC-Finers, respectively. ρ is the density of each one of the oil fractions entering the hydrotreaters.

Process fuel is consumed in certain units in the upgrading stage. The specific fuel demands (F) of each producer, according to upgrading scheme are calculated in the OSOM-BC with equations 2-26 to 2-28. FRL and FRD are parameters that set the fuel requirements of LC-Fining and Delayed coking units, respectively.

$$F_{U\text{-}1,P_i} = (VTB + ATB_F)_{P_i} \cdot FRL \quad (2\text{-}26)$$

$$F_{U\text{-}2,P_i} = VTB_{P_i} \cdot FRD \quad (2\text{-}27)$$

$$F_{U\text{-}3,P_i} = VTB_{P_i} \cdot FRL \quad (2\text{-}28)$$

2.2.6 Total energy demands

The energy demands of all producers in the base case are computed by adding individual energy commodities for all process stages, for all producers in the base case. The index k is used to differentiate specific energy demands of individual upgrading schemes. The equations below summarize the total energy demands of the OSOM-BC.

$$W = \sum_{P_i} (W_{H,P_i} + W_{E,P_i}) \tag{2-29}$$

$$P = \sum_{P_i} \left(P_{H,P_i} + P_{E,P_i} + PS_{P_i} + \sum_{k=1}^{3} P_{U\text{-}k,P_i} \right) \tag{2-30}$$

$$D = \sum_{P_i} D_{P_i} \tag{2-31}$$

$$S = \sum_{P_i} \left(S_{E,P_i} + \sum_{k=1}^{3} S_{U\text{-}k,P_i} \right) \tag{2-32}$$

$$SS = \sum_{P_i} SS_{P_i} \tag{2-33}$$

$$H = \sum_{P_i} \left(H_{T,P_i} + \sum_{k=1}^{3} H_{L\text{-}k,P_i} \right) \tag{2-34}$$

$$F = \sum_{P_i} \sum_{k=1}^{3} F_{P_i} \tag{2-35}$$

2.2.7 Energy supply

The OSOM-BC determines the aggregate energy demands from all stages, represented by circles in Figure 2-2, for all the SCO and bitumen producers in the base case. These demands, with the exception of diesel and process fuel, are satisfied by the energy-producing plants represented by boxes on the left side of the model superstructure in Figure 2-2. SB and SSB represent boilers generating steam at 6,300 kPa and 500 °C and 80% steam at 8,000 kPa, respectively. The former steam (S) is used in bitumen extraction as well as in upgrading operations. The latter (SS) is employed exclusively for SAGD operations. The steam production in boilers SB and SSB is given by the expressions:

$$S_b = \frac{HHV_{NG} \cdot PSP \cdot \eta_{B_b}}{\Delta HS_b} X_b \quad \forall \; b \in SB \tag{2-36}$$

$$SS_b = \frac{HHV_{NG} \cdot \eta_{B_b}}{\Delta HS_b} X_b \ \forall \ b \in SSB \tag{2-37}$$

Where η_B represents the thermal efficiency of the boiler, ΔHS is the enthalpy of the steam, HHV_{NG} is the high heating value of the natural gas fuel and PSP equals the percentage of boiler capacity used for steam production. X_b is the natural gas consumption of the boiler.

Boilers SB also produce hot water (W), required in bitumen hydrotransport and extraction:

$$W_b = \frac{HHV_{NG} \cdot (1 - PSP) \cdot \eta_{B_b}}{\Delta HW} X_b \ \forall \ b \in SB \tag{2-38}$$

And ΔHW above is the enthalpy of the hot water. Since the OSOM-BC is based on the current manner of operation in the Athabasca region oil sands industry, the power demands (P) are met by natural gas combined cycle power (NGCC) plants, according to equation (2-39). HRP is the specified heat rate of the NGCC plant and X_p is its natural gas consumption.

$$P_p = \frac{HHV_{NG}}{HRP_p} X_p \ \forall \ p \in NGCC \tag{2-39}$$

All the hydrogen (H) required for upgrading is produced in steam methane reforming (SMR) plants according to:

$$H_h = \frac{HHV_{NG}}{FCH} X_h \ \forall \ h \in SR \tag{2-40}$$

Where FCH equals the fuel consumption of SMR plants per unit of hydrogen produced. The steam reforming plant used in the model corresponds to the one described by Simbeck [19]. The power plants in the OSOM are modelled after the NGCC plant described in [39]. The steam boiler specifications are derived from [16]. The natural gas used in this study is Western Canadian, with a HHV of 38 MJ/Nm^3.

Two important features of the OSOM are its capability to accommodate power demands in excess of those calculated for oil sands operations and the option to use internally-produced refinery gas for hydrogen production. The power demands of all producers in the OSOM-BC are increased by a user-supplied factor, to account for power demands for subsidiary operations not included in the OSOM. In addition to the above,

the user can specify electricity generation for export, which is then added to the power demands corresponding to oil sands operations. This is useful if an oil producer decided to increase revenue by selling its excess power to the local grid.

The hydrogen demands in the OSOM-BC are calculated for the upgrading processes of all producers. Given that fuel gases are generated during upgrading (i.e., LC-Finer and coker gases), the model has the option to use all the produced sweet fuel gas as fuel in the hydrogen plants. This may potentially ease the amount of natural gas required for H_2 production, with valuable cost savings. By default, this option is inactive in the model.

2.2.8 CO_2 emissions

The model determines energy demands per process stage, per producer. These demands are broken down into the seven energy commodities listed in Figure 2-2. The OSOM-BC computes natural gas and diesel fuel demands associated with energy consumption for all oil producers, based on the natural gas requirements of all energy-producing units and process fuel demands for upgrading. Finally, the CO_2 emissions (E) due to natural gas and diesel fuel use for energy production in oil sands operations are computed in the OSOM, based on the emissions factors (FEF) for each fossil fuel [40]. Equations 2-41, 2-42, 2-43 and 2-44 show the CO_2 emissions of boilers (SB and SSB), hydrogen plants, and power plants, respectively.

$$E_b = \frac{FEF_{NG}}{\eta_{B_b} HHV_{NG}} \left(W_b \Delta HW + S_b \Delta HS_b \right) \forall\ b \in SB \tag{2-41}$$

$$E_b = \frac{FEF_{NG}}{\eta_{B_b} HHV_{NG}} SS_b \Delta HS_b \ \forall\ b \in SSB \tag{2-42}$$

$$E_h = HEF_h \cdot H_h \ \forall\ h \in SR \tag{2-43}$$

$$E_p = FEF_{NG} X_p \ \forall\ p \in NGCC \tag{2-44}$$

HEF is a model parameter, denoting the CO_2 emissions of SMR plants. The total CO_2 emissions from oil sands operations for the base case are given by:

$$E = \sum_{b \in SB} E_b + \sum_{b \in SSB} E_b + \sum_{h \in SR} E_h + \sum_{p \in NGCC} E_p + FEF_D \sum_{P_i} D_{P_i} + FEF_{NG} \sum_{P_i} \sum_{k=1}^{3} F_{k,P_i} \tag{2-45}$$

Where the last two terms in equation 2-45 represent the CO_2 emissions of diesel and process fuel, respectively.

CO_2 emissions from power and hydrogen production are reported according to their life-cycle components, as shown in Table 2-4. The aforementioned emission components were reported in life-cycle emissions and performance studies [39, 41].

Table 2-4 CO_2 emissions breakdown for hydrogen and power production plants

CO_2 Emissions source	NGCC (%)	SMR (%)
On-site - hydrogen production	-	82.3
On-site - electricity generation	84.4	2.5
Upstream - NG production & distribution	15.0	14.8
Upstream - construction & decommissioning	0.6	0.4
Total	100	100

An optional feature in the OSOM-BC is the calculation of other GHG emissions in addition to CO_2, such as CH_4 and N_2O. These two gases are linked to NGCC and SMR plants operations. The user has the option to include methane and nitrous oxide in the calculation of GHG emissions corresponding to hydrogen and power production, or else, calculate only CO_2 emissions in the above plants. The results for the 2003 case presented in Chapter 4 include CO_2, CH_4, and N_2O.

The OSOM-BC output includes energy demands per commodity, per producer; SCO and bitumen production per producer, as well as natural gas demands per commodity and per producer. The GHG emissions are reported per commodity and per producer; they can include CO_2, CH_4 and N_2O together, or CO_2 alone. The model also computes CO_2 or total GHG intensity for all producers, expressed as tonnes of CO_2 or CO_{2eq} per bbl of SCO or bitumen.

2.3 Future Production Scenarios

The future production scenarios (FPS) in the OSOM are based on forecasted SCO and bitumen production levels for the years 2012 and 2030, as specified in Table 2-1. In contrast to the base case, future production in the above years is anticipated to include SCO from SAGD bitumen. Thus, the OSOM-FPS determines energy demands for the combined bitumen and SCO production from producers A1-A3, B1-B3, and C. Another

noteworthy difference between the OSOM-BC and the FPS is the fact that while the former calculates CO_2 emissions from energy production in specified units (i.e., NGCC and SMR plants), the latter only quantifies the energy demands themselves. In other words, the OSOM-FPS does not make assumptions concerning the means by which each energy commodity is produced. This in practical terms denotes that the FPS output will determine the quantity and nature of the energy required to produce given quantities of SCO and bitumen but will not make any recommendations as to which technologies must be used to produce the required H_2, electricity, steam, etc.

The reader must at this point note that the OSOM-FPS has been expressly designed as a source of inputs for a second mathematical model, an optimization model which is the subject of Chapter 3. The model in question is conceived as an optimal planning tool for large-scale energy production incorporating CO_2 capture technologies to reduce the emissions from energy production in the oil sands industry. Accordingly, the optimization model is formulated to minimize the overall cost of producing H_2, steam, hot water, and power for the oil sands industry, while reducing total CO_2 emissions by a given percentage. The optimizer results determine the number of power and H_2 plants (and their types) as well as steam producers that will satisfy demands for the above commodities for the SCO and bitumen production rates in 2012 and 2030.

Thus, the role of the OSOM-FPS is chiefly to quantify the industry-wide demands for the energy commodities shown in Figure 2-6, for anticipated SCO and bitumen production levels in the years 2012 and 2030.

Producers A and C are modelled in the OSOM-BC. From a modelling perspective, producers B1-B3 are equivalent to producers C with the addition of an upgrading stage. Therefore, the energy demands of producers B are modelled based on the correlations used for producers C, plus the equations corresponding to the upgrading process. The upgrading process model section, which was originally developed for producers A in the OSOM-BC, is coupled with the SAGD model section also from the OSOM-BC, to model the operations of SCO production from thermal bitumen in the OSOM-FPS.

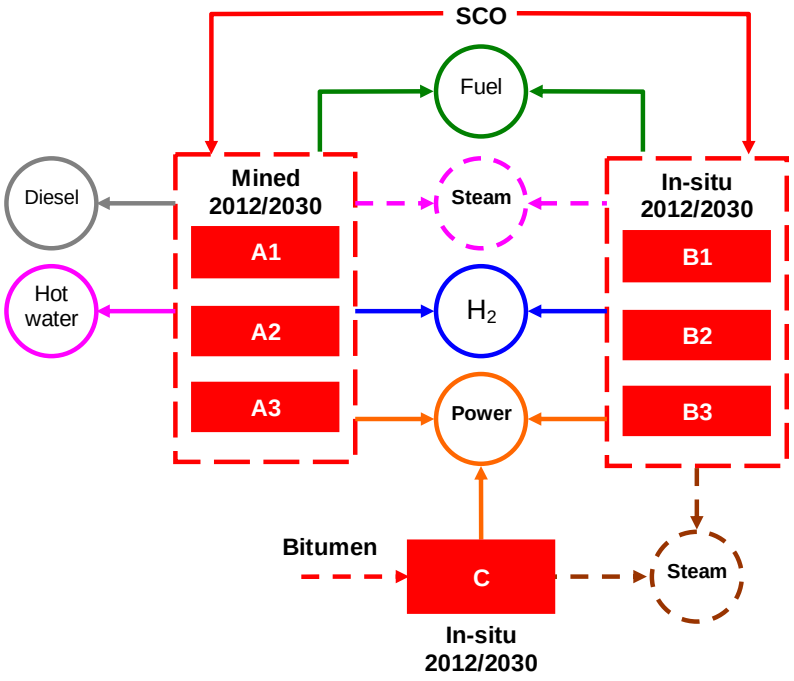

Figure 2-6 OSOM-FPS superstructure

The model sections for producers A and C in the OSOM-FPS are identical to those sections found in the OSOM-BC for these producers. The main difference is that the energy demands in the former scenario are a function of SCO and bitumen production and not of oil sands mining/extraction rates, as is the case in the latter. The OSOM-FPS output comprises the energy demands per commodity, per producer, for given bitumen and SCO production estimates for the years 2012 and 2030.

The results corresponding to the OSOM-BC and OSOM-FPS are discussed in Chapter 4. A list of the parameter values used in this study is presented in Appendix 1.

Chapter 3

GAMS Optimization Model

3.1 Overview

The superstructure of the optimization model is shown on Figure 3-1. Oil sands producers are shown on the right side in Figure 3-1, which is the energy demand side, consisting of the OSOM-BC and OSOM-FPS outputs. Fleet wide hot water (W), H_2 (H), process and SAGD steam (S/SS), power (P), and diesel (D) demands are calculated by the OSOM, for all years. These demands are represented by circles in Figure 3-1. All energy demands are met by three plant types (represented as boxes on the left in Figure 3-1): 1) boilers, 2) H_2 plants, and 3) power plants. These energy producers consume natural gas (X) or coal (Y). A third feedstock (Z) also appears in the model infrastructure, to denote the potential ability of some plants in the model to use alternative fuels such as petcoke or other bitumen residues. It is anticipated that future versions of the model will include petcoke-fuelled gasification plants and/or other plants (see Chapter 6). In this study, however, only natural gas and coal are used as fuels in all energy-producing plants.

CO_2 emissions in the superstructure are represented by (E) whereas CO_2 captured is symbolized by (CCO2). The oil products in the superstructure are mined SCO (MSCO), SAGD SCO (TSCO), and bitumen (BIT). The energy demand side in Figure 3-1 also shows the optional power (PEX) and hydrogen (HEX) demands for export (see sections 3.4.4 and 3.4.5) which in this study have a default value of zero. Oil sands producers A1-A3, B1-B3, and C, as defined in section 2.1 appear on the demand side. Their production capacity is divided into 2003 values and 2012/2030, according to the aggregate production estimates assumed for this study (see Table 2-1).

The objective of the optimization model is to find the most economical way to satisfy the fleet's demand for W, H, S, SS, and P, while at the same time meeting given CO_2 reduction targets according to the following problem statement:

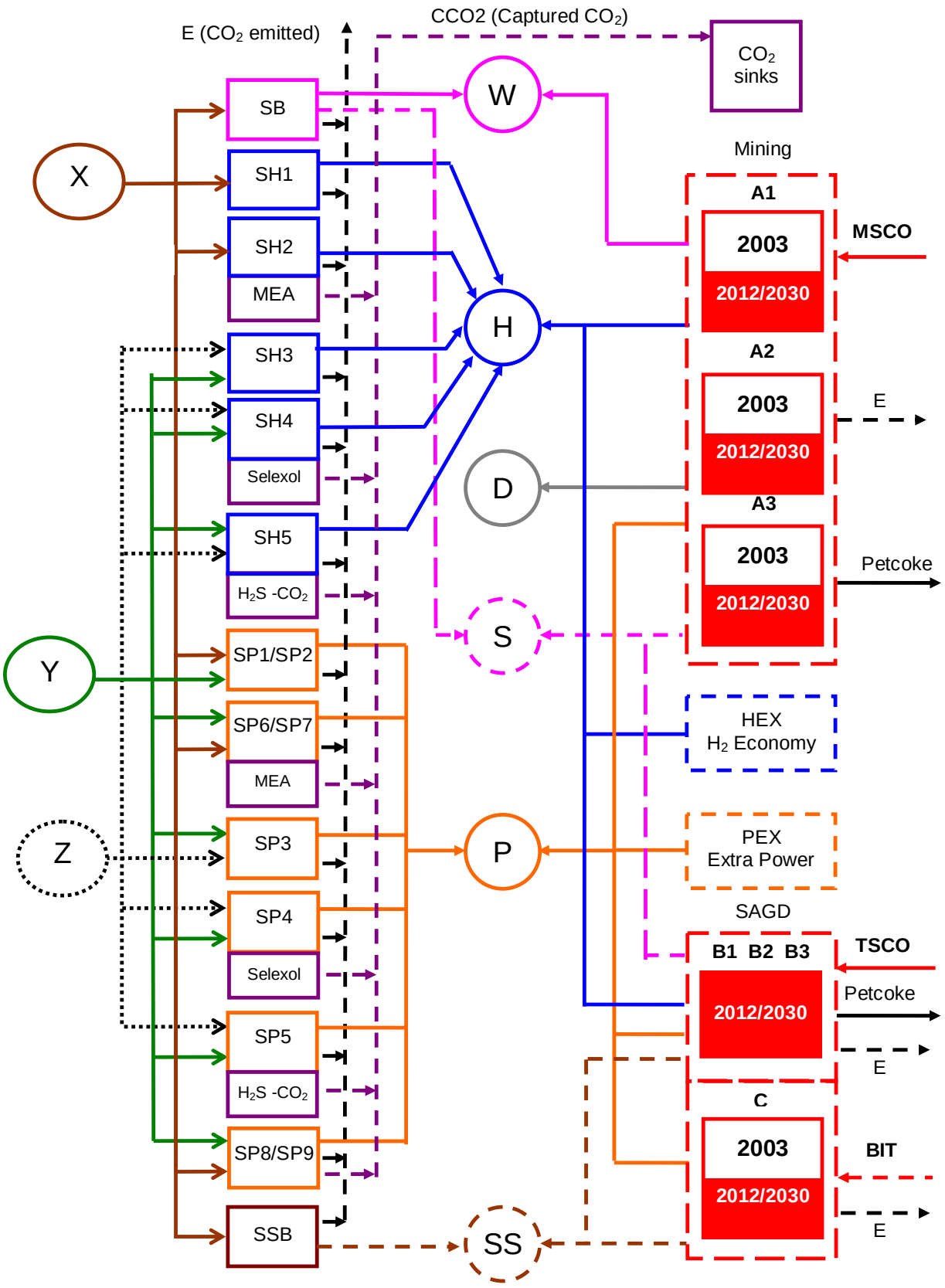

Figure 3-1. GAMS optimization model - Superstructure

What is the optimal combination of energy production technologies, feedstocks, and CO_2 capture processes to use in the oil sands industry that will satisfy future energy demands at minimal cost while meeting CO_2 reduction targets for given bitumen and SCO production levels?

The optimization model will determine the optimal energy infrastructure for a given combination of production levels of SCO and bitumen and CO_2 reduction targets. It does so by selecting the type and number of hydrogen plants, power plants, and boilers from a list of available energy production technologies, with and without CO_2 capture.

3.2 Plant Sets

Aside from conventional natural gas-fired boilers, several different power and hydrogen production technologies are available in the optimization model. A list of all such technologies in the form of plant sets is presented below. The reader must become familiar with the names of these plant sets, (left side of Figure 3-1) which appear throughout this chapter. The default number of units per set is shown in brackets. The default number of plants per set corresponds roughly to the oil sands industry energy demands in 2030. If larger energy outputs are to be optimized, the number of units in the pertinent sets must be increased.

3.2.1 Boilers

S_B = Natural gas-fired boilers producing process steam and hot water (def. 90)

S_{SB} = Natural gas-fired boilers producing SAGD steam (def. 150)

3.2.2 Hydrogen plants

S_{H_1} = Steam Methane Reforming (SMR) hydrogen plants without CO_2 capture (def. 120)

S_{H_2} = SMR hydrogen plants with 90% CO_2 capture – MEA (def. 120)

S_{H_3} = Coal gasification hydrogen plants without CO_2 capture (def. 30)

S_{H_4} = Coal gasification hydrogen plants with 90% CO_2 capture - Selexol (def. 30)

S_{H_5} = Coal gasification H_2 plants with 90% CO_2+ H_2S co-capture - Selexol (def. 30)

3.2.3 Power plants

S_{P_1} = NGCC power plants without CO_2 capture (def. 30)

S_{P_2} = PC (supercritical) power plants without CO_2 capture (def. 30)

S_{P_3} = IGCC power plants without CO_2 capture (def. 30)

S_{P_4} = IGCC power plants with 88% CO_2 capture - Selexol (def. 30)

S_{P_5} = IGCC power plants with 88% CO_2 + H_2S co-capture - Selexol (def. 30)

S_{P_6} = NGCC power plants with 90% CO_2 capture - MEA (def. 30)

S_{P_7} = PC (supercritical) power plants with 90% CO_2 capture - MEA (def. 30)

S_{P_8} = Natural gas Oxyfuel power plants with CO_2 capture (def. 30)

S_{P_9} = Coal Oxyfuel power plants with CO_2 capture (def. 30)

3.3 Indexes

In the optimization model, the following indexes are linked to variables and specific plant sets.

b = boiler

C = coal

D = demand

NG = natural gas

h = hydrogen plant

p = power plant

PF = process fuel

Thus, HHV_{NG} is used in this work to denote the High Heating Value of natural gas whereas $X_b \ \forall \ b \in S_B$ is the natural gas consumption in the set of boilers S_B.

3.4 Balances

The core of the optimization model consists of a series of equations relating the input parameters to process variables of interest (e.g., steam, coal consumption, CO_2 emissions). These equations are also mass and energy balances that link the energy supply side to the specified energy demands and are solved by the GAMS solvers. The balances featured in this section are organized according to variables.

3.4.1 Process steam

Steam at 6,300 kPa and 500 °C (as used by Syncrude) is produced in natural gas-fired boilers S_B. A portion of the boiler capacity is used for hot water (35 °C) production (see section 3.4.3). Additional steam from SMR plants might also be available, thus the total process steam supply in the fleet is given by:

$$S = \sum_{b \in S_B} S_b + \sum_{h \in S_{H_1}} S_h \geq S_D \tag{3-1}$$

The above equation is also a constraint, which specifies that the total process steam supply must be equal or greater than the fleet-wide demand. The amount of steam produced in the boilers is given by equation (3-2):

$$S_b = \frac{HHV_{NG} \cdot PSP \cdot \eta_{B_b}}{\Delta HS} X_b \ \forall \ b \in S_B \tag{3-2}$$

HHV_{NG} is the heating value of natural gas. PSP is the percentage of the boiler's capacity dedicated to steam production. The boiler's thermal efficiency is represented by ηb and ΔHS is the enthalpy of steam. The (optional) steam produced in SMR plants is calculated as follows:

$$S_h = SSR \cdot H_h \forall \ h \in S_{H_1} \tag{3-3}$$

SSR is a parameter that relates the amount of steam produced in hydrogen plants to the plant's hydrogen output. By default, the value of SSR in the optimizer is zero and thus, the steam output of SMR plants is also zero. The entirety of the steam in the

optimization by default comes from boilers. This is the case for all the results presented in Chapters 4 and 5.

3.4.2 SAGD steam

Steam at 8,000 kPa is used for SAGD bitumen extraction. The steam is produced in natural gas-fired boilers S_{SB}. The total SAGD steam production in the fleet is given by equation (3-4):

$$SS = \sum_{b \in S_{SB}} SS_b \geq SS_D \tag{3-4}$$

The above equation is also a constraint, which specifies that the total SAGD steam supply must be equal or greater than the fleet-wide demand.

The amount of SAGD steam produced in the boilers is given by equation 3-5:

$$SS_b = \frac{HHV_{NG} \cdot \eta_{B_b}}{\Delta HS} X_b \ \forall \ b \in S_{SB} \tag{3-5}$$

3.4.3 Hot water

In the optimization model, all hot water is produced in S_B boilers. The relationship between hot water supply and demand is given by the following equation:

$$W = \sum_{b \in S_B} W_b \geq W_D \tag{3-6}$$

The hot water produced in the NG boilers is defined by equation (3-7):

$$W_b = \frac{HHV_{NG} \cdot (1 - PSP) \cdot \eta_{B_b}}{\Delta HW} X_b \ \forall \ b \in S_B \tag{3-7}$$

where ΔHW is the enthalpy of the hot water leaving the boilers. The water is assumed to have a temperature of 35° C, as specified in [30].

3.4.4 Hydrogen

Hydrogen, which is used in bitumen upgrading, is produced in steam reforming- and IGCC-based plants, as shown below. A certain excess amount of hydrogen may be produced (HHE), which represents the hydrogen available for export.

$$H = \sum_{h \in S_{H_1} \cup S_{H_2}} H_h + \sum_{h \in \bigcup_{i=3}^{5} S_{H_i}} H_h \geq H_D + HHE \tag{3-8}$$

The H_2 produced in natural gas-based plants is defined by the following equation:

$$H_h = \frac{HHV_{NG}}{N_{H_h}} X_h \ \forall \ h \in S_{H_1} \cup S_{H_2} \tag{3-9}$$

where N_H is the energy required to produce a tonne of hydrogen. The hydrogen produced in gasification plants using coal as feedstocks is given by equation (3-10):

$$H_h = \frac{HHV_C}{N_{H_h}} Y_h \ \forall \ h \in \bigcup_{i=3}^{5} S_{H_i} \tag{3-10}$$

3.4.5 Power

The total power produced in the fleet is the sum of power produced in all power plants, plus the power co-generated in gasification hydrogen plants as shown in equation (3-11) below:

$$P = \sum_{p \in \bigcup_{i=1}^{9} S_{P_i}} P_p + \sum_{h \in \bigcup_{i=3}^{5} S_{H_i}} P_h \geq P_D + PEX + \sum_{h \in \bigcup_{i=1}^{2} S_{H_i}} P_h + P_{CO2} \tag{3-11}$$

PEX is the power for export generated in the fleet (optional). By default, this value is zero in the optimizer. P_h represents both the power co-generated in gasification hydrogen plants (left side of eq. 3-11) and the ancillary power requirements of SMR hydrogen plants (right side of eq. 3-11). P_{CO2} is the power required to transport the captured CO_2 to storage, as given by equation 3-12. PCT is a parameter representing the unitary power requirements for CO_2 transport (per 100 km segment) and PKM is the length of the pipeline. The value of PCT was provided by staff at the Alberta Research Council's Carbon and Energy Management Unit, using an in-house model for CO_2 transport [42].

$$P_{CO2} = \left(\sum_{h \in \bigcup_{i=2}^{5} S_{H_i}} C_h + \sum_{p \in \bigcup_{i=1}^{9} S_{P_i}} C_p \right) \cdot PCT \cdot \frac{PKM}{100} \tag{3-12}$$

The individual plant electricity generation is given by the following expressions:

$$P_p = \frac{HHV_{NG}}{HRP_p} X_p \ \forall \ p \in S_{P_1} \cup S_{P_6} \cup S_{P_8} \tag{3-13}$$

$$P_p = \frac{HHV_C}{HRP_p} Y_p \;\forall\; p \in \bigcup_{i=2}^{5} S_{P_i} \cup S_{P_7} \cup S_{P_9} \tag{3-14}$$

HRP symbolizes the heat rate of each power plant. Equations 3-13 and 3-14 represent the power produced in natural gas and coal power plants, respectively. Equation 3-15 is used to calculate both the ancillary energy requirements of SMR hydrogen plants and co-produced power from gasification plants. HPW is a parameter that represents the amount of power required/co-generated as a function of each plant's hydrogen output.

$$P_h = HPW_h \cdot H_h \;\forall\; h \in \bigcup_{i=1}^{5} S_{H_i} \tag{3-15}$$

3.4.6 Natural gas

Natural gas is consumed in boilers, hydrogen plants, and power plants. It is also used as process fuel for upgrading operations. Accordingly, the following equation is developed:

$$X = \sum_{b \in S_B \cup S_{SB}} X_b + \sum_{h \in S_{H_1} \cup S_{H_2}} X_h + \sum_{p \in S_{P_1} \cup S_{P_5} \cup S_{P_8}} X_p + X_{PF} \tag{3-16}$$

The optimizer will adjust each one of the variables in equation (3-16) as needed, to satisfy energy demands in the fleet and CO_2 reduction constraints. Currently, there is no constraint on the total amount of natural gas available for operations, nor on the units that can use natural gas as fuel. This in practical terms implies that the natural gas supply in the optimization is unlimited and that its price does not change as its demand increases. This study, however, includes sensitivity analyses to natural gas and coal prices. These analyses are the subject of Chapter 5.

3.4.7 Coal

Coal is consumed in hydrogen plants and power plants and it is also available as process fuel for upgrading operations according to equation (3-17):

$$Y = \sum_{h \in \bigcup_{i=3}^{5} S_{H_i}} Y_h + \sum_{p \in \bigcup_{i=2}^{5} S_{P_i} \cup S_{P_7} \cup S_{P_9}} Y_p + Y_{PF} \tag{3-17}$$

The amount of coal consumed in each plant is a function of its output, as determined by the optimizer. As with natural gas, no supply constraint is imposed on coal and its price does not vary with increased demand.

3.4.8 CO_2

All plants included in the optimizer consume fossil fuels, producing CO_2 as a by-product. The total CO_2 is the sum of CO_2 emitted and CO_2 captured, as shown in (3-18).

$$CO_2 = E + C \tag{3-18}$$

The total CO_2 emitted comes from boilers, hydrogen and power plants, as shown below. The terms of equation (3-19) correspond to boilers, NG and coal H_2 plants, and natural gas and coal power plants, in that order. The last two terms in (3-19) correspond to the CO_2 emissions from diesel and process fuel use in the OSOM, respectively.

$$E = \sum_{b \in S_B} E_b + \sum_{b \in S_{SB}} E_b + \sum_{h \in S_{H_1} \cup S_{H_2}} E_h + \sum_{h \in \bigcup_{i=3}^{5} S_{H_i}} E_h + \sum_{p \in S_{P_1} \cup S_{P_6} \cup S_{P_8}} E_p + \sum_{p \in \bigcup_{i=2}^{5} S_{P_i} \cup S_{P_7} \cup S_{P_9}} E_p + E_{DF} + E_{PF} \tag{3-19}$$

The total CO_2 captured in the fleet is given by equation (3-20):

$$C = \sum_{h \in S_{H_2}} C_h + \sum_{h \in S_{H_4} \cup S_{H_5}} C_h + \sum_{h \in S_{P_6} \cup S_{P_8}} C_p + \sum_{p \in S_{P_4} \cup S_{P5} \cup S_{P_7} \cup S_{P9}} C_p \tag{3-20}$$

The terms of (3-20) represent the CO_2 captured from NG and coal hydrogen plants, and natural gas and coal power plants, in that specific order. In the optimization model, no CO_2 captured is applied to steam boilers (S_B and S_{SB}).

The total CO_2 reduction is given by expression (3-21). The CO_2 emissions of the fleet must be equal or lesser than a user-defined reduction percentage, ERG, multiplied by the baseline emissions, as shown in (3-22). EBL represents the baseline CO_2 emissions of the base case, which is an input to the optimization model. In this study, this figure is determined by running the optimization model using only natural gas as fuel, no CO_2 capture, and employing exclusively SMR and NGCC plants for hydrogen and power production respectively. When using this approach, the baseline emissions and costs at any production level are equivalent to a “business as usual” (BAU) scenario. If another baseline scenario is desired, the user can simply run the optimizer using the desired feedstock(s), capture level and technologies and record the total CO_2 emissions of that

run. This value is then entered in a subsequent run as EBL with the desired set of conditions to be compared against the baseline case.

$$RED = EBL - E \tag{3-21}$$

$$E \leq EBL \cdot (1 - ERG) \tag{3-22}$$

The emissions from boilers are given by (3-23). The CO_2 emitted by H_2 plants and power plants are given in (3-24) and (3-25), respectively.

$$E_b = FEF_{NG} \cdot X_b \ \forall \ b \in S_B \cup S_{SB} \tag{3-23}$$

$$E_h = HEF_h \cdot H_h \forall \ h \in \bigcup_{i=1}^{5} S_{H_i} \tag{3-24}$$

$$E_p = EFP_p \cdot P_p \forall \ p \in \bigcup_{i=1}^{9} S_{P_i} \tag{3-25}$$

Parameters FEF, HEF, and EFP are the CO_2 emissions per unit of natural gas burned, hydrogen produced, and power generated, respectively. The CO_2 emissions resulting from diesel fuel and process fuel are given by equations (3-26) and (3-27).

$$E_{DF} = FEF_{DIE} \cdot D_D \tag{3-26}$$

$$E_{PF} = (FEF_{NG} \cdot X_{PF}) + (FEF_C \cdot Y_{PF} \cdot (ULC - ASH)) \tag{3-27}$$

where FEF represents the CO_2 emissions per unit of natural gas, diesel, and C in the coal. The last term in (3-27) adjusts the CO_2 emissions from coal burning by subtracting the mass of the coal that is ash (ASH) and thus, non CO_2-forming. ULC is the carbon content of the fuel as given in the ultimate analysis.

The CO_2 captured in hydrogen plants is a function of their output (eq. 3-28). Likewise, for power plants, the CO_2 captured is calculated depending on the power output of each particular plant, as seen in (3-29). CCH and CCP are parameters that relate the CO_2 captured to the unitary output of the power and hydrogen plants and are calculated on the basis of each technology's techno-economic performance.

$$C_h = CCH_h \cdot H_h \forall \ h \in S_{H_2} \cup S_{H_4} \cup S_{H_5} \tag{3-28}$$

$$C_p = CCP_p \cdot P_p \forall \ p \in \bigcup_{i=4}^{9} S_{P_i} \tag{3-29}$$

3.5 Binary Variables

In the optimization model, a number of binary variables are defined to quantify the number of units and plants present in the optimal energy infrastructures as well as to establish constraints.

Boilers

IB_b = 1 if boiler b exists in the infrastructure

= 0 otherwise $b \in S_B \cup S_{SB}$

Hydrogen plants

IH_h = 1 if plant h exists in the infrastructure

= 0 otherwise $h \in \bigcup_{i=1}^{5} S_{H_i}$

Power plants

IP_p = 1 if plant p exists in the infrastructure

= 0 otherwise $p \in \bigcup_{i=1}^{9} S_{P_i}$

3.6 Constraints

3.6.1 Energy producers

This set of constraints limits the number of boilers, H_2, and power plants that can exist at any given time in the optimization. Individual technologies can be excluded from the optimization by setting its number of plants to zero. Conversely, the user may choose to specify a limited number of a certain type of plants, or by deactivating a constraint associated with a certain technology, allow an unlimited number of such plants to exist.

Equations (3-30) to (3-32) show the general form of the constraints on the number of boilers, hydrogen, and power plants allowed in the optimizer, respectively.

$$\sum IB_b \le Integer\# \qquad \forall\ b \in S_B \cup S_{SB} \tag{3-30}$$

$$\sum IH_h \le Integer\# \qquad \forall\ h \in \bigcup_{i=1}^{5} S_{H_i} \tag{3-31}$$

$$\sum IP_p \le Integer\# \qquad \forall\ p \in \bigcup_{i=1}^{9} S_{P_i} \tag{3-32}$$

The reader must note that the integer numbers above should generally be equal to the number of units specified for individual plant sets (see section 3.2). For instance, the default number of boilers in the set S_B is 90. Therefore, a good integer number to be used in constraint (3-30) would be 50, or 90, but not 300. The latter could potentially cause execution errors, since the optimizer would be allowed to use up to 300 boilers, whereas the default specified number of boilers in the set (if unchanged) would be 90.

3.6.2 Energy supply

This set of constraints ensures that the total of each energy commodity produced in boilers, hydrogen, and power plants in the optimizer meets the demands specified by the user (and calculated by the OSOM). These equations were defined earlier, on the individual commodity balances.

$$\sum_{b \in S_B} S_b + \sum_{h \in S_{H_1}} S_h \ge S_D \tag{3-1}$$

$$\sum_{b \in S_{SB}} SS_b \ge SS_D \tag{3-4}$$

Equations (3-1) and (3-4) are the supply constraints on process and SAGD steam, respectively. Equation (3-6) shows the constraints on hot water production while equations (3-8) and (3-11) regulate the hydrogen and power production in the fleet, respectively. Equation (3-33) ensures that the demands for process fuel are met by either coal or natural gas, or a combination of both.

$$\sum_{b \in S_B} W_b \ge W_D \tag{3-6}$$

$$\sum_{h \in S_{H_1} \cup S_{H_2}} H_h + \sum_{h \in \bigcup_{i=3}^{5} S_{H_i}} H_h \ge H_D + HHE \tag{3-8}$$

$$\sum_{p \in \bigcup_{i=1}^{9} S_{P_i}} P_p + \sum_{h \in \bigcup_{i=3}^{5} S_{H_i}} P_h \ge P_D + PEX + \sum_{h \in \bigcup_{i=1}^{2} S_{H_i}} P_h + P_{CO2} \tag{3-11}$$

$$(X_{PF} \cdot HHV_{NG}) + (Y_{PF} \cdot 1000 \cdot HHV_C) = PF_D \cdot HHV_{NG} \tag{3-33}$$

3.6.3 Base case energy

Some constraints are introduced to allow the user to set the outputs of a sub-set of power and hydrogen plants to match the energy demands in 2003, the base case year in this study. This is desirable when optimizing the energy demands of the oil sands industry in a post-2003 time period, assuming that the energy infrastructure used in 2003 is still operational. In this study, a portion of the energy infrastructures of 2012 is identical to the 2003 infrastructure (refer to section 4.3.2.1). Thus the optimizer adds the optimal combination of plants required to meet the energy demands for 2012 to the existing 2003 plants. The base case energy supply constraints can be activated or deactivated by the user, for any given run.

Equations (3-34) to (3-36) define the base case energy supply for power, hydrogen plants, and process fuel, respectively. In 2003, all power is generated in NGCC plants and the hydrogen is produced in SMR plants, both without capture. Likewise, all process fuel is assumed to be natural gas. The base case energy constraints therefore, are based on these technologies, as seen below.

$$\sum P_p \geq P_D^{2003} \forall \; p \in S_{P_1} \tag{3-34}$$

$$\sum H_h \geq H_D^{2003} \forall \; h \in S_{H_1} \tag{3-35}$$

$$X_{PF} \geq PF_D^{2003} \tag{3-36}$$

3.6.4 Unit capacity

In addition to constraints on the energy supply of the fleet, an additional set of constraints is specified to ensure that the individual output of each energy producer in the infrastructure does not exceed its design capacity.

Equations (3-37) to (3-39) are the capacity constraints for boilers. SBC is the nominal capacity of each boiler in the fleet.

$$S_b \leq (SBC \cdot PSP) IB_b \quad \forall b \in S_B \tag{3-37}$$

$$S_b \leq SBC \cdot IB_b \quad \forall b \in S_{SB} \tag{3-38}$$

$$W_b \leq SBC \cdot (1 - PSP) \left(\frac{\Delta HS}{\Delta HW} \right) IB_b \quad \forall b \in S_B \tag{3-39}$$

The capacity constraints for individual hydrogen plants are given by the product of their design output (HCAP) and their specified availability factor (CF), as shown below.

$$H_h \leq HCAP_h \cdot CF_h \cdot IH_h \qquad \forall h \in \bigcup_{i=1}^{5} S_{H_i} \tag{3-40}$$

Similarly to hydrogen plants, the capacity constraints for individual power plants are given by the product of their nominal output (POUT) and their specified availability factor (CF), as shown in (3-41).

$$P_p \leq POUT_p \cdot CF_p \cdot IP_p \qquad \forall p \in \bigcup_{i=1}^{9} S_{P_i} \tag{3-41}$$

3.6.5 CO_2 reduction

A constraint is imposed on the allowed CO_2 emissions of the fleet of producers. It reduces the total emissions by a specified percentage, with respect to the baseline emissions for a given year. Equation (3-22) illustrates the CO_2 reduction constraint, which was introduced in section 3.4.8.

$$E \leq EBL \cdot (1 - ERG) \tag{3-22}$$

3.7 Objective function

The goal of the optimization is to minimize the total yearly cost of supplying all the energy required to sustain a given production level of SCO and bitumen in the oil sands industry. Accordingly, the following problem statement is formulated:

What is the optimal combination of energy production technologies, feedstocks, and CO_2 capture processes to use in the oil sands industry that satisfies energy demands at minimal cost while meeting GHG reduction targets for given bitumen/SCO production levels?

The objective function is defined as the annual costs of producing steam, hot water, hydrogen, and power plus the cost of supplying diesel and process fuel to the oil sands industry. In addition to these energy commodities, the model also accounts for the cost of transporting CO_2 to the sinks via pipeline and for storage/injection costs. Equation (3-42) expresses the objective function in a general form.

minimize [$P_{cost} + H_{cost} + S_{cost} + SS_{cost} + W_{cost} + F_{cost} + D_{cost} + CT_{cost} + CS_{cost}$] (3-42)

Each term in (3-42) comprises the capital, non-fuel operating, and fuel costs, where applicable. Equations (3-43) and (3-44) show the breakdown of the above costs in the optimizer for power and hydrogen plants, in that order.

$$P_{\cos t} = \sum_{p \in \bigcup_{i=1}^{9} S_{P_i}} \left[IP_p \cdot (CAP_p + OM_p) + t \cdot \left(P_p \cdot \frac{HRP_p}{1000} \cdot fuel_{cost} \right) \right] \tag{3-43}$$

$$H_{\cos t} = \sum_{h \in \bigcup_{i=1}^{5} S_{H_i}} \left[IH_h \cdot (CAP_h + OM_h) + t \cdot \left(\frac{fuel_{cost}}{1000} \cdot \left(X_h \cdot HHV_{NG} + Y_h \cdot HHV_C \right) \right) \right] \tag{3-44}$$

where CAP and OM are the fixed annual capital and non-fuel operating costs, respectively. These costs are calculated separately, as explained in section 3.8. The parameter *t* denotes the assumed hours per year for the economic analysis.

The costs of steam and hot water production consist only of the cost of water and fuel as show in (3-45) to (3-47).

$$S_{\cos t} = \sum_{b \in S_B} t \cdot \left[\left(X_b \cdot PSP \cdot \frac{HHV_{NG}}{1000} \cdot NG_{cost} \right) + \left(S_b \cdot water_{cost} \right) \right] \tag{3-45}$$

$$SS_{\cos t} = \sum_{b \in S_{SB}} t \cdot \left[\left(X_b \cdot \frac{HHV_{NG}}{1000} \cdot NG_{cost} \right) + \left(S_b \cdot water_{cost} \right) \right] \tag{3-46}$$

$$W_{\cos t} = \sum_{b \in S_B} t \cdot \left[\left(X_b \cdot (1 - PSP) \cdot \frac{HHV_{NG}}{1000} \cdot NG_{cost} \right) + \left(W_b \cdot water_{cost} \right) \right] \tag{3-47}$$

The costs of process fuel and diesel fuel are specified by (3-48) and (3-49).

$$F_{\cos t} = t \cdot \left[\left(X_{PF} \cdot \frac{HHV_{NG}}{1000} \cdot NG_{cost} \right) + \left(Y_{PF} \cdot HHV_C \cdot coal_{cost} \right) \right] \tag{3-48}$$

$$D_{\cos t} = t \cdot D_D \cdot diesel_{cost} \tag{3-49}$$

Finally, the CO_2 transport and storage/injection costs as a function are given by (3-50) and (3-51). The default pipeline length in the optimizer is 600 km, which covers CO_2 transport from Fort McMurray to a hub in Edmonton (400 km) and from Edmonton to nearby depleted oil fields (200 km radius), such as the Red Water Field [43].

$$CT_{\cos t} = t \cdot \left(\sum_{h \in \bigcup_{i=2}^{5} S_{H_i}} C_h + \sum_{p \in \bigcup_{i=1}^{9} S_{P_i}} C_p \right) \cdot CCT \cdot \frac{PKM}{100} \tag{3-50}$$

$$CS_{\cos t} = t \cdot \left(\sum_{h \in \bigcup_{i=2}^{5} S_{H_i}} C_h + \sum_{p \in \bigcup_{i=1}^{9} S_{P_i}} C_p \right) \cdot CST \tag{3-51}$$

The parameters CCT and CST are the unitary CO_2 transport cost per 100 km pipeline segment and the unitary CO_2 injection/storage cost, respectively. PKM represents the length of the pipeline (in km). The total CO_2 transport and storage costs are a function of the CO_2 captured and the length of the pipeline. The default value of CST is taken from [44]. This study features sensitivity analyses to CCT and CST, both of which are covered in Chapter 5.

3.8 Supporting Equations

In the optimization model, many equations are used in addition to the balances and objective function. For instance, the following set of equations is specified prior the objective function to calculate the amortization rate, the annual capital expenditure, and the annual non-fuel operating and maintenance costs for all plants.

$$AF_i = \frac{RET \cdot (1 + RET^{Book\ life_i})}{(1 + RET^{Book\ life_i}) - 1} \quad \forall i \in \bigcup_{j=1}^{5} S_{H_j} \cup \bigcup_{k=1}^{9} S_{P_k} \tag{3-52}$$

$$CAP_i = Design\ capacity_i \cdot CC_i \cdot AF_i \cdot ESC \qquad \forall i \in \bigcup_{j=1}^{5} S_{H_j} \cup \bigcup_{k=1}^{9} S_{P_k} \tag{3-53}$$

$$OM_i = Design\ capacity_i \cdot CC_i \cdot AOM_i \qquad \forall i \in \bigcup_{j=1}^{5} S_{H_j} \cup \bigcup_{k=1}^{9} S_{P_k} \tag{3-54}$$

Equation (3-52) calculates an annual amortization factor for all plants in the model, based on a desired annual capital charge rate (RET) and each plant's book life expressed in years. The default RET value in the model is 15 percent.

Equations (3-53) and (3-54) set the annual capital charges and non-fuel fixed and variable operating costs, as a function of the overnight costs of each plant. The amortization factors (AF) used in (3-53) are the same that were calculated in (3-52). The

parameter ESC allows for easy capital cost escalation due to external economic forces. In this work, the default plant CC values correspond to the year 2003 and are adjusted for the years 2012 and 2030, by manipulating the value of ESC (default = 1).

The non-fuel operating and maintenance costs factors AOM were taken from the literature for all power and hydrogen plants. In some instances, where a non-fuel O&M costs factor was not explicitly provided in a study, it was calculated by varying the value of AOM while keeping the capital and fuel portions of the unitary energy costs constant, until convergence with the reported unitary values was attained.

Chapter 5 includes sensitivity analyses to parameters RET and ESC for the years 2012 and 2030. The goal is to evaluate the effect of capital charge rates and capital cost escalation on the optimal energy infrastructures calculated by the model.

An additional set of equations is incorporated to the model to manipulate the outputs and convert them to useful information after the optimization has been completed. These equations make it possible to determine the energy costs for all products as well as their CO_2 intensities, based on the optimal solutions.

Equations (3-55) to (3-60) determine the average unitary commodity costs of the optimal infrastructure, excluding CO_2 transport and storage costs.

$$POW_{\cos t} = \frac{P_{\cos t}}{P \cdot t} \tag{3-55}$$

$$HYD_{\cos t} = \frac{H_{\cos t} + (P_h \cdot POW_{\cos t} \cdot t)}{H \cdot t} \qquad \forall h \in S_{H_1} \cup S_{H_2} \tag{3-56}$$

$$STM_{\cos t} = \frac{S_{\cos t}}{S \cdot t} \tag{3-57}$$

$$SST_{\cos t} = \frac{SS_{\cos t}}{SS \cdot t} \tag{3-58}$$

$$HOT_{\cos t} = \frac{W_{\cos t}}{W \cdot t} \tag{3-59}$$

$$PRO_{\cos t} = \frac{F_{\cos t}}{t \cdot \left[\left(\frac{X_{PF} \cdot HHV_{NG}}{1000} \right) + Y_{PF} \cdot HHV_C \right]} \tag{3-60}$$

The entirety of the CO_2 transport costs are due to CO_2 captured in hydrogen and power plants. Thus, the unitary cost of hydrogen and power is adjusted accordingly, as seen in (3-61) and (3-62). These equations give the average cost of a unit of power and hydrogen when CO_2 capture and transport is included in the cost.

$$POW_{cost}^{C+T} = \frac{P_{cost} + CT_{cost}^{P}}{P \cdot t} \tag{3-61}$$

$$HYD_{cost}^{C+T} = \frac{H_{cost} + ((P_h + P_{CO2}^{H}) \cdot POW_{cost}^{C+T} \cdot t) + CT_{cost}^{H}}{H \cdot t} \quad \forall h \in S_{H_1} \cup S_{H_2} \tag{3-62}$$

where CT_{cost}^{P} is the CO_2 transport cost corresponding to all the power plants and CT_{cost}^{H} is the transport cost of the CO_2 captured in all the hydrogen plants. Both of these variables are obtained from equation (3-50), by considering the CO_2 captured from either source on two separate equations.

The second term of equation (3-62) represents the cost of the ancillary power from hydrogen plants and of the power demands for transporting the CO_2 captured in hydrogen plants (P_{CO2}^{H}). The latter is obtained from equation (3-12), by neglecting the CO_2 captured in power plants.

The optimization model also determines the unitary costs of power and hydrogen when CO_2 capture, transport, and storage are considered. To do so, additional terms are added to expressions (3-61) and (3-62), to account for the additional cost due to CO_2 storage/injection as seen below.

$$POW_{cost}^{C+T+S} = \frac{P_{cost} + CT_{cost}^{P} + CS_{cost}^{P}}{P \cdot t} \tag{3-63}$$

$$HYD_{cost}^{C+T+S} = \frac{H_{cost} + ((P_h + P_{CO2}^{H}) \cdot POW_{cost}^{C+T+S} \cdot t) + CT_{cost}^{H} + CS_{cost}^{H}}{H \cdot t} \quad \forall h \in S_{H_1} \cup S_{H_2} \tag{3-64}$$

The advantage of separating the CO_2 transport and storage costs in the unitary costs of hydrogen and power is that by doing so, the impact of transport and storage on the final energy costs of SCO and bitumen can be quantified. Based on the above unitary costs, the energy cost breakdown per commodity can be computed for each product, using equations (3-65) to (3-71). For instance, expression (3-71) is the total calculated energy

cost per barrel of mined bitumen upgraded to SCO using the optimal energy infrastructure (excluding CO_2 transport and storage).

$$POW_{msco} = \frac{P_D^{msco} \cdot POW_{cost}}{SCO_{mined}} \tag{3-65}$$

$$HYD_{msco} = \frac{H_D^{msco} \cdot HYD_{cost}}{SCO_{mined}} \tag{3-66}$$

$$STM_{msco} = \frac{S_D^{msco} \cdot STM_{cost}}{SCO_{mined}} \tag{3-67}$$

$$HOT_{msco} = \frac{W_D^{msco} \cdot HOT_{cost}}{SCO_{mined}} \tag{3-68}$$

$$DIE_{msco} = \frac{D_D^{msco} \cdot diesel_{cost}}{SCO_{mined}} \tag{3-69}$$

$$PRO_{msco} = \frac{PF_D^{msco} \cdot HHV_{NG} \cdot PRO_{cost}}{1000 \cdot SCO_{mined}} \tag{3-70}$$

$$TOT_{msco} = POW_{msco} + HYD_{msco} + STM_{msco} + HOT_{msco} + DIE_{msco} + PRO_{msco} \tag{3-71}$$

Equation (3-65) gives the cost of power per barrel of mined SCO, excluding CO_2 transport and storage (POW_{cost} is used). In the optimization, the cost of power per barrel of SCO is also calculated taking into account CO_2 transport and storage, independently, as shown in (3-72) and (3-73) below.

$$POW_{msco}^{C+T} = \frac{P_D^{msco} \cdot POW_{cost}^{C+T}}{SCO_{mined}} \tag{3-72}$$

$$POW_{msco}^{C+T+S} = \frac{P_D^{msco} \cdot POW_{cost}^{C+T+S}}{SCO_{mined}} \tag{3-73}$$

The hydrogen costs per barrel of SCO are calculated with a set of equations of identical form as (3-72) and (3-73), using the values for H_2 calculated earlier (equations (3-62) and (3-64)). Finally, the energy costs of mined SCO with CO_2 transport and with CO_2 transport and storage are calculated using equations (3-74) and (3-75).

$$TOT_{msco}^{C+T} = POW_{msco}^{C+T} + HYD_{msco}^{C+T} + STM_{msco} + HOT_{msco} + DIE_{msco} + PRO_{msco} \tag{3-74}$$

$$TOT_{msco}^{C+T+S} = POW_{msco}^{C+T+S} + HYD_{msco}^{C+T+S} + STM_{msco} + HOT_{msco} + DIE_{msco} + PRO_{msco} \tag{3-75}$$

The energy costs (and breakdown) of bitumen and SAGD-derived SCO are determined with separate sets of equations identical to (3-65) to (3-75), by using the corresponding energy demands for each product, which are model inputs.

The optimization model also calculates the CO_2 intensities of all products by using a similar approach as that used to determine the energy cost breakdown. In the model, equations (3-76) to (3-81) serve to determine the unitary CO_2 emissions of each energy commodity while the overall CO_2 intensities of SCO and bitumen products are given by (3-82) to (3-84).

$$POW_{CO2} = \frac{1}{P} \cdot \sum_{p \in \bigcup_{i=1}^{9} S_{P_i}} E_p \tag{3-76}$$

$$HYD_{CO2} = \frac{1}{H} \cdot \sum_{h \in \bigcup_{i=1}^{5} S_{H_i}} E_h \tag{3-77}$$

$$STM_{CO2} = \frac{\sum_{b \in S_B} E_b \cdot PSP}{S} \tag{3-78}$$

$$SST_{CO2} = \frac{\sum_{b \in S_{SB}} E_b}{SS} \tag{3-79}$$

$$HOT_{CO2} = \frac{\sum_{b \in S_B} E_b \cdot (1 - PSP)}{W} \tag{3-80}$$

$$PRO_{CO2} = \frac{E_{PF}}{\left(\frac{X_{PF} \cdot HHV_{NG}}{1000} \right) + \left(Y_{PF} \cdot HHV_C \right)} \tag{3-81}$$

The total CO_2 emissions intensity of each product in the optimization is determined by adding up the individual CO_2 emissions corresponding to each of the energy commodities used divided by the barrels of product, as seen below.

$$MSCO_{CO2} = \frac{1}{SCO_{mined}} \left[\begin{array}{l} POW_{CO2} \cdot P_D^{msco} + HYD_{CO2} \cdot H_D^{msco} + \\ STM_{CO2} \cdot S_D^{msco} + HOT_{CO2} \cdot W_D^{msco} + \\ FEF_{DIE} \cdot D_D^{msco} + PRO_{CO2} \cdot \left(\frac{X_{PF} \cdot HHV_{NG}}{1000} \right) \end{array} \right] \tag{3-82}$$

$$TSCO_{CO2} = \frac{1}{SCO_{SAGD}} \left[\begin{array}{l} POW_{CO2} \cdot P_D^{ssco} + HYD_{CO2} \cdot H_D^{ssco} + \\ STM_{CO2} \cdot S_D^{ssco} + SST_{CO2} \cdot SS_D^{ssco} + \\ PRO_{CO2} \cdot \left(\frac{X_{PF} \cdot HHV_{NG}}{1000} \right) \end{array} \right] \quad (3\text{-}83)$$

$$BIT_{CO2} = \frac{1}{BIT} \left[POW_{CO2} \cdot P_D^{bit} + SST_{CO2} \cdot SS_D^{bit} \right] \quad (3\text{-}84)$$

In addition to the energy costs and CO_2 intensities per product (and their breakdown), the optimization model also reports the optimal energy infrastructure for the run as seen in Figure 3-2.

```
EQUATION  SELp1.L             =        0.00  Total # of NGCC
                                             plants
EQUATION  SELp2.L             =        0.00  Total # of PC plants
EQUATION  SELp3.L             =        0.00  Total # of IGCC
                                             plants
EQUATION  SELp4.L             =        0.00  Total # of IGCC w
                                             88% capture plants
EQUATION  SELp5.L             =        0.00  Total # of IGCC w
                                             88% co-capture plants
EQUATION  SELp6.L             =        0.00  Total # of NGCC w
                                             90% capture plants
EQUATION  SELp7.L             =        0.00  Total # of PC w 90%
                                             capture plants
EQUATION  SELp8.L             =        7.00  Total # of NG
                                             Oxyfuel w capture
                                             plants
EQUATION  SELp9.L             =        0.00  Total # of Coal
                                             Oxyfuel w capture
                                             plants


EQUATION  SELh1.L             =        1.00  Total # of SR plants
EQUATION  SELh2.L             =        1.00  Total # of SR w 90%
                                             capture plants
EQUATION  SELh3.L             =        0.00  Total # of IGCC H2
                                             plants
EQUATION  SELh4.L             =        0.00  Total # of IGCC H2 w
                                             90% capture plants
EQUATION  SELh5.L             =       21.00  Total # of IGCC H2 w
                                             90% co-capture plants
```

Figure 3-2. Sample GAMS optimal energy infrastructure

The GAMS input file of the optimization model is included in this manuscript as Appendix II. Chapter 4 presents the results of the optimization for the years 2012 and 2030. The sensitivity analyses for the optimal solutions are the subject of Chapter 5.

Chapter 4

Results and Discussion

In this chapter, the energy demands calculated by the OSOM will be presented alongside the optimal energy infrastructures and costs derived from the optimization model. Sections 4.1 and 4.2 cover the energy demands for the base case and the future production scenarios, respectively. Section 4.3 deals with the optimal energy infrastructures at varying CO_2 reduction levels for years 2012 and 2030 and their associated emissions intensities and costs. All costs and intensities are given on a per-barrel-of-oil basis and are presented according to product (bitumen, mined SCO, or SAGD SCO). The costs in this work are expressed in 2003 USD.

4.1 OSOM Base Case

The base case represents the manner of operation of oil sands producers in the year 2003. Accordingly, the OSOM calculates SCO production on the basis of the total oil sands mined by each producer in that particular year, which are found in [29]. While the technologies used for energy production in the oil sands are known in the year 2003, the same cannot be said of the future, i.e., years 2012 and 2030.Thus, the energy-related CO_2 emissions of the industry are determined only for the base case and not for the OSOM future production scenarios.

4.1.1 Energy demands

In the OSOM, the energy demands for oil sands operations are calculated for all producers and for all production stages, according to energy commodity. Table 4-1 shows the energy demands for the mining stage for producers A1-A3.

The diesel consumption of trucks is higher than that of shovels because there are more trucks than shovels in the reference mining fleet. This reflects the fact that a single shovel can load multiple trucks in the same amount of time that it takes for a truck to deliver its payload. Moreover, the shovels travel much shorter distances than trucks do.

Table 4-1. OSOM-BC energy demands in 2003 - Mining

Variable	Units	A1	A2	A3
Oil sands mined	tonne/h	17,402	17,405	5,126
Bitumen saturation	%	11.4	11.3	12.4
Diesel - Shovels	L/h	3,969	3,969	1,169
Diesel - Trucks	L/h	14,981	14,985	4,413
Total Diesel demands	L/h	18,950	18,954	5,582

In the bitumen Conditioning/Hydrotransport stage, the energy demands consist of hot water, steam, and electricity, as shown in Table 4-2. In the base case, only producer A1 uses bitumen conditioning, whereas the others hydrotransport the mined sand. This mirrors the way the industry operated in 2003, where the majority of the oil sands were subjected to the more energy-efficient hydrotransport process. By 2012 and afterward, all the mined sand is assumed to be hydrotransported.

Table 4-2. OSOM-BC energy demands in 2003 – Conditioning/Hydrotransport

Variable	Units	A1	A2	A3
Hot water - conditioning	tonne/h	1,030	N/A	N/A
Hot water - hydrotransport	tonne/h	4,291	5,222	1,538
Total hot water demands	tonne/h	5,321	5,222	1,538
Steam - conditioning	tonne/h	112	N/A	N/A
Power - hydrotransport	kW	38,577	65,176	20,417

Table 4-3 summarizes the energy demands of the bitumen extraction stage. Extraction is executed in two stages. In primary extraction, the oil sand slurry from conditioning/hydrotransport is diluted with hot water, causing the bitumen to rise to the surface as a froth. In secondary extraction, the froth is deaerated and diluted with naphtha and centrifuged to remove traces of sand and water. In all, the extraction processes consumes generous amounts of hot water, steam, and power, in addition to requiring naphtha solvent. The breakdown of these commodities is shown in Table 4-3.

From Table 4-3 it is evident that the power required to pump tailings to disposal ponds is very substantial. The production of tailings in the hot water process is elevated;

in fact, the OSOM-BC mass balances show that the ratio of tailings produced to bitumen recovered from the oil sand is 16, on a mass basis. Therefore, reductions in water requirements for bitumen extraction have a great potential to simultaneously cut energy demands in oil sands operations, and ultimately, their energy and emissions intensities.

Table 4-3. OSOM-BC energy demands in 2003 – Extraction

Variable	Units	A1	A2	A3
Hot water – primary extraction	tonne/h	7,139	7,140	2,103
Steam – secondary extraction	tonne/h	130	132	43
Naphtha – secondary extraction	tonne/h	1,299	1,324	428
Power – secondary extraction	kW	12,944	10,079	3,256
Power – tailings disposal	kW	100,771	126,975	38,681
Total power demands	kW	113,715	137,053	41,937

The energy demands of the bitumen upgrading stage are different for all producers, as it is a function of their particular upgrading scheme. Hence, the breakdown of these energy demands varies widely from producer to producer, as seen in Table 4-4.

Table 4-4. OSOM-BC energy demands in 2003 – Upgrading

Variable	Units	A1	A2	A3
Steam - Diluent Recovery	tonne/h	900	925	304
Steam - Vacuum Distillation	tonne/h	71	108	36
Steam – Fluid coking	tonne/h	326	N/A	N/A
Total steam demands	tonne/h	1,298	1,033	340
Power - LC Fining	kW	21,061	N/A	34,858
Power - Fluid Coking	kW	38,325	N/A	N/A
Power - Delayed Coking	kW	N/A	24,347	N/A
Total power demands	kW	59,386	24,347	34,858
Process fuel - LC Fining	Nm^3/h	3,135	N/A	5,190
Process fuel - Delayed Coking	Nm^3/h	N/A	25,103	N/A
Total process fuel demands	Nm^3/h	3,135	25,103	5,190
	GJ/h	119	995	197
Hydrogen – LC Fining	tonne/h	3.0	N/A	7.0
Hydrogen – Hydrotreatment	tonne/h	26.5	24.5	10.8
Total hydrogen demands	tonne/h	29.5	24.5	17.8

The power demands of producer A1 are more pronounced than the rest. This is due to the fact that its upgrading scheme involves coking and hydrocracking, both of which consume power. In contrast, producers A2 and A3 use only one primary upgrading step followed by hydrocracking, which requires less power overall. The upside of the upgrading scheme of A1 is that it achieves a higher overall bitumen conversion and produces less petcoke byproduct than that of A2.

One noteworthy difference in the upgrading stages among producers is the process fuel demands of producer A2, which are roughly nine times greater than those of A1. The former uses delayed coking, a process requiring more heat than either fluid coking or LC-Fining. In the OSOM-BC, natural gas is used as process fuel, which increases the cost of upgrading on a per barrel basis.

In addition to SCO produced from mined oil sands, the base case also includes production of bitumen via SAGD. The energy demands for this process consist of power and steam. Table 4-5 summarizes the demands for producer C.

Table 4-5. OSOM-BC energy demands in 2003 – Thermal (SAGD) bitumen

Variable	Units	C
Steam – SAGD	tonne/h	5,642
Power – SAGD	kW	45,120
Process fuel – lift gas	Nm^3/h	37,616

The steam demands for SAGD bitumen production are calculated in the base case on the basis of a steam-to-oil ratio (SOR) of 2.4. While the value of SOR is reservoir specific and may change over its productive life, 2.4 is a figure representative of an economically-feasible SAGD operation, not uncommon in commercial calculations [32].

Table 4-5 includes the amount of natural gas required for injection into the reservoir, which aids in pumping the produced bitumen out of the reservoir. The reader must note that this gas is later used in boilers for steam production, and is thus lumped with the natural gas demands for SAGD steam production in the OSOM.

The overall energy demands of each producer, according to energy commodity are computed in the OSOM-BC and presented in Table 4-6. The breakdown of these energy demands by commodity, expressed in GJ/h is shown in Table 4-7.

Table 4-6. OSOM-BC energy demands in 2003 – Producer comparison

Variable	Units	A1	A2	A3	C
Diesel	L/h	18,950	18,954	5,582	N/A
	L/bbl	1.96	2.14	1.43	N/A
Hot water	tonne/h	12,460	12,362	3,640	N/A
	tonne/bbl	1.29	1.39	0.93	N/A
Steam - Process	tonne/h	1,539	1,166	383	N/A
	tonne/bbl	0.16	0.13	0.10	N/A
Steam - SAGD	tonne/h	N/A	N/A	N/A	5,642
	tonne/bbl	N/A	N/A	N/A	0.39
Power – All stages	kW	211,678	226,577	97,212	45,120
Power – Ancillary	kW	21,168	22,658	9,721	4,512
Total power demands	kW	232,845	249,235	106,933	49,632
	kWh/bbl	24.1	28.1	27.4	3.4
Hydrogen	tonne/h	29.5	24.5	17.8	N/A
	MMSCF/h	12.5	10.4	7.5	N/A
	MMSCF/bbl	1,293	1,169	1,929	N/A
Process fuel	Nm^3/h	3,135	25,103	5,190	N/A
	GJ/h	119	995	197	N/A
	GJ/bbl	0.012	0.108	0.051	N/A

The base case results reveal that the unitary energy demands for SCO production are approximately 1.5 GJ/bbl. The energy intensity of producers A3 are the highest of all (1.55 GJ/bbl), followed by A1 and A2 (1.53 and 1.49 GJ/bbl). Published values of energy intensities in oil sands operations/heavy oil upgrading [40] for the year 2001 are 1.38 GJ/bbl. The upgrading scheme used in this study is unknown, thus direct comparison is not possible. Nevertheless, the OSOM-derived values seem reasonable.

The upgrading scheme has a strong influence over the energy intensity. For instance, although the energy requirements for mining and extraction of producers A1 and A3 are lower than those of A2, the latter's energy for upgrading is lower than that of

the former producers, which results in overall lower energy intensity. In other words, the base case results suggest that the energy intensity of SCO production from mined oil sands is proportional to the magnitude of the energy demands for the upgrading process.

In terms of energy consumption according to commodity, for the base case, the results reveal that steam generation is responsible for roughly half the energy demands of the fleet. Hydrogen, power, and hot water combined account for 46% of the total energy demands of the fleet while the share of process fuel and Diesel fuel is only 6%.

Table 4-7. OSOM-BC energy demands in 2003 – By commodity

Variable	Units	A1	A2	A3	C	Fleet
Diesel	GJ/h	726	726	214	0	1,665
Hot water	GJ/h	1,822	1,437	423	0	3,682
Steam	GJ/h	5,268	3,989	1,311	11,175*	21,742
Power	GJ/h	1,720	1,841	790	367	4,717
Hydrogen	GJ/h	5,157	4,282	3,114	0	12,553
Process fuel	GJ/h	119	955	197	0	1,272
Total per producer	GJ/h	14,812	13,229	6,049	11,541	45,631
Oil production	bbl/h	9,650	8,868	3,907	14,583	37,008
Energy Intensity	GJ/bbl	1.53	1.49	1.55	0.79	1.23

* Used for SAGD extraction, steam quality is different than that of process steam for mining/extraction operations

For bitumen production, the bulk of the energy demands is due to SAGD steam generation (97%). The energy intensity of producer C is 0.79 GJ/bbl bitumen produced. Although the above intensity value is lower than those corresponding to producers A1-A3, the reader must keep in mind that the product of the latter is upgraded bitumen, whereas the product of C is diluted bitumen (not upgraded).

4.1.2 GHG Emissions

Figure 4-1 presents the calculated GHG emissions intensity for SCO and bitumen according to producer and process stage. In mining operations (producers A1-A3), the bulk of the emissions come from the bitumen upgrading step, which accounts for approximately 70 percent of the process emissions for producers A1 and A2. The total calculated GHG intensity for these producers is 0.083 and 0.080 tonne CO_2 eq/bbl SCO,

respectively. The upgrading emissions of producer A3 represent 80 percent of its total GHG intensity, which was found to be 0.087 tonne CO_2 eq/bbl SCO. Its hydrogen-intensive upgrading scheme is the reason for such high value. The emissions distribution of the other process stages shows that roughly half of the non-upgrading emissions belong to the bitumen extraction stage. The first two process stages and the balance of the plants cause 15 percent of the total GHG emissions, on average. The mining and hydrotransport stages are less energy-intensive than extraction and upgrading, consuming only diesel fuel, hot water, and moderate amounts of electricity and steam. In contrast, bitumen extraction and upgrading require large quantities of steam, hot water and power, and in the case of the latter stage, also a good deal of H_2, as shown in Table 4-6.

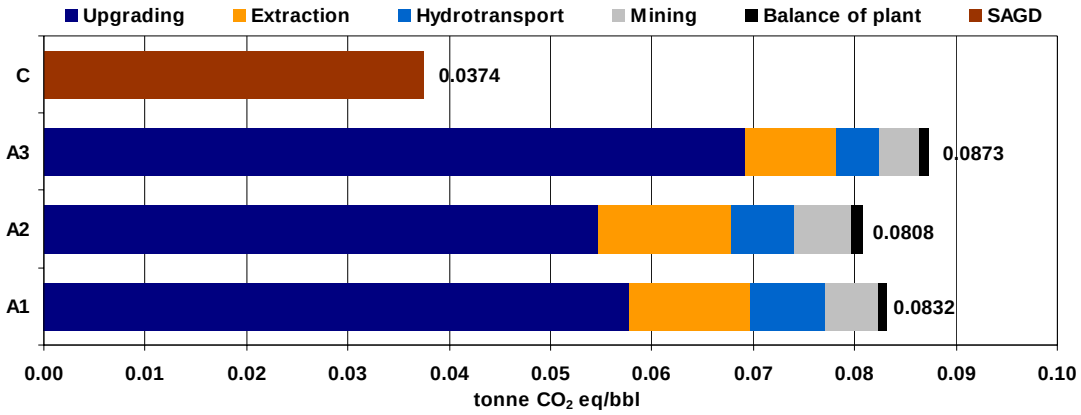

Figure 4-1. OSOM Base Case GHG emissions intensity by process stage in 2003

GHG emissions intensities reported in other studies [4, 10] correlate well with the values calculated by the OSOM for producers A1-A3. For instance, published values for mined bitumen upgraded to SCO range from 0.080 to 0.118 tonne CO_2 eq/bbl SCO [4] whereas the corresponding OSOM-BC values are 0.080 – 0.087 tonne CO_2 eq/bbl SCO.

The OSOM-BC values are always expected to be lower than those observed in commercial operations. The chief reasons for this are: 1) the OSOM does not include any fugitive emissions such as flaring, tailing ponds, land reclamations, etc and 2) the OSOM base case assumes that natural gas is the only fuel/feedstock for energy production. This was done to attenuate the complexity of modeling multiple fuel usage in multiple stages, with integration at the unit level, which is a common situation in the oil sands industry. Moreover, the quality and properties of the fuels used in oil sands plants, such as refinery gas, coker gas, fuel oil, and petcoke, vary widely from producer to producer, and even

from unit to unit. Hence, by assuming a single fuel for all operations, for al producers, these variations are eliminated and the performance of individual production schemes can be better studied.

The GHG emissions intensity of thermal bitumen production is relatively high, when compared to that of mined bitumen. In mining operations, diluted bitumen is available at the end of the extraction stage. The average GHG intensity of the mining, hydrotransport, and extraction stages is 0.022 tonne CO_2/bbl bitumen, for producers A1-A3. This value excludes fugitive emissions of tailing ponds or those generated during overburden removal. The emissions intensity associated with producing a barrel of bitumen via SAGD, on the other hand, is 0.0374 tonne CO_2/bbl bitumen, or 68% higher than the intensity of mined bitumen, excluding fugitive and overburden emissions.

The GHG emissions intensity for thermal bitumen production predicted by the OSOM (producer C) is lower than those from other studies [4, 10]. The published figures range from 0.052-0.060 tonne CO_2/bbl bitumen. It is unknown if these values include fugitive emissions (the OSOM does not consider these emissions). Also, the steam quality and SOR from the aforementioned studies is unknown. Hence, direct comparison of these values to the OSOM-BC GHG intensities is not possible.

Table 4-8. GHG emissions for all producers in tonne CO_2 eq/h (2003 average)

Producer	Hot water	Steam	Power	Hydrogen	Diesel	Process	CH4+N2O	Total
A1	86	248	81	281	51	6	51	803
A2	68	188	87	233	51	45	46	716
A3	20	62	37	169	15	9	29	341
C	0	526	17	0	0	0	3	546
Total	173	1023	222	683	116	60	129	2406

Of all the energy commodities consumed during SCO and thermal bitumen production, steam, hydrogen, and power are the most GHG-intensive. From Table 4-8, it can be seen that steam, H_2, and power are responsible for 80 percent of all GHG emissions in the Athabasca region oil sands industry in 2003. The individual contribution of each of the above is 42%, 28% and 10% of the total GHG emissions, respectively. The GHG emissions resulting from hot water production are the fourth largest, accounting for 7% of the total.

The results also show that 95 % of all emissions are CO_2, the rest being methane and nitrous oxide. These substances are emitted by power plants and H_2 plants, and for the most part, represent the GHG emissions upstream of the process, due to natural gas and coal production and transport. Their contribution to the total GHG emissions for the OSOM-BC is almost as significant as that of hot water. In the OSOM, these non-CO_2 emissions are calculated based on the emissions factors presented in [40, 41]. Furthermore, the combined calculated emissions from process fuel consumed during upgrading and diesel fuel were found to be relatively low, accounting for just 7 percent of the total, for all producers.

In mining operations alone, hydrogen production for upgrading is the leading source of GHG emissions, accounting for 37 percent of the total emissions. Steam and power represent 27 and 11 percent of total GHG emissions, respectively. The combined contribution of hot water production, diesel and process fuel use and non-CO_2 emissions is a quarter of the total GHG emissions of mining operations, which is estimated to be 1,860 tonne CO_2 eq/h by the OSOM-BC

The results from the OSOM-BC suggest that the GHG abatement efforts in oil sands operations should be focused on the upgrading stage. In other words, considerable opportunities exist for less CO_2-intensive production of steam, hydrogen, and power in the oil sands industry in Alberta.

4.2 OSOM Future Production Scenarios

The OSOM-FPS forecasts the demands for all energy commodities in the Athabasca region oil sands industry, based on the future bitumen and SCO production estimates shown in Table 2-1. All producers are active in the OSOM-FPS in the years 2012 and 2030.

The calculated energy demands for the Athabasca region oil sands industry are summarized in Tables 4-9 and 4-10. The total energy demands, according to commodity, as well as individual energy demands for the upgrading process are shown for all producers. This allows for a straightforward comparison of the magnitude of the energy required as a function of the upgrading process used to produce SCO, for different producers and/or bitumen extraction technologies. Also, the OSOM-FPS results show the

amounts of hydrogen and SAGD steam that could be potentially produced from internally generated fuel gas and solution gas, for producers A-B and B-C, respectively. This energy integration has the potential to reduce future fuel (natural gas, or other) requirements in hydrogen and steam production.

4.2.1 Year 2012

The projected energy demands for the oil sands industry in the year 2012 are shown in Table 4-9. Unlike the base case, oil sands operations in 2012 include producers B1-B3, which extract bitumen via SAGD and upgrade it to SCO. The results from the OSOM-FPS reveal that the energy intensity for these producers is, 1.93 GJ/bbl on average. This value is approximately 60 percent higher, on average, than that of producers A1-A3, which extract bitumen via mining.

In terms of energy demands of the fleet, the model results show that between 2003 and 2012, the total demand grows by a factor of 2.6, from 45 TJ/h to 120 TJ/h. Of all the commodities, hydrogen registered the sharpest increase, followed by SAGD steam between 2003 and 2012. This, unsurprisingly, reflects the addition of SCO production from SAGD in 2012, which is, as noted above, more energy intensive than that of mined SCO or SAGD bitumen. In 2003, the energy demands for hydrogen accounted for 27% of the fleet's total. In 2012, this figure increased to 33%. SAGD steam rose from 24% to 28% between 2003 and 2012. Nevertheless, the total combined energy demands for process and SAGD steam remains unchanged from 2003, accounting for roughly half of the energy demands of the entire fleet.

In absolute terms, producers A1-A3 lead all others in energy demands. Their combined demands are half of the fleet demands. Producers B1-B3 and producers C are responsible for 35% and 14% percent of the total energy demands, respectively. This trend is explained by the breakdown of the SCO and bitumen production. SCO from mining operations in 2012 is 975,000 bbl/d while SCO from SAGD operations is 525,000 bbl/d. Diluted bitumen production via SAGD is 500,000 bbl/d. The total energy demands associated with a certain product are thus, a function of its production level expressed in bbl/d and its energy intensity, expressed in GJ/bbl.

Table 4-9. OSOM-FPS projected energy demands of the oil sands industry in 2012

Variable	Units	A1	A2	A3	B1	B2	B3	C	Fleet
Diesel	L/h	31,654	28,945	14,880	N/A	N/A	N/A	N/A	75,479
	GJ/h	1,212	1,109	570					2,891
Hot Water	tonne/h	20,775	18,878	9,705	N/A	N/A	N/A	N/A	49,357
	GJ/h	2,414	2,194	1,128					5,736
Steam - Process	tonne/h	2,601	1,780	1,021	439	540	680	N/A	7,062
	GJ/h	8,902	6,091	3,494	1,503	1,848	2,329		24,167
Upgrading	tonne/h	2,235	1,578	907	439	540	680	N/A	6,380
Balance of plant	tonne/h	366	202	114	N/A	N/A	N/A		682
Steam - SAGD	tonne/h	N/A	N/A	N/A	2,052	2,989	3,765	8,061	16,866
	GJ/h				4,092	5,962	7,510	16,087	33,643
From solution gas	tonne/h	N/A	N/A	N/A	15	21	27	57	120
Power	MW	351.9	380.6	284.0	82.6	44.1	134.3	70.9	1,351.6
	GJ/h	2,600	2,811	2,105	610	334	1,000	524	9,983
Upgrading	MW	102.6	37.2	92.9	58.7	17.1	92.9	-	401.4
Balance of plant	MW	249.4	343.4	192.1	23.9	28.0	42.4	70.9	950.2
Hydrogen	tonne/h	50.9	37.4	47.5	21.5	17.3	47.5	N/A	222
	MMSCF/h	21.6	14.8	20.1	9.1	7.3	20.1		94
	GJ/h	9,170	6,732	8,547	3,874	3,107	8,547		39,976
From fuel gas	tonne/h	14.1	18.2	6.2	4.0	8.4	6.2		59
Process fuel	Nm3/h	5,415	38,335	13,835	7,538	17,639	13,835	N/A	96,651
	GJ/h	206	1,459	256	287	673	526		3,678
Total per producer	GJ/h	24,504	20,396	16,370	10,366	11,924	19,911	16,602	120,074
Oil production	bbl/h	16,667	13,542	10,417	5,208	6,250	10,417	20,833	83,333
Energy Intensity	GJ/bbl	1.47	1.51	1.57	1.99	1.91	1.91	0.80	1.44

4.2.2 Year 2030

The energy demands of the industry intensify by a factor of 2.7 between 2012 and 2030, totalling 319.5 TJ/h in 2030. This increase neatly follows the growth in SCO production in the same timeframe. Since the OSOM-FPS does not account for technological breakthroughs in oil sands operations, the specific energy intensities of bitumen and SCO remain unchanged between 2012 and 2030.

In 2030, the OSOM-FPS results reveal that much like between 2003 and 2012, the share of hydrogen and SAGD steam in the total energy demands rise again between 2012 and 2030. The former figure grows by one percentage point (34.3%) while the latter rises by 3 points (31%). The combined contribution of process and SAGD steam still remains at approximately 50 percent of the total.

Table 4-10. OSOM-FPS projected energy demands of the oil sands industry in 2030

Variable	Units	A1	A2	A3	B1	B2	B3	C	Fleet
Diesel	L/h	63,308	57,889	32,736	N/A	N/A	N/A	N/A	153,934
	GJ/h	2,425	2,217	1,254					5,896
Hot Water	tonne/h	41,550	37,755	21,351	N/A	N/A	N/A	N/A	100,655
	GJ/h	4,829	4,388	2,481					11,698
Steam - Process	tonne/h	5,202	3,560	2,246	1,405	2,160	2,722	N/A	17,296
	GJ/h	17,803	12,182	7,687	4,810	7,394	9,314		59,191
Upgrading	tonne/h	4,470	3,155	1,995	1,405	2,160	2,722	N/A	15,909
Balance of plant	tonne/h	732	404	251	N/A	N/A	N/A		1,387
Steam - SAGD	tonne/h	N/A	N/A	N/A	6,565	11,955	15,061	16,121	49,703
	GJ/h				13,096	23,847	30,041	32,157	99,140
From solution gas	tonne/h	N/A	N/A	N/A	47	85	107	114	353
Power	MW	703.9	761.2	627.1	264.2	180.7	541.3	141.8	3,220.4
	GJ/h	5,199	5,622	4,632	1,952	1,334	3,998	1,047	23,784
Upgrading	MW	204.1	74.3	204.4	187.7	68.6	371.7	-	1,112.0
Balance of plant	MW	498.8	686.8	422.7	76.5	112.0	169.6	141.8	2,108.4
Hydrogen	tonne/h	101.8	74.8	104.4	68.8	69.0	189.8	N/A	608.7
	MMSCF/h	43.1	31.7	44.2	29.1	29.2	80.4		257.7
	GJ/h	18,339	13,465	18,802	12,397	12,429	34,186		109,619
From fuel gas	tonne/h	30.3	36.4	13.7	14.9	33.6	24.0		154.8
Process fuel	Nm3/h	10,831	76,669	30,436	24,123	70,771	55,339	N/A	268,170
	GJ/h	412	2,917	1,158	918	2,693	2,106		10,204
Total per producer	GJ/h	49,008	40,791	36,015	33,172	47,697	79,646	33,204	319,532
Oil production	bbl/h	33,333	27,083	22,917	16,667	25,000	41,667	41,667	208,334
Energy Intensity	GJ/bbl	1.47	1.51	1.57	1.99	1.91	1.91	0.80	1.53

The most significant change in trends with respect to 2003 and 2012 is that by 2030 SCO from SAGD (producers B1-B3) is responsible for half of the total energy demands

of the fleet, followed by SCO from mining operations at 40% (A1-A3) and SAGD bitumen at 10%. The dramatic rise of the energy demands of producers B1-B3 from 35% to 50% of the total energy demands of the fleet is due to the combination of high anticipated production and SAGD SCO having the highest energy intensity of all products.

On a broader perspective, a comparison of Tables 4-9 and 4-10 reveals that steam, SAGD steam, hydrogen, and electricity are anticipated to have the highest demand growth during the overall period under study. Steam demands will increase by a factor of 2.3 between 2003 and 2012 and by 2.4 between 2012 and 2030. The demands for SAGD steam are projected to triple between 2003 and 2012 and triple again between 2012 and 2030. Likewise, hydrogen demands in the oil sands industry in Alberta will triple between 2003 and 2012 and grow by a factor of 2.7 thereafter. The increase in electricity demand is less than those observed for the above commodities, but still significant. The OSOM-FPS results reveal that between 2003 and 2012, electricity demands will roughly double, and increase 2.4 times between 2012 and 2030.

The OSOM-FPS results are valid only for the specified individual producer outputs for each year in Table 2-1. The reader must be aware that although the cumulative production estimates for 2012 and 2030 are invariable, the proportion of the total SCO produced by each producer is not. In other words, for a given year (2012 or 2030), it is possible to meet the thermal and mined SCO production targets with a wide variety of producer combinations. For instance; in 2012, the forecasted mined SCO production is specified at 975,000 bbl/d. This SCO could be entirely produced by producer A1, or by a combination of A1 and A3, or by a number of other producer combinations. The same is true of the thermal SCO future production estimates.

In the OSOM-FPS, different producer combinations will impact the total energy demand mix. For example, if most of the mined SCO comes from producer A3, the calculated hydrogen demands will be greater than if most of the SCO was supplied by producer A2. This behaviour of the model simply reflects the impact that different upgrading technologies have on the energy demands composition and magnitude, in the Athabasca region oil sands industry.

In this study, the individual contributions of each SCO producer were set to reflect the anticipated mid-term growth of producers in the region. However, the reader must keep in mind that the precise future output of each particular producer in the physical world is subject to uncertainty and to market/ economic forces. The former element is an inevitable part of forecasting while the latter can and will often change readily in response to a multitude of factors that are too numerous and complex to be accounted for in the model presented in this study. The OSOM model relies on known, commercially proven technologies that are currently used in the Canadian oil sands industry and to the best of the authors' knowledge, will continue to be applied in the foreseeable future (i.e., SAGD, LC-Fining, etc.) Thus, the use of future or experimental technologies for bitumen extraction and/or upgrading is beyond the scope of this work, as is the forecasting of a "most likely producer mix" subject to uncertainty and market/economic/technology forces. The OSOM-FPS calculates all energy demands based on user-specified production levels for all producers A, B, and C.

4.3 GAMS Optimization Model

A MILP (Mixed Integer Linear Program) optimization model has been developed to optimally meet the energy demands of the oil sands industry. The goal of this model is to minimize the total cost of producing all required energy commodities for the oil sands industry, while reducing CO_2 emissions by a given percentage for planned production capacity in the years 2012 and 2030. The results from the optimizer will determine the number power plants, hydrogen plants (and their types) that will satisfy the demands for specified SCO and bitumen production levels.

4.3.1 Year 2003: costs and emissions

Although energy production in 2003 is not optimized, the optimization model is used to calculate the costs of the energy required to produce SAGD bitumen and mined SCO. This is accomplished by deactivating all power and hydrogen plants in the optimizer, except for NGCC and SMR plants without capture. Hence, the assumed energy production infrastructure corresponding to the year 2003 is specified and its economics can be assessed using the GAMS model.

Since the focus of this study is the assessment of the economic and environmental impacts of energy production technologies and feedstocks in the oil sands industry, the unitary energy costs in $/bbl and the CO_2 intensities in tonne CO_2/bbl are used to measure the said impacts. This not only allows for consistent comparison among years, but can also be used to effortlessly assess the overall costs or intensities of any particular product in any year, or combinations of both, on the basis of the barrels produced.

The energy costs calculated by the optimizer for the year 2003 are $13.63/bbl and $4.37/bbl for SCO and bitumen, respectively. The annual energy costs for the fleet are $3.365 billion, including capital charges, fuel, and non-fuel operating expenses. In terms of emissions, the intensities for SCO and bitumen are 0.075 and 0.037 tonne CO_2/bbl, respectively. The total CO_2 emissions of the fleet are 2,249 tonne CO_2/h.

It is useful to remark at this point that the above costs are not the operating costs associated with SCO and bitumen production. They are rather the energy portion of the total operating costs. Hence, items such as non-energy-producing assets, overburden removal, and land reclamation are not covered in the costs presented above. Only energy-related capital and operating costs are contemplated in the GAMS optimization model, irregardless of the year and the product/oil sands producer mix.

The optimizer provides a wealth of economic and environmental data. For instance, the breakdown of the 2003 energy costs, as shown in graphical form in Figure 4-2 is available for all products, as a function of the energy infrastructure and feedstocks. The optimizer results reveal that for the 2003 case, hydrogen, steam, and hot water production account for over three quarters of the cost of producing a barrel of SCO, while for SAGD bitumen, the bulk of the energy costs is due to steam generation.

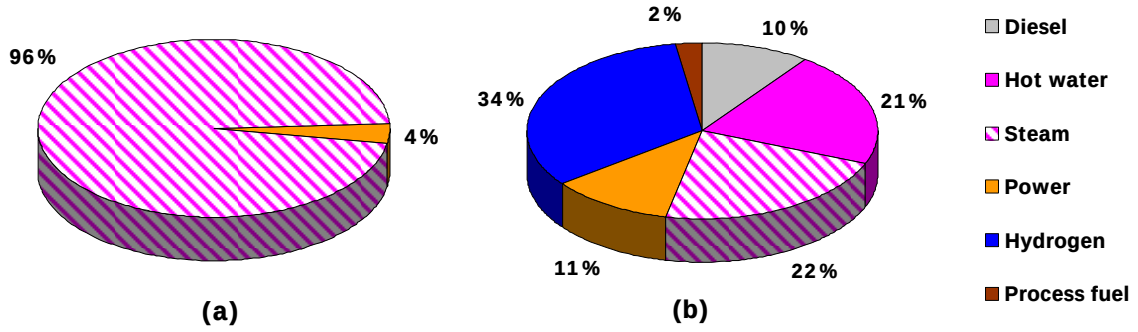

Figure 4-2. 2003 energy costs breakdown by commodity for (a) bitumen and (b) SCO

The costs calculated by the optimizer are a function of a large number of cost and other parameters. To realistically assess the energy costs in different years, however, only a limited number of parameters are assumed to change between 2003 and 2012. These parameters and their corresponding values for the timeframe under study are shown in Table 4-11. The rationale for the cost variation is, generally speaking, the anticipated escalation in fuel prices [47, 48] and the effect of inflation and construction materials on the capital costs of new plants. The specifics concerning the selected values for the years 2012 and 2030 will be discussed in later sections. The effect of fuel prices on the cost of energy and the optimal energy infrastructures will be discussed in Chapter 5.

Table 4-11. Economic assumptions for optimization in years 2012 and 2030

Parameter	Units	2003*	2012	2030
Overnight capital cost increase	%	0	50	100
Coal cost	$/GJ	1.9	2.2	3.0
Natural gas cost	$/GJ	6	9	12
Diesel cost	$/L	0.7	1.0	1.5
IGCC plant availability	%	80-85	83-88	90
CO_2 transport cost (600 km)	$/tonne CO_2 /100 km	N/A	1.2	1.4
CO_2 storage cost	$/tonne CO_2	N/A	6	8

* Reference year

4.3.2 Year 2012

The increase in oil sands production between 2003 and 2012 is the driver behind the growth in energy demands, as discussed earlier in section 4.2.1. The goal of the optimization model is to determine the best way to produce this energy at minimal cost and to reduce CO_2 emissions. In the following sections, the assumptions for the industry in 2012 will be discussed and the optimal costs and infrastructure for varying CO_2 reduction levels will be presented.

4.3.2.1 Baseline costs and emissions

The most important assumption for the optimization of energy demands in 2012 is that the power and hydrogen plants that existed in 2003 are still in operation in 2012.

Since the plant book lives of the above energy producers is between 20-30 years, plants that are operational in 2003 are assumed to be a fixed part of the energy infrastructure in 2012. This is accomplished in the optimization model by specifying a set of constraints concerning the energy demands in 2003, as explained in section 4.6.3.

Table 4-11 lists the assumed changes in economic parameters between 2003 and 2012. The overnight capital costs associated with building new plants rises by 50 percent with respect to 2003 levels. Likewise, the cost of fuels is assumed to escalate by a similar percentage [48].

A necessary parameter for the optimizer is the baseline CO_2 emissions of the fleet. In 2003, these emissions are easily calculated, since both the energy demands and the energy production technologies are known. In 2012, however, only the former are known, being in fact the OSOM-FPS demands. Speculating which technology or technologies will be used for hydrogen and power production in the oil sands industry by 2012 is a fruitless exercise. Hence, in this study, the baseline CO_2 emissions and energy costs are determined assuming a "business as usual" (BAU) scenario for the oil sands industry.

In this BAU situation, the technologies and feedstocks used in 2003 remain unchanged. Therefore, natural gas is used for power and hydrogen production, and no CCS is applied to any of the above plants. The advantage of using the BAU as the baseline for the optimization, is that it makes it possible to quantify the impacts of inaction, both on the technologic and environmental operations of the oil sands industry. Conversely, the BAU baseline is also a reference point to measure improvements in CO_2 intensity and energy costs associated with bitumen and SCO production.

Table 4-12. Baseline energy costs and CO_2 intensities comparison – 2012 and 2003

Product	2012		2003	
	$/bbl	tonne CO_2/bbl	$/bbl	tonne CO_2/bbl
Mined SCO	18.86	0.075	13.63	0.075
Thermal SCO	19.94	0.092	N/A	N/A
Bitumen	7.76	0.037	4.37	0.037

Table 4-12 summarizes the baseline energy costs and CO_2 intensities for the year 2012 and compares them with the year 2003. A comparison of values across products

within the year 2012 reveals that the energy cost for thermal SCO production is 6% higher than that of mined SCO. Table 4-12 also reveals that a 50 percent increase in the price of natural gas and diesel between 2003 and 2012 causes a 38% increase in the energy costs for SCO and 44% for bitumen, respectively. The CO_2 intensity of thermal SCO is roughly one-fifth higher than that of mined SCO, according to Table 4-12.

Cumulatively, the baseline CO_2 emissions for 2012 calculated by the optimizer are 5,887 tonne CO_2/h. Similarly, the total annual energy costs of the fleet are $11.95 billion. The above figures are 2.6 and 3.6 times higher than the emissions and energy costs of the oil sands industry in 2003, respectively.

4.3.2.2 Optimization results under CO_2 constraints

The economic and environmental impacts of the infrastructure employed for energy production vary depending on the specified CO_2 reduction target for the fleet of plants. A useful way to express these changes is by calculating the energy costs and CO_2 intensities per product as a function of the CO_2 reduction target/level. Table 4-13 summarizes the results for the year 2012 for varying CO_2 reduction levels.

Table 4-13. Optimal costs and emissions in 2012 under CO_2 constraints

Product	**Mined SCO**		**SAGD SCO**		**Bitumen**		**Fleet**	
CO_2 reduction	$/bbl	tonne CO_2/bbl	$/bbl	tonne CO_2/bbl	$/bbl	tonne CO_2/bbl	tonne CO_2 emitted	tonne CO_2 captured
Baseline*	18.86	0.075	19.94	0.092	7.76	0.037	5,887	0
0 %	17.09	0.075	18.12	0.094	7.71	0.037	5,887	1,379
10 %	17.14	0.067	18.25	0.081	7.70	0.038	5,298	2,237
20 %	17.51	0.057	18.56	0.073	7.72	0.037	4,710	2,593
25 %	21.43	0.052	22.48	0.069	7.86	0.036	4,415	1,857

* Reference – not optimized

The emissions of the base case and the zero percent reduction case are identical. However, the energy costs for all products are less in the latter case. The base case energy production infrastructure is not optimal. Hence, its energy costs are one-tenth higher compared to those of the optimized infrastructure.

The results from the optimizer reveal that energy cost savings are possible between zero percent capture level and 20 percent capture level, on the basis of the set of inputs in the year 2012. The calculated energy costs at 20 percent CO_2 reduction are 7 percent lower than the baseline costs, and the CO_2 intensities of the former are 21-23 percent lower than those of the latter for SCO.

On average, CO_2 capture levels in the mid-twenties can be achieved with energy costs that are on par with baseline costs. When capture levels approximate 25%, the energy costs escalate rapidly for all products. Table 4-13 shows that the highest CO_2 reduction level possible using the optimal energy infrastructure is 25%. At this level, energy costs are approximately 13% higher than baseline costs. However, important reductions in CO_2 intensities are also achieved. The CO_2 intensities reductions at maximum CO_2 capture are 31% and 26%, for mined and SAGD SCO, respectively.

The energy costs and CO_2 intensities of bitumen are not affected by changes in the energy infrastructure due to increased CO_2 capture levels. Even at maximum capture, the energy cost increase and CO_2 intensity decrease is only 1 percent with respect to the baseline. This is explained by the fact that power represents a nominal fraction of the energy requirements for bitumen production, compared to steam (see Table 4-7). Therefore, increases in the cost of power and reductions in power-related CO_2 emissions due to CO_2 capture have little impact on the final energy costs and intensities of bitumen.

The total energy costs are the sum of the energy production costs, plus the CO_2 capture costs, plus the costs of transporting the captured CO_2 and the costs of injecting it underground. The total energy costs are also a function of the individual commodity consumption per barrel, which is different for each product (see Tables 4-6 and 4-9).

The optimization results include a breakdown of the energy costs, which is presented in Table 4-14. The total energy costs for SCO production on Table 4-14 are divided into: energy production and capture (EC), CO_2 transport (T), and CO_2 injection/storage (S). The results for bitumen are excluded from Table 4-14, as its increase in energy cost due to CO_2 transport and storage is nil at capture levels below 25 percent and negligible at maximum capture (0.1%).

The bulk of the energy cost is due to energy production and CO_2 capture, both of which are set by the types and numbers of power and hydrogen plants used to produce the

energy. CO_2 transport and storage costs account for between 2-3.5% of the total energy costs, for all CO_2 capture levels shown in Table 4-14. With the specified distance of 600 km used in this study, CO_2 transport costs are marginally higher than injection/storage costs for both mined and SAGD SCO, by a fraction of a percentage point.

Table 4-14. Optimal energy costs breakdown for SCO in 2012 (in $/bbl)

Product	**Mined SCO**				**SAGD SCO**			
CO_2 reduction	EC	T	S	Total	EC	T	S	Total
Baseline*	18.86	N/A	N/A	18.86	19.94	N/A	N/A	19.94
0 %	16.80	0.16	0.13	17.09	17.79	0.19	0.14	18.12
10 %	16.67	0.26	0.21	17.14	17.70	0.31	0.24	18.25
20 %	16.97	0.31	0.23	17.51	17.93	0.36	0.27	18.56
25 %	21.03	0.23	0.17	21.43	22.06	0.24	0.18	22.48

EC = energy production and CO_2 capture, T = CO_2 transport (600 km), S = CO_2 injection/storage

* Reference – not optimized

The results from Table 4-14 reveal that CO_2 transport and storage costs for SAGD SCO are nominally higher than those of mined SCO. This is mostly due to the higher energy intensities of the former, which involve more CO_2 being produced and captured.

The CO_2 transport and storage costs for SCO rise steadily between 0-20% capture levels, peaking in the mid-twenties, and drop at maximum capture. This behaviour is linked to the rise in the number of coal-based energy producers between 0-20% capture and the subsequent transition to all-natural gas energy production with capture at the maximum CO_2 reduction level (see Table 4-15). Coal-based energy production with CO_2 capture produces more CO_2 per unit of energy than natural gas-based plants. Hence, more CO_2 needs to be captured, transported, and stored in the former case than in the latter.

The results from the optimizer suggest that CO_2 transport and storage cause only a modest increase in the cost of energy required for SCO production. This increase ranged between 29-54 cents/bbl for mined SCO and 33-63 cents/bbl for SAGD SCO, for CO_2 reduction levels between 0-25% in the year 2012.

4.3.2.3 Optimal energy infrastructures

The costs and emissions presented in Table 4-13 are a function of the infrastructure used to produce the energy. A unique infrastructure is chosen by the

optimizer based on the CO_2 emissions reduction level and other inputs specified by the user. A summary of the optimal infrastructures for 2012 is shown in Table 4-14.

The results from the optimizer shown in Table 4-15 reveal that certain technologies are chosen more often than others, while other are never selected irrespective of the capture level. NGCC plants and SMR plants appear throughout the entire range of capture levels. This is a constraint imposed on the optimizer, which is used to represent the plants from 2003 that are still active in 2012 (see section 4.3.2.1). According to the model results, 2 NGCC and 13 SMR plants from 2003 are still operating in 2012.

The results from Table 4-15 show that coal-fired IGCC power plants are absent from the optimal energy infrastructure. In contrast, all hydrogen production technologies are implemented at one point or another in 2012, and both natural gas and coal feedstocks are selected. Generally speaking, the optimization results suggest that natural gas-fuelled power plants and coal-based hydrogen plants are favoured in 2012 for CO_2 reduction levels between 0-20 percent. At maximum CO_2 reduction, only natural gas plants with CO_2 capture are used, excluding the existing non-capture 2003 plants.

Table 4-15. Optimal energy infrastructures for varying CO_2 reduction levels in 2012

CO_2 reduction	**P1**	**P2**	**P8**	**H1**	**H2**	**H3**	**H4**
Baseline*	4			40			
0 %	3			13		3	3
10 %	2	1		13		1	5
20 %	3			13			6
25 %	2		3	13	27		

P1 = NGCC, P2 = PC, P8 = NG Oxyfuel, H1 = SMR, H2 = SMR with CO_2 capture, H3 = H_2 IGCC, H4 = H_2 IGCC with CO_2 capture

* Reference – not optimized

The results from Table 4-15 are based on the assumption that CO_2 and H_2S co-capture, transport, and injection is not allowed. However, if this restriction is lifted, the optimal infrastructures change accordingly, as Table 4-16 shows.

The first noticeable difference between the 2012 optimal infrastructures with and without co-capture is that the maximum CO_2 reduction level rises from 25% to 25.7 %. This is due to the fact that the IGCC co-capture plants feature slightly lower CO_2

emissions per unit of hydrogen produced than SMR with capture plants [21]. Another difference between cases is the substitution of NG oxyfuel plants by NGCC plants with capture at 25 percent reduction.

Table 4-16. Optimal energy infrastructures in 2012 (Co-capture)

CO_2 reduction	**P1**	**P2**	**P6**	**P8**	**H1**	**H2**	**H3**	**H5**
Baseline*	4				40			
0 %	3				13		3	3
10 %	2	1			13		1	5
20 %	3				14	2		5
25 %	2		2		13			6
25.7 %	2			2	13			6

P1 = NGCC, P2 = PC, P6 = NGCC with CO_2 capture, P8 = NG Oxyfuel, H1 = SMR, H2 = SMR with CO_2 capture, H3 = H_2 IGCC, H5 = H_2 IGCC with CO_2 and H_2S co-capture

* Reference – not optimized

The implementation of CO_2 + H_2S co-capture technology, as shown in Table 4-16 brings cost-savings opportunities in oil sands operations in 2012. This technology completely replaced separate CO_2 and H_2S capture plants once the co-capture restriction in the optimizer was eliminated. The actual cost savings achieved are presented in Table 4-17, according to product.

Table 4-17. Optimal costs comparison between capture (A) and (B) co-capture cases in 2012

Product	**Mined SCO**		**SAGD SCO**		**Bitumen**	
CO_2 reduction	A	B	A	B	A	B
Baseline*	18.86	18.86	19.94	19.94	7.76	7.76
0 %	17.09	16.95	18.12	17.95	7.71	7.71
10 %	17.14	17.01	18.25	18.09	7.70	7.70
20 %	17.51	17.44	18.56	18.44	7.72	7.73
25 %	21.43	17.93	22.48	18.72	7.86	7.79
24.7 %	N/A	18.22	N/A	18.94	N/A	7.81

* Reference – not optimized

Between 0-20% CO_2 reductions, the savings for SCO products are modest (less than 2%). However, at levels above 20% reduction, the energy savings of the co-capture infrastructure over the no co-capture one are quite significant, reaching almost 20%. This is explained by the cost advantage of hydrogen from coal over hydrogen from NG under

CO_2 constraints. A tonne of hydrogen produced in an IGCC plant with co-capture is more economical than a tonne produced in an SMR plant with capture. Also, the co-capture case requires fewer power plants (NG oxyfuel) than the no co-capture case, which results in lower overall capital requirements.

The results from Table 4-17 must be interpreted with caution. Firstly, the viability of transporting H_2S-rich gas across long distances in populated areas may be questionable. Second, the capital costs of the pipeline required to transport such gas and the injection costs could be higher than those for CO_2 alone, which are the only ones used in this study, even for co-capture cases. Finally, the viability of sour CO_2 gas injection may be hampered by the characteristics of the depleted oil reservoir or deep formations.

Irrespective of the suitability of co-capture in CO_2-constrained oil sands operations in 2012, the optimization results highlight technologies of interest for further R&D. Among these, NGCC with and without capture, along with NG oxyfuel plants seem to offer advantages for power production in 2012. For hydrogen production, gasification-based plants seem to hold the greatest promise, as evidenced by the optimal results from Tables 4-15 and 4-16.

4.3.3 Year 2030

In 2030, according to the production estimates from [10] and summarized in Table 2-1, the total oil production is expected to reach 5 million bbl/d. Bitumen production will double between 2012 and 2030, while total SCO production will rise by a factor of 2.7 in the same period, to reach 4 million bbl/d. The optimal costs, emissions, and infrastructures for the oil sands based on the above production levels will be presented in this section.

4.3.3.1 Baseline costs and emissions

Unlike in the 2012 scenario, in 2030 no older plants are assumed to remain from previous years. The reason for this assumption is two-fold. First, the lapse between 2012 and 2030 is 18 years, which is very close to the book life of many power and hydrogen plants. Thus, rather than include aging plants in the optimizer for 2030, all plants are assumed to be new in this year. Secondly, between 2012 and 2030, the growth of the oil sands is expected to be more dramatic than between 2003 and 2012, reaching impressive

highs. Concurrently, the political and international pressure for cleaner oil sands operations is expected to also rise in the second decade of this millennium. This could effectively lead to the decommissioning of CO_2-intensive plants and their replacement with CO_2-capture ready units. To reflect this possible trend, the 2030 optimization models do not include any user-imposed restrictions with respect to the number of older plants that must remain active alongside newer plants chosen by the optimizer.

The economic assumptions for this year are summarized in Table 4-11. The overnight capital costs for all plants doubles between 2003 and 2030. This roughly corresponds to an annual plant cost index increase of 3.5%. While this number may sound alarming to some, the reality is that the capital and construction costs of plants in Alberta have doubled over the last five years, at the time of print. According to many industry insiders and analysts, the booming oil industry in Alberta combined with labour shortages and steel price increases will continue to push construction expenses upwards. Therefore, doubling the capital costs per unit of installed capacity for all plants in the optimization model is deemed a reasonable assumption, that for some, it might even be considered conservative.

The fuel costs between 2012 and 2030 are assumed to escalate by 50%, on average. Among these, natural gas has the highest price uncertainty. Natural gas price forecasts over the past 6 years have tended to underestimated future gas prices, sometimes by as much as 50% of observed prices [2, 45, 48]. Thus, in this work, a more "pessimistic" outlook of future natural gas prices is assumed, which seems to be more consistent with prices for the past 6 years. The approach on this work is to assume a price for a given year and then perform sensitivity analyses at a wide range of fuel prices, over a broad range. The results of such analyses are found in Chapter 5.

Other parameters that are subject to cost increases in 2030 are the assumed CO_2 transportation and storage costs. The former is affected by materials cost escalation as discussed earlier. The latter is assumed to rise as the difficulty of injecting CO_2 underground increases with reduced storage capacity over time. As a result, CO_2 transport costs increase roughly 20% between 2012 and 2030 while storage costs rise by 30% in the same period.

Finally, the availability of gasification-based plants is assumed to reach 90% in 2030. This assumption rests upon the fact that gasification is still in an early stage of its development cycle and major improvements can be likely expected by 2030. This is particularly true seeing that many companies in Europe, Asia, and North America have plans underway to build IGCC-based power to be commissioned by 2010-2012 [46].

Similarly to the year 2012, in 2030 the baseline energy costs and emissions are based on a BAU scenario for the production levels in the latter year. As such, the baseline emissions and costs represent the likely values associated with oil sands operations in 2030 if natural gas was used as fuel and no CO_2 capture was implemented. All improvements in costs and emissions are thus measured against the BAU baseline values in this project.

The baseline costs for 2030, along with those of 2012 and 2003 are shown in Table 4-18. The CO_2 intensities remain unchanged by 2030, as the baseline technologies and feedstocks for energy production are the same for all years. The energy cost increase due to higher natural gas prices in 2030 is 31%, on average, with respect to 2012.

Table 4-18. Baseline energy costs and CO_2 intensities comparison – 2003 - 2030

Product	2003		2012		2030	
	$/bbl	tonne CO_2/bbl	$/bbl	tonne CO_2/bbl	$/bbl	tonne CO_2/bbl
Mined SCO	13.63	0.075	18.86	0.075	24.70	0.075
Thermal SCO	N/A	N/A	19.94	0.092	26.22	0.092
Bitumen	4.37	0.037	7.76	0.037	10.15	0.037

On an industry-wide basis, the baseline energy costs in 2030 add up to $21.7 billion while the baseline CO_2 emissions calculated by the model are 15,659 tonne/h. These figures reveal that between 2012 and 2030, the energy costs rise by 80% while the emissions of the oil sands industry increase by a factor of 2.7 over the same period.

4.3.3.2 Optimization results under CO_2 constraints

Compared to 2012, in 2030, the maximum attainable CO_2 emissions reduction level is higher, reaching 39.7% (co-capture; no co-capture case maximum is 38.6%), as shown in Table 4-19. This figure is aided by the elimination of base case energy constraints (see section 3.6.3), which allows the optimizer unrestricted freedom to select

energy production technologies. The elimination of base case energy constraints is also responsible for the high disparity between the baseline and the 0% capture level, which is in fact, an optimized baseline case. In 2030, the energy costs of the former are roughly 20% higher than those of the latter. In other words, when the optimizer is given total freedom to choose technologies and feedstocks, the resulting energy costs are lower than when certain amount of energy must be produced with fixed technologies/feedstocks, as is the case in 2012 (see section 4.3.2.1).

Table 4-19. Optimal costs and emissions in 2030 under CO_2 constraints

Product	**Mined SCO**		**SAGD SCO**		**Bitumen**		**Fleet**	
CO_2 reduction	$/bbl	tonne CO_2/bbl	$/bbl	tonne CO_2/bbl	$/bbl	tonne CO_2/bbl	tonne CO_2 emitted	tonne CO_2 captured
Baseline*	24.70	0.075	26.22	0.092	10.15	0.037	15,659	0
0 %	20.21	0.077	21.87	0.091	9.96	0.038	15,659	6,887
	20.08	0.077	21.58	0.091	9.99	0.038	15,659	6,481
10 %	20.46	0.069	22.04	0.080	9.99	0.038	14,093	8,444
	20.34	0.069	21.80	0.081	10.01	0.038	14,093	7,977
20 %	20.74	0.060	22.28	0.070	10.00	0.038	12,527	9,971
	20.43	0.060	21.98	0.069	9.99	0.038	12,527	9,943
30 %	21.30	0.050	22.64	0.063	10.06	0.037	10,961	10,505
	20.92	0.050	22.24	0.062	10.05	0.037	10,961	10,835
35 %	22.09	0.044	23.02	0.060	10.17	0.036	10,178	11,539
	21.30	0.045	22.45	0.059	10.10	0.037	10,178	12,055
38 %	26.98	0.041	28.22	0.057	10.28	0.036	9,709	9,237
	22.09	0.041	23.01	0.057	10.17	0.036	9,709	11,777
38.6 %	29.49	0.040	31.03	0.057	10.32	0.036	9,615	7,756
	22.32	0.041	23.18	0.057	10.18	0.036	9,615	11,559
39.7 %	22.71	0.039	23.48	0.056	10.21	0.036	9,442	11,612

* Reference – not optimized

Note: shaded rows correspond to CO_2 and H_2S co-capture ca

Table 4-19 showcases the results corresponding to cases where CO_2 and H_2S co-capture is allowed (shaded areas) and when it is not, for identical CO_2 capture levels. The optimization results reveal that energy cost savings are possible up to a CO_2 reduction level of 36%, when co-capture is not implemented. On the other hand, if co-capture of CO_2 and H_2S is allowed, cost savings are possible across the full range of capture levels

shown on Table 4-19. These savings range between 8-19% with respect to the baseline energy costs, for both capture and co-capture cases.

The energy costs for all products rise as the CO_2 capture level increases. Taking the zero percent case as a reference, the cost increases at maximum CO_2 reduction are 46%, 42%, and 4%, for mined SCO, SAGD SCO, and bitumen, respectively. The zero percent capture case is chosen as a reference because it produces identical amounts of energy as the baseline, with equal CO_2 emissions, but using an optimized infrastructure. Thus, the cost penalty for capture (or co-capture) can be determined by comparing it to the most economical case with identical emissions to the baseline case.

When co-capture is allowed, the results form Table 4-19 show that at maximum CO_2 reduction, the increment in the energy costs of all products are relatively modest with respect to the optimal baseline. These cost increases are 13%, 11%, and 2% for mined SCO, SAGD SCO and bitumen, in that order. The energy infrastructure for the co-capture case consists of a smaller number of plants (lower capital costs) than that of the no co-capture case. Also, more plants in the former infrastructure are fuelled by coal than by natural gas (lower operating costs). The combination of the above two factors largely explains the difference in energy costs between the co-capture and capture cases, described above. A more detailed description of the reasons for the observed cost difference is given in section 4.3.3.3.

The impact of CO_2 reduction on individual product CO_2 intensities is significant for mined and SAGD SCO. The reductions in CO_2 intensities for these products range between 1.4% and 47% with respect to the baseline values. The intensity reductions when co-capture is allowed are marginally higher than those observed when co-capture is not allowed. In terms of products, mined SCO has the highest intensity reduction at 46-47% while the reduction for SAGD SCO is 39-40%, with respect to baseline CO_2 intensities. The CO_2 intensity of bitumen is unaffected by changes in overall CO_2 reduction levels, as explained previously in section 4.3.2.2.

The breakdown of the total SCO energy costs for 2030 is presented in Table 4-20. The breakdown of energy costs for bitumen is not included as the contribution of CO_2 transport and storage/injection is zero at CO_2 reduction levels below 35% and only 0.2% above that.

Table 4-20. Optimal energy costs breakdown for SCO in 2030 – no co-capture (in $/bbl)

Product	Mined SCO				SAGD SCO			
CO_2 reduction	EC	T	S	Total	EC	T	S	Total
Baseline*	24.70	N/A	N/A	24.70	26.22	N/A	N/A	26.22
0 %	19.58	0.33	0.30	20.21	21.11	0.40	0.36	21.87
10 %	19.68	0.41	0.37	20.46	21.10	0.49	0.45	22.04
20 %	19.82	0.48	0.44	20.74	21.17	0.59	0.52	22.28
30 %	20.32	0.52	0.46	21.30	21.46	0.63	0.55	22.64
35 %	20.97	0.60	0.52	22.09	21.77	0.67	0.58	23.02
38 %	26.05	0.50	0.43	26.98	27.22	0.54	0.46	28.22
38.6 %	28.71	0.42	0.36	29.49	30.21	0.45	0.37	31.03

EC = energy production and CO_2 capture, T = CO_2 transport (600 km), S = CO_2 injection/storage

* Reference – not optimized

Much like in 2012, the T+S costs of SAGD SCO are slightly higher than those of mined SCO in 2030. Likewise, the cost of transport is nominally higher than the storage/injection costs for both products. An important difference between 2012 and 2030 is that the combined T+S costs of the latter year account for 2.6-4.4% of the total energy costs. This is an increase of almost 2 percentage points with respect to 2012 values (2-3.5%). Two main reasons for this escalation is the increase in transport and storage costs in 2030 and differences in the composition of the energy infrastructures between years.

According to Table 4-20, the T+S costs for SCO peak at CO_2 reduction levels of 35% and decrease thereafter. The relative contribution of T+S to the total cost of energy per barrel of SCO reaches its minimum values at maximum CO_2 capture. This is due to the combination of very low overall CO_2 production (all plants are fuelled by natural gas) and high energy costs due to extensive CO_2 capture levels.

When co-capture is allowed, the energy cost breakdown changes, as shown in Table 4-21. All of the trends described above remain true for the co-capture case, with the exception of the relative contribution of T+S to the total cost of energy per barrel of SCO. In the no co-capture case, the minimum T+S value occurs at maximum CO_2 reduction level, whereas for co-capture, the minimum value occurs at zero capture. Also, although in both instances the T+S cost share peaks at CO_2 reduction levels of 35% and drops beyond that, the drop for no co-capture is roughly twice as sharp as for co-capture. In the former case, the T+S cost share goes from 5% at 35% CO_2 reduction to 2.6% at

maximum capture. In the co-capture case the T+S cost share drop between 35% and maximum CO_2 capture is half a percentage point for mined SCO and one-third of a percentage point for SAGD SCO.

Table 4-21. Optimal energy costs breakdown for SCO in 2030 – co-capture (in $/bbl)

Product	**Mined SCO**				**SAGD SCO**			
CO_2 reduction	EC	T	S	Total	EC	T	S	Total
Baseline*	24.70	N/A	N/A	24.70	26.22	N/A	N/A	26.22
0 %	19.48	0.32	0.28	20.08	20.86	0.38	0.34	21.58
10 %	19.61	0.39	0.34	20.34	20.92	0.46	0.42	21.80
20 %	19.51	0.49	0.43	20.43	20.88	0.58	0.52	21.98
30 %	19.90	0.54	0.48	20.92	21.05	0.63	0.56	22.24
35 %	20.12	0.62	0.56	21.30	21.18	0.67	0.60	22.45
38 %	20.94	0.61	0.54	22.09	21.74	0.68	0.59	23.01
38.6 %	21.20	0.6	0.52	22.32	21.92	0.67	0.59	23.18
39.7 %	21.58	0.6	0.53	22.71	22.21	0.68	0.59	23.48

EC = energy production and CO_2 capture, T = CO_2 transport (600 km), S = CO_2 injection/storage

* Reference – not optimized

In short, the optimization results show that at CO_2 reduction levels above 35%, the combined cost of CO_2 transport and storage expressed as a percentage of the total energy cost remains almost constant when co-capture is allowed. When co-capture is not allowed, the T+S cost share of the total energy cost diminishes by almost half in the same CO_2 reduction level range.

Unlike in the no co-capture case, when co-capture is allowed in the optimization, the contribution of T+S costs to the total energy costs for bitumen is higher. The optimizer results reveal that CO_2 transport and storage account for 0.1-0.3% of the total energy costs for bitumen in the latter case, for CO_2 reduction levels above 30%. In contrast, when co-capture is not permitted, these costs are fixed at 0.2% for CO_2 reduction levels of 35% and greater.

In absolute terms, the cost portion due to T+S ranges between 0.63-1.25 $/bbl SCO for no co-capture and 0.6-1.27 $/bbl SCO when co-capture is allowed in the optimal infrastructures. These figures are roughly twice as high as those calculated by the model for the year 2012. But, the maximum CO_2 reduction levels for the former year are significantly higher than that of the latter year (39.7% vs. 25%).

4.3.3.3 Optimal energy infrastructures

The infrastructures associated with the energy cost and CO_2 intensity data presented in Tables 4-19 to 4-21 are shown on Tables 4-22 and 4-23, for no co-capture and co-capture cases, respectively.

Table 4-22. Optimal energy infrastructures for varying CO_2 reduction levels in 2030 – no co-capture

CO_2 reduction	**P1**	**P2**	**P6**	**P8**	**H1**	**H2**	**H3**	**H4**
Baseline*	9				109			
0 %		5			1		8	14
10 %	1	5			1		4	17
20 %	1	5			1		1	20
30 %	6				1	1		21
35 %			7		1	1		21
38 %				10		65		9
38.6 %				12		106		1

P1 = NGCC, P2 = PC, P6 = NGCC with CO_2 capture, P8 = NG Oxyfuel, H1 = SMR, H2 = SMR with CO_2 capture, H3 = H_2 IGCC, H4 = H_2 IGCC with CO_2 capture

* Reference – not optimized

When co-capture is not allowed in the optimal infrastructures, power production without capture (NGCC and PC) is possible for CO_2 reduction levels of up to 30%. As CO_2 reductions approximate their limit, only natural gas-fired power plants with capture (NGCC with capture and NG Oxyfuel) are chosen, as shown in Table 4-22. Hydrogen production via gasification with and without capture is favoured for CO_2 reduction levels of 35% and lower. Above 35 percent CO_2 reduction, hydrogen production via SMR with capture is the dominant technology, although a small number of gasification plants with capture are still present even at maximum CO_2 reduction.

In 2030, when co-capture is not permitted, no coal-based power technology other than PC is chosen for the entire range of CO_2 reduction values. Similarly to the 2012 year, in 2030, natural gas-based power production technologies are favoured over coal-based technologies at high CO_2 reduction levels. Likewise, coal-based H_2 production is favoured for CO_2 reduction levels up to 35 percent. Above 35 percent, natural gas-based hydrogen production with capture is favoured over coal-based hydrogen.

If CO_2 and H_2S co-capture is permitted in 2030, the composition of the optimal infrastructure is quite different than when the opposite is true. The data on Table 4-23 reveal that: a) gasification-based hydrogen production is the predominant technology across the full range of CO_2 reduction levels and b) the power production technology mix is more varied when co-capture is allowed. Also, when co-capture is allowed, the maximum CO_2 reduction level rises by 1 percentage point.

Table 4-23. Optimal energy infrastructures for varying CO_2 reduction levels in 2030 –co-capture

CO_2 reduction	**P1**	**P2**	**P5**	**P6**	**P8**	**H1**	**H2**	**H3**	**H4**	**H5**
Baseline*	9					109				
0 %	1	5				1		8		13
10 %	1	5				1		5		16
20 %		6				1		1	1	19
30 %	3	2	1			1				21
35 %	2		4			1	1			21
38 %			1	6		1	1		1	20
38.6 %	1			7		1	1			21
39.7 %					7	1	1			21

P1 = NGCC, P2 = PC, P5 = IGCC with CO_2 and H_2S co-capture, P6 = NGCC with CO_2 capture, P8 = NG Oxyfuel, H1 = SMR, H2 = SMR with CO_2 capture, H3 = H_2 IGCC, H4 = H_2 IGCC with CO_2 capture, H5 = H_2 IGCC with CO_2 and H_2S co-capture

* Reference – not optimized

The most significant impact of co-capture in the optimal energy infrastructures is seen on the energy costs for all oil products. The lower costs observed due to H_2 production via gasification with co-capture is the combination of three main factors: 1) these plants feature the lowest CO_2 emissions of all H_2 production technologies. 2) The plants are fuelled by coal, which is a more economical fuel than natural gas. 3) All gasification-based H_2 plants included in this study co-produce modest amounts of power.

The above features of gasification-based co-capture plants combined have a large effect on the economics of energy production and, indirectly, on the composition of the power production plant fleet. For instance, as the CO_2 reduction level increases from 35% to 38%, in a no co-capture scenario (Table 4-22), the optimizer replaces H_2 gasification plants with SMR plants with capture. The latter plants have lower CO_2 emissions than the former, but they consume natural gas, driving the energy costs upward. SMR plants with

capture require external power to operate, which requires more plants to be added to the existing power plant fleet (10 vs. 7). However, since the overall fleet emissions must drop, the optimizer chooses oxyfuel plants instead of less expensive NGCC plants with capture. The final effect of increasing the CO_2 reduction from 35% to 38% is a sharp rise in both power and energy costs, due to more costly technologies and fuels.

Another factor that affects the composition of the power plant technology mix at increasing CO_2 reduction levels is the amount of captured CO_2 that needs to be transported and stored. In the optimization, CO_2 emissions can be reduced by either using natural gas as a fuel or capturing CO_2, or both. If CO_2 capture is the dominant mechanism for emissions abatement, the power requirements for CO_2 transport and storage/injection will rise. Conversely, if natural gas is used as a fuel for energy production, the power requirements for CO_2 transport and storage/injection will generally decrease due to lower captured CO_2 volumes. Combinations of the above CO_2 emissions reduction mechanisms will affect the number and nature of the power plants required.

An important observation concerning the relationship between the power plant technology and their numbers in each optimal infrastructure must be made. Invariably, when CO_2 capture is implemented, the capital and power costs will rise, while the efficiency and (often) net power output will decrease, with respect to no-capture plants. The latter explains, for instance, the observed increase in the total number of power plants at CO_2 reduction levels higher than 35% for the co-capture case in 2030. The NGCC plants without capture and the IGCC plants with co-capture have both higher power outputs than the NGCC plants with capture and oxyfuel plants. Thus, as CO_2 reduction levels increase, more plants are needed to sustain the total power output.

When analyzing the optimal infrastructures, the reader must keep in mind that the output of the power and hydrogen plants is not necessarily identical among plants for a given CO_2 reduction case or among different CO_2 reduction levels. The optimizer will choose the optimal output of each one of the plants featured in the infrastructures, subject to built-in maximum plant output constraints, which are a function of the user-specified plant availability factors.

All of the effects explained above interrelate in the optimization, sometimes with additive effects and sometimes with opposing ones. Hence, an *a priori* prediction of the

final shape of the optimal energy infrastructure for a particular set of inputs and CO_2 reduction level is a difficult endeavour. The optimization results, however, consistently yield the energy infrastructure that meets all constraints and satisfies the energy demands of the oil sands industry at minimal cost.

Two important conclusions can be drawn concerning the optimal energy infrastructures for 2030. Firstly, the most promising technologies for power production are predominantly natural gas-based: NGCC, with and without capture and oxyfuel. Supercritical coal plants are appealing at CO_2 reduction levels between 20-30%. Secondly, gasification-based technology for hydrogen production is attractive at most CO_2 reduction levels, in all its modes (co-capture, no capture, and capture). If CO_2 and H_2S co-capture is allowed, significant energy cost reductions can be attained via H_2 gasification. However, if co-capture is not permitted, H_2 production via SMR with CO_2 capture is imperative to achieve CO_2 reductions greater than 35 percent. This however, comes with a painful cost penalty.

On the basis of the optimal energy infrastructures for 2030, it seems that R&D efforts must focus on the improvement of the techno-economics of natural gas-based power production technologies, particularly NGCC with capture and oxyfuel. Concerning hydrogen production, the focus should be on gasification-based technologies. Of special interest is the improvement of the separate CO_2 and H_2S capture plant to reach the techno-economic performance of its co-capture counterpart. As seen in Table 4-19, H_2 production via gasification with co-capture offers dramatic cost reduction opportunities over all the other hydrogen production technologies featured in this study.

Figure 4-3 illustrates the impact of the optimal energy infrastructures on CO_2 emissions. In 2012, the optimal infrastructure allows for a maximum 25% reduction in emissions with respect to baseline values. In 2030, the maximum reduction rises to 39% of baseline emissions. In absolute terms, however, the CO_2 emissions between 2003 (baseline) and 2012 (optimal) double and increase by a factor of 2.2 between 2012 (optimal) and 2030 (optimal). The increased CO_2 emissions are caused by the dramatic increase in oil production in the Athabasca region, which is over five-fold between 2003 and 2030.

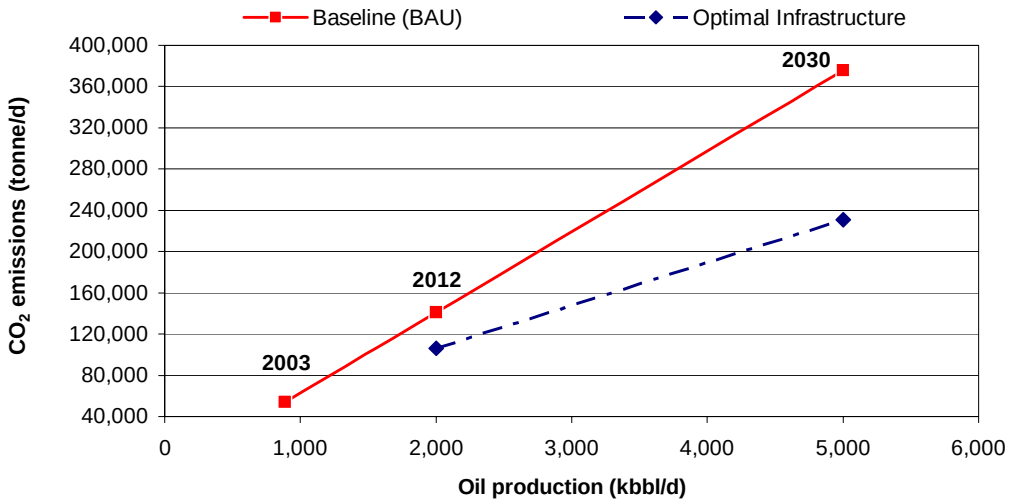

Figure 4-3. CO_2 emissions comparison baseline vs. optimal energy infrastructures 2003-2030

4.4 Model Limitations

The OSOM and GAMS models were developed on the basis of published data concerning oil sands operations, energy production, and CCS technologies. Nevertheless, there are limitations to the capabilities of these models. In this project, the limitations are due to the combination of two aspects.

Firstly, this project is, to the best knowledge of the researchers involved, the first attempt to model and optimize energy production in the oil sands industry as a whole, subject to CO_2 constraints. As such, some degree of simplification and a number of assumptions were necessary, given the frequent absence of information required. The latter sometimes involved incorporating technoeconomic data from a variety of studies that were not specific to energy generation and CO_2 emissions in the oil sands industry (i.e., factors from [39] and [41] were used to determine non-CO_2 GHG emissions from power and hydrogen production in the OSOM. It is the hope of the author that future developments in this area of study will improve the robustness of the models.

Secondly, the reader must bear in mind that the modelling and optimization of top-level large-scale plant networks inherently dictates that the level of detail within the model be limited. The above is necessary to improve the tractability and computational solution of large mixed integer linear optimization models, where size increases exponentially with the number of integer variables involved. Thus, in this work, some

sacrifice in complexity and a limited set of analysis options were needed to guarantee that the models could be solved using the software and computational resources at hand.

The model limitations are also associated with uncertainties surrounding costs and technological assumptions used when estimating future energy demands and their corresponding optimal energy infrastructures. Hence, the following discussion will focus on future fuel and technology costs and assumptions concerning future technological development and oil production levels in the oil sands industry.

4.4.1 Costs

Fuel. During the model analysis stage, only one study that featured fuel price forecasts extending to the year 2030 was found [48]. This study was not particular to the Alberta context. The reported natural gas costs in other mid-term forecasts varied widely from source to source [47, 48, 51, 52, 53]. Also, when current gas prices were compared to the above forecasts, the former were found to be different than the latter. The above facts called the suitability of the published costs into question, particularly for natural gas prices in the year 2030, where uncertainty is intuitively the highest. The approach in this work was then simplified by selecting natural gas prices which follow an annual escalation factor of 2.6% and 1.8% for coal in 2003-2030. The above escalation factors reflect the expectations concerning fossil fuels: natural gas production in Western Canada is rapidly declining while the abundant supply of coal [1] equal more stable prices.

The future fuel costs featured in this work are deliberately higher than those found elsewhere, to address the empirical observations concerning oil and natural gas prices, which have a tendency to surpass analysts' expectations. To further address these price uncertainties, this work features a comprehensive set of sensitivity analyses to natural gas and coal prices (Chapter 6) over a wide range of values, for all years under study.

Technology. The optimization model in its current form is limited in that it is does not incorporate potential cost reductions and technical improvements according to the concept of learning curves [49]. In the case studies featured in this work for 2012 and 2030, the overnight capital costs increase over time due to expectations of a sustained economic "boom" in the province of Alberta and because of sustained labour shortages and soaring construction expenses. Many projects which are currently under construction

have shown substantial cost overruns in the last decade [11, 50]. In light of the size of the bitumen reserves and potential sustained increase in oil prices in the foreseeable future, the assumptions of cost increases for new energy production plants in Alberta is deemed pertinent, within a macroeconomic framework.

4.4.2 Future SCO and Bitumen Production

Another area in the OSOM model which limits its capabilities is its reliance on third-party forecasted oil production levels. The user must specify the individual quantities of SCO and bitumen to be produced in a given year to estimate the energy demands of the industry for that particular production level and combination of producers. These OSOM-FPS inputs are susceptible to unpredictable market forces and socio-political events that affect the output of individual producers or the industry as a whole. In this work, the oil production levels are taken from a comprehensive study [10] that included the views of industry, government, and research organizations in Alberta. This *Oil Sands Technology Roadmap*, is in the opinion of the author, an adequate source of future production data for the oil sands industry.

4.4.3 Future Technologies

The inability to predict the extent and shape of the technological developments in both energy production and oil sands operations post-2003 is another drawback of the models. The factors that motivate the development and implementation of new technologies are numerous, often context-specific, and largely variable. While it is generally true that the more a technology is implemented, the lessons learned lead to improvements in performance and costs, an objective technique to predict the extent of such improvements in the oil sands industry is wanting. Thus, setting “technological scenarios” in 2012 and 2030 may rely heavily in conjectures. This affects the predictive capabilities of the optimization model; it is up to the user to decide the reference technologies to be used when determining and optimizing energy demands of future oil sands operations.

In this work, the approach selected was to analyse the effect of energy production technology at its current stage of development *if it were to replace the technology commonly used in the oil sands industry*. Therefore, future energy demands were

determined on the assumption that a “business as usual” (BAU) scenario is in effect between 2003 and 2030. The advantage of this approach is that it makes it possible to quantify the effect of technological inaction on the costs of producing energy and the resulting emissions of the oil sands industry. Additionally, it enables a comparison between a known, proven situation (BAU) and the alternative, tentative new technological framework (optimal energy infrastructures).

4.4.4 Modelling

Single-period optimization. The current GAMS model is only capable of optimizing energy demands for a single point in time and does not consider the incremental time and costs required for the construction of energy producing plants. This makes it impractical to develop an energy plan for the industry on a year-by year basis. In this work, the aim was to determine the optimal way to supply energy to the oil sands industry at specific points in time, for user-specified bitumen and SCO production levels.

Single plant sizes. A final shortcoming of the model is that all plants belonging to a particular technology set have identical sizes. While this is not an unreasonable assumption, it is possible that the incorporation of smaller or larger plants may further reduce the energy cost of the industry. The former may be applicable when a set of large plants operating at full capacity meet most of the energy demands, and a smaller plant operating at full capacity is more economical to build and operate than a large plant operating at fractional capacity. The latter plants have an increased potential to achieve cost reductions by their improved economies of scale.

Chapter 5

Sensitivity Analyses

In this chapter, the sensitivity of the GAMS model to process and economic parameters is evaluated. Section 5.1 deals with the OSOM while section 5.2 covers the sensitivity of the optimal energy infrastructures in 2012 and 2030 to a number of model parameters.

5.1 OSOM Base Case

The effect of changing OSOM parameters on the model output is entirely reflected on the magnitude and composition of the energy demands for the year 2003. The changes in the latter are ultimately evaluated in terms of the economic and environmental impacts of energy use in the oil sands industry, namely, in the values of the resulting energy costs and CO_2 intensities. In this analysis, the sensitivity of these variables to changes in the energy demands in 2003 is investigated.

The energy demands of each individual commodity were varied between ± 50% with respect to the original OSOM 2003 values, presented in Chapter 4. It is deemed that this range will adequately cover the impact of variations in the OSOM parameter values used in this study. Table 5-1 summarizes the sensitivity of energy costs and CO_2 intensities to changes in the magnitude of individual energy commodities for the year 2003. The data shown in Table 5-1 includes results for SCO and bitumen, as well as the change in the total CO_2 emissions of the fleet.

The energy costs of SCO are most sensitive to changes in hydrogen, hot water, and upgrading steam, in that specific order. The maximum cost variations are ± 16%, ± 10.6% and ±9.6%, for hydrogen, hot water, and steam, respectively, for changes of ± 50% in the magnitude of these commodities. The effects of diesel fuel and non-upgrading power on the energy cost are very similar, roughly ± 5% for a ± 50% change in magnitude. In contrast, the power for upgrading, non-upgrading steam, and process fuel have little effect on the energy costs of SCO, ranging from 0.5-1.5%.

Table 5-1. 2003 energy costs sensitivity to the demand of individual energy commodities

Variation	Mined SCO		Bitumen		Fleet
	$/bbl	tonne CO_2/bbl	$/bbl	tonne $_{CO2}$/bbl	tonne CO_2 emitted
OSOM base case values					
0%	13.64	0.075	5.38	0.037	2,249
Hot water (tonne/h)					
± 50%	± 10.6%	± 5.1%	0.0%	0.0%	± 3.8%
± 30%	± 6.3%	± 3.0%	0.0%	0.0%	± 2.3%
0%*	-7.1%	-10.1%	0.0%	0.0%	0.0%
SAGD steam (tonne/h)					
± 50%	0.0%	0.0%	± 48.1%	± 48.5%	± 11.7%
± 30%	0.0%	0.0%	± 28.9%	± 29.1%	± 7.0%
Process steam – upgrading (tonne/h)					
± 50%	± 9.6%	± 12.7%	0.0%	0.0%	9.5% / -9.6%
± 30%	± 5.8%	± 7.6%	0.0%	0.0%	5.7% / -5.8%
Process steam – balance of plant (tonne/h)					
± 50%	± 1.5%	± 2.0%	0.0%	0.0%	1.4% / -1.5%
± 30%	± 0.9%	± 1.2%	0.0%	0.0%	± 0.9%
Power – upgrading (kW)					
± 50%	± 0.9%	± 1.2%	± 0.1%	0.0%	± 0.9%
± 30%	± 0.5%	± 0.7%	0.0% / -0.1%	0.0%	± 0.5%
Power – balance of plant (kW)					
± 50%	± 5.0%	± 4.7%	± 2.0%	± 1.5%	± 3.9%
± 30%	± 2.0%	± 2.8%	± 0.9%	± 0.9%	± 2.3%
Hydrogen (tonne/h)					
± 50%	-16.0% / 16.5%	± 19.1%	± 0.1%	0.0%	± 14.7%
± 30%	-9.3% / 9.8%	± 11.5%	± 0.1%	0.0%	± 8.8%
100%	32.5%	38.2%	-0.1%	0.0%	-29.5%
Process fuel (GJ/h)					
± 50%	-1.2% / 1.3%	± 1.8%	0.0%	0.0%	± 1.3%
± 30%	-0.7% / 0.8%	± 1.1%	0.0%	0.0%	± 0.8%
Diesel fuel (L/h)					
± 50%	± 5.0%	± 3.5%	0.0%	0.0%	± 2.6%
± 30%	± 3.0%	± 2.1%	0.0%	0.0%	± 1.6%

* hot water from plant waste heat

The energy costs for bitumen production are mostly sensitive to variations in the SAGD steam and to a much lesser degree, to the power demands. The relationship between SAGD steam and energy cost is nearly proportional for bitumen, whereas a power demands variation of ± 50% changes the energy cost by 1-2%. The sensitivity results reveal that bitumen energy costs are slightly affected by changes in power demands for upgrading and hydrogen production. Although bitumen production does not require these commodities, variations in their order of magnitude change the number of power plants and their output. This in turn alters the cost of electricity, which causes the energy costs of bitumen to vary.

In terms of CO_2 intensities, Table 5-1 reveals that the intensities of SCO are most sensitive to changes in hydrogen, upgrading steam, non-upgrading power, and hot water demands. On the contrary, the SCO energy cost is less sensitive to changes in process fuel, power for upgrading, diesel fuel and steam for bitumen extraction.

The sensitivity of CO_2 intensity of bitumen in 2003 follows the same trend as the energy costs. Only changes in the magnitude of SAGD steam have a significant impact on the intensity values for bitumen. Doubling or halving the power demands only change the CO_2 intensity of bitumen by 1-1.5%.

On a fleet scale, the total CO_2 emissions are chiefly sensitive to changes in hydrogen, SAGD steam, and upgrading steam demands. The response to ± 50% variation on the magnitudes of these commodities resulted in changes of ± 15%, ± 12%, and ± 10%, respectively. Changes in hot water, power, process, and diesel fuel demands all have a marginal effect on the cumulative CO_2 emissions of the fleet.

The analysis shown on Table 5-1 includes a scenario, labelled “0-FH”, in which hot water demands are met without the need to burn fuel in the boilers. This sensitivity scenario was developed to account for the possibility of using waste heat from upgrading processes to heat all the water needed for bitumen extraction in SCO production. If this was feasible, the sensitivity analysis reveals that the energy costs would be lowered by 7% while the CO_2 intensities would drop by 10%, both of which are significant improvements over the base case scenario.

The sensitivity analysis for the 2003 case also includes a case in which hydrogen demands are double of what the OSOM computed. This scenario was introduced to

explore the possibility of producing aromatics-free synthetic crude, which requires deep hydrotreatment of the oil fractions. Such product is attractive to certain refiners in the Southern United States, who are ill-equipped to handle conventional synthetic crude from Alberta. Doubling the hydrogen demands is more than the anticipated process demands for deep hydrotreated SCO. The results from the analysis reveal that doubling the hydrogen demands for SCO production would increase the energy cost by a third, while causing the CO_2 intensity to rise by almost 40%. Also, the fleet CO_2 emissions would rise by roughly 30%.

In addition to variations in the magnitudes of the energy demands for individual commodities, the sensitivity of the energy cost to the cost of natural gas was also investigated. Figure 5-1 shows the energy costs for bitumen and SCO production in 2003 as a function of natural gas prices.

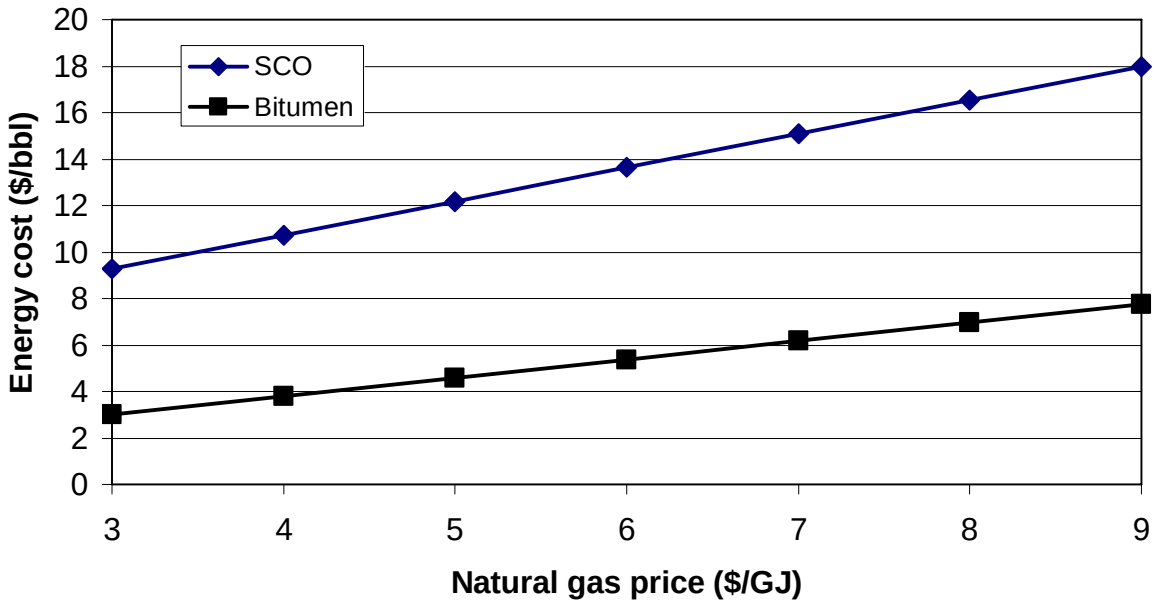

Figure 5-1. 2003 energy costs sensitivity to natural gas prices

The natural gas prices range between 3 and 9 $/GJ. These values represent a ± 50% variation in prices with respect to the assumed value of $6/GJ in 2003. According to Figure 5-1, the energy cost of SCO varies by ± 32% while that of bitumen is ± 44%, in response of a ± 50% change in the price of natural gas.

Figure 5-1 provides a reasonable estimate of energy costs at different fuel prices. For instance, the energy costs of bitumen production via SAGD reported in [10] are

$4.50/bbl at a natural gas price of $5/GJ. The cost calculated by the model for an identical natural gas price is $4.58/bbl. The latter value is in close agreement with the previously published figure.

5.2 GAMS Optimization Model

The optimal solutions for the years 2012 and 2030 were subjected to sensitivity analyses similar to those presented previously for the year 2003. However, since the optimization model changes the hydrogen and power plants only, the sensitivity analyses in this section are limited to hydrogen and power demands. Also, the analyses for 2012 and 2030 include process parameters like IGCC availability and CO_2 pipeline length. These are not part of the 2003 analyses because the energy infrastructure in this year did not include IGCC plants or CO_2 capture.

Concerning the sensitivity to economic parameters, the analyses for 2012 and 2030 cover CO_2 transport and injection/storage costs, capital costs and annual capital charges, in addition to fuel costs (natural gas and coal).

Finally, the sensitivity analyses in the remainder of this chapter will be presented for cases where CO_2 and H_2S co-capture is allowed as well as when co-capture is not permitted. In both instances the sensitivity analyses are performed at the maximum CO_2 reduction level. So for instance, in 2012, the maximum CO_2 reduction level for the no co-capture optimal solution is 25% whereas the corresponding value for the co-capture solution is 25.7%. The reader must note, however, than in certain special cases, CO_2 reduction levels other than the maximum are chosen for the sensitivity analyses. This is a necessity imposed on the analysis by virtue of the optimal energy infrastructure calculated by the model at maximum capture. For example, if the analysis involves variations in the price of coal and the optimal infrastructure at maximum capture excludes plants that use this fuel, a lower CO_2 reduction level that includes the required plants is chosen instead. This thus enables the study of the effect of different coal prices on the energy costs using optimal energy infrastructures, at CO_2 reduction levels as close to the maximum as possible.

Also, the maximum number of each plant that can be chosen is unrestricted for the analyses, but limited by the specified number of plants per set. The default values for these sets are large enough to allow unconstrained optimal energy infrastructures.

5.2.1 Year 2012

The sensitivity of the energy cost and CO_2 reductions (when applicable) to process and economic parameters are presented next for co-capture and no co-capture optimal solutions. The energy costs are expressed as a percentage variation with respect to the optimal case solution presented in Chapter 4. The analyses also include the optimal energy infrastructures over the range of parameter values, when pertinent.

5.2.1.1 Sensitivity to process variables and parameters

Table 5-2 shows a summary of the energy costs sensitivities to process variables and parameters in 2012. SCO costs are mainly affected by changes in hydrogen and power demands and to a lesser degree by steam boiler efficiencies. Bitumen is moderately sensitive to variations in steam boiler efficiencies and to a lesser degree, by power demands fluctuations. On the other hand, variations in IGCC plant availability and CO_2 pipeline length have a negligible effect on SCO energy costs and no effect on the bitumen costs. IGCC plant availability variations, however, change the optimal energy infrastructures slightly as do changes in hydrogen demands.

Each of the above sensitivities is discussed in detail in the remainder of this section along with the sensitivities of the co-capture optimal energy infrastructures.

The hydrogen demands were varied between -50% and 100% with respect to the optimal solution at maximum capture. Tables 5-3 and 5-4 summarize the results of the analysis for the no co-capture and co-capture solutions, respectively. The results show that the energy costs drop by 24% and 29% for mined and SAGD SCO respectively, when the hydrogen demands are reduced by 50%. On the other hand, if the hydrogen demands double, the energy costs rise by 29% for mined SCO and 32% for SAGD SCO. The variations in hydrogen demands have a negligible effect on the energy costs of bitumen, for both the co-capture and no co-capture solutions.

The co-capture solution is less sensitive to changes in hydrogen demands than the no co-capture case. When the demands are reduced by 50%, the energy costs of mined and SAGD SCO decrease by 18% and 22%, respectively. When the hydrogen demands double, the energy costs rise by 24% and 26% for mined and SAGD SCO.

Table 5-2. 2012 energy cost sensitivity to process variables and parameters summary

Variation	Mined SCO $/bbl	SAGD SCO $/bbl	Bitumen $/bbl	Infrastructure changes?
Reference values				
0%	21.43	22.48	7.86	N/A
Hydrogen demands (tonne/h)				
100%	29%	32%	0.1%	No
50%	17%	19%	0.1%	No
-50%	-24%	-29%	0.2%	Yes
Power demands (kW)				
100%	11%	5%	4%	No
50%	6%	3%	2%	No
-50%	-7%	-3%	-2%	No
IGCC plant availability (%)				
95	-2%	-2%	0%	No
90	-1%	-1%	0%	Yes
85			Reference	
80	0%	0%	0%	No
75	1%	1%	0%	Yes
Steam boiler thermal efficiency (%)				
100	-2.6%	-4.4%	-9.6%	No
95	-1.3%	-2.3%	-4.8%	No
90*	-6.8%	0.2%	0%	No
85	1.5%	2.4%	5.0%	No
75	4.9%	7.8%	14.9%	No
CO_2 pipeline length (km)				
1200	1%	1%	0%	No
1000	0.7%	1.2%	0%	No
800	0.4%	0.7%	0%	No
600			Reference	
400	-0.3%	-0.6%	0%	No
300	-0.5%	-0.9%	0%	No

* hot water from plant waste heat

Table 5-3. 2012 energy costs sensitivity to hydrogen demands ($/bbl) – no co-capture

Variation	Mined SCO	SAGD SCO	Bitumen	Max. CO_2 reduction
100%	29%	32%	0.1%	11.3%
50%	17%	19%	0.1%	18.1%
0	21.43	22.48	7.86	25.0%
-33%	-15%	-18%	0.1%	29.6%
-50%	-24%	-29%	0.2%	31.8%

In terms of CO_2 reductions, the co-capture solution offers a slight advantage over the no co-capture solution. However, the gap between the former and latter narrows as the hydrogen demands decrease and increases as the demands rise, as seen in Tables 5-3 and 5-4.

Table 5-4. 2012 energy costs sensitivity to hydrogen demands ($/bbl) – co-capture

Variation	Mined SCO	SAGD SCO	Bitumen	Max. CO_2 reduction
100%	24%	26%	0.4%	12.7%
50%	13%	15%	0.1%	19.2%
0	18.22	18.94	7.81	25.7%
-33%	-11%	-14%	0.2%	30.0%
-50%	-18%	-22%	0.2%	32.2%

The power and energy production technologies in the energy infrastructures of the co-capture solution remain unchanged throughout the full range of hydrogen demands. In the no co-capture case however, the energy infrastructure changes slightly at ± 50% hydrogen demands, as shown in Table 5-5. From this data, it is evident that increases in the hydrogen demands affect the number of power plants in the optimal infrastructure. Since the hydrogen plants are SMR-based, their ancillary power demands rise as their numbers increase, which in turn, requires more power plants. This also explains why the energy costs of bitumen rise slightly as hydrogen demands increase.

The sensitivity against changes in power demands was also studied. Tables 5-6 and 5-7 present the results of these analyses for the no co-capture and co-capture cases, respectively.

Table 5-5. 2012 energy infrastructure sensitivity to hydrogen demands – no co-capture

Variation	P1	P6	P8	H1	H2	H4
100%	2		4	26	54	
50%	2	1	3	20	41	
0	2		3	13	27	
-33%	2		3	9	18	
-50%	2		3	7	12	1

P1 = NGCC, P6 = NGCC with CO_2 capture, P8 = NG Oxyfuel, H1 = SMR, H2 = SMR with CO_2 capture, H4 = H_2 IGCC with CO_2 capture

When co-capture is disallowed, mined SCO is the most sensitive to changes in power demands. SAGD SCO and bitumen are similarly sensitive to variations in power demands. A reduction of 50% in the power demands results in a drop of 7%, 3%, and 2% in the energy costs of mined SCO, SAGD SCO, and bitumen, respectively. On the other hand, when the power demands double, the energy costs increase by 11%, 5%, and 4% for mined, SAGD SCO, and bitumen, in that order.

Table 5-6. 2012 energy costs sensitivity to power demands ($/bbl) – no co-capture

Variation	Mined SCO	SAGD SCO	Bitumen	Max. CO_2 reduction
100%	11%	5%	4%	21.2%
50%	6%	3%	2%	23.1%
0	21.43	22.48	7.86	25.0%
-33%	-4%	-2%	-1%	26.2%
-50%	-7%	-3%	-2%	26.9%

In the co-capture case, the sensitivities of mined and SAGD SCO to power demands are slightly higher than those of their no co-capture counterpart solutions. The sensitivity of bitumen remains the same, however.

The effect of power demands on the maximum CO_2 reduction levels is similar in the co-capture and no co-capture cases, as seen in Tables 5-6 and 5-7. A 50% reduction in power demands results in approximately a 2 percentage point increase in CO_2 reduction of the fleet. Conversely, a doubling of the demands causes the CO_2 reduction level decrease of roughly 4 percentage points. The effect of power demands on the maximum

CO_2 reduction level attainable is much less dramatic than that of hydrogen demands, for both co-capture and no co-capture optimal solutions.

Table 5-7. 2012 energy costs sensitivity to power demands ($/bbl) – co-capture

Variation	Mined SCO	SAGD SCO	Bitumen	Max. CO_2 reduction
100%	13%	6%	4%	21.9%
50%	7%	3%	2%	23.8%
0	18.22	18.94	7.81	25.7%
-33%	-6%	-3%	-2%	27.0%
-50%	-8%	-4%	-2%	27.6%

In terms of the optimal energy infrastructures, the results reveal that like with the hydrogen demands, the energy technologies in the co-capture solutions remain unchanged. The energy infrastructure in the no co-capture case suffers a slight change in response to a 33% decrease in power demands, but not at any other level, as shown in Table 5-8. Thus, the optimal energy infrastructures are essentially unaffected by changes in power demands for both co-capture and no co-capture cases, in the range of power demand values featured in this study.

Table 5-8. 2012 energy infrastructure sensitivity to power demands – no co-capture

Variation	P1	P8	H1	H2	H4
100%	3	5	13	27	
50%	3	4	13	27	
0	2	3	13	27	
-33%	1	3	13	25	1
-50%	1	2	13	27	

P1 = NGCC, P8 = NG Oxyfuel, H1 = SMR, H2 = SMR with CO_2 capture, H4 = H_2 IGCC with CO_2 capture

IGCC plants are often featured in the optimal energy infrastructures of the years 2012 and 2030, at multiple CO_2 reduction levels. This technology however, is still in the early stages of its development cycle. Therefore, there is some uncertainty associated with its performance. Specifically, disagreements concerning IGCC plant availability are common in the energy modeling field.

To address this issue, in this study the IGCC plant availability (capacity) factor is varied between 75% and 95%. The reader must note that the plant availability of other technologies is not included in the sensitivity analyses because: a) several technologies never appear in the optimal energy infrastructures, and b) many energy production technologies, such as NGCC plants, are fairly developed and their availability is close to its limit, which is in fact, the value that is used in the optimization model.

The optimal no co-capture energy infrastructure for 2012 at maximum CO_2 reduction is comprised only of natural gas-based plants. Hence, it is impossible to study its sensitivity to changes in the availability of IGCC plants at maximum CO_2 reduction. To deal with this, the optimal energy infrastructure at the nearest CO_2 reduction level (20%) is chosen instead as the reference point for the sensitivity analysis.

Table 5-9 summarizes the results of the model sensitivity to IGCC plant availability for the no co-capture and the co-capture cases.

Table 5-9. 2012 energy costs sensitivity to IGCC plant availability ($/bbl)

Availability	Mined SCO		SAGD SCO	
	no co-capture	co-capture	no co-capture	co-capture
95%	-2%	-2%	-2%	-2%
90%	-1%	0%	-1%	-1%
83%/88%	21.43	18.22	22.48	18.94
85%	0%	0%	0%	0%
80%	0%	0%	0%	0%
75%	1%	1%	1%	2%

The results show that the energy costs for both co-capture and no co-capture solutions are almost equally insensitive to changes in IGCC plant availability. Also, the energy costs of bitumen are unaffected by changes in IGCC plant availability. On the other hand, the sensitivity of mined and SAGD SCO energy costs ranges between -2% and 1% for a ± 10 percentage points variation.

The analysis results reveal that an IGCC plant availability of 85% is equivalent to a combination of 83% availability for hydrogen IGCC plants and 88% availability for IGCC power plants, which is the reference point for the analyses.

The energy infrastructures for both the co-capture and no co-capture optimal solutions also behave similarly. The energy technology mix in both cases is unaltered at the majority of IGCC availability values, with the exception of 75% and 90%, where SMR plants with capture appear in addition to IGCC plants, as seen in Table 5-10.

The steam demands, both for process and SAGD steam in 2012 are significant. They also account for a sizeable portion of the energy costs of all products. Hence, this study includes a sensitivity analysis to the steam boilers' thermal efficiency, ranging from 75% to 100%. The latter value was chosen to investigate the magnitude of the savings due to operation at an ideal maximum. The analysis also includes a case in which all of the hot water required is produced using waste heat from the plants, which saves some fuel in the boilers, similar to the case described earlier in section 5.1.

Table 5-10. 2012 energy infrastructure sensitivity to IGCC plant availability – co-capture

Availability	P1	P8	H1	H2	H5
95%	2	2	13		5
90%	2	2	13	2	5
83%/88%	2	2	13		6
85%	2	2	13		6
80%	2	2	13		6
75%	2	2	13	2	6

P1 = NGCC, P8 = NG Oxyfuel, H1 = SMR, H2 = SMR with CO_2 capture, H4 = H_2 IGCC with CO_2 and H_2S co-capture

The results of the analysis reveal that among products, bitumen is the most sensitive to variations in boiler thermal efficiency, followed by SAGD SCO, and mined SCO. The energy cost increase at 75% thermal efficiency is 15%, 8%, and 5%, in the above order, while the maximum possible cost savings at 100% efficiency is approximately 10%, 5%, and 3% for bitumen, SAGD SCO, and mined SCO, respectively.

As shown in Table 5-11, the maximum CO_2 reduction level possible when the boiler efficiency drops to 75% is roughly 15%. Conversely, at 100% efficiency, the corresponding CO_2 reduction value is 30%, or 5 percentage points above the reference case.

Table 5-11. 2012 energy costs sensitivity to boiler thermal efficiency ($/bbl) – no co-capture

Efficiency	Mined SCO	SAGD SCO	Bitumen	Max. CO_2 reduction
100%	-2.6%	-4.4%	-9.6%	30.1%
95%	-1.3%	-2.3%	-4.8%	27.7%
90%	21.43	22.48	7.86	25.0%
90%*	-6.8%	0.2%	0.0%	25.0%
85%	1.5%	2.4%	5.0%	22.0%
75%	4.9%	7.8%	14.9%	14.8%

* hot water from plant waste heat

The results for the co-capture case are shown on Table 5-12. These figures show that in general, the co-capture solutions are slightly more sensitive to changes in boiler thermal efficiency than their no co-capture counterparts. Nevertheless, the order of energy cost sensitivity among products is identical to that of the no co-capture case. Also, the changes in CO_2 reduction at 75% and 100% efficiency are marginally greater than those of the no co-capture case.

Table 5-12. 2012 energy costs sensitivity to boiler thermal efficiency ($/bbl) – co-capture

Efficiency	Mined SCO	SAGD SCO	Bitumen	Max. CO_2 reduction
100%	-3.1%	-5.3%	-9.7%	30.8%
95%	-1.6%	-2.7%	-4.8%	28.4%
90%	18.22	18.94	7.81	25.7%
90%*	-8.3%	0.0%	0.0%	25.7%
85%	1.8%	2.9%	5.0%	22.7%
75%	5.7%	9.1%	15.0%	15.5%

* hot water from plant waste heat

If the heat required for hot water production is provided by waste heat from the oil sands plants, only the energy costs of mined SCO are reduced in both co-capture and no co-capture cases. The energy savings due to this situation are more than twice those caused by 100% steam boiler efficiency, as seen in Tables 5-11 and 5-12.

A process parameter that was tested in this study is the length of the CO_2 pipeline connecting the sources to the sinks in Alberta. The pipeline length was varied between half and double its original value, as shown on Table 5-13.

Table 5-13. 2012 energy costs sensitivity to CO_2 pipeline length ($/bbl)

Length (km)	Mined SCO		SAGD SCO	
	no co-capture	co-capture	no co-capture	co-capture
1200	1.0%	1.8%	1.0%	2.0%
1000	0.7%	1.2%	0.7%	1.3%
800	0.4%	0.7%	0.4%	0.7%
600	21.43	18.22	22.48	18.94
400	-0.3%	-0.6%	-0.4%	-0.7%
300	-0.5%	-0.9%	-0.5%	-1.0%

The results of this analysis show that the energy costs of bitumen are insensitive to the CO_2 pipeline length, whereas mined and SAGD SCO are only marginally sensitive to this model parameter. In the no co-capture case, both products have an identical sensitivity, which ranges between -0.5% and 1% of the original SCO energy costs. In the co-capture case, SAGD SCO is slightly more sensitive to pipeline length than mined SCO. On the other hand, the co-capture solutions are roughly twice as sensitive as the no co-capture ones. This is explained by a higher increase in the amount of CO_2 to be transported in the former case. Or in other words, more CO_2 must be captured and transported in the co-capture case (coal-fired plants) than in the no co-capture (gas-fired plants) case at maximum CO_2 reduction levels. Also, the increase in transport length is accompanied by an increase in power demands for booster compressors along the pipeline, which in turn drives the CO_2 production and capture upward.

5.2.1.2 Sensitivity to economic parameters

In this section, the model output sensitivity to a number of key economic parameters is presented. Unlike in the year 2003, in 2012 coal is available for energy production, in addition to natural gas. Table 5-14 presents the results of the economic sensitivity analyses at a glance.

Table 5-14. 2012 energy cost sensitivity to economic parameters summary

Value	Mined SCO $/bbl	SAGD SCO $/bbl	Bitumen $/bbl	Infrastructure changes?
Reference values				
N/A	21.43	22.48	7.86	N/A
Natural gas prices ($/GJ)				
12	22%	27%	30%	No
9		Reference		
6	-22%	-27%	-30%	Yes
Coal prices ($/GJ)				
6.0	11%	12%	0%	Yes
3.0	2.3%	2.5%	0%	No
2.2		Reference		
1.4	-2.3%	-2.5%	0%	No
Annual capital charge rate (%)				
30	11.6%	10.5%	1.4%	No
15		Reference		
7.5	-5.3%	-4.8%	-0.6%	No
Overnight capital costs (% increase)				
200	23.8%	21.5%	2.9%	No
100	11.9%	10.8%	1.5%	No
50	6.4%	5.7%	0.8%	No
0		Reference		
-50	-5.6%	-5.1%	-0.6%	No
CO_2 transport costs ($/tonne CO_2/100km)				
2.4	1%	1%	0%	No
1.2		Reference		
0.6	-1.4%	-1.6%	0%	No
CO_2 injection/storage costs ($/tonne CO_2)				
12	0.8%	0.8%	0%	No
6		Reference		
3	-0.4%	-0.4%	0%	No

Figures 5-2 and 5-3 show the energy cost sensitivity to natural gas and coal prices. The price of natural gas used in the analysis ranges from 5-12 $/GJ. The lower

price is identical to the one used in 2003, while the latter corresponds to the natural gas price assigned to the 2030 year.

Among products, the analysis results show that bitumen is the most sensitive to variations in natural gas prices, followed by SAGD and mined SCO. Their energy costs in the above order are ± 30%, ± 27%, and ± 22% in response to a ± 33% fluctuation in the price of natural gas, for the no co-capture case. The energy prices for SCO in the co-capture solution are less sensitive to variations in natural gas price by 4-5 percentage points than the no co-capture case. However, the bitumen energy cost sensitivity to natural gas prices is identical for both co-capture and no co-capture solutions. Thus, only the values for the no co-capture case are plotted in Figure 5-2.

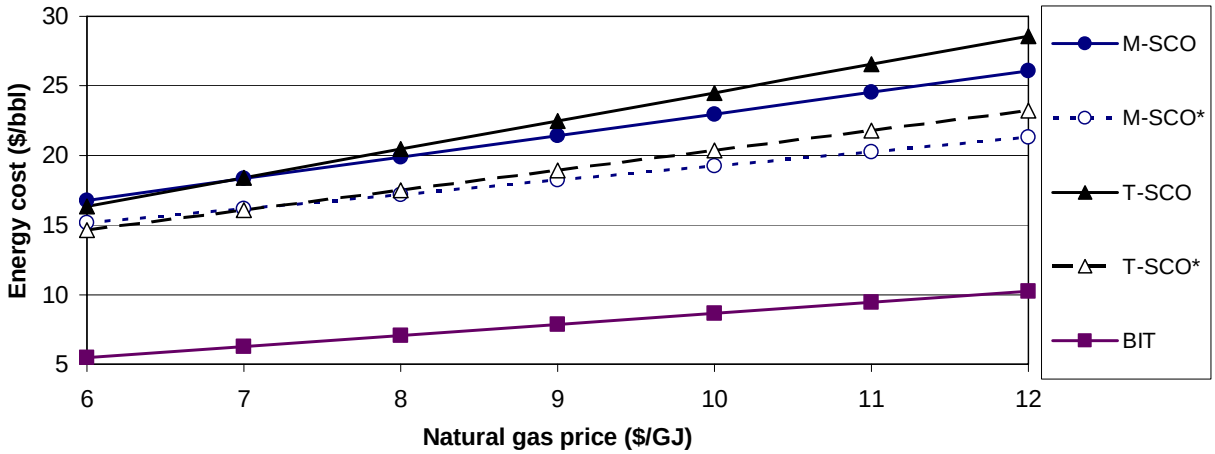

Figure 5-2. 2012 energy costs sensitivity to natural gas prices (* co-capture)

Figure 5-3 showcases the energy cost sensitivity to fluctuations in coal price. The energy costs of bitumen were excluded from Figure 5-3, as they are insensitive to changes in the price of coal. SCO, both mined and SAGD is moderately sensitive to coal prices. A 33% drop in the price of coal results in an energy cost decrease of roughly 2.5% while a doubling in the price of coal causes the energy costs of SCO to rise between 5-8%. The model results also reveal that the co-capture solution is slightly less sensitive to changes in the price of coal than the no co-capture case.

The upper limit in this analysis corresponds to a coal price of $6/GJ. This value is considered extremely high and above its anticipated level for the year 2012. The sensitivity analysis is extended to this level to allow for comparison with natural gas fuel at the same price, if the reader is interested in such a comparison. From Figure 5-3, it is

seen that when the price of coal almost triples in magnitude, it causes the energy cost of SCO to rise between 10-12%.

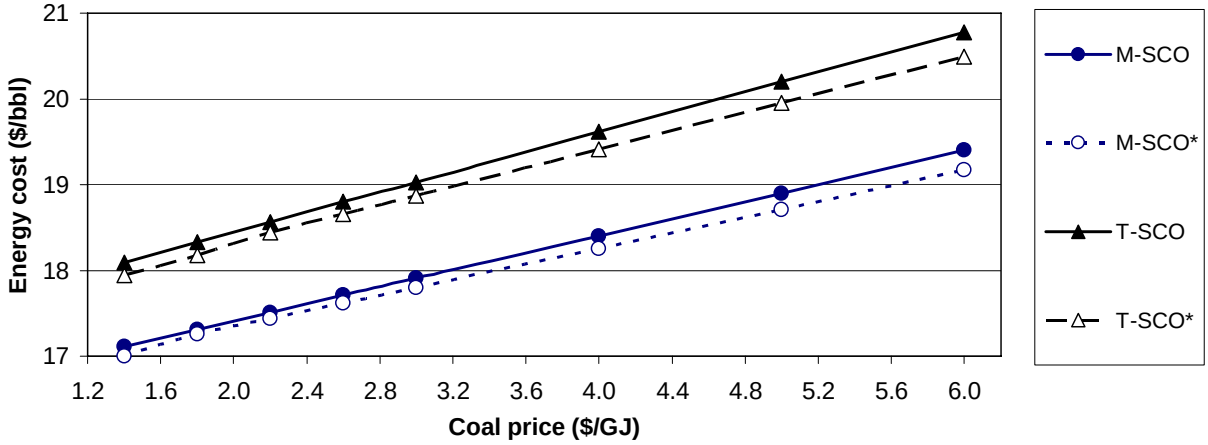

Figure 5-3. 2012 energy costs sensitivity to coal prices (* co-capture)

The composition of the optimal energy technology mix for the co-capture solution is sensitive to extreme coal price fluctuations while the no co-capture solution is only slightly affected at the highest coal price of $6/GJ. Table 5-15 shows the changes in the optimal energy infrastructure due to coal price fluctuations. These results suggest that in the co-capture case, IGCC H_2 plants with separate H_2S and CO_2 capture (H4) are more attractive at lower coal prices than co-capture (H5) plants. Likewise, at extreme coal prices, SMR plants with CO_2 capture tends to be more attractive than coal IGCC plants.

Table 5-15. 2012 energy infrastructure sensitivity to coal prices – co-capture

Coal price	P1	P5	H1	H2	H4	H5
6.0	3		15	1		5
5.0	3		14	2		5
4.0	3		14	2		5
3.0	3		14	2		2
2.6	3		14	2		5
2.2	3		14	2		5
1.8	2	1	16		1	4
1.4	3		13		4	2

P1 = NGCC, P5 = IGCC with CO_2 and H_2S co-capture, H1 = SMR, H2 = SMR with CO_2 capture, H4 = H_2 IGCC with CO_2 capture, H5 = H_2 IGCC with CO_2 and H_2S co-capture

Another parameter that was evaluated in this study is the annual capital charge rate. The range used in the analysis is 7.5% to 30%, which corresponds to a drop of 50% and a doubling of the reference value of 15%, respectively. The results of this analysis are shown in Figure 5-4.

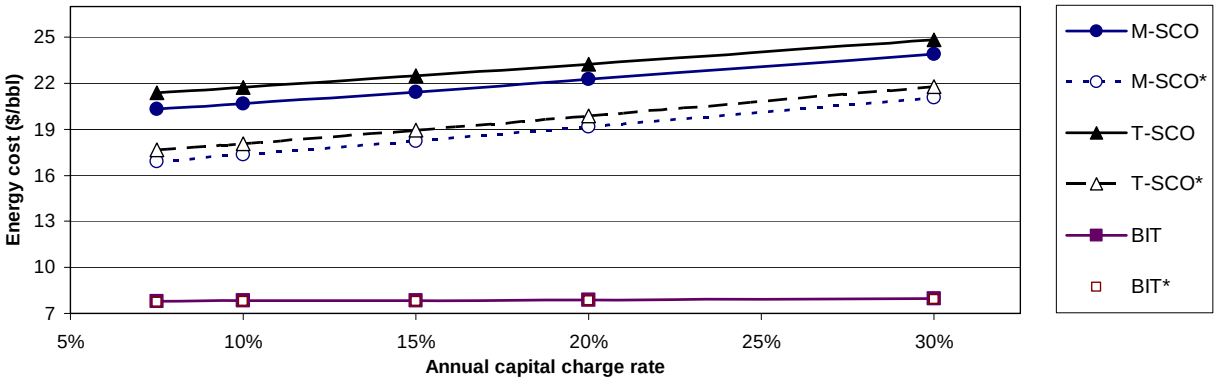

Figure 5-4. 2012 energy costs sensitivity to annual capital charge rate (* co-capture)

Mined SCO is the most sensitive product to fluctuations in capital charge rate, followed by SAGD SCO. Bitumen has a very low sensitivity to the capital charge rate. The model results show that a doubling in the value of the former parameter translates into an increase of approximately 11% in the energy cost of SCO and less than 2% in the case of bitumen.

When comparing the co-capture solutions against the no co-capture ones, the former are moderately more sensitive than the latter by roughly four percentage points, but only for SCO. The sensitivity of bitumen energy costs is the same in either case. This is due to the fact that the bulk of the energy costs of bitumen consist of fuel and water, and equipment costs are negligible in comparison.

A key economic parameter associated with energy costs in oil sands operations is the capital costs of hydrogen and power plants. In recent years, capital costs in Alberta have experienced an unprecedented rise. This trend is expected to continue as long as oil sands operations continue to expand. Therefore, this study features a sensitivity analysis to plant overnight costs, which ranges from -50% to 200% of the anticipated 2012 costs.

In a similar fashion as in the sensitivity to capital charge rates, the energy costs of bitumen are very mildly affected by changes in capital costs, as seen in Figure 5-5. The energy costs of SCO, on the other hand, show a moderate sensitivity to variations in plant overnight capital costs. A 50% drop in capital costs causes an approximate decrease of

5% and of 8% in the energy costs of SCO for the no co-capture and co-capture cases, respectively. Conversely, a doubling of the capital costs results in an 11% increase in the energy costs of the former and 16% in the latter. Tripling the overnight capital costs of all the plants in the optimal energy infrastructures at maximum CO_2 reduction causes the energy costs of SCO to rise by approximately 22% in the no co-capture case and by 30% in the co-capture case. These results suggest that the optimal co-capture energy infrastructure is more sensitive to capital charges than the no co-capture one.

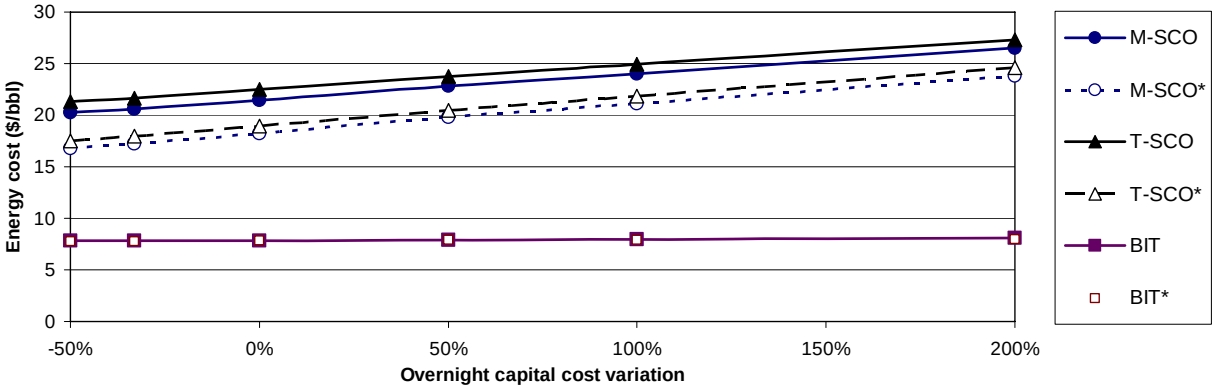

Figure 5-5. 2012 energy costs sensitivity to overnight plant capital costs (* co-capture)

The results of the sensitivity analysis to overnight capital costs variation shows that there is no change in the technologies included in the no co-capture case. In the co-capture case, the energy production technology mix remains unchanged throughout the entire range of capital cost values, with the exception of the 200% increase point. At this point only, one oxyfuel power plant is replaced by a NGCC with CO_2 capture.

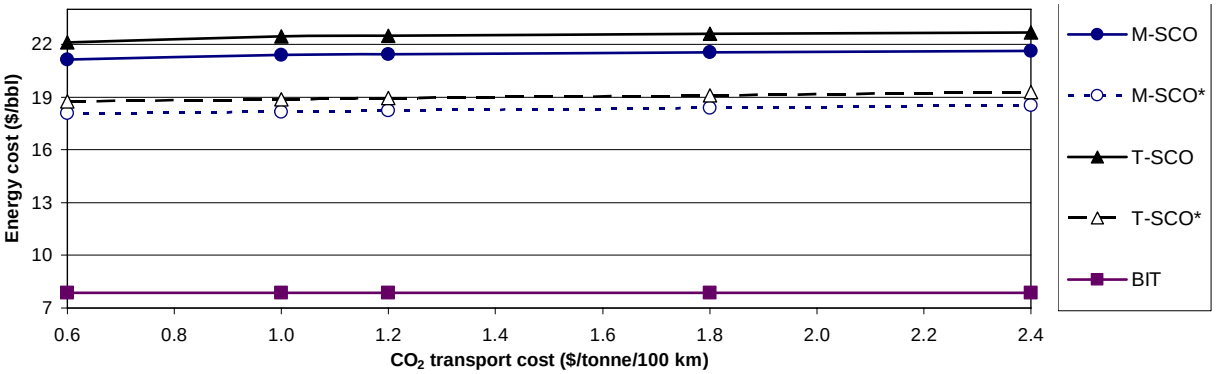

Figure 5-6. 2012 energy costs sensitivity to CO2 transport costs (* co-capture)

Last of the analyses is the sensitivity to CO_2 transport and storage costs. These parameters were varied between -50% and 100% for both the co-capture and no co-

capture cases, at maximum CO_2 reduction. The results of the analyses are shown in Figures 5-6 and 5-7.

The energy costs of SCO have a low sensitivity to fluctuations in the CO_2 transport costs and bitumen is insensitive to them. A 50% reduction in the CO_2 transport cost causes a decrease of roughly 1.5% and 1% in the energy costs of SCO in the no co-capture and the co-capture cases, respectively. Doubling the transport cost, on the other hand, causes a sharper increase in the energy costs of SCO in the co-capture case than in the no co-capture case. This is related to the larger amount of CO_2 captured in the former case than in the latter, which results in higher CO_2 transport costs.

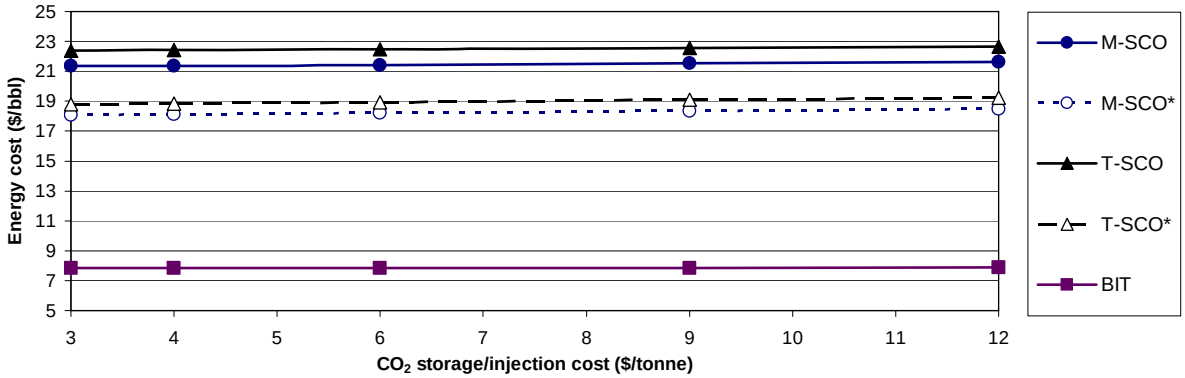

Figure 5-7. 2012 energy costs sensitivity to CO2 injection/storage costs (* co-capture)

CO_2 injection/storage costs have a marginal effect on SCO energy costs and a null effect on bitumen costs. In the no co-capture case, the energy cost variation over the entire range of storage costs is less than ± 1%. The co-capture solutions are slightly more sensitive to fluctuations in CO_2 storage costs than the no co-capture cases, but even a tripling in the storage costs causes only a 1.5% increase in the energy costs of SCO. The optimal energy infrastructures of the co-capture and no co-capture cases are completely unaffected by changes in the CO_2 transport and storage costs within the value ranges covered in this study.

5.2.2 Year 2030

In this section, the sensitivity of energy costs to process and economic parameters is presented. Unless explicitly mentioned, all reference values for the sensitivity analyses correspond to the energy costs at the highest CO_2 reduction level, which are 38.6% (no co-capture) and 39.7% (co-capture) for the optimal solutions.

5.2.2.1 Sensitivity to process variables and parameters

The energy costs sensitivity to variations in process variables/parameters is summarized in Table 5-16. A discussion of each of these sensitivities follows.

Table 5-16. 2030 energy cost sensitivity to process variables and parameters summary

Variation	Mined SCO $/bbl	SAGD SCO $/bbl	Bitumen $/bbl	Infrastructure changes?
Reference values				
0%	29.49	31.03	10.32	N/A
Hydrogen demands (tonne/h)				
100%	18%	21%	-0.8%	Yes
50%	11%	13%	-0.3%	No
-50%	-27%	-32%	0%	No
Power demands (kW)				
100%	11%	4%	5%	No
50%	7%	3%	3%	No
-50%	-10%	-5%	-3%	No
IGCC plant availability (%)				
95	-1%	-1%	0%	No
90			Reference	
85	1%	1%	0%	Yes
80	2%	2%	0%	No
75	3%	4%	0%	No
		Steam boiler thermal efficiency (%)		* hot water from plant waste heat
100	-2.8%	-4.5%	-9.8%	No
95	-1.2%	-2.0%	-4.9%	No
90*	-6.8%	0%	0%	No
85	1.5%	2.4%	5.0%	No
75	5.0%	7.8%	15.1%	No
CO_2 pipeline length (km)				
1200	1.4%	1.4%	0%	No
1000	0.9%	1.0%	0%	No
800	0.5%	0.5%	0%	No
600			Reference	
400	-0.5%	-0.6%	0%	No
300	-0.8%	-0.8%	0%	No

The demands for hydrogen and power are the two process variables that are used in the sensitivity analyses for the year 2030. The results of the sensitivity to H_2 demands are shown in Tables 5-17 and 5-18, for no co-capture and co-capture solutions.

Table 5-17. 2030 energy costs sensitivity to hydrogen demands ($/bbl) – no co-capture

Variation	Mined SCO	SAGD SCO	Bitumen	Max. CO_2 reduction
100%	18%	21%	-0.8%	32.9%
50%	11%	13%	-0.3%	35.9%
0	29.49	31.03	10.32	38.6%
-33%	-17%	-19%	0.1%	40.0%
-50%	-27%	-32%	0.0%	40.7%

The energy costs of thermal SCO are the most sensitive to variation in hydrogen demands, followed by mined SCO. Bitumen is little affected by changes in hydrogen demands, as seen in Tables 5-17 and 5-18. The co-capture case is less sensitive to decreases and more sensitive to increases in the hydrogen demands than the no co-capture case. A 50% drop in demands results in a 27-32% decrease in SCO energy costs for the no co-capture solution whereas the corresponding drop for the co-capture case is 14-18%. When hydrogen demands double, the SCO energy costs of the co-capture case rise by 29-33% while the SCO energy costs of the no co-capture case rise by 18-21%.

Table 5-18. 2030 energy costs sensitivity to hydrogen demands ($/bbl) – co-capture

Variation	Mined SCO	SAGD SCO	Bitumen	Max. CO_2 reduction
100%	29%	33%	-0.2%	35.9%
50%	12%	14%	-0.3%	38.0%
0	22.71	23.48	10.21	39.7%
-33%	-9%	-12%	0.4%	40.7%
-50%	-14%	-18%	0.6%	41.2%

Concerning CO_2 reductions, the no co-capture solutions are more sensitive to fluctuations in hydrogen demands than the co-capture ones. This reflects in higher attainable CO_2 reductions when hydrogen demands drop and vice versa. This behaviour

is related to the nature of the no co-capture energy infrastructures. As hydrogen demands mount, more IGCC plants are operational, which in turn drives the CO_2 emissions upward. In the co-capture case, the increase in hydrogen demands is met by a combination of IGCC and SMR plants with capture, which have lower CO_2 emissions than the IGCC plants in the no co-capture case.

Table 5-19. 2030 energy infrastructure sensitivity to hydrogen demands – co-capture

Variation	P6	P8	H1	H2	H4	H5
100%		8		58	1	30
50%		7		4	1	30
0%		7	1	1		21
-33%	1	7	1	1		14
-50%	1	7	1			11

P6 = NGCC with CO_2 capture, P8 = NG Oxyfuel, H1 = SMR, H2 = SMR with CO_2 capture, H4 = H_2 IGCC with CO_2 capture, H5 = H_2 IGCC with CO_2 and H_2S co-capture

The optimal energy infrastructure plant mix of the no co-capture case remains largely constant throughout the range of hydrogen demands. The same is not true of the co-capture optimal infrastructures. As seen in Table 5-19, the energy infrastructures mix in the co-capture case is affected by changes in hydrogen demands. Nevertheless, in both no co-capture and co-capture cases, it is the gasification plants that absorb the bulk of the changes in hydrogen demands.

Table 5-20. 2030 energy costs sensitivity to power demands ($/bbl) – no co-capture

Variation	Mined SCO	SAGD SCO	Bitumen	Max. CO_2 reduction
100%	11%	4%	5%	38.2%
50%	7%	3%	3%	38.5%
0	29.49	31.03	10.32	38.6%
-33%	-6%	-4%	-2%	38.6%
-50%	-10%	-5%	-3%	38.6%

The results of the energy cost sensitivity to power demands are shown in Tables 5-20 and 5-21. Bitumen is modestly affected by these fluctuations whereas mined SCO is

the most sensitive to changes in the power demands. On the other hand, the energy costs of SAGD SCO are slightly more sensitive to power demands than those of bitumen.

Table 5-21. 2030 energy costs sensitivity to power demands ($/bbl) – co-capture

Variation	Mined SCO	SAGD SCO	Bitumen	Max. CO_2 reduction
100%	16%	8%	5%	39.4
50%	9%	5%	3%	39.6
0	22.71	23.48	10.21	39.7
-33%	-6%	-3%	-2%	39.7
-50%	-10%	-4%	-3%	39.8

The optimal energy infrastructures for the co-capture case are more sensitive to changes in power demands than those of the no co-capture case. As seen in Table 5-22, NGCC plants with CO_2 capture appear at power demand variations of 100% and -33%. In the no co-capture case, the power production technology (NG Oxyfuel) remains unchanged throughout the full range of power demands values.

Table 5-22. 2030 energy infrastructure sensitivity to power demands – co-capture

Variation	P6	P8	H1	H2	H5
100%	1	15	1	1	21
50%		12	1		22
0%		7	1	1	21
-33%	2	3	1	1	21
-50%		3	1	1	21

P6 = NGCC with CO_2 capture, P8 = NG Oxyfuel, H1 = SMR, H2 = SMR with CO_2 capture, H5 = H_2 IGCC with CO_2 and H_2S co-capture

Unlike hydrogen demands, variation in power demands has a negligible effect on the maximum attainable CO_2 reduction in both the co-capture and no co-capture cases. The variation over the entire range of power demands for the former is ± 0.3 percentage points and ± 0.4 for the latter, with respect to their respective CO_2 reduction levels. In other words, a doubling/halving of the power demands will cause a drop of less than half a percentage point in the maximum attainable CO_2 reductions in both cases.

The sensitivity of energy costs to IGCC plant availability is also studied for the year 2030. Similarly to the year 2012, in 2030 the no co-capture optimal energy infrastructure at maximum CO_2 reduction (36.8%) excludes IGCC plants. Thus, the analysis was carried out at a CO_2 reduction level of 35%, in which a fair number of IGCC plants exist. The co-capture solutions are unaffected by the above situation, so its analysis to IGCC plant availability was performed at maximum CO_2 reduction.

The sensitivities of no co-capture and co-capture solutions to changes in IGCC plant availability are identical over the range of availability values in this study, as seen in Table 5-23. The sensitivity of SCO energy costs to IGCC plant availability is low and null for bitumen. The effect of different IGCC plant availability factors on SCO energy costs is identical for all such factors, except for the lowest availability factor. In the latter case, SAGD SCO energy costs are slightly more sensitive to IGCC availability than mined SCO costs.

Table 5-23. 2030 energy costs sensitivity to IGCC plant availability ($/bbl)

Availability	Mined SCO		SAGD SCO	
	no co-capture	co-capture	no co-capture	co-capture
95%	-1%	-1%	-1%	-1%
90%	22.09	22.71	23.02	23.48
85%	1%	1%	1%	1%
80%	2%	2%	2%	2%
75%	3%	3%	4%	4%

Variations in IGCC plant availabilities have a null effect on the energy technologies mix in both the co-capture and no co-capture optimal energy infrastructures. Over the full spectrum of availability factors, the same technologies are used for power and hydrogen production and only their number of plants change.

A sensitivity analysis to steam boiler thermal efficiency was carried out in 2030, identical to the one described in section 5.2.1.1 for the year 2012. The results of the 2030 analysis are summarized in Tables 5-24 and 5-25.

The energy costs of bitumen are the most sensitive to fluctuations in boiler thermal efficiencies. SAGD SCO energy costs are roughly half as sensitive as those of bitumen, while the energy costs of mined SCO are approximately a third as sensitive as

the bitumen ones. The co-capture solutions are slightly more sensitive than the no co-capture ones to changes in boiler efficiency for SCO only. The bitumen energy costs sensitivity to boiler efficiency is the same in either case.

Table 5-24. 2030 energy costs sensitivity to boiler thermal efficiency ($/bbl) – no co-capture

Efficiency	Mined SCO	SAGD SCO	Bitumen	Max. CO_2 reduction
100%	-2.8%	-4.5%	-9.8%	43.7%
95%	-1.2%	-2.0%	-4.9%	41.3%
90%*	-6.8%	0.0%	0.0%	38.6%
90%	29.49	31.03	10.32	38.6%
85%	1.5%	2.4%	5.0%	35.6%
75%	5.0%	7.8%	15.1%	28.4%

* hot water from plant waste heat

The impact of steam boiler efficiency variations on CO_2 reduction levels is significant and quite similar in magnitude for both co-capture and no co-capture solutions. Reducing the efficiency values to 75% causes the maximum CO_2 reduction level to drop by 10 percentage points whereas at 100% efficiency the CO_2 reduction level elevates by roughly 5 percentage points.

Table 5-25. 2030 energy costs sensitivity to boiler thermal efficiency ($/bbl) – co-capture

Efficiency	Mined SCO	SAGD SCO	Bitumen	Max. CO_2 reduction
100%	-3.6%	-5.9%	-9.9%	44.7%
95%	-1.9%	-3.0%	-5.0%	42.3%
90%*	-9.0%	0.0%	0.0%	39.7%
90%	22.71	23.48	10.21	39.7%
85%	1.9%	3.1%	5.0%	36.7%
75%	5.9%	9.6%	15.3%	29.4%

* hot water from plant waste heat

If waste heat from oil sands operations is enough to produce all the hot water required for bitumen extraction, the energy costs of mined SCO can be reduced by approximately 7% and 9% for no co-capture and capture cases, respectively. This special case affects only mined SCO, since no other oil sands product requires hot water.

The optimal energy infrastructures of the no co-capture case are unaffected by variations in steam boiler efficiencies. The same is not true of the co-capture case, as seen in Table 5-26. Energy cost savings are possible at both ends of the range of efficiency values, thanks to slightly less expensive power generation as one Oxyfuel plant is replaced by a NGCC with capture.

Table 5-26. 2030 energy infrastructure sensitivity to boiler thermal efficiency – co-capture

Availability	P6	P8	H1	H2	H5
100%	1	6	1	1	21
95%	1	6	1	1	21
90%		7	1	1	21
85%		7	1	1	21
75%	1	6	1	1	21

P6 = NGCC with CO_2 capture, P8 = NG Oxyfuel, H1 = SMR, H2 = SMR with CO_2 capture, H5 = H_2 IGCC with CO_2 and H_2S co-capture

The last process parameter evaluated in 2030 is the CO_2 transport pipeline length. Generally speaking, all products are marginally affected by variations in pipeline length (see Table 5-27). The energy costs of SAGD SCO are somewhat more sensitive to pipeline length than mined SCO, whereas bitumen is almost completely unaffected by this parameter. Comparatively, however, the co-capture solutions are more sensitive to pipeline length fluctuations than their no co-capture counterparts. For example, doubling the length of the pipeline causes the SCO energy costs to rise by 3% in the former case while the increase for the latter case is roughly 1.5%.

Table 5-27. 2030 energy costs sensitivity to CO_2 pipeline length ($/bbl)

Length (km)	Mined SCO		SAGD SCO	
	no co-capture	co-capture	no co-capture	co-capture
1200	1.4%	3.3%	1.4%	3.2%
1000	0.9%	2.5%	1.0%	2.2%
800	0.5%	1.2%	0.5%	1.1%
600	22.09	22.71	23.02	23.48
400	-0.5%	-1.1%	-0.6%	-1.1%
300	-0.8%	-1.3%	-0.8%	-1.5%

Lengthening the CO_2 transport pipeline length affects the optimal energy infrastructures in the co-capture case only. Table 5-28 shows that as the length increases, so does the number of power plants in the infrastructure. This is caused by the additional power required to drive the booster compressors in the lengthened pipeline and by its corresponding rise in CO_2 captured due to the extra power requirements.

Table 5-28. 2030 energy infrastructure sensitivity to CO_2 transport pipeline length – co-capture

Length (km)	P1	P6	P8	H1	H2	H5
1200			8	1	1	21
1000			8	1	1	21
800	1		7	1	1	21
600			7	1	1	21
400		1	6	1	1	21
300			7	1	1	21

P1 = NGCC, P6 = NGCC with CO_2 capture, P8 = NG Oxyfuel, H1 = SMR, H2 = SMR with CO_2 capture, H5 = H_2 IGCC with CO_2 and H_2S co-capture

5.2.2.2 Sensitivity to economic parameters

The economic parameters evaluated in the sensitivity analyses in 2030 are presented in Table 5-29 along with their corresponding impacts on energy costs. From this table, it is evident that all energy costs are sensitive to changes in natural gas costs. Also, SCO energy costs in 2030 are moderately sensitive to variations in coal prices, annual capital charge rates, and overnight capital costs. Bitumen energy costs are largely insensitive to all parameters but natural gas prices. Finally, the results indicate that all energy costs are insensitive to changes in CO_2 transport and injection/storage costs. An in-depth analysis and discussion of each individual sensitivity is covered in the rest of this chapter.

The sensitivity of the model output to coal and natural gas prices was evaluated. For 2030, natural gas costs range from 5-18 $/GJ while coal costs values included in the analysis vary from 1.9-6 $/GJ. Figures 5-8 and 5-9 present the results of these sensitivity analyses.

The most sensitive of the products is bitumen. Its energy costs appear to vary almost equally to changes in natural gas prices, for both no co-capture and co-capture

cases. Thermal SCO is the next most sensitive product, varying ± 40% and ± 30% in the no co-capture and co-capture solutions, respectively, when gas prices vary by ± 50%.

Table 5-29. 2030 energy cost sensitivity to economic parameters summary

Value	Mined SCO $/bbl	SAGD SCO $/bbl	Bitumen $/bbl	Infrastructure changes?
Reference values				
N/A	22.49	31.03	10.32	N/A
Natural gas prices ($/GJ)				
18	32%	40%	46%	No
12		Reference		
6	-32%	-40%	-46%	No
Coal prices ($/GJ)				
6.0	10.1%	11.7%	0%	No
5.0	6.8%	7.8%	0%	No
3.0		Reference		
1.9	-4.3%	-3.9%	-0.5%	Yes
Annual capital charge rate (%)				
30	13.2%	12.2%	1.6%	No
15		Reference		
7.5	-6.0%	-5.6%	-0.7%	No
Overnight capital costs (% increase)				
200	26.9%	24.8%	3.3%	No
100	13.6%	12.5%	1.6%	No
50	6.8%	6.3%	0.9%	No
0		Reference		
-50	-6.8%	--6.3%	-0.8%	No
CO_2 transport costs ($/tonne CO_2/100km)				
2.8	1.3%	1.3%	0%	No
1.4		Reference		
0.7	-0.6%	-0.6%	0%	No
CO_2 injection/storage costs ($/tonne CO_2)				
16	1.2%	1.2%	0%	No
8		Reference		
4	-0.6%	-0.6%	0%	No

The sensitivity of mined SCO energy costs to natural gas prices is significant, but lower than those of SAGD SCO and bitumen. The energy costs of the former are roughly 10 percentage points smaller than those of the latter, for co-capture and no co-capture cases alike. In both instances, the optimal energy infrastructures composition remains unchanged throughout the range of natural gas prices.

The sensitivity to coal prices was conducted at a CO_2 reduction level of 35% in the no co-capture case while the co-capture analysis was performed at maximum reduction (39.7%). The former level was required since no coal-fuelled plants exist at maximum CO_2 reduction.

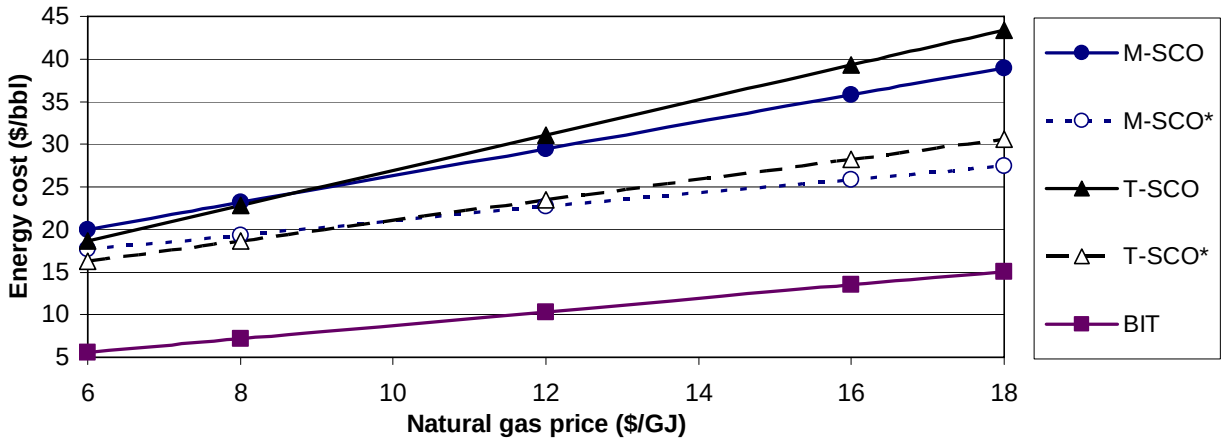

Figure 5-8. 2030 energy costs sensitivity to natural gas prices (* co-capture)

The energy costs of bitumen are insensitive to changes in coal prices and thus are not plotted on Figure 5-9. The energy costs of SCO are modestly affected by variations in coal prices. In the co-capture solutions, the energy costs of mined SCO are less sensitive than those of SAGD SCO.

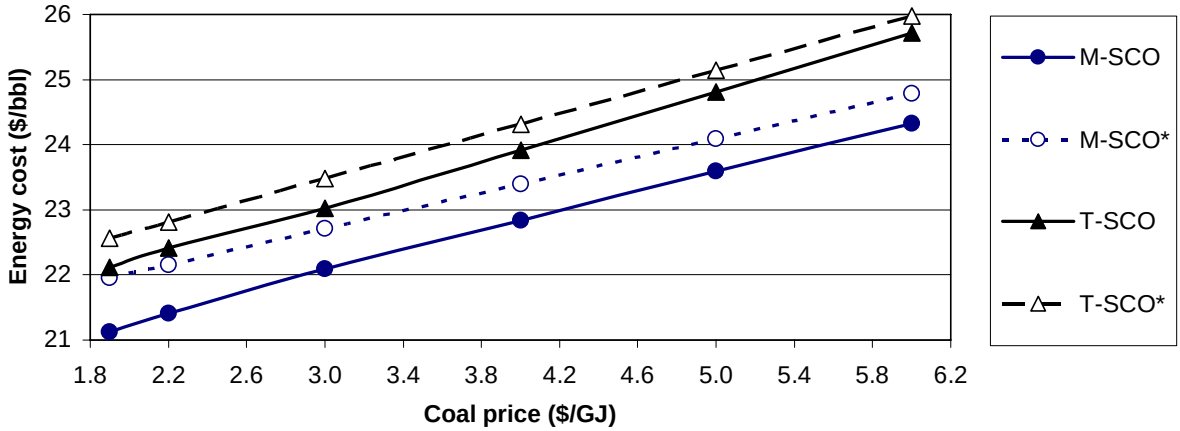

Figure 5-9. 2030 energy costs sensitivity to coal prices (* co-capture)

The composition of the optimal energy infrastructures of the co-capture solutions is insensitive to coal prices. In contrast, the optimal plant mix in the no co-capture cases changes when coal prices are lowered, as shown in Table 5-30. This response is significant, as the results suggest that coal oxyfuel plants are preferred over NGCC plants at moderate CO_2 reductions and low coal prices in 2030. This is the only instance where coal oxyfuel plants appear in the entire series of sensitivity analyses in this study.

Table 5-30. 2030 energy infrastructure sensitivity to coal prices – no co-capture

Coal price ($/GJ)	P6	P9	H1	H2	H4
6.0	7		1	1	21
5.0	7		1	1	21
4.0	7		1	1	21
3.0	7		1	1	21
2.2	1	5	1	1	21
1.9	1	5	1	1	21

P6 = NGCC with CO_2 capture, P8 = coal oxyfuel H1 = SMR, H2 = SMR with CO_2 capture, H4 = H_2 IGCC with CO_2 capture

The next economic parameter evaluated is the annual capital charge rate. The results of this analysis, carried over values ranging from 7.5-30%, are shown on Figure 5-10. These results show that bitumen is nominally sensitive to variations in annual capital charges. Mined SCO, on the other hand is somewhat more sensitive that SAGD SCO in no co-capture cases. For co-capture solutions, the effects of capital charge rates on energy costs are identical for mined and SAGD SCO. Generally speaking, however, the co-capture solutions are more sensitive to variations in annual capital charge rates than their no co-capture equivalents. This applies only to SCO, however.

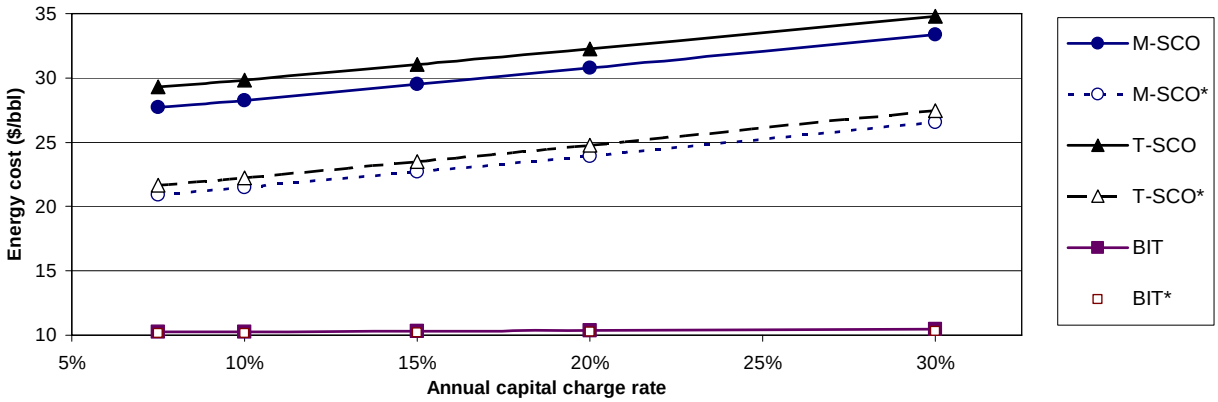

Figure 5-10. 2030 energy costs sensitivity to annual capital charge rates (* co-capture)

The overnight capital costs of power and hydrogen plants increased between 2012 and 2030 in the model results presented in Chapter 4. Nevertheless, a sensitivity analysis is performed, with the aim of investigating the extent of the impact that higher-than-predicted plant capital costs have on energy costs.

The results of the energy cost sensitivity to changes in overnight capital costs are summarized in Figure 5-11. It is evident that increases in capital costs have a significant impact on the energy costs of SCO but only a mild one on the energy costs of bitumen. This is due to the fact that large increases in the capital cost of power plants affect only the power costs. The energy costs of bitumen consist mostly of steam, so large increases in the cost of power have a minimal impact on the overall energy costs.

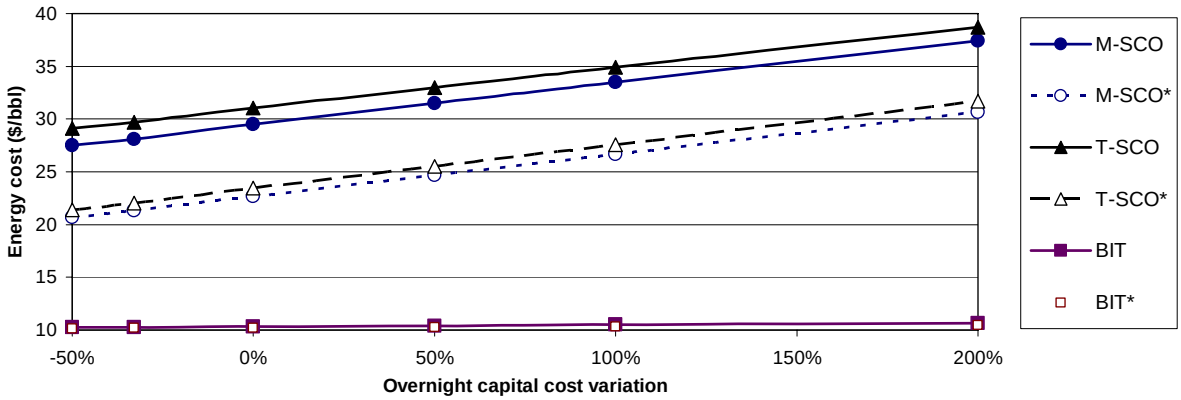

Figure 5-11. 2030 energy costs sensitivity to overnight plant capital cost (* co-capture)

Tripling the overnight capital costs of all available plants in the optimization model results in a substantial increase in the energy costs of SCO. For the no co-capture case, the increase is roughly 25% while the co-capture case increase is higher, reaching 35%, with respect to the reference energy costs. The sensitivity of mined SCO in the former case is slightly higher than that of SAGD SCO, whereas in the latter case, both mined and SAGD SCO are equally sensitive to variations in capital costs.

A most relevant result of this analysis is the fact that the optimal energy infrastructures for co-capture and co-capture scenarios are unaffected by changes in plant capital costs. This reinforces the confidence in the compositions of the above optimal energy infrastructures, even when capital costs rise due to changes in the local economy.

Concerning the sensitivity of the model results to CO_2 transport costs, the analysis results suggest that their effect on energy costs is insignificant, as seen in Figure 5-12. In

fact, the sensitivity of bitumen costs to CO_2 transport costs is null. For SCO, doubling the CO_2 transport costs result in an energy cost increase of 1.3% and of 2.5% for no co-capture and co-capture solutions, respectively. The energy infrastructures are as insensitive to CO_2 transport costs as the energy costs. Their composition remains unchanged for all CO_2 transport cost values used in this analysis.

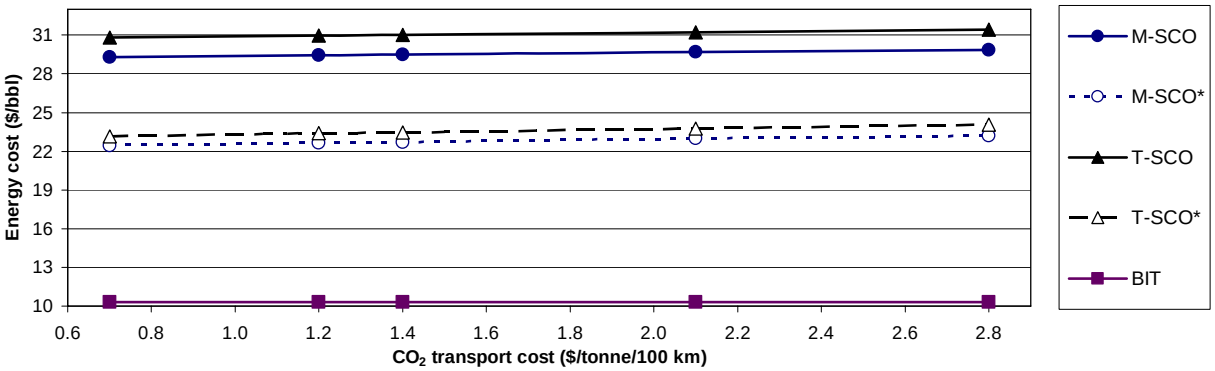

Figure 5-12. 2030 energy costs sensitivity to CO_2 transport costs (* co-capture)

The energy costs sensitivity to the CO_2 injection/storage cost is shown in Figure 5-13. Similarly to the CO_2 transport costs, the energy costs are not sensitive to changes in storage/injection costs. Co-capture solutions are roughly twice as responsive to injection costs as the no co-capture ones, yet their energy costs variation range is less than ± 2.5%. Just as with CO_2 transport costs, the energy infrastructures at maximum CO_2 reduction are unchanged by variations in CO_2 storage/injection costs.

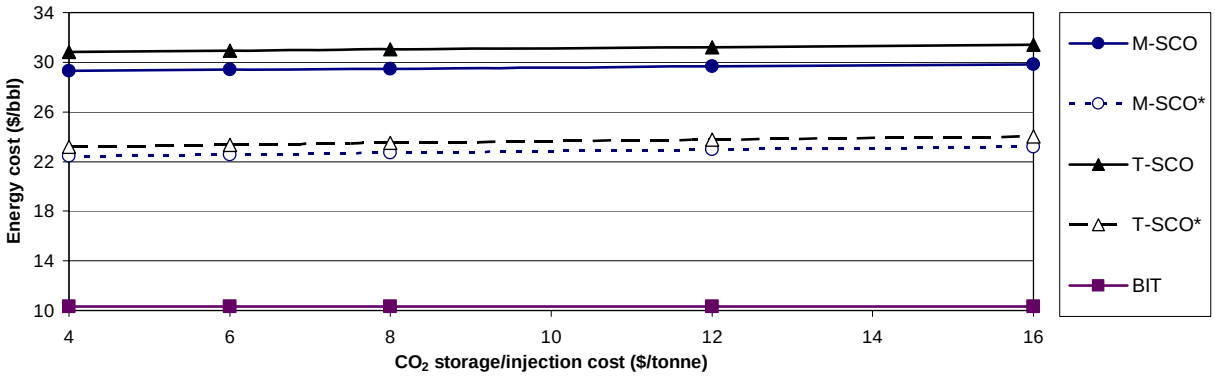

Figure 5-13. 2030 energy costs sensitivity to CO_2 injection/storage costs (* co-capture)

Chapter 6

Conclusions and Recommendations

6.1 OSOM Base Case and Future Production Scenarios

In the OSOM base case (2003), the bitumen upgrading to SCO is the most CO_2-intensive of all the process stages, accounting for 70-80% of the total GHG emissions in mining operations. The total calculated CO_2 intensity of SCO ranges from 0.080 to 0.087 tonne CO_2 eq/bbl. On the other hand, the calculated GHG intensity of thermally-produced bitumen is 0.037 tonne CO_2 eq/bbl. The energy costs of oil sands operations in 2003 are $13.63/bbl and $5.37/bbl for SCO and bitumen, respectively.

Of all the energy consumed in the oil sands industry in 2003, steam, H_2, and power are the leading sources of GHG emissions, accounting for approximately 80% of the total emissions. In SCO production, H_2 is the single largest source of CO_2, (37%) while steam and power are responsible for 27% and 11% of the total, respectively. Moreover, 95% of all GHG emissions in the base case are CO_2 while CH_4 and N_2O account for the remaining 5%. These non-CO_2 emissions are more significant than the total emissions from diesel fuel use in mining operations in 2003.

The demands for SAGD steam, process steam, hydrogen, and power will experience an explosive growth between 2003 and 2030. The demands for SAGD steam are poised to triple between 2003 and 2012 and triple again between 2012 and 2030. The H_2 demands of the oil sands industry in Alberta will likewise triple between 2003 and 2012 and grow by a factor of 2.7 thereafter. Process steam demands will roughly double between 2003 and 2012 and increase by a factor of 2.4 by 2030. The escalation in electricity demands follows a very similar pattern as the above steam demands.

6.2 GAMS Optimal Energy Infrastructure and Costs

The optimal energy infrastructures for 2012 reveal that the maximum attainable CO_2 reduction level is 25% with respect to baseline emissions. NGCC and NG Oxyfuel power

plants and coal gasification H_2 plants are favoured for CO_2 reduction levels under 20%. At 25% CO_2 reduction, only NG Oxyfuel and SMR plants with CO_2 capture are used, in addition to the existing 2003 plants. The optimization results suggest that the above-mentioned technologies hold the greatest promise for optimal CO_2-constrained oil sands operations in 2012.

Two chief conclusions can be drawn concerning the optimal energy infrastructures for 2030. Firstly, the most prominent technologies for power production (as selected by the optimizer) are natural gas-based: NGCC, with and without capture and oxyfuel. Supercritical coal plants are appealing only at CO_2 reduction levels between 20-30%. Secondly, gasification-based H_2 production is attractive at most CO_2 reduction levels. However, H_2 production via SMR with CO_2 capture is imperative to achieve CO_2 reductions greater than 35%. This nonetheless, comes with a sizeable cost penalty.

Based on the optimal energy infrastructures, it seems that R&D efforts must focus on improving the techno-economics of natural gas-based power production, particularly oxyfuel and NGCC with capture. Concerning H_2 production, the focus should be on gasification. Of special interest is the enhancement of the separate CO_2 and H_2S gasification plant to reach the technoeconomic performance of its co-capture counterpart.

With the 2012 optimal energy infrastructures, moderate energy cost savings (~7%) are possible for CO_2 reduction levels under 20%, with respect to the baseline. Achieving maximum CO_2 reductions (25%), however, results in an average 13% rise in energy costs. CO_2 transport and storage costs account for between 2-3.5% of the total energy costs of SCO for all feasible CO_2 reduction levels but are negligible for bitumen.

In 2030, the maximum attainable CO_2 emissions reduction level is 38.6% with respect to the baseline emissions. The optimization results also reveal that energy cost savings between 9-18% are possible up to a CO_2 reduction level of 36%. The energy costs increase by roughly 20% (SCO) and 2% (bitumen) with respect to baseline costs at maximum CO_2 reduction. Mined SCO has the largest CO_2 intensity reduction (46%), followed by SAGD SCO (39%). The CO_2 intensity of bitumen is practically constant for all CO_2 reduction levels. CO_2 transport and storage/injection costs account for ~5% (SCO) of its total energy cost while for bitumen, they represent less than 0.5% the total energy costs, but only at CO_2 reduction levels higher than 30%.

An important finding from this work is that attaining CO_2 reductions greater than 25% (2012) and 39% (2030) necessitates specific CO_2 mitigation strategies for steam generation processes. The magnitude of the combined CO_2 emissions from SAGD and process steam generation represents almost half of the total for 2030. By capturing CO_2 from steam generation, or otherwise reducing its emissions, substantial CO_2 reductions can be attained, on top of those accomplished by the optimal energy infrastructures.

Optimal energy infrastructures featuring co-capture of CO_2 and H_2S offer attractive energy cost reductions compared to infrastructures where co-capture is not allowed, for CO_2 reduction levels greater than 20%. The use of co-capture-enabled infrastructures also increases the maximum attainable CO_2 reduction levels by roughly 1%. An ideal setting for co-capture infrastructures is when sour CO_2 injection is technically feasible and CO_2 transport occurs in unpopulated areas or in short distances (the former is sink-dependent while the latter address safety concerns).

6.3 Sensitivity Analyses

This study features an extensive set of sensitivity analyses for all products and optimal solutions. The 2003 energy costs of SCO are most sensitive to changes in H_2, upgrading steam, and hot water, in that specific order. The relationship between SAGD steam demands and energy cost is nearly proportional. The OSOM base case sensitivity to natural gas prices is significant. On an industry scale, the total CO_2 emissions are chiefly sensitive to changes in H_2, SAGD steam, and upgrading steam demands. Changes in the demands of other commodities have a marginal effect on the CO_2 emissions.

The sensitivity of base case SCO costs and intensities to an ultra-H_2-intensive upgrading process was carried out. This analysis serves to investigate the impacts of producing almost aromatics-free synthetic crude, an attractive product for refineries in the Southern USA. The analysis reveal that doubling the 2003 H_2 demands for SCO production would increase its energy cost by a third, while causing the CO_2 intensity to rise by almost 40%. Also, the fleet CO_2 emissions would rise by roughly 30%.

The most sensitive of the products to variations in natural gas prices is bitumen. Its energy costs appear to vary almost equally to changes in gas prices. Thermal SCO is the next most sensitive product, while the sensitivity of mined SCO energy costs to gas

prices is lower than those of SAGD SCO and bitumen. In 2012 and 2030, the composition of the optimal energy infrastructures is unaffected throughout the range of gas prices. The sensitivity analyses to coal prices show that the energy costs of bitumen are insensitive to coal prices while the SCO costs are mildly affected by these variations.

A key result of this study is the fact that the optimal energy infrastructures for co-capture and no co-capture scenarios are unaltered by changes in plant capital costs. This reinforces the confidence in the optimal energy infrastructures, even when capital costs rise due to changes in the economy. The energy costs of bitumen are insensitive to changes in capital costs. The energy costs of SCO show a moderate sensitivity to variations in plant capital costs. Another parameter that was evaluated in this study is the annual capital charge rate. Mined SCO shows a mild sensitivity to fluctuations in capital charge rate, followed by SAGD SCO. Bitumen is insensitive to the capital charge rate.

In terms of sensitivity to CO_2 transport and storage costs, the results show that the energy costs of SCO have a very low sensitivity to fluctuations in these costs while bitumen is insensitive to them. Doubling the transport and storage costs increases the energy costs by less than 2%. Finally, the optimal energy infrastructures are unaffected by changes in the CO_2 transport and storage costs within the value ranges of this study.

A process parameter that was tested in this study is the length of the pipeline connecting the CO_2 sources to the sinks in Alberta. The pipeline length was varied between half and double its original value of 600 km. The results of this analysis show that in 2012 and 2030 the energy costs of bitumen are almost completely unaffected by changes in the pipeline length, whereas mined and SAGD SCO costs are only marginally sensitive to this parameter, rising less than 2% when the length doubles.

In addition to costs, the sensitivity of the optimal solutions to changes in IGCC plant availability was investigated. The 2012 and 2030 optimization results show that the energy costs are almost insensitive to changes in IGCC plant availability. These changes also have a nil effect on the mix of technologies in the optimal energy infrastructures.

6.4 Recommendations

In this section, the most relevant future directions of research and development for this study are summarized and discussed. The areas of development are organized in no particular order and no priority is assigned to the possible future R&D avenues.

A multi-period optimization model based on the current model must be developed. While the current optimization model is capable of optimizing energy demands for a given oil sand production level, it is desirable to determine the optimal growth patterns for the industry when CO_2 constraints and economic fluctuations are considered an inherent part of the model. Such a multi-period model would enable the users to determine the long-term financial and environmental impacts of proposed CO_2 mitigation strategies or their absence in the oil sands industry. The GAMS optimization model presented in this study has laid down the foundations for such a model. Its transparent and scalable architecture lends it great flexibility for further development.

Incorporate technological advancements in oil sand operations and energy production to the OSOM and optimization models. This applies to the OSOM future production scenarios. It is advantageous that the OSOM-FPS accounts for anticipated energy reductions/increases brought about by new and improved technologies in bitumen extraction and upgrading. SAGD extraction and bitumen upgrading are the top two areas where the energy intensity of operations may change between the present and the years 2012 and 2030. In the former, reductions in steam intensity and solvent-assisted extraction are being researched currently, as they have great potential to reduce the water and energy demands of the SAGD process. In the latter, increased demand for aromatics-free SCO may drive hydrogen demands to higher levels in the short term.

Add partially upgraded bitumen to the product mix in the OSOM and optimization models. According to officials from North American Oil Sands, in the future, oil sand companies will market “sour synthetic crude”, in addition to fully upgraded SCO and diluted bitumen. This sour synthetic is essentially bitumen that has been processed in a coker but not hydrotreated. This product is expected to be sold to refineries in the USA and perhaps new Asian customers. The OSOM and optimization models could be expanded to cover this new product, using the basic architecture and the equations corresponding to existing bitumen extraction and upgrading processes.

Incorporate nuclear-based energy production to the optimization model energy technologies database. Initially (between the present and 2012), only nuclear power would be available and some of it could potentially be used to produce hydrogen via electrolysis. Over the long term (post-2020), however, hydrogen production using termochemical processes integrated with nuclear reactors may become commercially available and could then, be added to the optimization model. The reader must note that currently, hydrogen production via nuclear exists only at a conceptual stage, with commercial prospects ranging 20-30 years into the future.

Simulation of more gasification-based energy production technologies is required. Current interest in gasification of bitumen residues in Alberta is high. According to Jacobs Canada, energy production from gasification of asphaltenes is economically attractive at current oil and energy prices. Other bitumen-derived gasification feedstocks that must be investigated include petcoke, pitch, and raw bitumen. Additionally, it would be advisable to also include biomass in the proposed mix of technologies for further study as potential sources of energy for oil sands operations. The techno-economics of all of the above gasification plants must be determined in an Alberta-specific environment that includes CCS technologies. The resulting data could then be added to the optimization model.

Add an option to the optimization model to pipeline bitumen from Fort McMurray to the Greater Edmonton Area for upgrading. Currently, at least three major upgraders operating in the area have been announced. They are expected to begin operations between the years 2010 and 2015. Therefore, the optimization model should incorporate a way to account for this new infrastructure. The model has already been prepped for such a modification: the energy demands for upgrading of all products are separate model inputs that can be manipulated independently of all other energy demands. This should simplify the modifications required to the GAMS code to implement the said feature.

Incorporate CO_2 credits/taxes to the optimization model. It is worthy to study the financial impact that an eventual CO_2 trading market would have on the energy costs of oil sands operations, and more importantly, on the shape of the optimal energy

infrastructures determined by the model. A sensitivity analysis to increasing CO_2 prices is highly desirable and useful.

Investigate new ways to produce low-GHG intensive SAGD and process steam. One major lesson learned during this project is that deep CO_2 emissions reductions in the oil sands industry will be unattainable unless the sizeable emissions from steam production can be mitigated. GHG-free steam production is one of the greatest challenges ahead for the oil sands industry, which is only worsened by the water availability issues that accompany oil sands operations growth. The optimization model can be modified to explore the financial and environmental impacts of, for instance, using H_2 as fuel in boilers for steam production, or steam production using electrical boilers. In both the above scenarios, H_2 and power would be produced in plants with built-in CO_2 capture.

Add poly-generation and co-generation plants a to the optimization model. A fourth year project based on IGCC plant models featured in this study was carried out between January and April, 2007. The project attempted to simulate a coal gasification plant producing power, steam, and hydrogen, which has the potential to supply the above commodities to oil sands operators at reduced costs relative to separate boilers, power, and hydrogen plants. In addition to cost reductions, such a plant with CO_2 capture can also reduce the GHG intensity associated with power, steam, and hydrogen production, with highly promising environmental benefits for SCO and bitumen production. More of the power plants featured in the GAMS model should be modeled as co-generation plants and their techno-economics formally assessed for inclusion in the model.

Incorporate the economics of EOR and ECBM to the optimization model. The economic benefit of injecting CO_2 in aging oil fields must be clearly known, preferably as a function of oil prices and CO_2 capture costs. Adding such economic data to the model would be challenging, as the economics of EOR and ECBM are very site-specific. Nevertheless, it is necessary to have at least an approximate idea of the economic impact of using CO_2 in the above two applications.

References

[1] National Energy Board. (2003). *Canada's Energy Future. Scenarios for Supply and Demand to 2025*. National Energy Board Publications Office. Calgary, Canada.

[2] National Energy Board. (2006). *Canada's Oil Sands Opportunities and Challenges to 2015: An Update*. National Energy Board Publications Office. Calgary, Canada.

[3] Lee, S. (1996). *Alternative Fuels*. Taylor & Francis, Washington, United States.

[4] McCulloch, M., Raynolds, M., Wong, R. (2006). *Carbon Neutral 2020: A Leadership Opportunity in Canada's Oil Sands*. The Pembina Institute. Drayton Valley, Canada.

[5] Lakeman, B., Gunter, W., Brown, K. (2006) *Establishing and Implementing a Management Framework for CO_2 Capture and Geological Storage Activities: CANiCAP and CANiSTORE – A Canadian Case study*. Proceedings of the GHGT-8 Conference. Trondheim, Norway, June, 2006.

[6] Gunter, B., Bachu, S. (2003). *Canadian Sedimentary Basins: Carbon Dioxide Storage Opportunities*. Presentation at the Canadian Clean Coal Roadmap Workshop, Calgary, Alberta, Canada, March 20-21, 2003

[7] De Malherbe, R., Doswell, S.J., Mamalis, A.G., de Malherbe, M.C. (1983). *Synthetic Crude from Oil Sands*. VDI-Verlag GmbH. Düsseldorf, Germany.

[8] http://www.syncrude.ca. Accessed on August, 2007.

[9] http://www.suncor.ca. Accessed on August, 2007.

[10] Alberta Chamber of Resources. (2004). *Oil Sands Technology Roadmap Unlocking the Potential*. Alberta Chamber of Resources. Edmonton, Canada.

[11] http://www.longlake.ca/default.asp. Accessed on August, 2007.

[12] http://www.eub.gov.ab.ca/BBS/new/newsrel/2000/nr2000-17.htm. Accessed on August, 2007.

[13] Meyers, R.A. (1984). *Handbook of Synfuels Technology*. McGraw-Hill Inc., California, United States.

[14] http://www.hydrocarbonprocessing.com/handbooks//contents2.html. Accessed on August, 2007.

[15] Lott, R., Lee, L.K. (2003). *Upgrading of Heavy Crude Oils and Residues with (HC)3 ™ Hydrocracking Technology*. Paper presented at the 2003 American Institute of Chemical Engineers annual conference. April 2, 2003. New Orleans, United States.

[16] Harrell, G. (2002). *Steam System Survey Guide*. Report ORNL/TM-2001/263.: Oak Ridge National Laboratory. Tennessee, United States.

[17] Thambimuthu, K. (2003). *Clean Coal Roadmap 'Strawman.'* Presentation at the 1st Canadian Clean Coal Technology Roadmap. Calgary, Alberta, Canada. March 21-21, 2003.

[18] Simbeck, D, Chang, E. (2002). *Hydrogen Supply: Cost estimate for Hydrogen Pathways – Scoping Analysis*. Report NREL/SR-540-32525. National Renewable Energy Laboratory. Colorado, United States.

[19] Simbeck, D. R. (2004). *Hydrogen Costs with CO_2 Capture*. Proceedings of the GHGT-7 Conference. Vancouver, Canada, September, 2004.

[20] Kruse, B., Grinna, S., Buch, C. (2002). *Hydrogen – Status and Possibilities*. The Bellona Foundation. Oslo, Norway.

[21] Chiesa, P., Consonni, S., Kreutz, T., Williams, R. (2005). *Co-production of hydrogen, electricity, and CO_2 from coal with commercially ready technology. Part A: Performance and emissions.* International Journal of Hydrogen Energy. 30:747, 2005.

[22] Kreutz, T., Williams, R., Consonni, S., Chiesa, P. (2005). *Co-production of hydrogen, electricity, and CO_2 from coal with commercially ready technology. Part B: Economic analysis*. International Journal of Hydrogen Energy. 30:769, 2005.

[23] Schultz, K. R., Brown, L.C., Besenbruch, G.E. (2003). *Large-scale production of hydrogen by nuclear energy for the hydrogen economy*. Proceedings of the National Hydrogen Association Annual Conference. April 6-9, 2003. Washington, United States.

[24] Rubin, E.S., Rao, A. B., Chen, C. (2004). *Comparative assessments of fossil fuel power plants with CO_2 capture and storage*. Proceedings of the GHGT-7 Conference. Vancouver, Canada, September, 2004.

[25] Jordal, K., Anhede, A., Yan, J., Strömberg, L. (2004). *Oxyfuel combustion for coal-fired power generation with CO_2 capture – opportunities and challenges*. Proceedings of the GHGT-7 Conference. Vancouver, Canada, September, 2004.

[26] Ordorica-Garcia, G., Douglas, P., Croiset, E., Zheng, L. (2006). *Technoeconomic evaluation of IGCC power plants for CO_2 avoidance*. Energy Conversion and Management. 47:2250, 2006.

[27] Ordorica-Garcia, G. (2003). E*valuation of Combined-Cycle Power Plants for CO_2 Avoidance*. Master's thesis. University of Waterloo, Canada, 2003.

[28] Davison, J. (2007). *Performance and costs of power plants with capture and storage of CO_2*. Energy. 32:7, 2007.

[29] Alberta Energy and Utilities Board. (2004). *Alberta Oil Sands Annual Statistics for 2003*. Report ST 2003-43. Alberta Energy and Utilities Board. Calgary, Canada.

[30] http://www.syncrude.ca/users/folder.asp?FolderID=5726. Accessed on July, 2006.

[31] http://www.alfalaval.com/digitalassets/2/file10080_0_PD41493e.pdf. Accessed on January 2007.

[32] OPTI Canada. (2002). *OPTI Canada Long Lake Project Application for Commercial Approval. Volume 1 Sections A, B, and C.* Application submitted to the Alberta Energy Utilities and Board. Calgary, Canada.

[33] Sunderland, B. (2001).*Hydrogen Production, Recovery and Use at Syncrude*. Presentation at the EFI Conference on Technologies to Enable the Hydrogen Economy. April 22-24, 2001. Tucson, United States.

[34] Schumacher, M. (1982). *Heavy Oil and Tar Sands Recovery and Upgrading International Technology*. Noyes Data Corporation. Park Ridge, United States.

[35] Van Driesen, R., Caspers, J., Campbell, A.R., Lunin, G. *LC-Fining Upgrades Heavy Crudes*. (1979). Hydrocarbon Processing. 58:5, 1979.

[36] Sadorah, R., Shell Canada, personal communication (2005)

[37] http://www.coptechnologysolutions.com/thruplus_delayed_coking/thruplus/tech_specs/index.htm. Accesed on August, 2007.

[38] Yui, S., Chung, K.H. (2001). *Processing oil sands bitumen is Syncrude's R&D focus*. Oil & Gas Journal. 99:17, 2001.

[39] Spath, P. L., Mann, M. K. (2000). *Life Cycle Assessment of a Natural Gas Combined-Cycle Power Generation System*. Report NREL/TP-570-27715. National Renewable Energy Laboratory. Colorado, United States.

[40] Nyober, J. (2003). *A Review of Energy Consumption in Canadian Oil Sands Operations, Heavy Oil Upgrading 1990, 1994 to 2001*. Canadian Industry Energy End-use Data and Analysis Centre. Vancouver, Canada.

[41] Spath, P. L., Mann, M. K. (2001). *Life Cycle Assessment of Hydrogen Production via Natural Gas Steam Reforming*. Report NREL/TP-570-27637. National Renewable Energy Laboratory. Colorado, United States.

[42] Faltinson, J. Carbon and energy Management, Alberta Research Council, personal communication. February, 2007.

[43] Gunter, B., Chalaturnyk, R. (2004). *The CANiSTORE Program. Planning Options for Technology and Knowledge Base Development for the Implementation of Geological Storage Research, Development and Deployment in Canada*. Alberta Research Council. Edmonton, Canada.

[44] Mitchell, B, Van Ham, J. (2006). *Canada's CO_2 Capture and Storage Technology Roadmap*. CANMET Energy Technology Centre. Ottawa, Canada.

[45] Stambler, I. (2002). *Calpine sees coal-based IGCC plants generating power for $40 per MWh*. Gas Turbine World. 32:4.

[46] http://www.netl.doe.gov/publications/brochures/pdfs/Gasification_Brochure.pdf. Accessed on August, 2007.

[47] USA Energy Information Administration. (2007). *Annual Energy Outlook 2007 With Projections to 2030*. Report DOE/EIA-0383(2007). U.S. Department of Energy. Washington, United States.

[48] Walden, T. (2006). *Relative Costs of Electricity Generation Technologies*. Canadian Energy Research Institute. Calgary, Canada.

[49] Rubin, E.S., Taylor, M.R., Yeh, S., Hounshell, D.A. (2004). *Learning curves for environmental technology and their importance for climate change policy analysis*. Energy. 29:9-10, 2004.

[50] http://www.transalta.com/transalta/webcms.nsf/0/76FEA6403BECE73F8725728A007019DF?OpenDocument. Accessed on September, 2007.

[51] IEA (2005). World Energy Outlook. OECD/IEA. http://www.iea.org//textbase/nppdf/free/2005/weo2005.pdf. Accessed on August, 2007.

[52] http://www.chapeng.ab.ca/forecast0701.htm. Accessed on September, 2007.

[53] http://eetd.lbl.gov/EA/EMP/reports/53587_memo.pdf. Accessed on September, 2007.

Appendix I – OSOM Parameter Values

ERS =	3.1	[kW/tonne bitumen]
f =	refer to Table 2-2	[l/h]
FCH =	174,910	[MJ/tonne H_2]
FEF =	0.00179	[tonne CO_2/Nm^3 natural gas]
	0.00270	[tonne CO_2/l diesel]
FRD =	153	[MJ/tonne feed]
FRL =	93	[MJ/tonne feed]
HDR =	934	[MJ/tonne feed]
HEF =	9.52	[tonne CO_2/tonne H_2]
HFC =	1058	[MJ/tonne feed]
HHG =	0.0027	[tonne/bbl feed]
HHV =	38.05	[MJ/Nm^3]
HLG =	0.0027	[tonne/bbl feed]
HLH =	0.020	[tonne/tonne feed]
HLL =	0.014	[tonne/tonne feed]
HNP =	0.0021	[tonne/bbl feed]
HRP =	7.39	[MJ/kWh]
HVD =	214	[MJ/tonne feed]
PDC =	23.2	[kW/tonne feed]
PFC =	36.4	[kW/tonne feed]
PLH =	99.7	[kW/tonne feed]
PLL =	99.7	[kW/tonne feed]
PSP =	74.4	[%]
SCS =	70	[mass %]
SF =	2.1	[mass %]
SOL =	2	[tonne gas/tonne bitumen]
SOR =	2.4	[tonne steam/tonne bitumen]
SSE =	0.04	[tonne steam/tonne froth]
WWE =	0.41	[tonne water/tonne oil sand]
ΔHS =	3415	[MJ/tonne process steam]
	2469	[MJ/tonne SAGD steam]
ΔHW =	115	[MJ/tonne]
η_B =	90	[%]
ρ =	0.118	[tonne/bbl naphtha]
	0.145	[tonne/bbl LGO]
	0.154	[tonne/bbl HGO]

Appendix II – GAMS Model Input File

```
$Title Oil Sands Operations Optimization - Year 2030 (Guillermo Ordorica-Garcia - Author)
$Ontext
This model determines the best combination of hydrogen plants,
power plants, feedstocks, and CO2 capture processes to use in the
oil sands industry to satisfy future energy demands at minimal cost
while meeting CO2 reduction targets for specified SCO and bitumen production levels
$Offtext
Sets
NGB natural gas boilers (steam @ 950 psig and 500 C - Upgrading)      /NGB1*NGB90/
SGB natural gas boilers (steam @ 8000 kPa - SAGD)                     /SGB1*SGB150/
SP1 NGCC power plants                                                 /NG1*NG30/
SP2 PC power plants                                                   /PC1*PC30/
SP3 IGCC power plants                                                 /IG1*IG30/
SP4 IGCC w 88% CO2 capture plants                                     /IGC1*IGC30/
SP5 IGCC w 88% CO2+H2S co-capture plants                              /IGCO1*IGCO30/
SP6 NGCC w 90% capture power plants                                   /NGC1*NGC30/
SP7 PC w 90% capture power plants                                     /PCC1*PCC30/
SP8 NG Oxyfuel w capture power plants                                 /NGOX1*NGOX30/
SP9 Coal Oxyfuel w capture power plants                               /COOX1*COOX30/
SR steam reforming H2 plants                                          /SR1*SR120/
SH2 steam reforming w 90% capture H2 plants                           /SRC1*SRC120/
SH3 IGCC H2 plants                                                    /IGH1*IGH30/
SH4 IGCC w 90% capture H2 plants                                      /IGHC1*IGHC30/
SH5 IGCC w 90% co-capture H2 plants                                   /IGHCO1*IGHCO30/;
* ---------------------- SCALAR LIST ----------------------------------
* Fleet demands (SCO+BIT production correspond to OSTR year 2030 = OSOM FPS 2030)
*       Diesel
scalar DCS Diesel for current mined SCO production (l\h)              /43486/
scalar DNS Diesel for NEW mined SCO production (l\h) 113062           /113062/
*       Hot water
scalar WCS Water for current SCO production (tonne\h)                 /28462/
scalar WNS Water for NEW mined SCO production (tonne\h)               /73901/
*       Steam - Upgrading
scalar SCMU Steam for current mined SCO - UPGRADING (tonne\h)         /2671/
```

scalar SNTU Steam for NEW thermal SCO - UPGRADING (tonne\h) /6279/
scalar SNMU Steam for NEW mined SCO - UPGRADING (tonne\h) /6958/
* Steam - Balance of Plants
scalar SCMS Steam for current mined SCO - PLANT (tonne\h) /417/
scalar SNTS Steam for NEW thermal SCO - PLANT (tonne\h) /0/
scalar SNMS Steam for NEW mined SCO - PLANT (tonne\h) /987/
* Steam - SAGD
scalar SCTB Steam for current thermal BITUMEN - SAGD (tonne\h) /5602/
scalar SNTB Steam for NEW thermal BITUMEN - SAGD (tonne\h) /10404/
scalar SNTSS Steam for NEW thermal SCO - SAGD (tonne\h) /32994/
* Electricity - Balance of plants
scalar PCTB Power for current thermal BITUMEN - PLANT (kWh) /49632/
scalar PCMS Power for current mined SCO - PLANT (kWh) /470422/
scalar PNTB Power for NEW thermal BITUMEN - PLANT (kWh) /92174/
scalar PNTS Power for NEW thermal SCO - PLANT (kWh) /358654/
scalar PNMS Power for NEW mined SCO - PLANT (kWh) /1209466/
* Electricity - Upgrading
scalar PCMSU Power for current mined SCO - UPGRADING (kWh) /118591/
scalar PNTSU Power for NEW thermal SCO - UPGRADING (kWh) /663580/
scalar PNMSU Power for NEW mined SCO - UPGRADING (kWh) /344197/
* Hydrogen - UPGRADING
scalar HCMS H2 for current mined SCO - UPGRADING (tonne\h) /71.8/
scalar HNTS H2 for NEW thermal SCO - UPGRADING (tonne\h) /333.4/
scalar HNMS H2 for NEW mined SCO - UPGRADING (tonne\h) /205.1/
scalar HHE Hydrogen for H2 Economy (tonne\h) /0/
* Process fuel for Upgrading
scalar NGCMS NG for current mined SCO - UPGRADING (Nm3\h) /33428/
scalar NGNTS NG for NEW thermal SCO - UPGRADING (Nm3\h) /144469/
scalar NGNMS NG for NEW mined SCO - UPGRADING (Nm3\h) /94432/
* Fleet products
* SCO production
scalar CMSCO Current mined SCO (bbl\h) /22425/
scalar NTSCO NEW thermal SCO (bbl\h) /83333/
scalar NMSCO NEW mined SCO (bbl\h) /60908/
* Diluted Bitumen production
scalar CTB Current thermal BITUMEN (bbl\h) /14583/
scalar NTB NEW thermal BITUMEN (bbl\h) /27083/

```
*       Petcoke production
scalar CKCMS Coke from current mined SCO (tonne\h)                    /500/
scalar CKNTS Coke from NEW thermal SCO (tonne\h)                       /908/
scalar CKNMS Coke from NEW mined SCO (tonne\h)                        /1217/
*       Fuel gas production
scalar FGCMS Fuel gas from current mined SCO (tonne\h)                /0/
scalar FGNTS Fuel gas from NEW thermal SCO (tonne\h)                  /0/
scalar FGNMS Fuel gas from NEW mined SCO (tonne\h)                    /0/
* CO2 reduction input parameters
scalar CO2B Baseline CO2 emissions (tonne\h)                          /15658.95/
scalar ERG CO2 reduction percentage (%)                               /0.3967/
scalar CCT CO2 transport cost ($\tonne CO2\100 km)                    /1.40/
scalar PKM CO2 pipeline length (km)                                   /600/
scalar PCT Compression power for CO2 trans (kWh\tonne CO2)            /1.34/
scalar CST CO2 underground injection cost ($\tonne CO2)               /8.0/
* CO2 emissions factors
scalar FEFC Coal (tonne CO2\tonne coal)                               /3.7/
scalar FEFD Diesel (tonne CO2\l diesel)                               /0.0027/
scalar FEFNG NG (tonne CO2\Nm3 NG)                                    /0.00179/
scalar HEFSR H2 SR plant (tonne CO2\tonne H2)                         /8.992/
scalar HEFH2 H2 SR w 90% capture plant (tonne CO2\tonne H2)           /1.050/
scalar EFSP1 NGCC plant (tonne CO2\kWh)                               /0.000367/
scalar EFSP2 PC plant (tonne CO2\kWh)                                 /0.000811/
scalar EFSP3 IGCC plant (tonne CO2\kWh)                               /0.000800/
scalar EFSP4 IGCC w 88% capture (tonne CO2\kWh)                       /0.000131/
scalar EFSP5 IGCC w 88% co-capture (tonne CO2\kWh)                    /0.000118/
scalar EFSP6 NGCC w 90% capture (tonne CO2\kWh)                       /0.000043/
scalar EFSP7 PC w 90% capture (tonne CO2\kWh)                         /0.000107/
scalar EFSP8 NG Oxyfuel w capture (tonne CO2\kWh)                     /0.000012/
scalar EFSP9 Coal Oxyfuel w capture (tonne CO2\kWh)                   /0.000084/
scalar EFSH3 IGCC H2 plant (tonne CO2\tonne H2)                       /18.732/
scalar EFSH4 IGCC w 90% capture H2 plant (tonne CO2\tonne H2)         /1.502/
scalar EFSH5 IGCC w 90% co-capture H2 plant (tonne CO2\tonne H2)      /0.810/
* CO2 capture factors
scalar CCSH2 CO2 captured SR w 90% capture (tonne CO2\tonne H2)       /9.446/
scalar CCSH4 CO2 captured IGCC w 90% capture (tonne CO2\tonne H2)/17.262/
scalar CCSH5 CO2 captured IGCC w 90% co-cap (tonne CO2\tonne H2) /17.262/
```

```
scalar CCSP4 CO2 captured IGCC w 88% (tonne CO2\kWh)                 /0.000911/
scalar CCSP5 CO2 captured IGCC w 88% co-capture (tonne CO2\kWh)      /0.000842/
scalar CCSP6 CO2 captured NGCC w 90% (tonne CO2\kWh)                 /0.000387/
scalar CCSP7 CO2 captured PC w 90% capture (tonne CO2\kWh)           /0.000959/
scalar CCSP8 CO2 captured NG Oxyfuel w capture (tonne CO2\kWh)       /0.000403/
scalar CCSP9 CO2 captured Coal Oxyfuel w capture (tonne CO2\kWh)     /0.000831/
* Coal properties  (Highvale mine, AB)
scalar ULTC C content from Ultimate analysis (%)                     /0.63/
scalar ASH unburned carbon converted to ash (%)                      /0.17/
scalar HHVC coal HHV (MJ\kg)                                         /24.05/
* NG properties (Western Canadian)
scalar HHVNG NG HHV (MJ\Nm3)                                         /38.05/
scalar LHVNG NG LHV (MJ\Nm3)                                         /34.59/
* Petcoke properties (TBD)
scalar LHVK Petcoke LHV (MJ\kg)                                      /33.60/
* Refinery Gas properties
scalar LHVFC Fuel gas LHV - Meyers (MJ\kg)                           /4.64/
scalar LHVLC LC Fining fuel gas - Shafeen (MJ\kg)                    /10.6/
* Conversion Factors
scalar BBL bbl to m3 (m3\bbl)                                        /0.1589873/
scalar H2D H2 density (SCF\tonne)                                    /423300/
scalar NM3 Nm3 to SCF (SCF\Nm3)                                      /33.40/
scalar BTU BTU to MJ (BTU\MJ)                                        /948/
* Economics - Miscellaneous
scalar USD USD->CAD exchange rate (USD\CAD)                          /1.000/
scalar CWT boiler feed water cost (USD$\tonne)                       /1.5/
scalar RET annual capital charge rate (%)                            /0.15/
scalar t annual operating hours (h\yr)                               /8760/
scalar LOC Location factor for capital costs (%)                     /1/
scalar CVR Capital cost escalation factor for sensitivity (%)        /2/
* Economics - Fuel prices
scalar CCL coal cost (USD$\GJ)                                       /3.0/
scalar CNG NG cost (USD$\GJ)                                         /12.0/
scalar CCK petcoke cost (USD$\GJ)                                    /0.4/
scalar CDI Diesel cost (USD$\l)                                      /1.5/
* Economics - Plant availability/capacity factors
scalar CFSR annual CF for SR plants (%)                              /0.90/
```

```
scalar CFH2 annual CF for SR w 90% capture plants (%)                /0.90/
scalar CFH3 annual CF for IGCC H2 plants (%)                         /0.83/
scalar CFH4 annual CF for IGCC w 90% capture H2 plants (%)           /0.83/
scalar CFH5 annual CF for IGCC w 90% co-capture H2 plants (%)        /0.83/
scalar CFNG annual CF for NGCCs (%)                                  /0.90/
scalar CFPC annual CF for PCs (%)                                    /0.90/
scalar CFIG annual CF for IGCCs (%)                                  /0.88/
scalar CFP4 annual CF for IGCCs w 88% capture (%)                    /0.88/
scalar CFP5 annual CF for IGCCs w 88% co-capture (%)                 /0.88/
scalar CFP6 annual CF for NGCCs w 90% capture (%)                    /0.90/
scalar CFP7 annual CF for PCs w 90% capture(%)                       /0.90/
scalar CFP8 annual CF for NG Oxyfuel w capture (%)                   /0.90/
scalar CFP9 annual CF for Coal Oxyfuel w capture (%)                 /0.90/
* Economics - Plant operating/book lives
scalar LH1 operating life - SR   (yr)                                /30/
scalar LH2 operating life - SR w 90% capture (yr)                    /30/
scalar LH3 operating life - IGCC H2 (yr)                             /30/
scalar LH4 operating life - IGCC w 90% capture H2 (yr)               /30/
scalar LH5 operating life - IGCC w 90% co- capture H2 (yr)           /30/
scalar LP1 operating life - NGCC (yr)                                /30/
scalar LP2 operating life - PC (yr)                                  /30/
scalar LP3 operating life - IGCC (yr)                                /30/
scalar LP4 operating life - IGCC w 88% capture (yr)                  /30/
scalar LP5 operating life - IGCC w 88% co-capture (yr)               /30/
scalar LP6 operating life - NGCC w 90% capture (yr)                  /30/
scalar LP7 operating life - PC w 90% capture (yr)                    /30/
scalar LP8 operating life - NG Oxyfuel w capture (yr)                /30/
scalar LP9 operating life - Coal Oxyfuel w capture (yr)              /30/
* Economics - Plant O&M Factors (as a % of total plant capital cost)
scalar OH1 O&M factor for SR (default = 0.060)                       /0.0600/
scalar OH2 O&M factor for SR w 90% capture (default = 0.060)         /0.0600/
scalar OH3 O&M factor for IGCC H2 (default = 0.0356)                 /0.0356/
scalar OH4 O&M factor for IGCC H2 w 90% cap (default = 0.0356)       /0.0356/
scalar OH5 O&M factor for IGCC H2 w 90% co-cap (default = 0.0356)    /0.0356/
scalar OP1 O&M factor for NGCC (default = 0.0180)                    /0.0180/
scalar OP2 O&M factor for PC (default = 0.0380)                      /0.0380/
scalar OP3 O&M factor for IGCC (default = 0.0264)                    /0.0264/
```

```
scalar OP4 O&M factor for IGCC w 88% capture (default = 0.0252)      /0.0252/
scalar OP5 O&M factor for IGCC w 88% co-capture (def = 0.0262)      /0.0262/
scalar OP6 O&M factor for NGCC w 90% capture (default = 0.0370)     /0.0370/
scalar OP7 O&M factor for PC w 90% capture (default = 0.0494)       /0.0494/
scalar OP8 O&M factor for NG Oxyfuel w capture (def = 0.0860)       /0.0860/
scalar OP9 O&M factor for Coal Oxyfuel w capture (def = 0.0760)     /0.0760/
* Economics - Plant capital costs
scalar SRCC SR H2 plants (USD$\tonne H2\h)                          /11127828/
scalar SR90 SR H2 w 90% capture plants (USD$\tonne H2\h)            /17766023/
scalar H3CC IGCC H2 plants (USD$\tonne H2\h)                        /23784493/
scalar H4CC IGCC H2 w 90% capture plants (USD$\tonne H2\h)          /25065340/
scalar H5CC IGCC H2 w 90% co-capture plants (USD$\tonne H2\h)       /23380064/
scalar PCCC PC power plants (USD$\kW)                               /1234/
scalar NGCC NGCC power plants (USD$\kW)                             /567/
scalar IGCC IGCC power plants (USD$\kW)                             /1764/
scalar IG88 IGCC w 88% capture power plants (USD$\kW)               /2400/
scalar IG88C IGCC w 88% cocapture power plants (USD$\kW)            /1886/
scalar NG90 NGCC w 90% capture power plants (USD\kW)                /931/
scalar PC90 PC w 90% capture power plants (USD\kW)                  /1983/
scalar NGOX NG Oxyfuel w capture power plants (USD\kW)              /1246/
scalar COOX Coal Oxyfuel w capture power plants (USD\kW)            /1952/
* Boiler specifications
scalar SBC NG boiler capacity (tonne steam\h)                       /340/
scalar PSP percentage of capacity used for steam (%)                /0.8191/
* NOTE: PSP must be adjusted whenever hot water or steam demands change so that no excess
steam or water is produced in the boilers
scalar EFC coal boiler thermal efficiency (%)                       /0.83/
scalar EFN NG boiler thermal efficiency (%)                         /0.90/
scalar DHW Enthalpy of W @ 35 C (MJ\tonne W)                        /115/
* Upgrading and extraction steam - 915 psig, 500C
scalar DHS Delta H (MJ\tonne S)                                     /3415/
scalar HST Enthalpy of steam (@ 915 psig\500 C)                     /3415/
scalar HFW Enthalpy of feedwater (assumed T = 80 C)                 /335/;
DHS = HST-HFW;
* SAGD steam - 8,000 kPa, 80% quality
scalar DHSS Delta H (MJ\tonne S)                                    /2469/
scalar HSTS Enthalpy of SAGD steam (@ 8000 kPa)                     /2469/
```

```
scalar HFWS Enthalpy of SAGD feedwater (Opti-Nexen)                    /674/;
DHSS = HSTS-HFWS;
scalar SSR Steam produced in SR plants (tonne\tonne H2)                /0/
* Heat rates for all plants
scalar NH1 fuel consumption in SR plants (MJ\tonne H2)                 /174886/
scalar SRpow power consumption in SR plant (kWh\tonne H2)              /707/
scalar NH2 fuel consumption in SR w 90% cap plants (MJ\tonne H2)       /204174/
scalar H2pow power cons in SR w 90% cap plant(kWh\tonne H2)            /2061/
scalar NH3 fuel consumption in IGCC H2 plants (MJ\tonne H2)            /208978/
scalar H3pow power co-generation in IGCC H2plant (kWh\tonne H2)        /2443/
scalar NH4 fuel consumption in IGCC w 90% H2 plants (MJ\tonne H2)      /208978/
scalar H4pow power co-generation in IGCC w 90% H2 (kWh\tonne H2)       /1212/
scalar NH5 fuel cons in IGCC w 90% co-cap H2 plants (MJ\tonne H2)      /208978/
scalar H5pow power co-gen in IGCC w 90% co-cap H2 (kWh\tonne H2)       /1091/
scalar HRSP1 HR of NGCCs (MJ\kWh)                                      /7.17/
scalar HRSP2 HR of PCs (MJ\kWh)                                        /9.16/
scalar HRSP3 HR of IGCCs (MJ\kWh)                                      /8.757/
scalar HRSP4 HR of IGCCs w 88% capture (MJ\kWh)                        /11.060/
scalar HRSP5 HR of IGCCs w 88% co-capture (MJ\kWh)                     /10.174/
scalar HRSP6 HR of NGCCs w 90% capture (MJ\kWh)                        /8.411/
scalar HRSP7 HR of PCs w 90% capture (MJ\kWh)                          /12.040/
scalar HRSP8 HR of NG Oxyfuel w capture (MJ\kWh)                       /7.699/
scalar HRSP9 HR of Coal Oxyfuel w capture (MJ\kWh)                     /9.722/
* ---------------------- PARAMETER LIST -------------------------
* Fleet demands to be optimized
Parameter PD Total power demands to be optimized (kWh);
PD = PCTB+PNTB+(PNTS+PNTSU)+(PCMS+PCMSU)+(PNMS+PNMSU)
Parameter SD Total steam (950 psig) demands to be optimized (tonne\h);
SD = (SNTS+SNTU)+(SNMS+SNMU)+(SCMS+SCMU)
Parameter SSD Total steam (SAGD) demands to be optimized (tonne\h);
SSD = SCTB+SNTB+SNTSS
Parameter WD Total hot water demands to be optimized (tonne\h);
WD = WCS+WNS
Parameter DD Total diesel fuel demands (l\h);
DD = DCS+DNS
Parameter HD Total hydrogen demands to be optimized (tonne\h);
HD = HCMS+HNTS+HNMS+HHE
```

* Installed Capacity - Hydrogen plants

Parameter HSRmax(SR) SR H2 plants (tonne\h);

HSRmax(SR) = 6.25

Parameter H2max(SH2) SR w 90% capture H2 plants (tonne\h);

H2max(SH2) = 6.25

Parameter H3max(SH3) IGCC H2 plants (tonne\h);

H3max(SH3) = 32.09

Parameter H4max(SH4) IGCC w 90% capture H2 plants (tonne\h);

H4max(SH4) = 32.09

Parameter H5max(SH5) IGCC w 90% co-capture H2 plants (tonne\h);

H5max(SH5) = 32.09

* Installed Capacity - Power plants

Parameter PSP1max(SP1) NGCC plants (kW);

PSP1max(SP1) = 507000

Parameter PSP2max(SP2) PC plants (kW);

PSP2max(SP2) = 524000

Parameter PSP3max(SP3) IGCC plants (kW);

PSP3max(SP3) = 538877

Parameter PSP4max(SP4) IGCC w 88% plants (kW);

PSP4max(SP4) = 447965

Parameter PSP5max(SP5) IGCC w 88% co-cap plants (kW);

PSP5max(SP5) = 513262

Parameter PSP6max(SP6) NGCC w 90% capture plants (kW);

PSP6max(SP6) = 432000

Parameter PSP7max(SP7) PC w 90% capture plants (kW);

PSP7max(SP7) = 492000

Parameter PSP8max(SP8) NG Oxyfuel w capture plants (kW);

PSP8max(SP8) = 440000

Parameter PSP9max(SP9) Coal Oxyfuel w capture plants (kW);

PSP9max(SP9) = 532000

* Ammortized capital factors

Parameter AH1(SR) Factor for SR (%);

AH1(SR) = (RET*((1+RET)**LH1))/(((1+RET)**LH1)-1)

Parameter AH2(SH2) Factor for SR w 90% capture (%);

AH2(SH2) = (RET*((1+RET)**LH2))/(((1+RET)**LH2)-1)

Parameter AH3(SH3) Factor for IGCC H2 (%);

AH3(SH3) = (RET*((1+RET)**LH3))/(((1+RET)**LH3)-1)

```
Parameter AH4(SH4) Factor for IGCC H2 w 90% capture  (%);
AH4(SH4) = (RET*((1+RET)**LH4))/(((1+RET)**LH4)-1)
Parameter AH5(SH5) Factor for IGCC H2 w 90% co-capture  (%);
AH5(SH5) = (RET*((1+RET)**LH5))/(((1+RET)**LH5)-1)
Parameter AP1(SP1) Factor for NGCC (%);
AP1(SP1) = (RET*((1+RET)**LP1))/(((1+RET)**LP1)-1)
Parameter AP2(SP2) Factor for PC (%);
AP2(SP2) = (RET*((1+RET)**LP2))/(((1+RET)**LP2)-1)
Parameter AP3(SP3) Factor for IGCC (%);
AP3(SP3) = (RET*((1+RET)**LP3))/(((1+RET)**LP3)-1)
Parameter AP4(SP4) Factor for IGCC w 88% capture (%);
AP4(SP4) = (RET*((1+RET)**LP4))/(((1+RET)**LP4)-1)
Parameter AP5(SP5) Factor for IGCC w 88% co-capture (%);
AP5(SP5) = (RET*((1+RET)**LP5))/(((1+RET)**LP5)-1)
Parameter AP6(SP6) Factor for NGCC w 90% capture (%);
AP6(SP6) = (RET*((1+RET)**LP6))/(((1+RET)**LP6)-1)
Parameter AP7(SP7) Factor for PC w 90% capture (%);
AP7(SP7) = (RET*((1+RET)**LP7))/(((1+RET)**LP7)-1)
Parameter AP8(SP8) Factor for NG Oxyfuel w capture (%);
AP8(SP8) = (RET*((1+RET)**LP8))/(((1+RET)**LP8)-1)
Parameter AP9(SP9) Factor for Coal Oxyfuel w capture (%);
AP9(SP9) = (RET*((1+RET)**LP9))/(((1+RET)**LP9)-1)
* Annual production of H2 and power
Parameter SRprod(SR) Annual H2 production in SMR (tonne H2\yr);
SRprod(SR) = HSRmax(SR)*t*CFSR
Parameter H2prod(SH2) Annual H2 production in SMR w 90% capture (tonne H2\yr);
H2prod(SH2) = H2max(SH2)*t*CFH2
Parameter H3prod(SH3) Annual H2 production in IGCC (tonne H2\yr);
H3prod(SH3) = H3max(SH3)*t*CFH3
Parameter H4prod(SH4) Annual H2 production in IGCC w 90% capture (tonne H2\yr);
H4prod(SH4) = H4max(SH4)*t*CFH4
Parameter H5prod(SH5) Annual H2 production in IGCC w 90% co-capture (tonne H2\yr);
H5prod(SH5) = H5max(SH5)*t*CFH5
Parameter NGprod(SP1) Annual power generation in NGCCs (kWh\yr);
NGprod(SP1) = PSP1max(SP1)*t*CFNG
Parameter PCprod(SP2) Annual power generation in PCs (kWh\yr);
PCprod(SP2) = PSP2max(SP2)*t*CFPC
```

Parameter IGprod(SP3) Annual power generation in IGCCs (kWh\yr);

IGprod(SP3) = PSP3max(SP3)*t*CFIG

Parameter P4prod(SP4) Annual power generation in IGCCs w 88%(kWh\yr);

P4prod(SP4) = PSP4max(SP4)*t*CFP4

Parameter P5prod(SP5) Annual power generation in IGCCs w 88% co-capture (kWh\yr);

P5prod(SP5) = PSP5max(SP5)*t*CFP5

Parameter P6prod(SP6) Annual power generation in NGCCs w 90% capture (kWh\yr);

P6prod(SP6) = PSP6max(SP6)*t*CFP6

Parameter P7prod(SP7) Annual power generation in PCs w 90% capture (kWh\yr);

P7prod(SP7) = PSP7max(SP7)*t*CFP7

Parameter P8prod(SP8) Annual power generation in NG Oxyfuel w capture (kWh\yr);

P8prod(SP8) = PSP8max(SP8)*t*CFP8

Parameter P9prod(SP9) Annual power generation in Coal Oxyfuel w capture (kWh\yr);

P9prod(SP9) = PSP9max(SP9)*t*CFP9

* Annual capital costs of all plants

Parameter SRcap(SR) annual capital cost of SR H2 (USD$\year);

SRcap(SR) = HSRmax(SR)*SRCC*AH1(SR)*CVR

Parameter H2cap(SH2) annual capital cost of SR w 90% capture H2 (USD$\year);

H2cap(SH2) = H2max(SH2)*SR90*AH2(SH2)*CVR

Parameter H3cap(SH3) annual capital cost of IGCC H2 (USD$\year);

H3cap(SH3) = H3max(SH3)*H3CC*AH3(SH3)*CVR

Parameter H4cap(SH4) annual capital cost of IGCC H2 w 90% capture (USD$\year);

H4cap(SH4) = H4max(SH4)*H4CC*AH4(SH4)*CVR

Parameter H5cap(SH5) annual capital cost of IGCC H2 w 90% co-capture (USD$\year);

H5cap(SH5) = H5max(SH5)*H5CC*AH5(SH5)*CVR

Parameter NGcap(SP1) annual capital cost of NGCC power (USD$\year);

NGcap(SP1) = PSP1max(SP1)*NGCC*AP1(SP1)*CVR

Parameter PCcap(SP2) annual capital cost of PC power (USD$\year);

PCcap(SP2) = PSP2max(SP2)*PCCC*AP2(SP2)*CVR

Parameter IGcap(SP3) annual capital cost of IGCC power (USD$\year);

IGcap(SP3) = PSP3max(SP3)*IGCC*AP3(SP3)*CVR

Parameter P4cap(SP4) annual capital cost of IGCC w 88% capture power (USD$\year);

P4cap(SP4) = PSP4max(SP4)*IG88*AP4(SP4)*CVR

Parameter P5cap(SP5) annual capital cost of IGCC w 88% co-capture power (USD$\year);

P5cap(SP5) = PSP5max(SP5)*IG88C*AP5(SP5)*CVR

Parameter P6cap(SP6) annual capital cost of NGCC w 90% capture power (USD$\year);

P6cap(SP6) = PSP6max(SP6)*NG90*AP6(SP6)*CVR

Parameter P7cap(SP7) annual capital cost of PC w 90% capture power (USD$\year);
P7cap(SP7) = PSP7max(SP7)*PC90*AP7(SP7)*CVR
Parameter P8cap(SP8) annual capital cost of NG Oxyfuel w capture power (USD$\year);
P8cap(SP8) = PSP8max(SP8)*NGOX*AP8(SP8)*CVR
Parameter P9cap(SP9) annual capital cost of Coal Oxyfuel w capture power (USD$\year);
P9cap(SP9) = PSP9max(SP9)*COOX*AP9(SP9)*CVR
* Annual non-fuel O&M costs of all plants
Parameter SRom(SR) annual O&M cost of SR H2 (USD$\year);
SRom(SR) = HSRmax(SR)*SRCC*OH1
Parameter H2om(SH2) annual O&M cost of SR w 90% capture H2 (USD$\year);
H2om(SH2) = H2max(SH2)*SR90*OH2
Parameter H3om(SH3) annual O&M cost of IGCC H2 (USD$\year);
H3om(SH3) = H3max(SH3)*H3CC*OH3
Parameter H4om(SH4) annual O&M cost of IGCC H2 w 90% capture (USD$\year);
H4om(SH4) = H4max(SH4)*H4CC*OH4
Parameter H5om(SH5) annual O&M cost of IGCC H2 w 90% co-capture (USD$\year);
H5om(SH5) = H5max(SH5)*H5CC*OH5
Parameter NGom(SP1) annual O&M costs of NGCC power (USD$\year);
NGom(SP1) = PSP1max(SP1)*NGCC*OP1
Parameter PCom(SP2) annual O&M cost of PC power (USD$\year);
PCom(SP2) = PSP2max(SP2)*PCCC*OP2
Parameter IGom(SP3) annual O&M cost of IGCC power (USD$\year);
IGom(SP3) = PSP3max(SP3)*IGCC*OP3
Parameter P4om(SP4) annual O&M cost of IGCC w 88% capture power (USD$\year);
P4om(SP4) = PSP4max(SP4)*IG88*OP4
Parameter P5om(SP5) annual O&M cost of IGCC w 88% co-capture power (USD$\year);
P5om(SP5) = PSP5max(SP5)*IG88C*OP5
Parameter P6om(SP6) annual O&M cost of NGCC w 90% capture power (USD$\year);
P6om(SP6) = PSP6max(SP6)*NG90*OP6
Parameter P7om(SP7) annual O&M cost of PC w 90% capture power (USD$\year);
P7om(SP7) = PSP7max(SP7)*PC90*OP7
Parameter P8om(SP8) annual O&M cost of NG Oxyfuel w capture power (USD$\year);
P8om(SP8) = PSP8max(SP8)*NGOX*OP8
Parameter P9om(SP9) annual O&M cost of Coal Oxyfuel w capture power (USD$\year);
P9om(SP9) = PSP9max(SP9)*COOX*OP9
* ---------- VARIABLE LIST ----------
Positive Variables

* Steam

Sngb(NGB) Steam produced in NG boilers (tonne\h)

Ssgb(SGB) Steam (SAGD) produced in SGB boilers (tonne\h)

Sh1(SR) Steam produced in SR H2 plants (tonne\h)

S915 Fleetwide 915 steam production (tonne\h)

S8000 Fleetwide 8000 steam production (tonne\h)

* Hot water

Wngb(NGB) Hot water produced in NG boilers (tonne\h)

WAT Fleetwide hot water production (tonne\h)

* Hydrogen

Hh1(SR) H2 produced in SR plants (tonne\h)

Hh2(SH2) H2 produced in SR w 90% capture plants (tonne\h)

Hh3(SH3) H2 produced in IGCC H2 plants (tonne\h)

Hh4(SH4) H2 produced in IGCC H2 w 90% capture plants (tonne\h)

Hh5(SH5) H2 produced in IGCC H2 w 90% co-capture plants (tonne\h)

H2 Fleetwide H2 production (tonne\h)

* Power

Pp1(SP1) Power generated in NGCC plants (kW)

Pp2(SP2) Power generated in PC plants (kW)

Pp3(SP3) Power generated in IGCC plants (kW)

Pp4(SP4) Power generated in IGCC w 88% capture plants (kW)

Pp5(SP5) Power generated in IGCC w 88% co-capture plants (kW)

Pp6(SP6) Power generated in NGCC w 90% capture plants (kW)

Pp7(SP7) Power generated in PC w 90% capture plants (kW)

Pp8(SP8) Power generated in NG Oxyfuel w capture plants (kW)

Pp9(SP9) Power generated in Coal Oxyfuel w capture plants (kW)

Ph1 Power requirements of SR H2 plants (kW)

Ph2 Power requirements of SR w 90% capture H2 plants (kW)

Ph3 Power co-produced in IGCC H2 plants (kW)

Ph4 Power co-produced in IGCC H2 w 90% capture plants (kW)

Ph5 Power co-produced in IGCC H2 w 90% co-capture plants (kW)

Phco2 Power requirements for CO2 transport for H2 plants (kW)

Ppco2 Power requirements for CO2 transport for power plants (kW)

POW Fleetwide power production (kW)

* NG Feedstock

Xngb(NGB) NG consumed in NG boilers (Nm3\h)

Xsgb(SGB) NG consumed in SG boilers (Nm3\h)

Xh1(SR) NG consumed in SR plants (Nm3\h)

Xh2(SH2) NG consumed in SR w 90% capture plants (Nm3\h)

Xp1(SP1) NG consumed in NGCC plants (Nm3\h)

Xp6(SP6) NG consumed in NGCC w 90% capture plants (Nm3\h)

Xp8(SP8) NG consumed in NG Oxyfuel w capture plants (Nm3\h)

Xpf NG used as upgrading process fuel (Nm3\h)

Xfl Fleet NG consumption (Nm3\h)

* Coal Feedstock

Yp2(SP2) Coal consumed in PC plants (tonne\h)

Yp3(SP3) Coal consumed in IGCC plants (tonne\h)

Yp4(SP4) Coal consumed in IGCC w 88% capture plants (tonne\h)

Yp5(SP5) Coal consumed in IGCC w 88% co-capture plants (tonne\h)

Yp7(SP7) Coal consumed in PC w 90% capture plants (tonne\h)

Yp9(SP9) Coal consumed in Coal Oxyfuel w capture plants (tonne\h)

Yh3(SH3) Coal consumed in IGCC H2 plants (tonne\h)

Yh4(SH4) Coal consumed in IGCC H2 w 90% capture plants (tonne\h)

Yh5(SH5) Coal consumed in IGCC H2 w 90% co-capture plants (tonne\h)

Ypf Coal used as upgrading process fuel (tonne\h)

* Fuel gas consumption in H2 SR plants (optional)

Fh1(SR) Fuel gas consumed in SR plants (tonne\h)

* CO2 Emitted

Engb CO2 emitted by NG boilers (tonne\h)

Esgb CO2 emitted by SG boilers (tonne\h)

Eh1 CO2 emitted by SR plants (tonne\h)

Eh2 CO2 emitted by SR w 90% capture plants (tonne\h)

Eh3 CO2 emitted by IGCC H2 plants (tonne\h)

Eh4 CO2 emitted by IGCC H2 w 90% capture plants (tonne\h)

Eh5 CO2 emitted by IGCC H2 w 90% co-capture plants (tonne\h)

Ep1 CO2 emitted by NGCC plants (tonne\h)

Ep2 CO2 emitted by PC plants (tonne\h)

Ep3 CO2 emitted by IGCC plants (tonne\h)

Ep4 CO2 emitted by IGCC plants w 88% capture (tonne\h)

Ep5 CO2 emitted by IGCC plants w 88% co-capture (tonne\h)

Ep6 CO2 emitted by NGCC w 90% capture plants (tonne\h)

Ep7 CO2 emitted by PC w 90% capture plants (tonne\h)

Ep8 CO2 emitted by NG Oxyfuel w capture plants (tonne\h)

Ep9 CO2 emitted by Coal Oxyfuel w capture plants (tonne\h)

EDF CO2 emissions from diesel fuel use (tonne\h)

EPF CO2 emissions from process fuel use (tonne\h)

EHI CO2 emissions from H2 produced from plant off-gas (tonne\h)

EH2 CO2 emissions from H2 produced internally (tonne\h)

* CO2 Captured

CCh2 CO2 captured in SR w 90% capture plants (tonne\h)

CCh4 CO2 captured in IGCC H2 w 90% capture plants (tonne\h)

CCh5 CO2 captured in IGCC H2 w 90% co-capture plants (tonne\h)

CChyd Total CO2 captured in H2 plants (tonne\h)

CCp4 CO2 captured in IGCC plants w 88% capture (tonne\h)

CCp5 CO2 captured in IGCC plants w 88% co-capture (tonne\h)

CCp6 CO2 captured in NGCC w 90% capture plants (tonne\h)

CCp7 CO2 captured in PC w 90% capture plants (tonne\h)

CCp8 CO2 captured in NG Oxyfuel w capture plants (tonne\h)

CCp9 CO2 captured in Coal Oxyfuel w capture plants (tonne\h)

CCpow Total CO2 captured in power plants (tonne\h)

Binary Variables

* The following variables determine whether a unit/plant exists in the fleet

INGB(NGB) NG boilers

ISGB(SGB) SG boilers

IH1(SR) SR plants

IH2(SH2) SR with 90% capture plants

IH3(SH3) IGCC H2 plants

IH4(SH4) IGCC H2 with 90% capture plants

IH5(SH5) IGCC H2 with 90% co-capture plants

IP1(SP1) NGCC plants

IP2(SP2) PC plants

IP3(SP3) IGCC plants

IP4(SP4) IGCC plants w 88% capture

IP5(SP5) IGCC plants w 88% co-capture

IP6(SP6) NGCC w 90% capture plants

IP7(SP7) PC w 90% capture plants

IP8(SP8) NG Oxyfuel w capture plants

IP9(SP9) Coal Oxyfuel w capture plants

Variables

* The following variables apply to the entire fleet

Pcost total annual power cost (USD$\yr)

Hcost total annual hydrogen cost (USD$\yr)

Wcost total annual cost of hot water (USD$\yr)

Scost total annual 915 steam cost (USD$\yr)

SScost total annual 8000 steam cost (USD$\yr)

Fcost total annual process fuel cost (USD$\yr)

Dcost total annual diesel fuel cost (USD$\yr)

CTHcost total annual CO2 transport cost - H2 plants (USD$\yr)

CTPcost total annual CO2 transport cost - power plants (USD$\yr)

CSHcost total annual CO2 storage cost - H2 plants (USD$\yr)

CSPcost total annual CO2 storage cost - power plants (USD$\yr)

COST total annual energy cost of the fleet (USD$\yr)

CO2E total CO2 emissions (tonne\h)

CCO2 total CO2 captured (tonne\h)

NGnb total NG consumption in NG boilers (Nm3\h)

NGsb total NG consumption in SG boilers (Nm3\h)

NGh1 total NG consumption in SR plants (Nm3\h)

NGh2 total NG consumption in SR w 90% capture plants (Nm3\h)

NGp1 total NG consumption in NGCC plants (Nm3\h)

NGp6 total NG consumption in NGCC w 90% capture plants (Nm3\h)

NGp8 total NG consumption in NG Oxyfuel w capture plants (Nm3\h)

NGpf total NG consumption for process fuel (Nm3\h)

NGtot total NG consumption (Nm3\h)

Ch3 total coal consumption in IGCC H2 plants (tonne\h)

Ch4 total coal consumption in IGCC H2 w 90% capture plants (tonne\h)

Ch5 total coal consumption in IGCC H2 w 90% co-capture plants (tonne\h)

Cp2 total coal consumption in PC plants (tonne\h)

Cp3 total coal consumption in IGCC plants (tonne\h)

Cp4 total coal consumption in IGCC w 88% capture plants (tonne\h)

Cp5 total coal consumption in IGCC w 88% co-capture plants (tonne\h)

Cp7 total coal consumption in PC w 90% capture plants (tonne\h)

Cp9 total coal consumption in Coal Oxyfuel w capture plants (tonne\h)

Cpf total coal consumption for process fuel (tonne\h)

Ctot total coal consumption (tonne\h)

FGtot total fuel gas consumption in SR plants for H2 production (tonne\h)

PEX Excess power available for export (kW)

* Costing variables of optimal fleet

Punit total cost of producing power ($\kW)

H2cost total cost of producing H2 ($\tonne)

S9cost total cost of raising 950 steam and producing hot water ($\tonne)

S8cost total cost of raising 8000 steam ($\tonne)

HWcost total cost of producing hot water ($\tonne)

* Unitary energy costs of optimal fleet

NMScost total energy cost of mined SCO ($\bbl SCO)

NTScost total energy cost of thermal SCO ($\bbl SCO)

NTBcost total energy cost of thermal bitumen ($\bbl bitumen)

* Turn coal (process fuel) on/off by fixing its value to zero

Variable Ypf Coal for process fuel in upgrading (tonne\h);

*Ypf.fx = 0;

* ---------- EQUATION LIST ----------

Equations

* Steam production

STMngb(NGB) Total steam produced in NG boilers (tonne\h)

STMsgb(SGB) Total steam produced in SG boilers (tonne\h)

STMh1(SR) Total steam produced in SR plants (tonne\h)

STM8000 Fleetwide 8000 steam production (tonne\h)

STM915 Fleetwide 915 steam production (tonne\h)

* Hot water production

WATngb(NGB) Total hot water produced in NG boilers (tonne\h)

HWAT Fleetwide hot water (35 C) production (tonne\h)

* H2 production

H2h1(SR) Total H2 produced in SR plants (tonne\h)

H2h2(SH2) Total H2 produced in SR w 90% capture plants (tonne\h)

H2h3(SH3) Total H2 produced in IGCC H2 plants (tonne\h)

H2h4(SH4) Total H2 produced in IGCC H2 w 90% capture plants (tonne\h)

H2h5(SH5) Total H2 produced in IGCC H2 w 90% co-capture plants (tonne\h)

HYD Fleetwide H2 production (tonne\h)

* Power generation / ancillary consumption

POWp1(SP1) Total power generated in NGCC plants (kW)

POWp2(SP2) Total power generated in PC plants (kW)

POWp3(SP3) Total power generated in IGCC plants (kW)

POWp4(SP4) Total power generated in IGCC w 88% capture plants (kW)

POWp5(SP5) Total power generated in IGCC w 88% co-capture plants (kW)

POWp6(SP6) Total power generated in NGCC w 90% capture plants (kW)

POWp7(SP7) Total power generated in PC w 90% capture plants (kW)

POWp8(SP8) Total power generated in NG Oxyfuel w capture plants (kW)

POWp9(SP9) Total power generated in Coal Oxyfuel w capture plants (kW)

POWh1 Total power consumption of SR plants (kW)

POWh2 Total power consumption of SR w 90% capture plants (kW)

POWh3 Total power co-generated in IGCC H2 plants (kW)

POWh4 Total power co-generated in IGCC H2 w 90% capture plants (kW)

POWh5 Total power co-generated in IGCC H2 w 90% co-capture plants (kW)

POWhco2 Total power consumption for CO2 transport of H2 plants (kW)

POWpco2 Total power consumption for CO2 transport of power plants (kW)

POWtot Total power generated fleetwide (kW)

POWex Total excess power generated fleetwide (kWh)

* NG consumption

NGngb NG consumption in NG boilers (Nm3\h)

NGsgb NG consumption in SG boilers (Nm3\h)

NGsh1 NG consumption in SR plants (Nm3\h)

NGsh2 NG consumption in SR w 90% capture plants (Nm3\h)

NGsp1 NG consumption in NGCC plants (Nm3\h)

NGsp6 NG consumption in NGCC w 90% capture plants (Nm3\h)

NGsp8 NG consumption in NG Oxyfuel w capture plants (Nm3\h)

NGprf NG consumption for upgrading process fuel (Nm3\h)

NG Fleet NG consumption (Nm3\h)

* Coal consumption

Csh3 Coal consumption in IGCC H2 plants (tonne\h)

Csh4 Coal consumption in IGCC H2 w 90% capture plants (tonne\h)

Csh5 Coal consumption in IGCC H2 w 90% co-capture plants (tonne\h)

Csp2 Coal consumption in PC plants (tonne\h)

Csp3 Coal consumption in IGCC plants (tonne\h)

Csp4 Coal consumption in IGCC w 88% capture plants (tonne\h)

Csp5 Coal consumption in IGCC w 88% co-capture plants (tonne\h)

Csp7 Coal consumption in PC w 90% capture plants (tonne\h)

Csp9 Coal consumption in Coal Oxyfuel w capture plants (tonne\h)

Cprf Coal consumption for process fuel (tonne\h)

C Fleet coal consumption (tonne\h)

* Fuel gas consumption (used for H2 production) - optional

FGsh1 Fuel gas consumption in SR plants (tonne\h)

* CO2 Emissions

CO2ngb Total emissions of NG boilers (tonne CO2\h)

CO2sgb Total emissions of SG boilers (tonne CO2\h)

CO2h1 Total emissions of SR plants (tonne CO2\h)

CO2h2 Total emissions of SR w 90% capture plants (tonne CO2\h)

CO2h3 Total emissions of IGCC H2 plants (tonne CO2\h)

CO2h4 Total emissions of IGCC H2 w 90% capture plants (tonne CO2\h)

CO2h5 Total emissions of IGCC H2 w 90% co-capture plants (tonne CO2\h)

CO2p1 Total emissions of NGCC plants (tonne CO2\h)

CO2p2 Total emissions of PC plants (tonne CO2\h)

CO2p3 Total emissions of IGCC plants (tonne CO2\h)

CO2p4 Total emissions of IGCC w 88% capture plants (tonne CO2\h)

O2p5 Total emissions of IGCC w 88% co-capture plants (tonne CO2\h)

CO2p6 Total emissions of NGCC w 90% capture plants (tonne CO2\h)

CO2p7 Total emissions of PC w 90% capture plants (tonne CO2\h)

CO2p8 Total emissions of NG Oxyfuel w capture plants (tonne CO2\h)

CO2p9 Total emissions of Coal Oxyfuel w capture plants (tonne CO2\h)

CO2diesel Total emissions from diesel fuel use (tonne CO2\h)

CO2pfuel Total emissions from process fuel use (tonne CO2\h)

CO2fleet Total emissions of the fleet (tonne CO2\h)

* CO2 Captured

CCO2h2 Total CO2 captured in SR w 90% capture plants (tonne CO2\h)

CCO2h4 Total CO2 captured in IGCC H2 w 90% capture plants (tonne CO2\h)

CCO2h5 Total CO2 captured in IGCC H2 w 90% co-capture plants (tonne CO2\h)

CCO2p4 Total CO2 captured in IGCC w 88% capture plants (tonne CO2\h)

CCO2p5 Total CO2 captured in IGCC w 88% co-capture plants (tonne CO2\h)

CCO2p6 Total CO2 captured in NGCC w 90% capture plants (tonne CO2\h)

CCO2p7 Total CO2 captured in PC w 90% capture plants (tonne CO2\h)

CCO2p8 Total CO2 captured in NG Oxyfuel w capture plants (tonne CO2\h)

CCO2p9 Total CO2 captured in Coal Oxyfuel w capture plants (tonne CO2\h)

CCO2hyd Total CO2 captured in all H2 plants (tonne CO2\h)

CCO2pow Total CO2 captured in all power plants (tonne CO2\h)

CCO2fleet Total captured CO2 production of the fleet (tonne CO2\h)

* Costs

POWER total annual cost of electricity (USD$\yr)

HYDROGEN total annual cost of hydrogen (USD$\yr)

STEAM total cost of 950 steam (USD$\yr)

SSTEAM total cost of 8000 steam (USD$\yr)

WATER total annual water cost (USD$\yr)

DIESEL total cost of diesel fuel (USD$\yr)

PROFUEL total cost of process fuel (USD$\yr)

CO2TRHYD total cost of transporting CO2 from H2 plants (USD$\yr)

CO2TRPOW total cost of transporting CO2 from power plants (USD$\yr)

CO2STHYD total cost of storing CO2 underground from H2 plants (USD$\yr)

CO2STPOW total cost of storing CO2 underground from power plants (USD$\yr)

FLEET Total annual cost of operating the fleet (USD$\yr)

* Energy producers constraints

SELngb Total # of NG boilers

SELsgb Total # of SG boilers

SELh1 Total # of SR plants

SELh2 Total # of SR w 90% capture plants

SELh3 Total # of IGCC H2 plants

SELh4 Total # of IGCC H2 w 90% capture plants

SELh5 Total # of IGCC H2 w 90% co-capture plants

SELp1 Total # of NGCC plants

SELp2 Total # of PC plants

SELp3 Total # of IGCC plants

SELp4 Total # of IGCC w 88% capture plants

SELp5 Total # of IGCC w 88% co-capture plants

SELp6 Total # of NGCC w 90% capture plants

SELp7 Total # of PC w 90% capture plants

SELp8 Total # of NG Oxyfuel w capture plants

SELp9 Total # of Coal Oxyfuel w capture plants

* Unit capacity constraints

CAPSngb(NGB) Total steam production capacity of NG boilers (tonne\h)

CAPSsgb(SGB) Total steam production capacity of SG boilers (tonne\h)

CAPSh1(SR) Total steam production capacity of SR plants (tonne\h)

CAPWngb(NGB) Total hot water production capacity of NG boilers (tonne\h)

CAPh1(SR) Total H2 production capacity of SR plants (tonne\h)

CAPh2(SH2) Total H2 production capacity of SR w 90% capture plants (tonne\h)

CAPh3(SH3) Total H2 production capacity of IGCC plants (tonne\h)

CAPh4(SH4) Total H2 production capacity of IGCC H2 w 90% capture plants (tonne\h)

CAPh5(SH5) Total H2 production capacity of IGCC H2 w 90% co-capture plants (tonne\h)

CAPp1(SP1) Total power generation capacity of NGCC plants (kWh)

CAPp2(SP2) Total power generation capacity of PC plants (kWh)

CAPp3(SP3) Total power generation capacity of IGCC plants (kWh)

CAPp4(SP4) Total power generation capacity of IGCC w 88% capture plants (kWh)

CAPp5(SP5) Total power generation capacity of IGCC w 88% co-capture plants (kWh)

CAPp6(SP6) Total power generation capacity of NGCC w 90% capture plants (kWh)

CAPp7(SP7) Total power generation capacity of PC w 90% capture plants (kWh)

CAPp8(SP8) Total power generation capacity of NG Oxyfuel w capture plants (kWh)

CAPp9(SP9) Total power generation capacity of Coal Oxyfuel w capture plants (kWh)

* Energy supply constraints

CAPS Total fleet steam supply constraint (tonne\h)

CAPSS Total fleet SAGD steam supply constraint (tonne\h)

CAPW Total fleet hot water supply constraint (tonne\h)

CAPH Total fleet H2 supply constraint (tonne\h)

CAPP Total fleet power supply constraint (tonne\h)

CAPF Total fleet upgrading process fuel supply constraint (MJ\h)

CAPG Total fleet fuel gas availability constraint (tonne\h)

* Base case supply contraints

BCPOWR The base case power demands must be met by NGCC plants without capture

BCHYDG The base case H2 demands must be met by SR plants without capture

BCFUEL The base case FG demands must be met by Natural gas

* CO2 reduction constraint

RED Overall CO2 emissions reduction (tonne\h)

;

* Steam production

STMngb(NGB) .. Sngb(NGB) =e= HHVNG*PSP*EFN/DHS*Xngb(NGB);

STMsgb(SGB) .. Ssgb(SGB) =e= HHVNG*EFN/DHSS*Xsgb(SGB);

STMh1(SR) .. Sh1(SR) =e= HHVNG*SSR*Xh1(SR);

STM915 .. S915 =e= Sum(NGB, Sngb(NGB));

STM8000 .. S8000 =e= Sum(SGB, Ssgb(SGB))+Sum(SR, Sh1(SR));

* Hot water production

WATngb(NGB) .. Wngb(NGB) =e= (HHVNG*(1-PSP)*EFN/DHW*Xngb(NGB));

HWAT .. WAT =e= Sum(NGB, Wngb(NGB));

* H2 production

H2h1(SR) .. Hh1(SR) =e= ((Xh1(SR)*HHVNG)+(Fh1(SR)*1000*LHVLC))/NH1;

H2h2(SH2) .. Hh2(SH2) =e= (Xh2(SH2)*HHVNG)/NH2;

H2h3(SH3) .. Hh3(SH3) =e= (Yh3(SH3)*HHVC)/NH3;

H2h4(SH4) .. Hh4(SH4) =e= (Yh4(SH4)*HHVC)/NH4;

H2h5(SH5) .. Hh5(SH5) =e= (Yh5(SH5)*HHVC)/NH5;

HYD .. H2 =e= Sum(SR, Hh1(SR))+Sum(SH2, Hh2(SH2))+

```
                Sum(SH3, Hh3(SH3))+Sum(SH4, Hh4(SH4))+
                Sum(SH5, Hh5(SH5));
* Power generation
POWp1(SP1) .. Pp1(SP1) =e= (HHVNG/HRSP1*Xp1(SP1));
POWp2(SP2) .. Pp2(SP2) =e= (HHVC/HRSP2*Yp2(SP2));
POWp3(SP3) .. Pp3(SP3) =e= (HHVC/HRSP3*Yp3(SP3));
POWp4(SP4) .. Pp4(SP4) =e= (HHVC/HRSP4*Yp4(SP4));
POWp5(SP5) .. Pp5(SP5) =e= (HHVC/HRSP5*Yp5(SP5));
POWp6(SP6) .. Pp6(SP6) =e= (HHVNG/HRSP6*Xp6(SP6));
POWp7(SP7) .. Pp7(SP7) =e= (HHVC/HRSP7*Yp7(SP7));
POWp8(SP8) .. Pp8(SP8) =e= (HHVNG/HRSP8*Xp8(SP8));
POWp9(SP9) .. Pp9(SP9) =e= (HHVC/HRSP9*Yp9(SP9));
POWh1 .. Ph1 =e= Sum(SR, Hh1(SR)*SRpow);
POWh2 .. Ph2 =e= Sum(SH2, Hh2(SH2)*H2pow);
POWh3 .. Ph3 =e= Sum(SH3, Hh3(SH3)*H3pow);
POWh4 .. Ph4 =e= Sum(SH4, Hh4(SH4)*H4pow);
POWh5 .. Ph5 =e= Sum(SH5, Hh5(SH5)*H5pow);
POWhco2 .. Phco2 =e= CChyd*PCT*(PKM/100);
POWpco2 .. Ppco2 =e= CCpow*PCT*(PKM/100);
POWtot .. POW =e=   Sum(SP1, Pp1(SP1))+Sum(SP2, Pp2(SP2))+Sum(SP3, Pp3(SP3))+
                    Sum(SP4, Pp4(SP4))+Sum(SP5, Pp5(SP5))+Sum(SP6, Pp6(SP6))+
                    Sum(SP7, Pp7(SP7))+Sum(SP8, Pp8(SP8))+Sum(SP9, Pp9(SP9))+
                    Ph3+Ph4+Ph5;
POWex .. PEX =e= POW-PD-Ph1-Ph2-Phco2-Ppco2;
* NG consumption
NGngb .. NGnb =e= Sum(NGB, Xngb(NGB));
NGsgb .. NGsb =e= Sum(SGB, Xsgb(SGB));
NGsh1 .. NGh1 =e= Sum(SR, Xh1(SR));
NGsh2 .. NGh2 =e= Sum(SH2, Xh2(SH2));
NGsp1 .. NGp1 =e= Sum(SP1, Xp1(SP1));
NGsp6 .. NGp6 =e= Sum(SP6, Xp6(SP6));
NGsp8 .. NGp8 =e= Sum(SP8, Xp8(SP8));
NGprf .. NGpf =e= Xpf;
NG .. NGtot =e=     NGnb+NGsb+
                    NGh1+NGh2+
                    NGp1+NGp6+NGp8+
                    NGpf;
```

```
*Coal consumption
Csh3 .. Ch3 =e= Sum(SH3, Yh3(SH3)/1000);
Csh4 .. Ch4 =e= Sum(SH4, Yh4(SH4)/1000);
Csh5 .. Ch5 =e= Sum(SH5, Yh5(SH5)/1000);
Csp2 .. Cp2 =e= Sum(SP2, Yp2(SP2)/1000);
Csp3 .. Cp3 =e= Sum(SP3, Yp3(SP3)/1000);
Csp4 .. Cp4 =e= Sum(SP4, Yp4(SP4)/1000);
Csp5 .. Cp5 =e= Sum(SP5, Yp5(SP5)/1000);
Csp7 .. Cp7 =e= Sum(SP7, Yp7(SP7)/1000);
Csp9 .. Cp9 =e= Sum(SP9, Yp9(SP9)/1000);
Cprf .. Cpf =e= Ypf;
C .. Ctot =e=     Ch3+Ch4+Ch5+
                  Cp2+Cp3+Cp4+Cp5+Cp7+Cp9+
                  Cpf;
* Fuel gas consumption
FGsh1 .. FGtot =e= Sum(SR, Fh1(SR));
* CO2 Emissions
CO2ngb .. Engb =e= Sum(NGB, Xngb(NGB)*FEFNG);
CO2sgb .. Esgb =e= Sum(SGB, Xsgb(SGB)*FEFNG);
CO2h1 .. Eh1 =e= Sum(SR, HEFSR*Hh1(SR));
CO2h2 .. Eh2 =e= Sum(SH2, HEFH2*Hh2(SH2));
CO2h3 .. Eh3 =e= Sum(SH3, EFSH3*Hh3(SH3));
CO2h4 .. Eh4 =e= Sum(SH4, EFSH4*Hh4(SH4));
CO2h5 .. Eh5 =e= Sum(SH5, EFSH5*Hh5(SH5));
CO2p1 .. Ep1 =e= Sum(SP1, FEFNG*Xp1(SP1));
CO2p2 .. Ep2 =e= Sum(SP2, EFSP2*Pp2(SP2));
CO2p3 .. Ep3 =e= Sum(SP3, EFSP3*Pp3(SP3));
CO2p4 .. Ep4 =e= Sum(SP4, EFSP4*Pp4(SP4));
CO2p5 .. Ep5 =e= Sum(SP5, EFSP5*Pp5(SP5));
CO2p6 .. Ep6 =e= Sum(SP6, EFSP6*Pp6(SP6));
CO2p7 .. Ep7 =e= Sum(SP7, EFSP7*Pp7(SP7));
CO2p8 .. Ep8 =e= Sum(SP8, EFSP8*Pp8(SP8));
CO2p9 .. Ep9 =e= Sum(SP9, EFSP9*Pp9(SP9));
CO2diesel .. EDF =e= DD*FEFD;
CO2pfuel .. EPF =e= (Xpf*FEFNG)+(Ypf*FEFC*(ULTC-ASH));
CO2fleet .. CO2E =e=    Engb+Esgb+
                        Eh1+Eh2+Eh3+Eh4+Eh5+
```

```
                    Ep1+Ep2+Ep3+Ep4+Ep5+Ep6+Ep7+Ep8+Ep9+
                    EDF+EPF;
* CO2 production
CCO2h2 .. CCh2 =e= Sum(SH2, CCSH2*Hh2(SH2));
CCO2h4 .. CCh4 =e= Sum(SH4, CCSH4*Hh4(SH4));
CCO2h5 .. CCh5 =e= Sum(SH5, CCSH5*Hh5(SH5));
CCO2p4 .. CCp4 =e= Sum(SP4, CCSP4*Pp4(SP4));
CCO2p5 .. CCp5 =e= Sum(SP5, CCSP5*Pp5(SP5));
CCO2p6 .. CCp6 =e= Sum(SP6, CCSP6*Pp6(SP6));
CCO2p7 .. CCp7 =e= Sum(SP7, CCSP7*Pp7(SP7));
CCO2p8 .. CCp8 =e= Sum(SP8, CCSP8*Pp8(SP8));
CCO2p9 .. CCp9 =e= Sum(SP9, CCSP9*Pp9(SP9));
CCO2hyd .. CChyd =e= CCh2+CCh4+CCh5;
CCO2pow .. CCpow =e= CCp4+CCp5+CCp6+CCp7+CCp8+CCp9;
CCO2fleet .. CCO2 =e= CCh2+CCh4+CCh5+
                    CCp4+CCp5+CCp6+CCp7+CCp8+CCp9;
* Cost - Power generation
POWER .. Pcost =e=  Sum(SP1, IP1(SP1)*NGcap(SP1))+
                    Sum(SP2, IP2(SP2)*PCcap(SP2))+
                    Sum(SP3, IP3(SP3)*IGcap(SP3))+
                    Sum(SP4, IP4(SP4)*P4cap(SP4))+
                    Sum(SP5, IP5(SP5)*P5cap(SP5))+
                    Sum(SP6, IP6(SP6)*P6cap(SP6))+
                    Sum(SP7, IP7(SP7)*P7cap(SP7))+
                    Sum(SP8, IP8(SP8)*P8cap(SP8))+
                    Sum(SP9, IP9(SP9)*P9cap(SP9))+
                    Sum(SP1, IP1(SP1)*NGom(SP1))+
                    Sum(SP2, IP2(SP2)*PCom(SP2))+
                    Sum(SP3, IP3(SP3)*IGom(SP3))+
                    Sum(SP4, IP4(SP4)*P4om(SP4))+
                    Sum(SP5, IP5(SP5)*P5om(SP5))+
                    Sum(SP6, IP6(SP6)*P6om(SP6))+
                    Sum(SP7, IP7(SP7)*P7om(SP7))+
                    Sum(SP8, IP8(SP8)*P8om(SP8))+
                    Sum(SP9, IP9(SP9)*P9om(SP9))+
                    (Sum(SP1, Pp1(SP1)*HRSP1/1000*CNG)+
                    Sum(SP2, Pp2(SP2)*HRSP2/1000*CCL)+
```

```
                    Sum(SP3, Pp3(SP3)*HRSP3/1000*CCL)+
                    Sum(SP4, Pp4(SP4)*HRSP4/1000*CCL)+
                    Sum(SP5, Pp5(SP5)*HRSP5/1000*CCL)+
                    Sum(SP6, Pp6(SP6)*HRSP6/1000*CNG)+
                    Sum(SP7, Pp7(SP7)*HRSP7/1000*CCL)+
                    Sum(SP8, Pp8(SP8)*HRSP8/1000*CNG)+
                    Sum(SP9, Pp9(SP9)*HRSP9/1000*CCL))*t;
* Cost - Hydrogen production
HYDROGEN .. Hcost =e=       Sum(SR, IH1(SR)*SRcap(SR))+
                            Sum(SH2, IH2(SH2)*H2cap(SH2))+
                            Sum(SH3, IH3(SH3)*H3cap(SH3))+
                            Sum(SH4, IH4(SH4)*H4cap(SH4))+
                            Sum(SH5, IH5(SH5)*H5cap(SH5))+
                            Sum(SR, IH1(SR)*SRom(SR))+
                            Sum(SH2, IH2(SH2)*H2om(SH2))+
                            Sum(SH3, IH3(SH3)*H3om(SH3))+
                            Sum(SH4, IH4(SH4)*H4om(SH4))+
                            Sum(SH5, IH5(SH5)*H5om(SH5))+
                            (Sum(SR, Xh1(SR)*HHVNG/1000*CNG)+
                            Sum(SH2, Xh2(SH2)*HHVNG/1000*CNG)+
                            Sum(SH3, Yh3(SH3)*HHVC/1000*CCL)+
                            Sum(SH4, Yh4(SH4)*HHVC/1000*CCL)+
                            Sum(SH5, Yh5(SH5)*HHVC/1000*CCL))*t;
* Cost - process generation
STEAM .. Scost =e=      (Sum(NGB, Xngb(NGB)*PSP*HHVNG/1000*CNG)+
                        Sum(NGB, Sngb(NGB)*CWT))*t;
* Cost - SAGD steam generation
SSTEAM .. SScost =e= (Sum(SGB, Xsgb(SGB)*HHVNG/1000*CNG)+
                        Sum(SGB, Ssgb(SGB)*CWT))*t;
* Cost - Hot water production
WATER .. Wcost =e=      (Sum(NGB, Xngb(NGB)*(1-PSP)*HHVNG/1000*CNG)+
                        Sum(NGB, Wngb(NGB)*CWT))*t;
* Cost - Process fuel
PROFUEL .. Fcost =e=     (Xpf*HHVNG/1000*CNG*t)+(Ypf*HHVC*CCL*t);
* Cost - Diesel fuel
DIESEL .. Dcost =e=      (DD*CDI*t);
* Cost - CO2 Transport
```

```
CO2TRHYD .. CTHcost =e=  CChyd*t*CCT*(PKM/100);
CO2TRPOW .. CTPcost =e=  CCpow*t*CCT*(PKM/100);
* Cost - CO2 Storage
CO2STHYD .. CSHcost =e= CChyd*t*CST;
CO2STPOW .. CSPcost =e= CCpow*t*CST;
* Cost - Fleet total (objective function)
FLEET .. COST =e=      Pcost+Hcost+Scost+SScost+Wcost+Fcost+Dcost+
                       CTHcost+CTPcost+
                       CSHcost+CSPcost;
* Energy producers constraint
SELngb .. Sum(NGB, INGB(NGB)) =l= 90;
SELsgb .. Sum(SGB, ISGB(SGB)) =l= 150;
SELh1 .. Sum(SR, IH1(SR)) =l= 120;
SELh2 .. Sum(SH2, IH2(SH2)) =l= 120;
SELh3 .. Sum(SH3, IH3(SH3)) =l= 30;
SELh4 .. Sum(SH4, IH4(SH4)) =l= 30;
SELh5 .. Sum(SH5, IH5(SH5)) =l= 30;
SELp1 .. Sum(SP1, IP1(SP1)) =l= 30;
SELp2 .. Sum(SP2, IP2(SP2)) =l= 30;
SELp3 .. Sum(SP3, IP3(SP3)) =l= 30;
SELp4 .. Sum(SP4, IP4(SP4)) =l= 30;
SELp5 .. Sum(SP5, IP5(SP5)) =l= 30;
SELp6 .. Sum(SP6, IP6(SP6)) =l= 30;
SELp7 .. Sum(SP7, IP7(SP7)) =l= 30;
SELp8 .. Sum(SP8, IP8(SP8)) =l= 30;
SELp9 .. Sum(SP9, IP9(SP9)) =l= 30;
* Energy supply constraints
CAPS .. Sum(NGB, Sngb(NGB))+Sum(SR, Sh1(SR)) =g= SD;
CAPSS .. Sum(SGB, Ssgb(SGB)) =g= SSD;
CAPW .. Sum(NGB, Wngb(NGB)) =g= WD;
CAPH .. H2 =g= HD;
CAPP .. POW =g= PD+Ph1+Ph2+Phco2+Ppco2;
CAPF .. (Xpf*HHVNG)+(Ypf*1000*HHVC) =e= (NGCMS+NGNTS+NGNMS)*HHVNG;
CAPG .. FGtot =l= FGNTS+FGNMS;
* Base case energy constraints
*BCPOWR .. Sum(SP1, Pp1(SP1)) =g= PCTB+PCMS+PCMSU;
*BCHYDG .. Sum(SR, Hh1(SR)) =g= HCMS;
```

```
*BCFUEL .. Xpf =g= NGCMS;
* Unit capacity constraints
CAPSngb(NGB) .. Sngb(NGB) =l= (SBC*PSP)*INGB(NGB);
CAPSsgb(SGB) .. Ssgb(SGB) =l= SBC*ISGB(SGB);
CAPWngb(NGB) .. Wngb(NGB) =l= SBC*(1-PSP)*(DHS/DHW)*INGB(NGB);
CAPSh1(SR) .. Sh1(SR) =l= SSR*HSRmax(SR)*NH1*IH1(SR)*CFSR;
CAPh1(SR) .. Hh1(SR) =l= HSRmax(SR)*IH1(SR)*CFSR;
CAPh2(SH2) .. Hh2(SH2) =l= H2max(SH2)*IH2(SH2)*CFH2;
CAPh3(SH3) .. Hh3(SH3) =l= H3max(SH3)*IH3(SH3)*CFH3;
CAPh4(SH4) .. Hh4(SH4) =l= H4max(SH4)*IH4(SH4)*CFH4;
CAPh5(SH5) .. Hh5(SH5) =l= H5max(SH5)*IH5(SH5)*CFH5;
CAPp1(SP1) .. Pp1(SP1) =l= PSP1max(SP1)*IP1(SP1)*CFNG;
CAPp2(SP2) .. Pp2(SP2) =l= PSP2max(SP2)*IP2(SP2)*CFPC;
CAPp3(SP3) .. Pp3(SP3) =l= PSP3max(SP3)*IP3(SP3)*CFIG;
CAPp4(SP4) .. Pp4(SP4) =l= PSP4max(SP4)*IP4(SP4)*CFP4;
CAPp5(SP5) .. Pp5(SP5) =l= PSP5max(SP5)*IP5(SP5)*CFP5;
CAPp6(SP6) .. Pp6(SP6) =l= PSP6max(SP6)*IP6(SP6)*CFP6;
CAPp7(SP7) .. Pp7(SP7) =l= PSP7max(SP7)*IP7(SP7)*CFP7;
CAPp8(SP8) .. Pp8(SP8) =l= PSP8max(SP8)*IP8(SP8)*CFP8;
CAPp9(SP9) .. Pp9(SP9) =l= PSP9max(SP9)*IP9(SP9)*CFP9;
* CO2 emissions reduction constraint
RED .. CO2E =e= CO2B*(1-ERG)
;
Model OSOMbc /all/;
option optcr =0;
Solve OSOMbc using mip minimizing COST;
* ------------------ Post-solve calculations --------------------------
* Cost of power and hydrogen IF operating at full capacity
parameter P1fue Unit fuel cost of NGCC ($\kWh);
P1fue = HRSP1/1000*CNG
parameter P1cost Baseload unit cost of NGCC power (cents\kWh);
P1cost = (((NGcap('NG1')+NGom('NG1'))/NGprod('NG1'))+ P1fue)*100
parameter P2fue Unit fuel cost of PC ($\kWh);
P2fue = HRSP2/1000*CCL
parameter P2cost unit cost of PC power (cents\kWh);
P2cost = (((PCcap('PC1')+PCom('PC1'))/PCprod('PC1'))+ P2fue)*100
parameter IGfue Unit fuel cost of IGCC ($\kWh);
```

IGfue = HRSP3/1000*CCL

parameter IGpow Unit power cost produced in IGCC (cents\kWh);

IGpow = (((IGcap('IG1')+IGom('IG1'))/IGprod('IG1'))+IGfue)*100

parameter P4fue Unit fuel cost of IGCC w 88% capture ($\kWh);

P4fue = HRSP4/1000*CCL

parameter P4pow Unit power cost produced in IGCC w capture (cents\kWh);

P4pow = (((P4cap('IGC1')+P4om('IGC1'))/P4prod('IGC1'))+P4fue)*100

parameter H1cost Unit cost of H2 - base case ($\tonne H2);

H1cost = (BChyd+BChe)/(HCMS*t)

parameter SCOcost Unit cost of SCO ($\bbl);

display P1cost, P2cost, IGpow, P4pow;

Scalars

* Average CO2 emissions of energy commodities

POWco2 average CO2 emissions of electricity (tonne CO2\kW)

HYDco2 average CO2 emissions of H2 (tonne CO2\tonne H2)

STMco2 average CO2 emissions of 950 steam (tonne CO2\tonne steam)

SSTco2 average CO2 emissions of 8000 steam (tonne CO2\tonne steam)

HOTco2 average CO2 emissions of hot water (tonne CO2\tonne water)

DIEco2 average CO2 emissions of diesel fuel (tonne CO2\l diesel)

PROco2 average CO2 emissions of process fuel (tonne CO2\GJ fuel)

* Average cost of energy commodities

POWcost average cost of electricity (USD$\kWh produced)

POWtcost average cost of electricity including CO2 transport (USD\kWh)

POWtscost average cost of electricity including CO2 transport and storage (USD\kWh)

HYDcost average cost of hydrogen (USD$\tonne H2 produced)

HYDtcost average cost of hydrogen including CO2 transport (USD\tonne H2)

HYDtscost average cost of hydrogen including CO2 transport and storage (USD\tonne H2)

HYDstcost average cost of hydrogen including CO2 transport and storage (USD\tonne H2)

STMcost average cost of 950 steam (USD$\tonne steam produced)

SSTcost average cost of 8000 steam (USD$\tonne steam produced)

HOTcost average cost of hot water (USD$\tonne hot water produced)

DIEcost average cost of diesel fuel (USD$\l)

PROcost average cost of process fuel (USD$\GJ)

* Optimal energy costs per bbl of product (Excluding Transport)

MSCcost optimized unitary cost of mined SCO without CO2 transport (USD$\bbl SCO produced)

TSCcost optimized unitary cost of thermal SCO without CO2 transport (USD$\bbl SCO produced)

TBIcost optimized unitary cost of thermal bitumen without CO2 transport (USD$\bbl BIT produced)

* Optimal CO2 emissions intensity per bbl of product

MSCco2 optimal CO2 intensity of mined SCO (tonne CO2\bbl SCO produced)

TSCco2 optimal CO2 intensity of thermal SCO (tonne CO2\bbl SCO produced)

TBIco2 optimal CO2 intensity of thermal BITUMEN (tonne CO2\bbl BIT produced)

* Optimal Energy Cost breakdown

* Mined SCO

POWmsc Cost of power per bbl of mined SCO (USD$\bbl SCO produced)

POWtsmsc Cost of power per bbl of mined SCO including CO2 transport and storage (USD$\bbl SCO produced)

HYDmsc Cost of H2 per bbl of mined SCO (USD$\bbl SCO produced)

HYDtsmsc Cost of H2 per bbl of mined SCO including CO2 transport and storage (USD$\bbl SCO produced)

STMmsc Cost of steam per bbl of mined SCO (USD$\bbl SCO produced)

HOTmsc Cost of hot water per bbl of mined SCO (USD$\bbl SCO produced)

DIEmsc Cost of diesel per bbl of mined SCO (USD$\bbl SCO produced)

PROmsc Cost of process fuel per bbl of mined SCO (USD$\bbl SCO produced)

TOTmsc Total energy cost per bbl of mined SCO excluding storage (USD$\bbl SCO produced)

FINmsc Total energy cost per bbl of mined SCO including storage (USD$\bbl SCO produced)

* SAGD SCO

POWtsc Cost of power per bbl of thermal SCO (USD$\bbl SCO produced)

POWtstsc Cost of power per bbl of thermal SCO including CO2 transport and storage (USD$\bbl SCO produced)

HYDtsc Cost of H2 per bbl of thermal SCO (USD$\bbl SCO produced)

HYDtstsc Cost of H2 per bbl of thermal SCO including CO2 transport and storage (USD$\bbl SCO produced)

STMtsc Cost of steam per bbl of thermal SCO (USD$\bbl SCO produced)

SSTMtsc Cost of SAGD steam per bbl of thermal SCO (USD$\bbl SCO produced)

PROtsc Cost of process fuel per bbl of thermal SCO (USD$\bbl SCO produced)

TOTtsc Total energy cost per bbl of thermal SCO excluding storage (USD$\bbl SCO produced)

FINtsc Total energy cost per bbl of thermal SCO including storage (USD$\bbl SCO produced)

* SAGD BITUMEN

POWtb Cost of power per bbl of thermal BITUMEN (USD$\bbl SCO produced)

POWtstb Cost of power per bbl of thermal BITUMEN including CO2 transport and storage (USD$\bbl SCO produced)

SSTMtb Cost of SAGD steam per bbl of thermal BITUMEN (USD$\bbl SCO produced)

TOTtb Total energy cost per bbl of thermal BITUMEN excluding storage (USD$\bbl SCO produced)

FINtb Total energy cost per bbl of thermal BITUMEN including storage (USD$\bbl SCO produced)

;

* Cost - Optimized unitary commodity costs

POWcost = Pcost.l/POW.l/t;

POWtcost = (Pcost.l+CTPcost.l)/POW.l/t;

POWtscost = (Pcost.l+CTPcost.l+CSPcost.l)/POW.l/t;

HYDcost = (Hcost.l+((Ph1.l+Ph2.l)*POWcost*t))/H2.l/t;

HYDtcost = (Hcost.l+((Ph1.l+Ph2.l+Phco2.l)*POWtcost*t)+CTHcost.l)/H2.l/t;

HYDtscost = (Hcost.l+((Ph1.l+Ph2.l+Phco2.l)*POWtscost*t)+CTHcost.l+CSHcost.l)/H2.l/t;

STMcost = Scost.l/S915.l/t;

SSTcost = SScost.l/S8000.l/t;

HOTcost = Wcost.l/WAT.l/t;

DIEcost = CDI;

PROcost = Fcost.l/((Xpf.l*HHVNG/1000*t)+(Ypf.l*HHVC*t));

* Cost - Optimized unitary energy costs (excluding CO2 transport and storage)

MSCcost = (((DCS+DNS)*CDI)+
((WCS+WNS)*HOTcost)+
((SCMU+SCMS+SNMU+SNMS)*STMcost)+
((PCMS+PCMSU+PNMS+PNMSU)*POWcost)+
((HCMS+HNMS)*HYDcost)+
((NGCMS+NGNMS)*HHVNG/1000*PROcost))/(CMSCO+NMSCO);

TSCcost = (((SNTU+SNTS)*STMcost)+(SNTSS*SSTcost)+
((PNTS+PNTSU)*POWcost)+(HNTS*HYDcost)+
(NGNTS*HHVNG/1000*PROcost))/NTSCO;

TBIcost = (((SCTB+SNTB)*SSTcost)+((PCTB+PNTB)*POWcost))/(CTB+NTB);

* Optimal energy cost breakdown - Mined SCO

POWmsc = ((PCMS+PCMSU+PNMS+PNMSU)*POWtcost)/(CMSCO+NMSCO);

POWtsmsc = ((PCMS+PCMSU+PNMS+PNMSU)*POWtscost)/(CMSCO+NMSCO);

HYDmsc = ((HCMS+HNMS)*HYDtcost)/(CMSCO+NMSCO);

HYDtsmsc = ((HCMS+HNMS)*HYDtscost)/(CMSCO+NMSCO);

STMmsc = ((SCMU+SCMS+SNMU+SNMS)*STMcost)/(CMSCO+NMSCO);

HOTmsc = ((WNS+WCS)*HOTcost)/(CMSCO+NMSCO);

DIEmsc = ((DCS+DNS)*CDI)/(CMSCO+NMSCO);

PROmsc = ((NGCMS+NGNMS)*HHVNG/1000*PROcost)/(CMSCO+NMSCO);

TOTmsc = POWmsc+HYDmsc+STMmsc+HOTmsc+DIEmsc+PROmsc;

```
FINmsc = POWtsmsc+HYDtsmsc+STMmsc+HOTmsc+DIEmsc+PROmsc;
* Optimal energy cost breakdown - SAGD SCO
POWtsc = ((PNTS+PNTSU)*POWtcost)/NTSCO;
POWtstsc = ((PNTS+PNTSU)*POWtscost)/NTSCO;
HYDtsc = (HNTS*HYDtcost)/NTSCO;
HYDtstsc = (HNTS*HYDtscost)/NTSCO;
STMtsc = ((SNTU+SNTS)*STMcost)/NTSCO;
SSTMtsc = (SNTSS*SSTcost)/NTSCO;
PROtsc = (NGNTS*HHVNG/1000*PROcost)/NTSCO;
TOTtsc = POWtsc+HYDtsc+STMtsc+SSTMtsc+PROtsc;
FINtsc = POWtstsc+HYDtstsc+STMtsc+SSTMtsc+PROtsc;
* Optimal energy cost breakdown - Thermal BITUMEN
POWtb = ((PCTB+PNTB)*POWtcost)/(CTB+NTB);
POWtstb = ((PCTB+PNTB)*POWtscost)/(CTB+NTB);
SSTMtb = ((SCTB+SNTB)*SSTcost)/(CTB+NTB);
TOTtb = POWtb+SSTMtb;
FINtb = POWtstb+SSTMtb;
* Optimal unitary CO2 emissions of energy commodities
POWco2 = (Ep1.l+Ep2.l+Ep3.l+Ep4.l+Ep5.l+Ep6.l+Ep7.l+Ep8.l+Ep9.l)/POW.l;
HYDco2 = (Eh1.l+Eh2.l+Eh3.l+Eh4.l+Eh5.l)/H2.l;
STMco2 = (Engb.l*PSP)/S915.l;
SSTco2 = (Esgb.l)/S8000.l;
HOTco2 = (Engb.l*(1-PSP))/WAT.l;
DIEco2 = FEFD;
PROco2 = (EPF.l)/((Xpf.l*HHVNG/1000)+(Ypf.l*HHVC));
* Optimal CO2 intensities of all products
MSCco2 =        (((DCS+DNS)*DIEco2)+
                ((WCS+WNS)*HOTco2)+
                ((SCMU+SCMS+SNMU+SNMS)*STMco2)+
                ((PCMS+PCMSU+PNMS+PNMSU)*POWco2)+
                ((HCMS+HNMS)*HYDco2)+
                ((NGCMS+NGNMS)*HHVNG/1000*PROco2))
                /(CMSCO+NMSCO);
TSCco2 =        (((SNTU+SNTS)*STMco2)+(SNTSS*SSTco2)+
                ((PNTS+PNTSU)*POWco2)+(HNTS*HYDco2)+
                (NGNTS*HHVNG/1000*PROco2))/NTSCO;
TBIco2 =        (((SCTB+SNTB)*SSTco2)+((PCTB+PNTB)*POWco2))/(CTB+NTB);
```

```
display DIEcost, PROcost, HOTcost, STMcost, POWcost, HYDcost, H1cost;
display BCtot, COST.l, BCsco, MSCcost, TSCcost, BCbit, TBIcost;
display POWmsc, HYDmsc, STMmsc, HOTmsc, DIEmsc, PROmsc, TOTmsc;
display POWco2, HYDco2, STMco2, SSTco2, HOTco2, DIEco2, PROco2;
option decimals =5;
display CO2sco, CO2bit, MSCco2, TSCco2, TBIco2;
option decimals =2;
display CO2E.l, CCO2.l, MSCcost, TOTmsc, FINmsc, TSCcost,TOTtsc, FINtsc, TBIcost, TOTtb,
FINtb ;
display Phco2.l, Ppco2.l, PD, PEX.l, CTHcost.l, CSHcost.l, CTPcost.l, CSPcost.l;
display HYDcost, HYDtcost, HYDtscost, POWcost, POWtcost, POWtscost;
display SELp1.l, SELp2.l, SELp3.l, SELp4.l, SELp5.l, SELp6.l, SELp7.l, SELp8.l, SELp9.l;
display SELh1.l, SELh2.l, SELh3.l, SELh4.l, SELh5.l;
```